Analysis of Oxidative Stress in Sperm in Early Embryonic Development

Dissertation

zur
Erlangung der naturwissenschaftlichen Doktorwürde
(Dr. sc. nat.)

vorgelegt der
Mathematischen-naturwissenschaftlichen Fakultät

der
Universität Zürich

von

Sarah Luisa Wyck

aus Deutschland

Promotionskommission
PD Dr. Raffaella Santoro (Leitung der Dissertation und Vorsitz)
Prof. Dr. Hanspeter Nägeli
Prof. Dr. Heinrich Bollwein
PD Dr. Paolo Cinelli
Prof. Dr. Petra Hajkova

Zürich, 2018

Summary

Infertility affects around 15% of all couples of reproductive age, with about 50% being associated with abnormalities in the male. Reactive oxygen species (ROS)-induced oxidative stress is well known to play a major role in male infertility. However, how oxidative DNA lesions in sperm affects early development remains elusive. Using cattle as model, we show that oxidative stress induces DNA damage in sperm and causes an arrest at later stages of embryo development, close to the onset of embryonic genome activation. Reactive oxygen species (ROS)-induced oxidative stress is well known to play a major role in male infertility. However, how oxidative DNA lesions in sperm affects early development remains elusive. Using cattle as model, we show that oxidative stress induces DNA damage in sperm and causes an arrest at later stages of embryo development, close to the onset of embryonic genome activation. The levels of DNA damage response did not directly correlate with the degree of developmental defects. Instead, damaged paternal genome showed an impairment of zygotic active DNA demethylation, a process that has been linked with the base excision repair (BER) pathway. Quantitative immunofluorescence analysis and ultrasensitive LC-MS-based measurements revealed that oxidative DNA lesions in sperm impair active DNA demethylation at paternal pronuclei, without affecting 5-hydroxymethylcytosine (5hmC), a TET3-mediated 5-methylcytosine modification that has been linked to paternal DNA demethylation in mouse embryos. Thus, active DNA demethylation in bovine embryos does not necessarily depend on the 5hmC pathway. Recruitment of the BER component X-ray repair cross-complementing protein 1 (XRCC1) to damaged paternal pronuclei indicates that oxidative DNA lesions are repaired by BER-mediated pathways and that this process occurs at the expense of DNA demethylation. Together, the data demonstrate that oxidative stress in sperm has an impact not only on DNA integrity but also on the dynamics of epigenetic reprogramming, which may harm the paternal genetic and epigenetic contribution to the developing embryo and affect embryo development and embryo quality. Last, but not least the results revealed species-specific epigenetic differences between bovine and mouse embryos and gametes that will facilitate the understanding of the dynamics of DNA methylation in early development.

Zusammenfassung

Unfruchtbarkeit betrifft rund 15% der Paare im fortpflanzungsfähigen Alter wobei, rund 50% der Fälle auf Unfruchtbarkeit im Mann zurück geführt werden können. Man weiss, dass dabei durch reaktive Sauerstoffspezies induzierter oxidativer Stress eine bedeutende Rolle spielt. Wie genau oxidative Läsionen in Spermien die embryonale Frühentwicklung beeinflussen, ist bis jetzt allerdings schwer fassbar. Wir konnten in Kühen zeigen, dass oxidativer Stress in Spermien DNA Schädigungen erzeugt und damit einen Arrest in späteren Stadien der frühen Embryonalentwicklung, unmittelbar zu Beginn der embryonalen Genomaktivierung, herbeiführt. Das Ausmaß der DNA Reparatur Antwort korrelierte nicht direkt mit dem Ausmaß der Entwicklungsdefekte. Stattdessen zeigte das beschädigte väterliche Genom eine Beeinträchtigung in der aktive DNA Demethylierung in der Zygote, einem Prozess der mit dem Basen-Exzisionsreparatur Signalweg in Verbindung gebracht wird. Quantitative Immunfluoreszenzanalysen und ultra-sensitive LC-MC basierte Messungen ergaben, dass oxidative DNA Läsionen in Spermien die aktive DNA Demethylierung im väterlichen Vorkern verunmöglichen, ohne dabei 5-hydroxymethylcytosine, eine durch TET3 herbeigeführte Modifikation von 5-methylcytosine, die in Mausembryonen mit der DNA Demethylierung auf dem väterlichen Genom in Verbindung gebracht wurde, zu beeinflussen. Diese Ergebnisse deuten darauf hin, dass die aktive DNA Demethylierung in Kuhembryonen nicht zwingendermassen von dem 5hmC Signalweg abhängt. Die Rekrutierung der BER Komponente X-ray repair cross-complementing protein 1 (XRCC1) vom mütterlichen zum väterlichen Vorkern indiziert, dass oxidative Läsionen durch den BER-indizierten Signalweg repariert werden können und dass dieser Prozess zu Lasten der DNA Demethylierung geht. Zusammengefasst zeigen die Daten, dass oxidativer Stress nicht nur einen Einfluss auf die DNA Integrität, sondern auch auf die Dynamik der epigenetischen Reprogrammierung hat, die den väterlichen genetischen und epigenetischen Beitrag zur Embryoentwicklung schädigen und die Embryonalentwicklung und Embryoqualität in Mitleidenschaft ziehen können. Nicht zuletzt ergaben die Resultate speziesspezifische epigenetische Unterschiede zwischen Embryonen und Gameten von Kühen und Mäusen, die das Verständnis der Dynamik der DNA Methylierung in der frühen Embryonalentwicklung fördern.

Abbreviations

5caC	5-carboxycytosine
5fC	5-formylcytosine
5hmC	5-hydroxymethylcytosine
5mC	5-methylcytosine
8-oxoG	7,8-dihydro-8-oxoguanine
AGG/MPG	alkyl guanine glycosylase/methyl purine glycosylase
AMH	anti-Mullerian hormone
Ape1	apurinic endonuclease 1
APOBEC1	apolipoprotein B mRNA-editing en- zyme catalytic polypeptide 1
ART	assisted reproductive technologies
AS	Angelman syndrome
ATM	ataxia telangiectasia Mutated
ATP	adenosine triphosphate
ATR	ataxia telangiectasia And Rad3 Related
BER	base excision repair
BW	Beckwith-Wiedemann
CChIP	establishing the carrier-chromatin immunoprecipitation
CDX2	caudal type homeobox 2
CGI	CpG island
CL	corpus luteum
Dam-ID	DNA adenine methyltransferase identification
DDR	DNA damage response
DMR	differentially methylated region
DNA	desoxyribonucleic acid
DNMT	DNA methyltransferase
Dppa3	developmental pluripotency-associated protein 3
DSB	double strand break
EGA	embryonic genome activation
EpiLCs	epiblast-like cells
EpiSCs	epiblast stem cells
EZH2	enhancer of zeste homologue 2

FapyG	2,6-diamino-4-hydroxy-5-formamidopyrimidine
FEN1	flap-endonuclease 1
FSH	follicle-stimulating hormone
γH2AX	phosphorylated H2A.X
GRR	germline reprogramming responsive
GV	germinal vesicle
HAT	histone acetyltransferases
HDAC	histone deacetylases
HMGB1	nonhistone protein high mobility group box 1
HP1	heterochromatin protein 1
HR	homologous recombination
IAP	intracisternal A-particles
ICM	inner cell mass
ICR	imprinted control regions
ICSI	intracytoplasmatic sperm injection
IVF	*in vitro* fertilization
IVP	*in vitro* production
LAD	lamina associated domains
LH	luteinizing hormone
LigI	ligase I
LINE-1	long interspersed element 1
lncRNA	long non-coding RNA
LOS	large offspring syndrome
Mbd4	methyl CpG binding domain protein 4
mESC	mouse embryonic stem cells
MMR	mismatch repair
mPN	maternal pronucleus
NER	nucleotide excision repair
NHEJ	non-homologous end-joining
NLB	nucleolar-like bodies
NTH1	endonuclease III-like protein 1
NuRD	nucleosome remodelling and histone deacetylation
OCT4	octamer-binding transcription factor 4

OGG1	8-oxoguanine DNA glycosylase 1
PARP1	poly(ADP-Ribose)-Polymerase 1
PCNA	proliferating cell nuclear antigen
PGC	primordial germ cells
PGCLCs	PGC-like cells
PIKK	phosphatidylinositol 3-kinase-like protein kinase
PMF	primordial follicle
PNKP	polynucleotide kinase/phosphatase
Polβ	polymerase beta
pPN	paternal pronucleus
Pramel7	PRAME-like 7
PRC	polycomb repressive complex
PRDM14	PR domain containing 14
PTEN	phosphatase and tensin homolog deleted on chromosome 10
PTM	posttranslational modification
ROS	reactive oxygen species
RPA	replication protein A
SCNT	somatic cell nuclear transfer
SINE	short interspersed nuclear element
SMUG1	single-strand-selective monofunctional uracil glycosylase 1
SOX2	sex determining region Y-box 2
SRS	Silver-Russel syndrome
SSA	single strand annealing
SSB	single strand break
TDG	thymine DNA glycosylase
TET	ten-eleven translocation
TFIIH	transcription factor II H
TNP	transition protein
TOP2B	topoisomerase 2B
TP53BP1	tumour suppressor p53-binding protein 1
UHRF1	ubiquitin-like plant homeodomain and RING finger 1
UNG	uracil glycosylases
Xi	inactivated X-chromosome

Xp	paternal X-chromosome
XRCC1	X-ray repair cross-complementing protein 1
ZGA	zygotic genome activation

Table of Contents

1. Introduction

1.1 Epigenetic regulation

In 1942 Waddington coined the term epigenetics, which he defined as changes in phenotype without changes in genotype, to explain aspects of development for which there was little mechanistic understanding (Allis and Jenuwein, 2016). Today, epigenetics refers to the study of changes in gene function that are mitotically and/or meiotically heritable and that do not entail a change in DNA sequence.

The best known epigenetic modifications are DNA methylation and histone post-transcriptional modifications, including methylation, acetylation, ubiquitination and phosphorylation (Jenuwein and Allis, 2001). In the following sections, I will describe in details how DNA methylation is regulated and its functional impact in cellular process (see **1.1.1**). The establishment and role of histone modifications will be described in the context of gametogenesis and early embryogenesis (see **1.4** and **1**.**5**).

1.1.1 DNA methylation

DNA methylation is a heritable epigenetic mark involving the covalent transfer of a methyl group to the C-5 position of the cytosine ring by DNA methyltransferases (DNMTs), which use S-adenosyl-L-methionine (SAM) as methyl group donor (**Fig. 1**). In plants, cytosines are methylated in both symmetrical (CG or CHG) and asymmetrical (CHH, where H is A, T, or C) contexts. In mammals, approximately 70–80% of the cytosines in CpG dyads are methylated on both strands. In general, CpG methylation is highly prevalent in repetitive sequences and in gene bodies but rare at CpG islands within housekeeping promoters (Ambrosi et al., 2017; Chen and Riggs, 2011).

In mammals, DNA methylation is involved in the repression of single genes or entire chromosomes (as in the case of X chromosome inactivation) and is essential for genomic imprinting by guiding allele-specific gene expression. Moreover, DNA methylation is required for the silencing of repetitive elements, thereby maintaining genome stability. Defects in DNA methylation are closely associated with cancer; epigenetic hallmarks of cancer include global DNA hypomethylation and locus-specific hypermethylation of CpG islands (CGIs) (Suzuki and Bird, 2008).

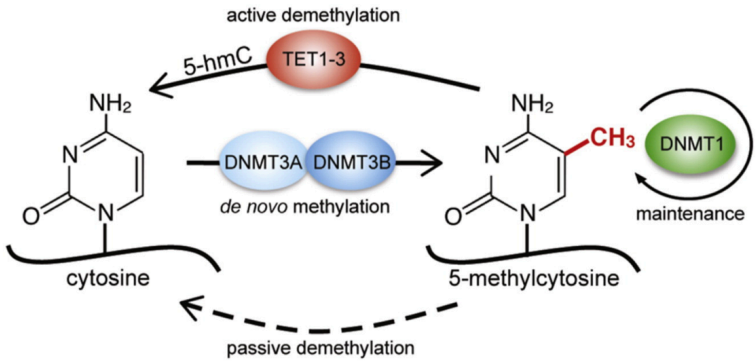

Figure 1. Key players in the DNA methylation and demethylation pathway. *De novo* methylation is established via DNMT3A/B mediated addition of a methylgroup to the 5th carbon at the cytosine base. DNA methylation is maintained through the presence of DNMT1 that is present during replication. Image taken from (Ambrosi et al., 2017).

In mammals, three conserved DNA methyltransferases (DNMTs) are responsible for DNA methylation (**Fig. 2**) (Li et al., 1992a; Okano et al., 1999a).

DNMT3A and DNMT3B are the *de novo* methyltransferases whereas DNMT1 is the maintenance DNA methyltransferase (DNMT1) (Goll and Bestor, 2005). Recently, DNMT3C has been identified as a new member of the DNMT family (Barau et al., 2016). *Dnmt3C* is a *de novo* DNA methyltransferase gene that evolved via a duplication of *Dnmt3B* in rodent genomes and was previously annotated as a pseudogene. DNMT3C is the enzyme responsible for methylating the promoters of evolutionarily young retrotransposons in the male germ line and this specialized activity is required for mouse fertility (Barau et al., 2016).

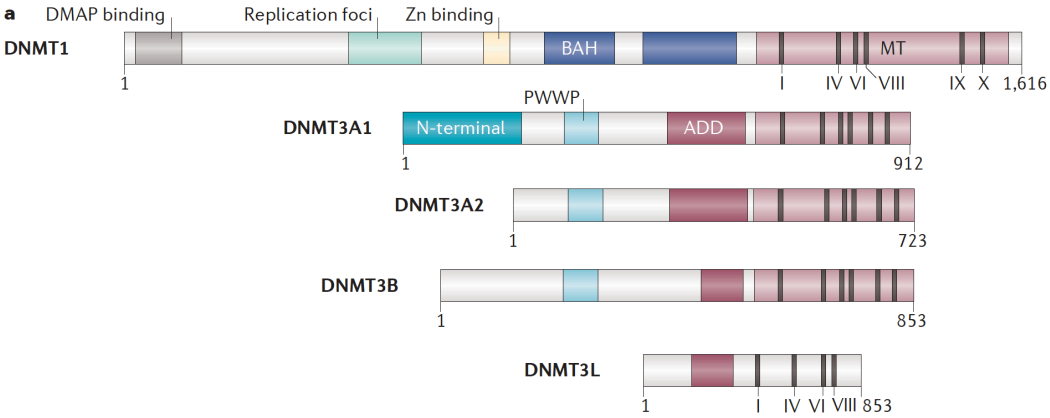

Figure 2. The structure of DNA methyltransferase proteins. Domain architecture of DNA methyltransferase 1 (DNMT1), DNMT3A1, DNMT3A2, DNMT3B and DNMT3-like (DNMT3L) and major DNMT3A splice isoforms. DNMT3B has also a number of additional isoforms that are not depicted here. Protein length is indicated (length given as number of amino acids). Domain abbreviations: ADD, ATRX-DNMT3-DNMT3L (related to the plant homology (PHD)-like domain of regulator ATRX); BAH, Bromo adjacent homology domain; DMAP, DNMT1-associated protein; PWWP, Pro-Trp-Trp-Pro. MT is the catalytic methyltransferase domain, and I, IV, VI, IX and X are motifs in the catalytic domain: motif I allows the binding of the methyl group donor *S*-adenosyl methionine. Motifs I and X are for cofactor binding, and motifs VIII and IX are for DNA binding. Image taken and modified from (Jurkowska et al., 2011).

All DNMTs share a similar, multi-domain architecture. The variable N-terminus contains several regulatory domains and the C-terminal regions harbour the catalytic methyltransferase (MT) domain (**Fig. 2**). The N-terminal domains strongly differ between DNMT1 and DNMT3 proteins and could play an important role in specifying their activity along the genome (Ambrosi et al., 2017). For example, the N-terminal part of DNMT1 contains domains that mediate anchoring to the replication fork (Leonhardt et al., 1992; Suetake et al., 2006).

Since DNA methylation is highly dynamic and varies in a global and local context, DNA methylation removal is considered as an integral part of the epigenetic regulatory network (Ambrosi et al., 2017). DNA methylation can be removed through several mechanisms. Passive DNA demethylation is achieved via DNA replication in the absence of DNMT1 activity. Active DNA demethylation has been proposed to be a multistep process that is initiated by modifications of the methylated cytosine or methyl group, followed by removal of the modified base via a DNA repair mechanism.

The details of DNA methylation and DNA demethylation processes are described in the following paragraphs.

1.1.1.1. *De novo* DNA methylation

DNMT3A and DNMT3B establish *de novo* DNA methylation (Law and Jacobsen, 2010). DNMT3L lacks the catalytic C-terminus and is therefore catalytically inactive but through its interaction with other *de novo* DNMTs is able to modulate their activity (Jurkowska et al., 2011; Ooi et al., 2007; Wu and Zhang, 2014). Deletion of *Dnmt3b* in mice is embryonically lethal whereas *Dnmt3a*$^{-/-}$ mice survive to full term and die around 4 weeks of age (Okano et al., 1999a). In mice, DNMT3A is mainly expressed in oocytes and early embryos, being responsible for establishing the imprints in both gametes. DNMT3B is expressed in later pre-implantational embryos and plays a role after the zygotic genome activation and the establishment of the methylation mark after embryonic reprogramming.

The most N-terminal part of DNMT3A and DNMT3B is highly variable and is involved in interactions with DNA and nucleosomes (Jeong et al., 2009) (**Fig. 2**). The ATRX-DNMT3-DNMT3L domain of DNMT3A, DNMT3B, and DNMT3L interacts with histone H3 tails and this association is blocked by the methylation of the lysine-4 residue of histone (H3K4me3) (Ooi et al., 2007; Otani et al., 2009). The PWWP domain of DNMT3A and DNMT3B contains a conserved aromatic cage that recognizes

histone H3 lysine-36 trimethylation (H3K36me3) *in vitro* and *in vivo* (Baubec et al., 2015; Dhayalan et al., 2010) and is also required for the localisation to pericentromeric repeats (Chen et al., 2004). In contrast, DNMT3C and DNMT3L lack the PWWP domain (Barau et al., 2016). The shorter isoform of DNMT3A that is predominantly expressed in embryonic stem cells, DNMT3A2, also lacks the PWWP domain (Chen et al., 2002). Recent analyses revealed that DNMT3A isoforms (DNMT3A1 and DNMT3A2) differ in their genomic binding and DNA methylation activity at regulatory sites (Manzo et al., 2017). The longer isoform DNMT3A1 preferentially localizes to the methylated shores of bivalent CpG island promoters in a tissue-specific manner and coincides with elevated hydroxymethylcytosine (5-hmC) deposition, suggesting an involvement of this isoform in mediating turnover of DNA methylation at these sites.

1.1.1.2. Maintenance of DNA methylation

DNA methylation is a heritable epigenetic mark. Maintenance of DNA replication during cell division is mediated by DNMT1. Deletion of mouse *Dnmt1* is lethal at/after gastrulation (Li et al., 1992a). In mice, the *Dnmt1* locus encodes two functionally identical isoforms: a somatic (*Dnmt1s*) and an oocyte-specific isoform (*Dnmt1o*) (Gaudet et al., 1998; Mertineit et al., 1998).

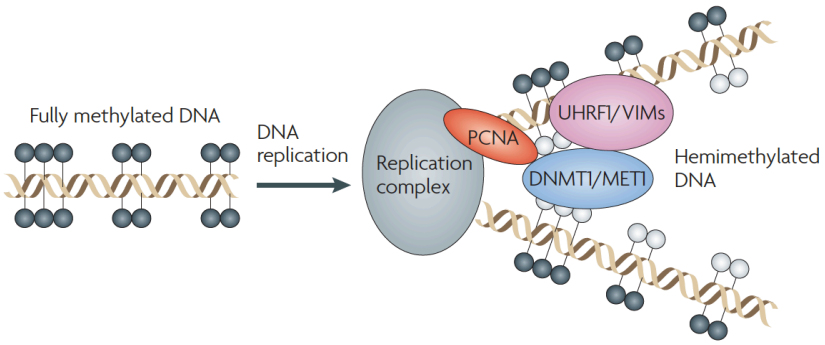

Figure 3. Model depicting the maintenance of CG methylation during replication. DNMT1 is proposed to be recruited to replication foci through interactions with UHRF1 - a SET- or RING-associated (SRA) domain protein that specifically interacts with hemimethylated DNA - and with proliferating cell nuclear antigen (PCNA). After being recruited, DNMT1 functions to maintain methylation patterns by restoring the hemimethylated DNA to a fully methylated state. Black and white circles represent methylated and unmethylated cytosines, respectively. Image taken and modified from (Law and Jacobsen, 2010).

Due to the semiconservative nature of DNA replication, a DNA sequence carrying symmetrical methylation marks on both strands gives rise to two hemi-methylated double strands (**Fig. 3**). During replication DNMT1 is targeted to hemimethylated DNA in order to re-establish symmetrically methylated CpGs. DNMT1 CXXC do-

main, located at the N-terminus, displays a preferential binding to unmethylated CpG dinucleotides while inhibiting the binding of the active site of DNMT1 to the DNA, thus preventing *de novo* methylation (Song et al., 2011a). DNMT1 associates with replication foci (Edwards et al., 2017; Leonhardt et al., 1992; Urieli-Shoval et al., 1983). Early studies showed that DNMT1 is recruited to replication foci by an interaction with the proliferating cell nuclear antigen (PCNA) component of the replication machinery (Chuang et al., 1997). However, disruption of this interaction only resulted in a minor reduction in DNA methylation (Spada et al., 2007).

DNMT1 was shown to interact with ubiquitin-like plant homeodomain and RING finger 1 (UHRF1) protein (Bostick, 2007; Kishikawa et al., 2003) (**Fig. 3**). UHRF1 binds to hemimethylated DNA and facilitates the targeting of DNMT1 to hemimethylated DNA (Bostick, 2007). The SET- or RING-associated (SRA) domain of UHRF1 specifically binds to hemimethylated CG dinucleotides (Arita et al., 2008; Hashimoto et al., 2008). Mutations in UHRF1 cause a severe decrease in DNA methylation and have led to a model in which UHRF1 recruits DNMT1 to hemimethylated DNA (Bostick, 2007; Sharif et al., 2007).

The functional separation of *de novo* and maintenance DNMT activities is, however, not completely tight as originally thought. Studies in *Dnmt3a/3b* deficient mouse embryonic stem cells (mESCs) revealed that DNMT1 alone was not sufficient to completely maintain DNA methylation levels, suggesting that *de novo* methyltransferase activities are also required for fully maintenance of DNA methylation (Chen et al., 2003; Liang, 2002).

1.1.1.3. Passive and active DNA demethylation

Although in most cases DNA methylation is a stable epigenetic mark, reduced levels of methylation are observed during development in plants and mammals. This net loss of methylation can either occur passively, by replication in the absence of functional maintenance methylation pathways, or actively, by removing methylated cytosines.

Passive demethylation takes place in a replication dependent manner in the absence of the maintenance methylation (Howlett and Reik, 1991; Rougier et al., 1998). Passive mechanism depends on repeated DNA replication and therefore cannot account for the rapid loss of DNA methylation in slowly or non-dividing cells. Furthermore, this mechanism does not allow locus-specific, but only global, removal of DNA methylation marks (Messerschmidt et al., 2014).

The existence of mechanisms for active DNA demethylation was proposed to explain the global reduction in DNA methylation in the absence of replication. Important examples are the demethylation of paternal pronuclei (pPN) in pre-replicative zygotes and during the epigenetic reprogramming of primordial germ cells (PGCs) (Hajkova, 2002; Mayer et al., 2000; Oswald et al., 2000; Sasaki and Matsui, 2008). In contrast to the enzymatically controlled, straightforward methylating mechanism, a direct DNA demethylase capable of breaking carbon-carbon bonds has not been identified. Instead, several alternative, active demethylation mechanisms have been proposed (Wu and Zhang, 2010). There is a certain consensus that active DNA demethylation is a multistep process that is initiated by modifications at cytosines followed by their replacement by DNA repair-mediated mechanisms.

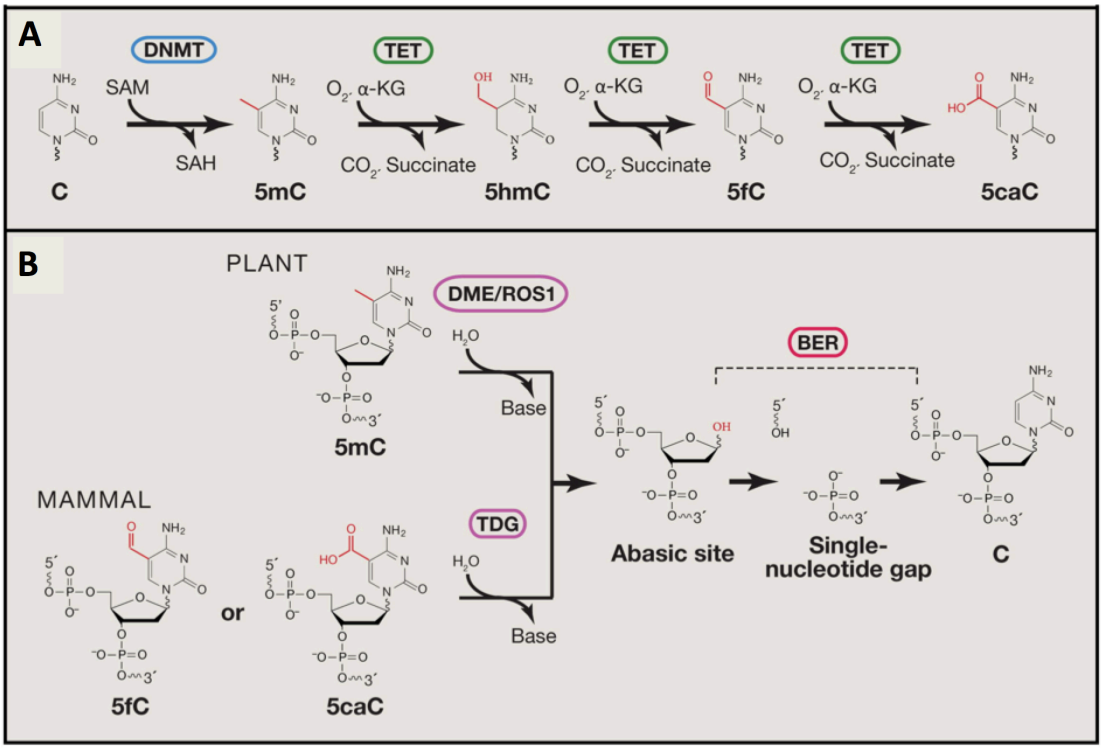

Figure 4. The step-wise cytosine modification pathway that includes cytosine methylation by DNMTs and iterative oxidation of 5mC by TET proteins. As Fe(II)/α-ketoglutarate (α-KG)-dependent dioxygenases, TET proteins use a base-flipping mechanism to flip the target base out of the duplex DNA into the catalytic site. TET enzymes use molecular oxygen as a substrate to catalyse oxidative decarboxylation of α-KG, yielding CO_2, enzyme-bound succinate, and a reactive high-valent Fe(IV)-oxo intermediate. The enzyme-bound Fe(IV)-oxo intermediate reacts with 5mC/5hmC/5fC to generate 5hmC/5fC/5caC, with a net oxidative transfer of the single oxygen atom to the substrate, resulting in regeneration of the Fe(II) species. Base excision repair of 5mC (in plants) or 5fC/5caC (in mammals) was proposed to complete DNA demethylation. In mammals, oxidized 5mC bases (5fC/5caC), could be excised by thymine DNA glycosylase TDG. TDG is a monofunctional DNA glycosylase, so other proteins are required to provide the AP lyase activity to remove the sugar ring to generate a single-nucleotide gap. Modified after (Wu and Zhang, 2014).

5hmC and TET family of dioxygenases have been implicated in active DNA demethylation (Tahiliani, 2009). 5hmC was originally discovered in T2, T4, T6 bacteriophage genomes (Jesaitis, 1957). TET enzymes drive the oxidation of 5mC, forming

5hmC (**Fig. 4**). Accordingly, in mouse embryonic stem cells (mESCs) 5hmC was dependent on TET expression (Ito, 2010; Tahiliani et al., 2009). Iterative oxidation steps result in further oxidised intermediates like 5-formylcytosein (5fC) and 5-carboxylcytosine (5caC) (He et al., 2011; Ito et al., 2011; Pfaffeneder et al., 2011) (**Fig. 4**). However, the abundance of 5fC and 5caC is at least one order of magnitude lower than 5hmC (He et al., 2011; Ito et al., 2011).

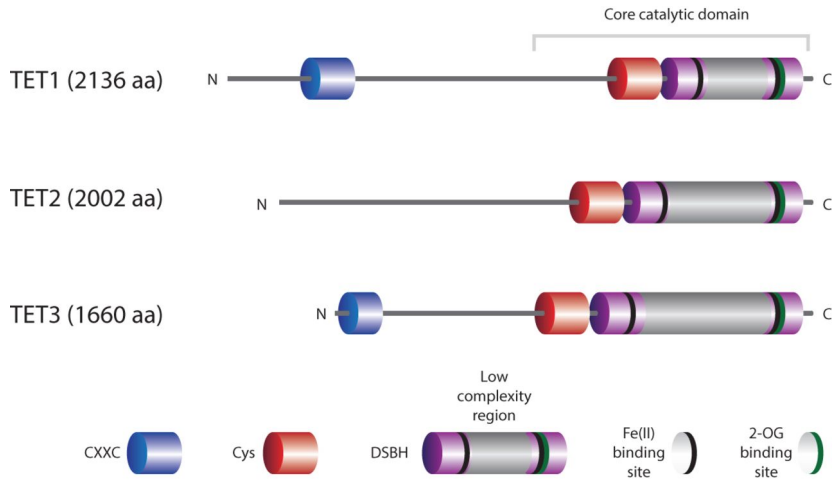

Figure 5. Domain structure of TET proteins. The C-terminal core catalytic domain shared by all TET enzymes consists of the DSBH domain, a cysteine-rich (Cys) domain, and binding sites for the Fe(II) and 2-OG cofactors. The DSBH domain contains a large low-complexity region of unknown function. TET1 and TET3 have an N-terminal CXXC domain that can bind directly to DNA and facilitate recruitment to genomic target sites. Taken from (Rasmussen and Helin, 2016).

The TET protein family contains three family members TET1, TET2 and TET3 (**Fig. 5**). TETs contain a core catalytic domain wherein, with the use of molecular oxygen, the oxidation of 5mC to 5hmC is driven (Kohli and Zhang, 2013). TETs belong to the family of Fe(II)/a-KG-dependent oxygenases and their enzymatic activity is conserved between human and mice (Ito et al., 2010). All TET proteins contain a conserved double-stranded β-helix (DSBH) domain, a cysteine-rich domain, and binding sites for the cofactors Fe(II) and 2-oxoglutarate (2-OG) that together form the core catalytic region in the C-terminus. Structural studies suggest that this core catalytic region preferentially binds cytosines in a CpG context but does not interact with surrounding DNA bases and shows little or no specificity for flanking DNA sequences (Hashimoto et al., 2014; Hu et al., 2015). In addition to their catalytic domain, TET1 and TET3 have an N-terminal CXXC zinc finger domain that can bind DNA. CXXC are supposed to bind unmethylated CpGs that might help the TET recruitment to CpG-rich promoters (Frauer et al., 2011; Ko et al., 2013; Lee et al., 2001; Xu et al., 2012; Zhang et al., 2010).

TET1 and TET2 are expressed during early embryonic development and in the inner cell mass (ICM). TET3 was shown to be highly expressed in oocytes and zygotes until 2-cell stage. In zygotes, TET3 was mainly found on the paternal pronucleus whereas TET1 and TET2 expression could be detected only later in development (Gu, 2011; Shen et al., 2014). The pattern of TET expression during gametogenesis and embryogenesis seems to be conserved among species, with the exception of sheep where TET3 expression was lower relative to mice (Jafarpour et al., 2017). Knockout (KO) of *Tet1/2* resulted in surviving pups, but *Tet1* KO led to a reduction in litter size, whereas *Tet2* deletion increased the susceptibility to leukaemia (Dawlaty et al., 2011; Moran-Crusio et al., 2011). In mESCs double KO (*Tet1/2*) and triple KO (*Tet1/2/3*) decreased the global 5hmC level and DNA methylation was found increased at enhancers (Hon et al., 2014; Lu et al., 2014).

TETs have been proposed to play a crucial role during active DNA demethylation of the paternal pronucleus (pPN) in zygotic development. The pPN of pre-replicative mouse zygotes contains substantial amounts of 5hmC but lacks 5mC and depletion of TET3 affects 5hmC and 5mC patterns (Gu, 2011; Iqbal et al., 2011; Wossidlo, 2011). However, these initial results were obtained with immunofluorescence (IF) analysis using antibodies specifically recognizing 5mC or 5hmC, which did not allow absolute quantifications. Recent studies have started to weaken the model by which TET-mediated 5hmC is responsible for active DNA demethylation. Reduced representation bisulfite sequencing (RRBS) analysis estimated that around 75% of demethylated loci in the paternal pronucleus and around 87% of demethylated loci in the female pronucleus do so by a replication-dependent mechanism with or without the activity of TET3 (Guo et al., 2014a). Moreover, recent results have revealed that in mouse zygotes the loss of paternal 5mC and accumulation of 5hmC are temporally disconnected, with a first wave of DNA demethylation that is independent of 5hmC followed by zygotic *de novo* DNA methylation activities that trigger TET3-driven cytosine hydroxylation (Amouroux et al., 2016). Finally, it was recently shown that in mouse PCGs 5hmC was not a prerequisite for 5mC loss and that TET1 played a role in maintaining but not driving DNA demethylation (Hill et al., 2018). Thus, the conversion of 5mC to 5hmC might not implicit to active DNA demethylation.

Several mechanisms have been proposed for the role in the DNA demethylation process by TET-mediated cytosine hydroxymethylation. A replication-dependent passive

dilution of oxidized 5mC has been proposed due to the loss of 5hmC during preimplantation in a DNA replication-dependent manner (Inoue et al., 2011; Inoue and Zhang, 2011). Indeed, 5hmC may aid passive DNA demethylation even in the presence of DNMT1, which itself has low affinity for 5hmC hemimethylated DNA (Valinluck and Sowers, 2007). Accordingly, genome-scale DNA methylation maps for both the paternal and maternal genomes in mouse zygotes indicated that TET3 facilitates DNA demethylation largely by coupling with DNA replication (Shen et al., 2014).

It has also been proposed a DNA repair-mediated excision of modified 5mC as part of the active DNA demethylation process. Early studies have proposed that AID (activation-induced deaminase)/APOBEC (apolipoprotein B mRNA-editing enzyme complex) family of cytidine deaminases may theoretically deaminate 5hmC to generate 5-hydroxyuracil (5hmU) (Guo et al., 2011). The resulting 5hmU·G mismatch can be repaired by DNA glycosylases such as TDG and SMUG1 (Cortellino et al., 2011). However, subsequent studies showed that AID/APOBEC proteins exhibit no detectable deaminase activity against 5hmC in *in vitro* biochemical assays or in cells overexpressing these enzymes, challenging the biochemical plausibility of this proposed mechanism (Nabel et al., 2012). One potential explanation for the negligible activity of AID/APOBEC on 5hmC is that the relatively bulky steric size of 5-position substituent may have a significant negative impact on deaminase activity (Wu and Zhang, 2014).

Several evidences exist that the base excision repair (BER) pathway might play a crucial role in excising the modified cytosine base and replace it by an unmodified one. A similar mechanism was already observed in plants (Kohli and Zhang, 2013). For example, pharmacological inactivation of BER core components - APE1 (apurinic/apyrimidinic endonuclease) and PARP1 (poly(ADP-ribose) polymerase family, member 1) - resulted in zygotes with significantly higher levels of DNA methylation in the paternal pronucleus (Hajkova et al., 2010). 5mC is prone to hydrolytic deamination, resulting in the base thymine or uracil instead of cytosine, which leads to T:G mismatches and mutations in the genome. The two DNA glycosylases methyl-CpG binding domain 4 (MBD4) and thymine-DNA-glycosylase (TDG) were shown to be able to excise deamination products of 5mC, thereby creating an abasic site (Hardeland et al., 2001; Krokan et al., 2002; Zhu, 2009). Although both glycosylases harbour 5mC glycosylase activity, increasing evidence tend towards TDG as being

the main driver in excising modified 5mC. TDG was shown to interact with several transcription factors, chromatin modifiers and DNMTs (Dalton and Bellacosa, 2012). Additionally, TDG was inevitable for early embryonic development and T:G mismatches, arising from the from the deamination of 5mC or 5hmC, are known substrates of TDG (Cortazar et al., 2011; Cortellino, 2011; Guo et al., 2011). Furthermore, TDG robustly excises 5fC and 5caC *in vitro*, whereas no direct activity on excising C, 5mC and 5hmC could have been detected (He et al., 2011; Maiti and Drohat, 2011). However, recent studies fail to detect a role in DNA demethylation mediated by TDG in embryo since TDG deletion from the zygote has not effect on DNA demethylation (Guo et al., 2014a). The glycosylase implicated in zygotic DNA demethylation remains yet to be identified.

To summarize, two main pathways have been considered for the removal of oxidised 5mC forms, either TDG/BER dependent mechanisms or replication dependent dilution. However, alternative mechanisms have been proposed for the active loss of modified cytosines, including the ability of DNMT3A and DNMT3B to directly dehydroxylase 5hmC (Chen et al., 2012) and the direct decarboxylation of 5caC (Schiesser et al., 2012). Both reactions result in an unmodified C without the contribution of the BER machinery (Schiesser et al., 2012).

1.2 Gametogenesis

A Gamete is a cell that contains a haploid set of chromosomes and possess the ability to fuse with another gamete in sexually reproducing organisms in order to form an embryo. Each sex of sexually reproducing organisms produces a distinct type of gamete. The gamete produced by the female organism is called oocyte and the male counterpart is referred to as sperm. Both gametes differ in morphology, in cellular content, their maturation process and their reproductive capability.

The maturation process of sperm and oocytes is called gametogenesis, which is a multistep process that includes the proliferation and differentiation of primordial germ cells (PGCs) in order to form the mature gametes.

In mice, ~30-40 PGCs appear on embryonic development day 7.5 (E7.5) in the extra embryonic mesoderm (Ginsburg et al., 1990). PGCs further migrate to the genital ridges, the precursor of the gonads, and at around E10.5 ~1000 PGCs colonize the embryonic gonadal primordia (Saitou and Miyauchi, 2016). Germ cell derived transcription factors like BLIMP1, PRDM14, OCT4 or NANOG were shown to be detrimental for proliferation, migration and survival of the germ cell progenitors (Sánchez and Smitz, 2012). During the migration to the genital ridges, sex determination starts, whereby the “default” gender seems to be female. Differentiation to testes is only induced under the influence of the Y-linked gene Sry, since XX gonads lack the SRY they differentiate towards the uterine fate (Bowles and Koopman, 2010). Thus, the differentiation of germ cells into either oocytes or spermatozoa is not dependent on the set of chromosomes but depends rather on the differentiated form of the genital ridges. Therefore XY germ cells can give rise to oocytes when the genital ridges differentiated into ovaries and XX germ cells can differentiate to sperm in a XY environment (Bowles and Koopman, 2010). The male PGCs proliferate in the embryonic testes until they undergo mitotic arrest and further differentiate at E13.5 into prospermatogonia. The female PGCs in contrast are arrested in the first meiotic prophase where they remain until puberty before they terminally differentiate into mature oocytes.

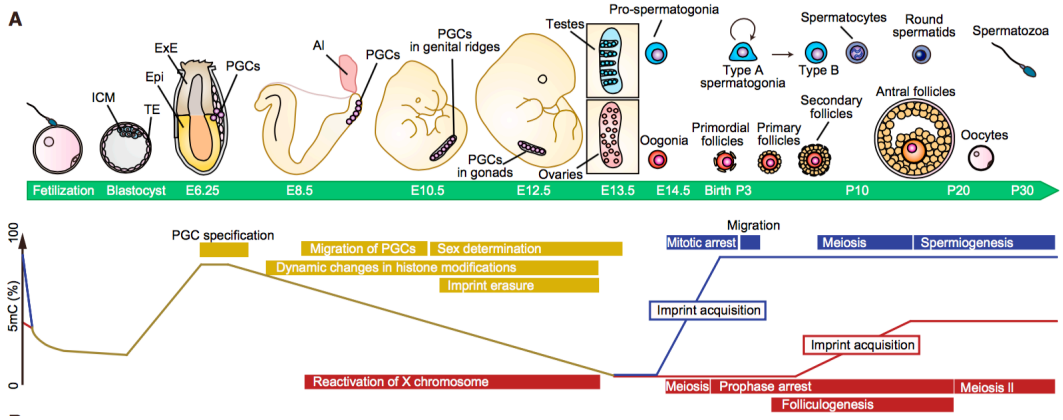

Figure 6. **Gametogenesis within the mouse life cycle.** PGC precursor cells are first observed around E6.0, differentiating in a small PGC founder population (20 cells) that arises around E7.25. They proliferate very fast and double within 16 hours, until they stop proliferation around E13.5. The following cycle of oocyte and spermatozoa maturation contains the onset of meiosis, where only one replicative cycle is followed by two meiotic divisions in order to form a haploid mature gamete. The timing and outcome of the meiotic cycle is sex-specific and results in 4 haploid mature spermatozoa constantly produced during lifetime of a male individual but results in only one mature oocyte and its polar bodies that are extruded prior to fertilization after puberty in the female organism. Folliculogenesis is a major factor driving oogenesis. Several epigenetic factors are also involved in successful gametogenesis that will be discussed in detail later. Taken from (Saitou and Miyauchi, 2016).

Spermatogonial stem cells (Type A spermatogonia) are present throughout the reproductive lifespan in males. After birth, spermatogonial precursors are constantly recruited for undergoing differentiation, leading to a constant production of mature spermatozoa. In contrast, in females, the oocyte progenitors are arrested in prophase of meiosis I in primordial follicles and they become activated in a cyclic manner after puberty during the female reproductive cycle, in doing so folliculogenesis plays a bearing role (**Fig. 6**). The onset and duration of the different phases in mitosis and meiosis differ substantially in spermatogenesis and oogenesis and will be discussed in more details in the following paragraphs.

Gametogenesis starts with a plethora of mitotic cycles leading to the proliferation of the germ cells. Mitosis starts after a replication cycle is finished; the two sister chromatids in one cell become separated in order to form two genetically identical daughter cells. Mitosis is subdivided in several phases, starting with the prophase right after replication, where the replicated chromosomes condense and the mitotic spindle is assembled. In the following stage the nuclear envelope is destroyed and the chromosomes are attached to the spindle apparatus. Once attached to the spindle, the chromosomes are arranged in the equatorial plane of the cell, where each sister chromatid assembles with the opposite pole of the cell. During anaphase the chromosomes separate by shortening the kinetochore microtubules and the cell poles start to diverge leading to a more stretched shape of the cell. The reduction of the kinetochore length

pulls the sister chromatids apart to the opposite poles of the cell. Telophase marks the end of mitosis when the daughter chromosomes arrive at the spindle poles and a new nuclear envelope is reassembled. The stretched shape of the cell facilitates the constriction of the cell that is driven by actin and myosin filaments. Cytokinesis divides the cytoplasm and leads to the formation of two daughter cells containing one nucleus with a diploid set of chromosomes each (Alberts et al., 2008).

Meiosis is a highly specialized cell division process in sexual reproducing species only taking place during gametogenesis (**Fig. 7**). Pre-meiotic S-phase produces gamete precursors with a diploid set of chromosomes. Completion of S phase prior to meiosis takes longer than an usual S phase in mitosis. The reason might be the establishment of chiasmata that pair the homologous chromosomes to perform meiotic recombination and accurately separate the homologous chromosomes during meiosis (Handel and Schimenti, 2010). The prophase of the first meiotic division is subdivided into different sub-stages according to the structure and configuration of the chromosomes. In the leptotene stage, the homologous chromosomes are aligned but not yet paired. In this time, a scaffold complex is built consisting of several proteins, including SPO11, Mre11, Rad50 and NBS1 that induces programmed DNA double strand breaks necessary for the following meiotic recombination. Activation of the homologous repair and the recombinase machinery is triggered by these breaks and is an essential step for the further segregation of the chromosomes.

At the zygotene stage, the pairing of the chromosomes is completed and synapsis, the correct positioning of the chromosomes is initiated. Synapsis and recombination are completed in pachytene stage. Finally, the diplotene stage with desynapsis and the condensation of the chromosomes marks the end of the prophase (Handel and Schimenti, 2010). Meiotic recombination ensures genetic variety within the population (Handel and Schimenti, 2010). Missing crossover in the first meiotic division can lead to inaccurate separation of the chromosomes, which subsequently might result in aneuploidy. In human, gametic aneuploidy is the most common form of aneuploidy and mostly arises during the first meiotic division in oogenesis. Male and female meiotic division results in sex-specific outcomes. In male organisms, the first meiotic division leads to two secondary spermatocytes whereas only one secondary oocyte with a polar body is formed in females (**Fig. 7**).

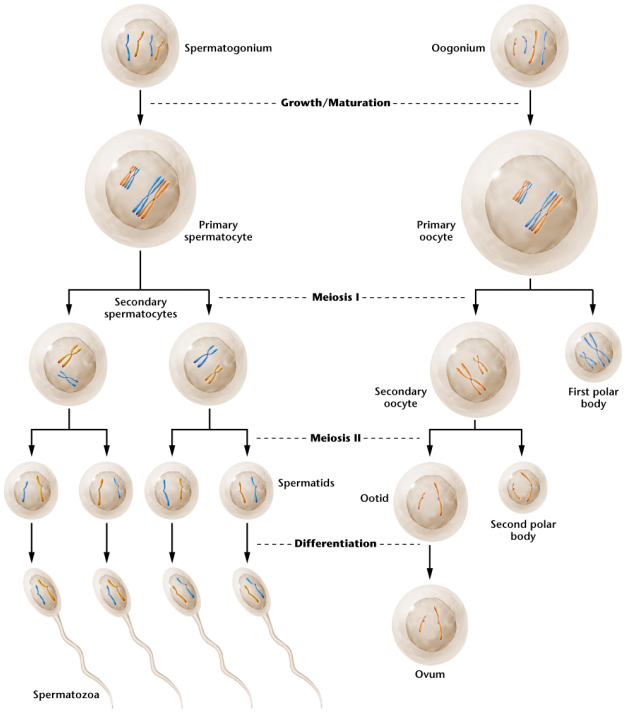

Figure 7. **Gametogenesis.** PGCs first undergo sex determination followed by several mitotic cycles. Spermatogonia further differentiate to primary spermatocyte while entering the meiotic cycle. Primary spermatocytes further differentiate into two diploid secondary spermatocytes and result after the second meiotic cycle in four haploid spermatids that undergo spermiogenesis, the last maturation step. Primary oocytes are arrested in prophase of meiosis I, resuming meiosis leads to the extrusion of the first polar body and during the second meiotic cycle a second polar body.

The first meiotic division is followed by a second meiotic division, where the sister chromatids loosen theirs contacts and become separated. The onset and the outcome of the second meiotic division are sex-specific. In males, this second meiotic division occurs directly after the first one and results in four haploid spermatids. In deep contrast stands the female organism, where the second meiotic division is performed in the context of the female reproductive cycle starting with puberty. The second meiotic division in females results in a haploid oocyte and a second polar body that is extruded during maturation (Handel and Schimenti, 2010) (**Fig. 7**). The following paragraphs describe the sex specific maturation, oogenesis and spermatogenesis, of gametes.

1.2.1 Oogenesis

In mice, around E13.5, the gonads are colonized and female PGCs undergo several mitotic divisions with an incomplete cytokinesis that results in the formation of "germ cell cysts" or "germ cell nests" (Pepling, 2006). Once the nests are established, mitosis is stopped and meiosis is induced prior to follicle formation.

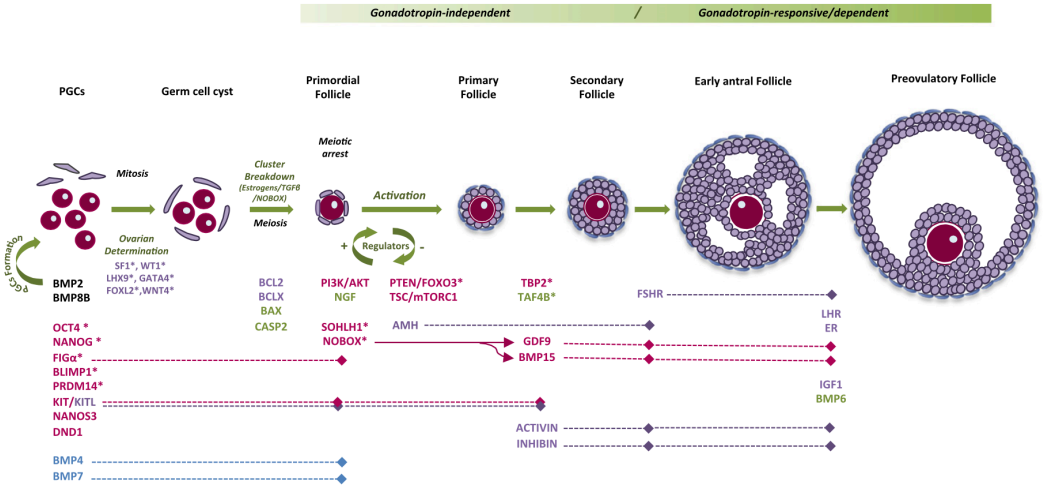

Figure 8. Oogenesis and folliculogenesis. Oogenesis starts with the colonization of the genital ridges with oogonia. Pre-mature oocytes are arranged in nests. During the formation of the primordial follicle, the oocyte stays meiotically arrested. Several factors reactivate the folliculogenesis during the female reproductive cycle. When an antral cavity is formed, the follicle matures in a gonadotropin dependent manner until the mature oocyte is released from the ovulatory follicle. Taken from (Sánchez and Smitz, 2012).

All the oocyte precursor cells start their meiotic program synchronously to become primary oocytes that further commit lineage specification according to the female-lineage specific program (Ginsburg et al., 1990; Handel and Schimenti, 2010). Start of meiosis is indicated with the start of the prophase, where homologous chromosomes pair and recombination or crossing over takes place. In the female reproductive tract, meiotic I prophase is arrested until puberty, when the oocytes start to mature within the female reproductive cycle induced by the luteinizing hormone (LH) surge that marks the start of the final maturation step by inducing ovulation (Handel and Schimenti, 2010; Hunt and Hassold, 2008). The later oocytes are still assembled in nests, which break down during meiotic arrest, and the oocytes become surrounded by pre-granulosa cells initiating primordial follicle (PMF) formation (**Fig. 8**). Folliculogenesis is a further milestone in oogenesis. During the nest breakdown many oocytes undergo apoptosis. Each PMF contains an oocyte arrested at the diplotene stage of the prophase of the first meiotic division that depicts the entire pool of germ cells during the whole female reproductive lifespan (Sánchez and Smitz, 2012). The PMFs become activated by the signalling of the PTEN (phosphatase and tensin homolog deleted on chromosome 10)/PI3K (phosphatidylinositol 3 kinase) pathway, that is involved in several cellular processes and is active in primordial and primary follicles (Cantley, 2002). Disturbances in the PI3K pathway either lead to cell cycle arrest and apoptosis or alterations in the activation of PMFs (Castrillon et al., 2003; Liu et al., 2006). PMFs are constantly recruited in waves to undergo folliculogenesis and further devel-

op into secondary pre-antral follicles, as a response to chemical signalling pathways of the oocytes and also of the surrounding cells. The anti-Mullerian hormone (AMH) is controlling the amount of PMFs being activated for further maturation and the ones that stay silent. Morphological changes occur on the surrounding flattened granulosa cells when PMFs develop to primary follicles, which are surrounded by single-layered cuboidal granulosa cells (Sánchez and Smitz, 2012). The development of the pre-antral follicles, primordial, primary to the secondary follicular stage, seems to be gonadotropin (FSH, LH) independent (**Fig. 8**) and rather depend on locally secreted factors. Pre-antral follicles further develop into antral follicles this goes along with significant morphological changes like the proliferation of pre-antral follicle granulosa cells, an increase in follicular size and the formation of an antral cavity (**Fig. 8**). Once the antral cavity is formed and the granulosa cells are differentiated into cumulus and mural cells, the oocyte receives the capacity of going further in oogenesis, by resuming meiosis. The further antral stages of folliculogenesis and the ovulation are gonadotropin dependent, at which only a small amount of these antral follicles responds to the signalling of the pituitary hormones, the follicle-stimulating hormone (FHS) and the luteinizing hormone (LH) and start growing to the dominant ovulatory follicle while the rest of the follicles undergoes programmed cell death (Pepling and Spradling, 2001). The remaining somatic cells after ovulation undergo a last step of differentiation by forming the corpus luteum (CL). The CL produces progesterone that is inevitably needed to maintain the presumable pregnancy. Follicle formation seems to be species-specific, in humans the formation of follicles is initiated prior birth, whereas in mice follicles are formed right after birth (Pepling, 2006).

1.2.2 Spermatogenesis

Spermatogenesis is the maturation of spermatozoa derived from PGCs (**Fig. 9**). Spermatogonial stem cells are rare (0.03 % of all germ cells) and represent the founder population for the following spermatogenesis process (Tegelenbosch and de Rooij, 1993). In male mammals, spermatogonial stem cells are present from birth onwards, therefore mature spermatozoa can be continuously produced throughout the reproductive lifetime in the male organism (Handel and Schimenti, 2010).

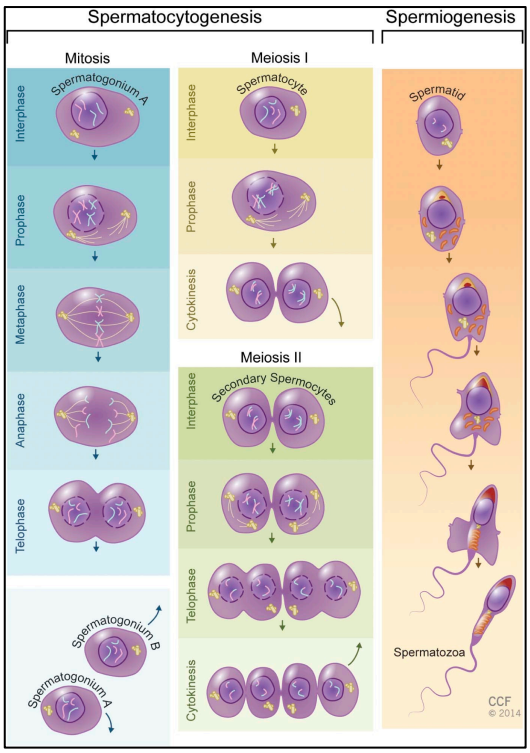

Figure 9. **Spermatogenesis.** PGCs undergo several mitotic divisions resulting in type A and B spermatogonia. Type A spermatogonia represent the stem cell pool, renewing the spermatogonial stock, whereas type B spermatogonia enter the meiotic cycle undergoing differentiation. The first meiotic cycle results in two diploid daughter spermatocytes, the result of the second meiotic division is four haploid secondary spermatocytes that further mature during spermiogenesis and are released to the lumen as mature spermatozoa. Taken from (Gunes et al., 2015).

Spermatogenesis is divided into three phases. First, the proliferative phase, within which all the primitive germ cells (spermatogonia) undergo several mitotic divisions, resulting in pro-spermatogonia arrested in mitosis in the semniferous tubules. During this phase paternal epigenetic marks, such as imprints, are established (Kato, 2007; Kobayashi et al., 2013; Kubo et al., 2015; Seisenberger, 2012). Three types of spermatogonia exist. Type A spermatogonia is the most primitive undifferentiated stage and contains almost no heterochromatin in contrast to intermediate type spermatogonia that contain some heterochromatin and Type B spermatogonia that harbour large amounts of heterochromatin. Type A spermatogonia represent the stem cell pool, having stem cell properties such as self-renewal capacity and they are also able to differentiate into intermediate type spermatogonia.

The second phase of spermatogenesis is the meiotic phase. The first meiotic division is reductive and separates homologous chromosomes, producing two secondary spermatocytes (Hann et al., 2011). The second meiotic division occurs immediately after the first division resulting in an equatorial division and the separation of sister chromatids. The net result of this process is the production of four haploid spermatids. Meiosis in males is initiated at puberty during prophase of meiosis I when homolo-

gous chromosomes pair and synapse. Prophase I is divided into four stages based on the morphology of the XY bivalent and the synaptic progression of the autosomal bivalents. The meiotic phase is followed by the finale maturation step called spermiogenesis (Chocu et al., 2012). Spermiogenesis goes along with drastic chromatin rearrangements and structural changes. The process is divided into four phases: Golgi phase, the cap phase, formation of the tail and the maturation stage (Gunes et al., 2015). The head and axoneme formation is characterised by the Golgi phase. During this phase, spermatozoal DNA undergoes packaging with specific nuclear proteins called transition proteins, which will be then replaced by protamines. During the cap phase, the elongation of spermatid and acrosomal cap formation takes place, followed by the elongation of one of the centrioles by manchette, which is required for the differentiation into the tail. The last stage is the phagocytosis of residual bodies by Sertoli cells.

Spermatozoa are small cells with only a small amount of cytoplasma that carry the densely packed spermatozoal DNA. Sperm chromatin packaging is an important step in the maturation of spermatids, however the exact mechanism remains largely unknown (Rathke et al., 2014). To reduce the volume of the sperm chromatin, the histone-bound chromatin of the progenitor cells undergo replacement of the histones with protamines. Prior to protamination, the histones are replaced by specific nuclear proteins, transition protein 1 and 2 (Steger et al., 2001). In the later progress of maturation, these proteins will then be replaced by protamines. Protamines are 5-8 kDa arginine-rich proteins and are expressed during late stage spermatogenesis in the sperm head (further details will be found in **1.4.3**). The resulting highly condensed structure of chromatin has been proposed to protect the sperm chromatin during its transition from the male to the female genital tract and to a certain extent from oxidative damage or even mechanical stress (Hwang and Lamb, 2012; McKAY et al., 1986; Meistrich et al., 2003; Rooney and Zhang, 1999; Torregrosa et al., 2006).

In the next step of spermiogenesis further morphological changes take place, such as the reduction of the cytoplasma, the formation of the sperm tail through elongation of one of the centrioles and the formation of an acrosomal cap that contains enzymes necessary for the fusion with the zona pellucida of the oocyte (**Fig. 10**). The formation of the tail is indispensable for the progressive motility of the spermatozoa, which is needed to cover big distances within the female reproductive tract. The tail rises from one of the centrioles at the opposite site of the acrosome. The flagellum

consists of four different parts: (1) the neck that contains two centrioles; (2) the mid-piece that is surrounded by mitochondria, providing energy; (3) the principle piece consisting of fibre elements and (4) the end-piece. The sperm head contains the highly condensed chromatin that is released to the oocyte after fertilization. In the last maturation step, phagocytosis occurs in order to phagocyte the residual bodies of Sertoli cells (Zini and Agarwal, 2012).

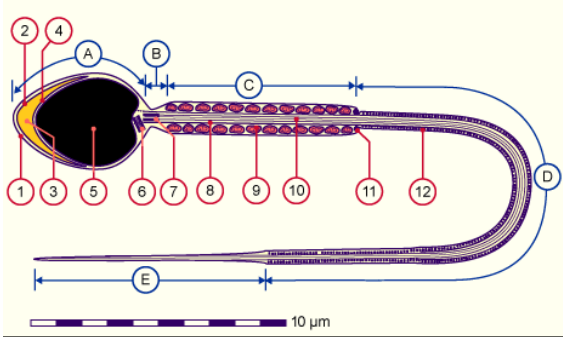

Figure 10. Structure of a mature sperm. 1) Plasma membrane 2) Outer acrosomal membrane 3) Acrosome 4) Inner acrosomal membrane 5) Nucleus 6) Proximal centriole 7) Rest of the distal centriole 8) Thick outer longitudinal fibres 9) Mitochondrion 10) Axoneme 11) Anulus 12) Ring fibre A) Head B) neck C) Mid piece D) Principal piece E) Endpiece. Taken from (http://www.embryology.ch/anglais/cgametogen/spermato05.html).

1.3 Embryogenesis

Fertilization refers to the fusion of the two haploid gametes that results in a zygote with a diploid set of chromosomes. Fertilization is a multifactorial process, involving the migration of the sperm through the female genital tract to the oviduct, where fertilization takes place in mammals, followed by sperm penetration into the oocyte. After fertilization, the sperm chromatin undergoes drastic structural and epigenetic changes, such as the replacement of the protamines with maternally provided and newly synthesized histones or the active loss of DNA demethylation (the details of this process is described in **1.5**) (Hwang and Lamb, 2012; Meistrich et al., 2003). Although both the gametes provide their own haploid genome for the formation of the zygote, all additional components such as RNAs and proteins derive from the maternal oocyte (Zhou and Dean, 2015).

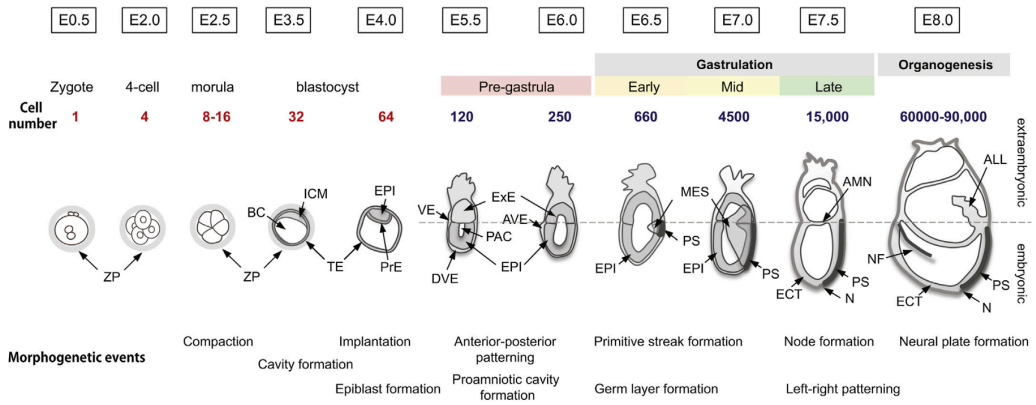

Figure 11. Embryogenesis in mice. After fertilization the zygote is formed. During the first several cell cleavages, the size of the embryo is not increased. The formation of the blastocyst goes along with several morphological changes and consists of cells of three cell lineages. Gastrulation is an important step in establishing the body plan of the growing embryo and is initiated after implantation. Following gastrulation the organs are formed during organogenesis. Taken from (Kojima et al., 2014).

During the first cleavage stages, embryos show no increase in cell size. This results in a distribution of the initial amount of cytoplasm to the daughter cells during every cell division and the female factors are supposed to drive this development. The blastomeres undergo severe morphological changes like cell polarization, flattening and gap junction formation and at a certain time point (species specific) the embryonic genome becomes activated (**Fig. 11**) (Zhou and Dean, 2015).

The last stage in pre-implantational embryo development is the formation of the blastocyst. The blastocyst is characterized by the formation of a blastocoelic cavity that is formed around 16-32 cell stage and the allocation of the cells to the three cell lineages

(Motosugi et al., 2005). The blastocyst consists of three different cell types: trophectoderm (TE), the epiblast (EPI) and the primitive endoderm (PrE) (**Fig. 11**). Lineage specification for the future trophectodermal cells already takes place at the 4th and 5th cell division and they become connected by the formation of tight junctions and desmosomes. PrE cells specify during the 5th and 6th division (Aiken et al., 2004; Morris et al., 2010). While the blastocyst hatches out of the zona pellucida, the ICM forms two distinct cell populations. The most ventral layer becomes flat, separates from the rest of the ICM cells and forms the hypoblast. The hypoblast grows further along the trophectodermal cells within the inside of the blastocyst and counts as the primitive endoderm. The primitive endoderm and the throphectodermal cells give rise to the extraembryonic tissue, such as placenta (Tam and Loebel, 2007). The dorsal layer establishes the epiblast. These cells derive from the ICM and give rise to the three germ layers, endoderm, mesoderm and ectoderm (Oestrup et al., 2009).

After fertilization and prior to implantation, the embryo is transported from the oviduct to the uterus, where the embryo becomes implanted. After implantation, the pre-implantational epiblast undergoes morphological changes that lead to the formation of a post-implantational epiblast (**Fig. 11**). Subsequently, coordinated cell movements during gastrulation form distinct germ layers that differentiate into the various cell types of the tissue in a mature organism. Gastrulation is an important step during embryogenesis, placing the precursor cells in the correct place in the growing embryo to initiate correct organogenesis. Gastrulation starts with a local cellular invasion, forming the primitive streak (Kojima et al., 2014). The timing of the onset of gastrulation widely varies among species. For example the onset of the first cell cycles in *Xenopus laevis* (35 minutes post-fertilization (pf)), *Danio rerio* (15 minutes pf) and *Drosophila melanogaster* (15 minutes pf) leads to the initiation of gastrulation within hours after fertilization. In contrast, mammals have long cell cycles, where the first cleavage occurs only days after fertilization with the initiation of gastrulation 5-6 days after fertilization (Lee et al., 2014). After implantation the embryo undergoes dramatic changes in shape and size, whereby the volume increases about 40 fold due to the formation of tissue establishing the future extra-embryonic ectoderm (Tam and Behringer, 1997).

Organogenesis takes place at the end of gastrulation and is completed at the time of birth. Organogenesis-related genes initiate processes like vasculogenesis, organ formation, where the three germ layers give rise to the dedicated organs and neurogene-

sis (**Fig. 11**). Overall, organogenesis shifts the expression pattern away from pluripotency towards a more differentiate expression program.

1.3.1 Embryonic genome activation

Maternal to zygotic transition is an embryonic reprogramming event where the maternal transcription program is erased and a new embryonic program is established. The process of embryonic genome activation (EGA) is a stepwise process that requires structural and epigenetic changes on the chromatin. The gametes themselves are not (paternal) or only reduced (maternal) transcriptionally active. The start of embryonic genome activation differs among species, although embryonic genome activation displays a very important point during early embryonic development (Lee et al., 2014).
Zygotic genome activation in mice is the earliest amongst vertebrates and is seen from 1-cell stage on (Hamatani et al., 2004). Embryonic genome activation in pigs and cattle was shown to start not earlier than 4-cell stage (Bjerregaard et al., 2007; Braude et al., 1988; Graf et al., 2014). EGA is not even conserved within ruminants, since in sheep it was shown to start earliest at 8-cell stage (Crosby et al., 1988).

Mammalian embryonic genome activation is a stepwise process, whereby an earlier minor (800 genes) genome activation is followed by a major (3500 genes) wave of genome activation. The human genome is also activated in a minor wave at 1-cell stage followed by the major wave at 4-8 cell stage (Lee et al., 2014). There exist two general models of embryonic genome activation, the first the “nucleocytoplasmic (N/C) ratio” model claiming that the increase in nuclear material relative to the constant cytoplasm volume allows transcriptional repression, therefore these mostly maternal derived factors must be erased before transcription starts (Newport and Kirschner, 1982a, b). The second model is suggested as being a “maternal clock” that is independent on cell divisions but is triggered through the quantity and activity of maternal factors that, when reaching a certain level, enable transcription (Howe et al., 1995).
Independently of these models, the EGA depends on cell cycle regulation, chromatin structure and the activity of transcription factors. It was demonstrated in Xenopus and Drosophila that the cell cycle establishes a hierarchy of zygotic activated genes by transcribing short genes during the first short cell cycles, whereas longer genes are transcribed later in development.

The timing of EGA also depends on the chromatin state (see also **1.5**). Upon fertilization, the protamines in the paternal pronucleus are rapidly replaced by histones provided by the oocyte. These newly inserted histones contain transcriptional permissive histone marks, like H4 hyperacetylation, H3K9me and H3K27me. It has been proposed that the chromatin structure of the paternal genome (uncondensed relative to the maternal pronucleus and containing histone modified with active histone marks) might be the reason why, prior to the fusion of both genomes in mid/late S-phase, the paternal pronucleus contributes to the minor zygotic genome activation whereas the maternal pronucleus remains transcriptionally silent (Lee et al., 2014). Histone exchange plays also a major role during embryogenesis, since the gametic histones of the parental chromatins are replaced by somatic histone variants during replication. Transcription factors are clearly playing an essential role during EGA, by binding to repressed chromatin and thus inducing remodelling that leads to open chromatin and the binding of the transcription machinery to the promoters (Lee et al., 2014). All in all, EGA is a multifactorial process that needs to be highly coordinated to ensure an appropriate development of the embryo.

1.4 Chromatin and epigenetic modifications in gametes

In mice, primordial germ cells (PGCs), the precursors of both sperm and oocyte, arise from the extra-embryonic mesoderm at E7.25 (Saitou et al., 2002). Human PGCs (hPGCs) are specified around E12–E16 (developmental week 2) (von Meyenn et al., 2016). The nascent PGCs are successors of epiblast cells and as such they acquired layers of epigenetic information including DNA methylation and numerous histone modifications in a manner similar to other epiblast cells that will give rise to the soma (Hajkova, 2011). For example, early PGCs harbour mono-allelic parent-of-origin-specific differential methylation marks at imprinted genes. Therefore, PGCs must re-set their epigenome in order to suppress the somatic gene expression, including the erasure of the inherited imprinting marks followed by the establishment of new ones appropriate to their own sex. Epigenetic reprogramming involves erasure of DNA methylation, changes in histone modifications and histone variant composition as well as major changes in the nuclear architecture (**Fig. 12**).

Around E10.5-E11.5, following migration into the developing gonad, PGCs undergo genome-wide DNA demethylation, which includes erasure of genomic imprints as well as reactivation of the inactive X chromosome (Xi) in female embryos. At the time of sex determination in the fetal gonads, which in mice occurs at around E12.5, global DNA methylation levels are very low, and the methylomes of male and female primordial germ cells (PGCs) are very similar (Guibert et al., 2012; Seisenberger et al., 2012). This is the point where the epigenome reaches its most ‘naive’ state during development and represents the starting platform for the acquisition of new epigenetic information and genomic imprints that will be transmitted to the next generation through mature gametes (Hajkova, 2011). Establishment of *de novo* methylation proceeds in very different manners in the male and female germ lines. In the female germ line, cell division ceases and maternal imprints are asynchronously restored in the absence of any DNA replication, during post-natal oocyte growth (Lucifero et al., 2004; Obata and Kono, 2002). In male germ cells, *de novo* methylation of paternally imprinted genes is initiated at around E14.5 but occurs gradually and is only completed postnatal (Davis et al., 2000; Li et al., 2004).

Epigenetic modifications established during gametogenesis regulate transcription and other nuclear processes in gametes, but also have influences in the zygote, embryo and postnatal life (Stewart et al., 2016).

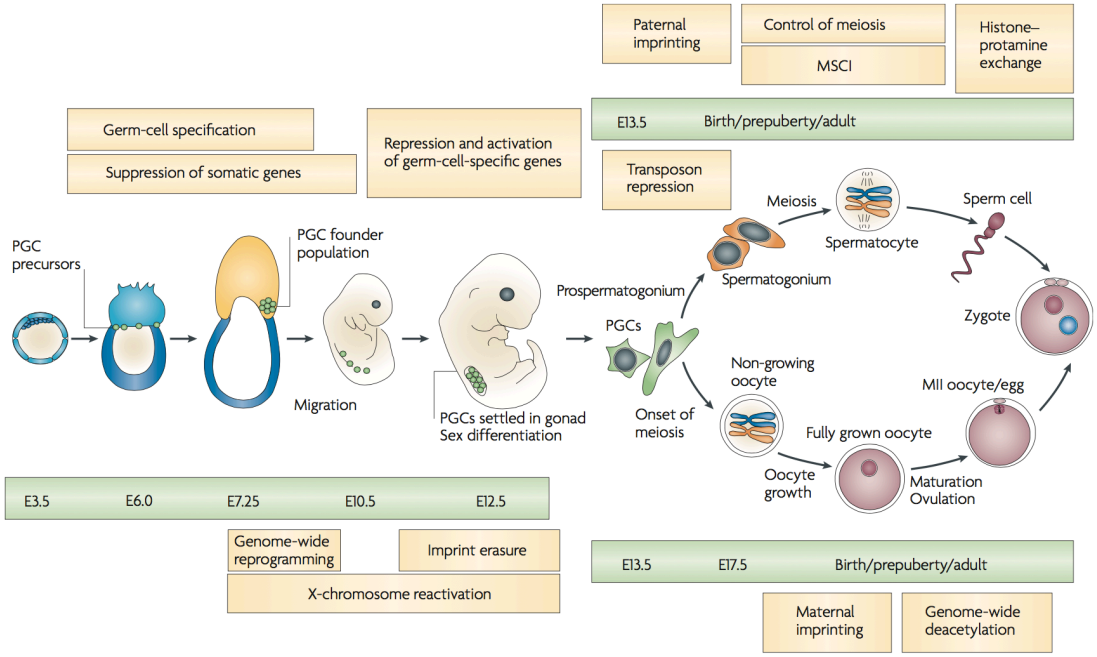

Figure 12. Germ cell development and the accompanying epigenetic modifications. PGC precursors migrate from the embryonic ectoderm to the future gonads. During this migration the somatic epigenetic pattern become erased, including imprint erasure and X-chromosome reactivation. Once the sex differentiation is performed, the respective gamete progenitors undergo sex-specific re-establishment of epigenetic marks. Taken from (Sasaki and Matsui, 2008).

1.4.1 Regulation of DNA methylation in gametogenesis

Studies in mice revealed that at E11.5, soon after their entry into the genital ridges, PGCs start to undergo pronounced changes in their nuclear architecture connected with the decondensation of heterochromatin, loss of chromocentres and increase in nuclear size (Hajkova et al., 2008). It has been suggested that epigenetic reprogramming in PGCs is divided in an early and a late phase. The early phase takes place during proliferation and migration of the PGCs to the genital ridges, whereas the late phase is a post-mitotic phase that starts once PGCs arrived at the genital ridges (Seisenberger, 2012; Vincent et al., 2013) (**Fig. 13**).

In the case of DNA methylation, the initial loss takes place before or during PGC migration to the genital ridges and seems to be due to dilution within the numerous replicative cycles. In contrast, sequences that carry long-term epigenetic memory (imprints, CpG islands on the X chromosome, germline-specific genes) only become demethylated upon entry of PGCs into the gonads (E11.5 and E12.5) (Guibert et al., 2012; Hajkova et al., 2002; Ito et al., 2010; Lane et al., 2003; Seisenberger, 2012) (**Fig. 13**).

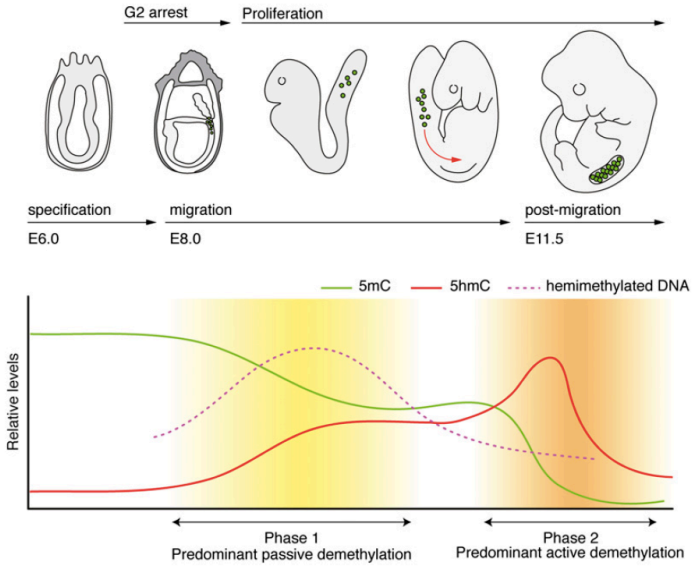

Figure 13. Biphasic demethylation dynamics in mouse PGCs. PGCs harbour high levels of somatic 5mC (green). During migration the 5mC levels are diluted by several replication cycles. After migration, the PGCs undergo a predominant active DNA demethylation cycle. Taken from (Messerschmidt et al., 2014).

Other studies, however, have suggested that the demethylation is taking place at the same time as the global demethylation wave (Kagiwada et al., 2013; Lee et al., 2002). Downregulation of *de novo* and maintenance DNA methyltransferase machineries (DNMT3A, DNMT3B and UHRF1) also cooperates in the global loss of DNA methylation (Kagiwada et al., 2013; Kurimoto, 2008; Seisenberger, 2012; Seki, 2005; Yabuta et al., 2006). Consequently, the 70% CG methylation found in the somatic precursor population of an embryo at E6.5 drops to approximately 5% methylation content in PGCs at E13.5 (Seisenberger et al., 2012). Because of the doubling time of post-migratory PGCs (approx. 16 h), it has been proposed that this phase of epigenetic reprogramming should include an active DNA demethylation process (Hajkova et al., 2002). Interestingly, during this process the upregulation of key factors involved in the base excision DNA repair (BER) pathway has been observed (Hajkova, 2010). A possible involvement of DNA deaminases AID or APOBEC1 in the active DNA demethylation has been proposed. However, the genetic ablation of *Aid* has only limited impact on the 5mC levels in PGCs and the expression of *Aid* is detectable only after the wave of DNA demethylation (Popp et al., 2010). Thus, AID-dependent deamination might not be the driving force in demethylating these sequences (Messerschmidt et al., 2014). Moreover, the expression of the mismatch glycosylase *Tdg* is not detectable and loss of *Mbd4* has no impact on germline development or fertility. The presence of 5hmC during the wave of DNA demethylation in PGCs let propose a role of

TETs in this process. However, recent results revealed that sequences depleted of 5hmC in E10.5 and E11.5 PGCs still underwent demethylation, indicating that loss of DNA demethylation can be independent of 5mC oxidation to 5hmC (Hill et al., 2018). These data were supported by the fact that 5mC was depleted in E13.5 PGCs from both *Tet1*$^{-/-}$ mice and wild-type mice. Interestingly, PGCs from *Tet1*$^{-/-}$ mice showed that 5mC levels were higher at specific DNA regions in E12.5 and E14.5, suggesting that TET1-mediated 5mC oxidation causes locus-specific DNA demethylation in PGCs after global DNA demethylation. Of note, was the specific presence of 5hmC on a class of genes, thereafter named germline reprogramming responsive (GRR) genes, which were activated in both sexes at E10.5. The observation that (1) TET1 associates with the promoters of GRR genes (Yamaguchi et al., 2012), (2) upregulation of GRR genes was less marked in PGCs from *TET1*$^{-/-}$ mice and (3) the difference in GRR gene expression was detected before any differences in the DNA methylation of these genes, strongly suggests that TET1 might activate transcription independently of DNA methylation. These results were also consistent with previous observations showing that deficiency of TET1 did not greatly affect the genome-wide demethylation in PGCs, but lead to defective DNA demethylation and decreased expression of a subset of meiotic genes (Yamaguchi et al., 2012). Together these results revealed that gonadal epigenetic reprogramming entails complex erasure of epigenetic information. However, how active DNA demethylation is achieved remains elusive.

At the time of sex determination in the fetal gonads, which in mice occurs at E12.5, global DNA methylation levels are very low, and the methylomes of male and female PGCs are very similar (Guibert et al., 2012; Seisenberger, 2012). Sex differentiation includes the establishment of the sex-specific epigenetic marks and *de novo* methylation establishment proceeds in very different manners in the male and female germ lines (Saitou et al., 2012; Sasaki and Matsui, 2008). Accordingly, the methylation content varies between the two mature gametes: 40% for oocytes, and approximately 80% for sperm (Kobayashi et al., 2012; Popp et al., 2010; Shirane et al., 2013). Interestingly, recent analyses of the cattle sperm methylome detected several megabase long domains of centromeric satellite clusters that were hypomethylated, suggesting that these regions might play a role during meiosis and their rapid transcriptional activation after fertilization (Zhou et al., 2018).

At E13.5, after the epigenetic erasure process, female gonocytes are arrested in meiot-

ic prophase, the state of the genome that constitutes the beginning of oogenesis (Dokshin et al., 2013). Therefore, the oocyte methylome is solely reflective of *de novo* methylation events. Oocyte growth and maturation are initiated postnatally in females, coincident with *de novo* DNA methylation through the combined and coordinated activities of DNMT3A/DNMT3L (Lucifero et al., 2007; Smallwood et al., 2011). Deletion of *Dnmt3a* or *Dnmt3l* in oocytes prevents oocyte-specific methylation of imprints and the resultant embryos cannot develop beyond mid-gestational stage due to abnormal expression of imprinted genes (Hata et al., 2002; Kaneda et al., 2010). However, the mechanisms leading to step-wise reacquisition of DNA methylation in oocytes remain elusive. High-resolution, genome-wide DNA methylation profiles have revealed that DNA methylation is established immediately prior to ovulation of the metaphase II (MII) oocyte (Smallwood et al., 2011; Smith et al., 2012). Among those genes with significant CpG-island methylation was the *de novo* DNA methyltransferase family member *Dnmt3b*, which, like *Dnmt1*, is transcriptionally silent at this time. This observation typifies an ever-growing concept where epigenetic modifiers are regulated by their cognate marks themselves (Dean, 2014).

In the male germline, *de novo* methylation is initiated at E13.5, in prospermatogonia or gonocytes that are arrested in mitosis. At E16.5, male PGCs already acquired 50% of the global DNA methylation (Kota and Feil, 2010). The male specific DNA methylation pattern is completely set at birth. Following methylation establishment, male gametes experience a proliferative burst before entering meiosis and beginning the process of differentiating into sperm. Therefore, the mature sperm methylome is kept throughout the multiple replication cycles right before the sperm progenitors enter meiosis and its methylome is a product of DNA methylation maintenance that must operate faithfully from birth in male mice (Davis et al., 2000; Henckel, 2009; Stewart et al., 2016). Unlike in oocytes, loss of DNA methylation during spermatogenesis causes infertility accompanied by a profound reduction in testis size (Stewart et al., 2016). Although the precise role of each methylation mark in the process of spermatogenesis is still unknown, studies of mutant mice demonstrated the involvement of methylation in genome imprinting and repression of transposable elements. Establishment of DNA methylation in male germ cells is initiated at repetitive sequences by a testis-specific class of small RNAs called PIWI-interacting RNAs (piRNAs), which derive from repeat sequences and are implicated in direct methylation and silencing of transposable elements in the male germline (Iwasaki et al., 2015). piRNAs appear to

act upstream of DNMT3L, as loss of DNMT3L does not affect piRNA expression, while piRNA deficiency leads to loss of methylation at transposable elements (Aravin et al., 2008; Kuramochi-Miyagawa et al., 2008). Similarly to oocytes, establishment of DNA methylation in sperm is primarily due to the activity of DNMT3A and its co-factor DNMT3L. Lack of *Dnmt3a* or *Dnmt3L* resulted in a global reduction in DNA methylation (Shirane et al., 2013). Moreover deletion of *Dnmt3a* but not *Dnmt3b* impaired spermatogenesis (Kaneda et al., 2004). DNMT3A mainly methylates the *H19* and *Dlk1/Gtl2* DMRs and a short interspersed repeat SineB1. Both *Dnmt3a* and *Dnmt3b* were shown to be involved in the methylation of *Rasgrf1* DMR and long interspersed repeats IAP and Line1 whereas only *Dnmt3b* was required for the methylation of the satellite repeats (Kato et al., 2007). Finally recent results have identified DNMT3C to play a crucial role in specifically methylating retrotransposons during gametogenesis in mouse (Barau et al., 2016). Abnormal sperm DNA methylation patterns have been associated with human subfertility, including aberrant methylation of both imprinted and non-imprinted genes in oligospermic men. Incorrect DNA methylation of the DAZL promoter in CpG island has also been associated with defective human sperms (Navarro-Costa et al., 2010). Analysis of spermatozoa from oligozoospermic men showed the occurrence of hypermethylation at several maternal DMRs or hypomethylation of H19 and intergenic-DMR was increased, particularly in patients with ejaculation volumes of $<10\times10^6$/ml (Dada et al., 2012; Pacheco et al., 2011). Therefore, in a clinical context, understanding the mechanisms underlying DNA methylation might be particularly important in order to develop therapeutic strategies for male genital system diseases caused by abnormal sperm DNA methylation.

1.4.2 Histone modifications in PGC reprogramming

In pre-migratory and migratory germ cells, histone modifications undergo orderly and extensive changes (Seki, 2005). Immunohistochemistry studies have shown that around E8.0 germ cells concomitantly and significantly reduce H3K9 dimethylation (H3K9me2) and DNA methylation. By contrast, at E8.5-9.0, germ cells substantially increase the levels of H3K27 trimethylation (H3K27me3), and maintain this state until at least E12.5. H3K4 methylation (H3K4me3) and H3K9 acetylation (H3K9ac), modifications associated with transcriptionally permissive/active chromatin, are similar in germ and surrounding somatic cells but germ cells transiently increase these

marks sharply upon their entry into the genital ridge. H3K9 trimethylation, a hallmark of centromeric heterochromatin, is kept relatively constant (Seki, 2005). The analysis of the genome-wide histone modification states has been limited since PGCs are specified in small numbers (~40) and are refractory to proliferation *in vitro,* making them intractable to quantitative analysis. The establishment of an *in vitro* system that recapitulates germ cell development made possible a better understanding of histone modifications changes in the PGC specification pathway in mice. This system is based on the induction of embryonic stem cells (ESCs) to form epiblast-like cells (EpiLCs), a cellular state highly similar to pre-gastrulating epiblasts but distinct from epiblast stem cells (EpiSCs). EpiLCs can be then induced into PGC-like cells (PGCLCs) with capacity for both spermatogenesis and oogenesis (Hayashi et al., 2011; Kurimoto and Saitou, 2015). This *in vitro* system allowed the dissecting of regulatory networks of the germline epigenome (Kurimoto and Saitou, 2015). For example, EpiLCs contain abundant bivalent gene promoters characterized by low H3K27me3, indicating a state primed for differentiation. PGCLCs initially lose H3K4me3 from many bivalent genes but subsequently regain this mark with concomitant upregulation of H3K27me3, particularly at developmental regulatory genes. PGCLCs progressively lose H3K9me2, including the loss at lamina-associated perinuclear heterochromatin, resulting in changes in the nuclear architecture. The mesodermal factor T was shown to recruit H3K27ac to activate BLIMP1, a transcriptional repressor that has a crucial role in the specification of PGCs in mice at E7.5. BLMP1 targets a broad range of targets, possibly through recruitment and spreading of H3K27me3.

1.4.3 Modifications of chromatin in spermatogenesis

During meiosis of male germ cells, the X and Y chromosomes are transcriptionally silenced by a series of chromatin-based events (Turner, 2015) (**Fig. 14**). The precise role of meiotic sex chromosome inactivation (MSCI) is unknown, but it is conserved and essential in all mammals studied so far and in more distant species such as *C. elegans.* MSCI starts at the pachytene stage of meiotic prophase I with phosphorylation of histone H2A variant X (γH2AX) mediated by Rad3-related (ATR) kinase (Ichijima et al., 2011; Royo et al., 2013). After that, both sex chromosomes undergo di- and trimethylation of histone H3 at lysine 9 (H3K9me2 and H3K9me3), ubiquitination of histone H2A (uH2A), and recruitment of heterochromatin protein 1 (HP1) (Baarends et al., 1999; Cowell et al., 2002; Khalil et al., 2004). At mid-pachytene further chro-

matin changes take place such as extensive deacetylation at histones H3 and H4, replacement of the canonical histones H3 (H3.1 and H3.2) by the histone variant H3.3 and methylation of the lysine 20 of histone H4 (H4K20me) (van der Heijden et al., 2007). All these chromatin modifications induce the sex chromosomes of mammalian spermatocytes to form a heterochromatic structure and a specialized nuclear territory at the periphery of the spermatocyte nucleus (the XY body), where both transcription and homologous recombination are restricted (Handel, 2004) (**Fig. 14**).

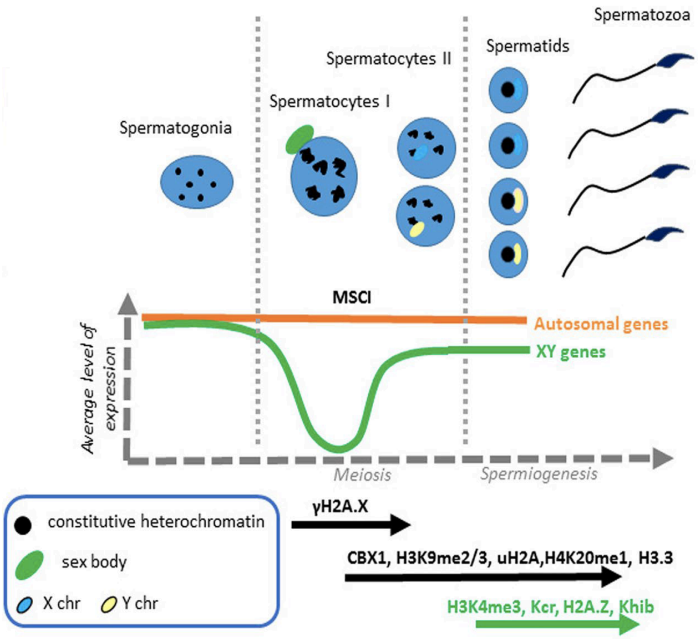

Figure 14. Schematic diagram of XY gene expression during mouse spermatogenesis. In spermatogonia, X and Y gene expression is comparable to that of autosomes. At the pachytene stage of meiosis I, XY genes are transcriptionally repressed by MSCI. After meiosis, XY gene expression is reactivated. The timing of appearance of the chromatin marks enriched on the sex chromosomes (as observed by immunofluorescence) during and after meiosis is represented under the schematic diagram. Taken from (Moretti et al., 2016).

The further presence of repressive chromatin structure (H3K9me2 and H3K9me3, HP1) also on the post-meiotic sex chromatin had suggested that XY gene silencing might persist also in spermatids (Khil et al., 2004; Namekawa et al., 2006). Accordingly, early work proposed that mouse spermatogenesis genes are relatively underrepresented on the X chromosome whereas female-biased genes are enriched on it and therefore the inactivation of the X chromosome in male meiosis might be a universal driving force for X-chromosome demasculinization (Khil et al., 2004). However, further analyses have demonstrated not only that the mouse X chromosome is enriched for spermatogenesis genes functioning before meiosis but also that approximately 18% of mouse X-linked genes are expressed in postmeiotic cells (Mueller et al., 2008).

The postmeiotic transcriptional reactivation of XY gene expression in spermatids coincides with changes in nucleosomal histones and histone modifications. Indeed, and in contrast to somatic cells, germ cells express many, spatiotemporally regulated sets of core histone variants (**Fig. 14**). Some of these histone variants are exclusively expressed in testes. In general, some of the histone variants are present from early meiotic spermatocytes through the late elongated spermatids, while some others are exclusively present in the haploid spermatids right before histone-to-protamine replacement (Bao and Bedford, 2016; Orsi et al., 2009). The testes specific histone 1 subtype variant (H1*t*) was detected in mid- to late-pachytene spermatocytes until elongation spermatid stage (Drabent et al., 1998). This histone variant seems to be particularly important to maintain the open chromatin structure necessary for meiotic recombination and histone replacement (De Lucia et al., 1994). The testes specific H1 variant, H1T2, is restricted to haploid spermatids. *H1t2*-KO mice showed severe defects such as infertility, abnormal spermatid elongation and defects in chromatin condensation, suggesting a major role of this histone variant in replacing histones by protamines (Martianov et al., 2005; Tanaka et al., 2005). Another testes specific H1 variant, HILS1, was only found in spermatids of mammalian testes and, as the others, is supposed to be involved in histone to protamine exchange (Bao and Bedford, 2016; Yan et al., 2003). Testes specific H2A variants were also detected (TH2A or TH2B). TH2B is the major testes specific histone variant and is expressed in the leptotene stage spermatocytes. Mice lacking both *TH2A* and *TH2B* were sterile, although the exact function of these histone variants in spermatogenesis remains elusive (Montellier et al., 2013; Shinagawa et al., 2015). A correlation between the decrease in expression of the somatic histone H2B and the increase of TH2B suggests a function of TH2B in postmeiotic germ cells (Montellier et al., 2013). The testes histone H3 variant (H3T) was found in testes and other somatic tissues (Govin et al., 2007). H3T incorporation resulted in unstable nucleosomes, suggesting a role during meiotic recombination (Tachiwana et al., 2010; Tachiwana et al., 2008).

Modifications at histones during spermatogenesis have also been detected. In spermatogenesis the phosphorylation of core histones has been particularly observed, but the function remains elusive (Govin et al., 2010; Song et al., 2011b). H2A, H2B and H4 are acetylated in spermatogonia and pre-leptotene spermatocytes, whereas in meiotic spermatocytes and round spermatids they are hypo-acetylated (Bao and Bedford, 2016). In elongating spermatids H4K5, H4K8, H4K16 are acetylated independent of

DNA replication (Awe and Renkawitz-Pohl, 2010; Eitoku et al., 2008; Govin et al., 2004; Lahn et al., 2002). Interestingly, the testis-specific member of acetyl lysine binding domain-containing protein, BRDT, was found to be specifically expressed in spermatocytes and haploid spermatids and deletion of one of its bromo domain resulted in male sterility (Shang et al., 2007; Shang et al., 2004). In support of the functional role of BRDT, treatment with bromodomain-specific small-molecule inhibitor JQ1 prevents recognition of acetylated histone H4 by BRDT and induced spermatogenic deficiency (Matzuk et al., 2012). Methylation of histone H3K79 methylation is exclusively detected in the elongating spermatids and accompanies H4 hyperacetylation prior to histone-to-protamine transition (Dottermusch-Heidel et al., 2014). The activity of poly(ADP-ribose) polymerases (mainly PARP1 and PARP2) was proposed to facilitate the removal of histone H1 linker and local chromatin decondensation through the coordination of topoisomerase 2B (TOP2B)-dependent DNA relaxation with histone-to-protamine exchange necessary for spermatid chromatin remodeling (Meyer-Ficca et al., 2011).

One of the dramatic chromatin changes that occur lies in the transition from a nucleosome-based chromatin to a protamine-based chromatin array, which requires the replacement of 90 – 95% of the histones by protamines (Govin et al., 2007; McCarrey et al., 2005). It is considered that this change in chromatin structure is a critical step for the fertilization, which requires realization of many physiological events including movement of sperm cells all along the female reproductive system, their attachment to zona pellucida, and penetration into the oocyte. The condensation of the haploid genome during spermiogenesis is not necessary for the paternal genome to participate in embryogenesis. Indeed, injection of round spermatids, whose chromatin is organized with histones, into oocytes generated embryos that develop into normal offspring (Kimura and Yanagimachi, 1995; Meistrich et al., 2003; Ogura et al., 1994). The fact that *de novo* DNA methylation in spermatogenesis occurs prior to histone-protamine exchange suggests that this highly condensed structure makes DNA inaccessible for further modifications.

While the morphological changes throughout all steps of spermatid development are well characterized, the molecular basis underlying the transition from histone-to-protamine replacement, remains largely unknown (Rathke et al., 2014). Protamines are basic proteins that are enriched for lysines and cysteine residues. They are located in nuclei, and synthetized during advanced stages of spermatogenesis. In both humans

and mice, there are two genes (Protamine 1, *Prm1*; Protamine 2, *Prm2*) clustered on the same chromosome (Balhorn, 2007). Both protamines are essential since genetic ablation of one of the two alleles causes infertility in mice (Cho et al., 2001). Protamines compact DNA very tightly by binding in the major groove of the DNA, end to end. Protamination goes along with somatic H4 hyperacetylation and DNA breaks (McPherson and Longo, 1993; Meistrich et al., 1992; Rathke et al., 2007). The transition from histones to protamines in mice starts around 156 hours after completion of meiosis, corresponding to the time when the spermatids are elongating, and takes in total around 120 - 126 hours (Rathke et al., 2014).

Transition proteins 1 and 2 (TNP1 and TNP2) have been implicated in the transition from histone-to-protamine replacement. TNP1 and TNP2 are expressed shortly before the protamine deposition and are arginine- and lysine-rich proteins binding to DNA. *In vitro* biochemical studies demonstrated that TNP1 tends to relax the DNA in the nucleosomal core particles, whereas TNP2 is prone to compact the nucleosomal DNA, suggesting that TNP2 is a DNA-condensing protein while TNP1 can promote the eviction of the nucleosomal histones (reviewed in (Bao and Bedford, 2016)). Both proteins appear to act redundantly since only mice with double KO of *Tnp1* and *Tnp2* showed a severe retention of histones (Meistrich et al., 2003; Zhao et al., 2004).

In mammals, however, removal of histones is generally not complete, with around 1% in mouse and 10% in human of histones still retained in sperm. In human and mouse spermatozoa strong enrichments of nucleosomes containing H3K27me3, H3K4me2 and H3K4me3 at promoters of distinct gene classes with defined expression programs during spermatogenesis and early embryonic development were shown (Brykczynska et al., 2010; Hammoud et al., 2009). Furthermore, remaining histones have been reported to stay associated with the paternal genome during *de novo* chromatin formation in the zygote after fertilization, supporting a model of epigenetic inheritance by nucleosomes between generations (Erkek et al., 2013; van der Heijden et al., 2008).

1.5 Chromatin and epigenetic modifications in early embryogenesis

As described in the previous chapters, oocyte and sperm are highly differentiated cells that contain a gamete-specific epigenetic pattern. After fertilization, the oocyte and sperm cells fuse to form the zygote. Consequently, in order to reset the gamete's epigenome to a totipotent state, both parental genomes undergo drastic epigenetic changes. Early pre-implantation development starts with the zygotic stage and ends after numerous cell cycles, once the blastocyst is formed (**Fig. 15**).

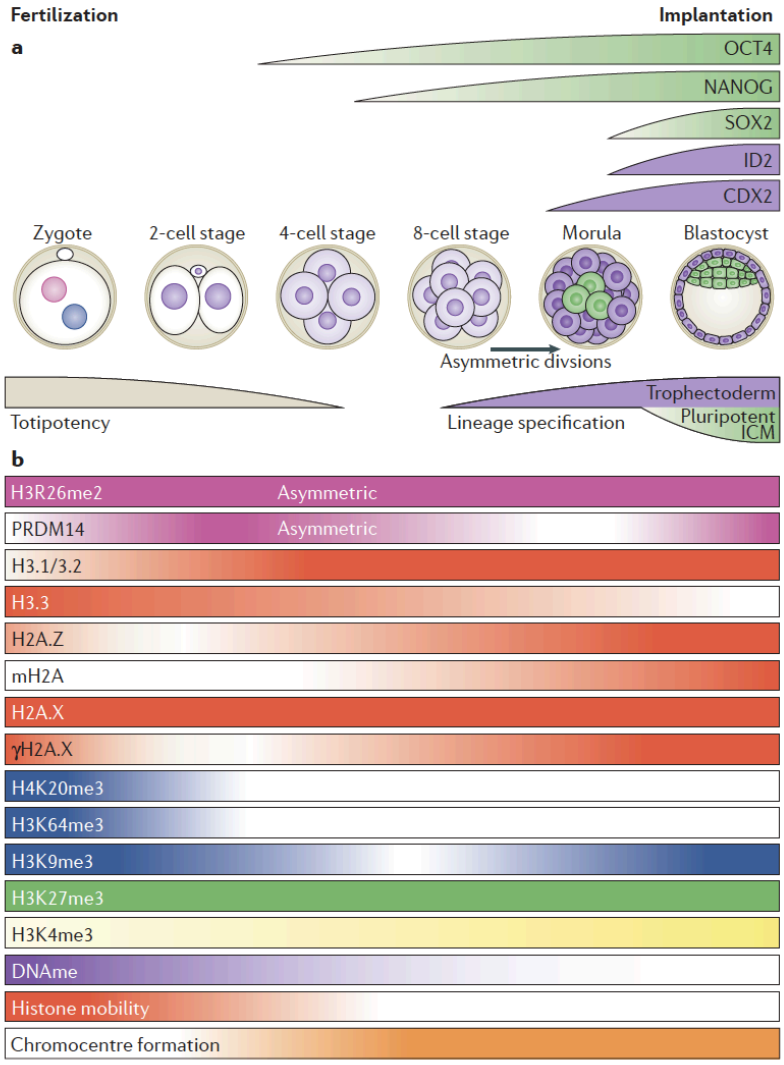

Figure 15. Transcription factors and global chromatin changes during early embryonic development in mouse. A) The transcription factors during early embryonic development are dynamically expressed at a certain time point of development. Cells from the ICM are depicted in green, whereas cells of the trophectoderm are represented in purple. The respective transcription factors are coded accordingly. B) The dynamics of histone modifications and histone variants during preimplantational embryo development are depicted. Pink: asymmetric distribution among cells within 4-cell stage embryos; red: histone variants; blue: constitutive heterochromatic post-translational modifications; green: facultative heterochromatic post-translational modifications; yellow: modifications of transcriptionally active chromatin; purple: DNA methylation; orange: nuclear architecture features. Taken from (Burton and Torres-Padilla, 2014).

Shortly after fertilization, the zygote presents epigenetic asymmetry between paternal and maternal genomes in zygotes. The most dramatic change is the loss of DNA methylation at paternal genome, a process proposed to be mediated by active DNA demethylation mechanisms as it is completed before the onset of DNA replication (Mayer et al., 2000; Oswald et al., 2000). Conversely, the maternal genome undergoes replication-dependent DNA demethylation (passive demethylation), further adding to a parental epigenetic asymmetry in the zygote. This parental specific epigenetic pattern is not only limited to DNA methylation but also includes histone modifications and histone variants. One possible explanation why epigenetic asymmetry between the two genomes might occur is that the protamine-histone exchange takes place on the paternal genome shortly after fertilization. Indeed, this process requires extensive chromatin remodelling and, consequently, might facilitate the establishment of new epigenetic marks.
In the next paragraphs, I will describe how these epigenetic changes are established during early embryonic development.

1.5.1 Regulation of DNA methylation in early embryogenesis

Shortly after zygote formation, the mature sperm genome is globally DNA demethylated, with exception of a limited number of loci including parental imprints and active retrotransposons, which are protected from demethylation to ensure embryonic viability (Mayer et al., 2000; Oswald et al., 2000; Seisenberger et al., 2012). Similar DNA methylation pattern has been detected in several mammals (i.e. human, mouse, rat and cattle) whereas in other species, such as pigs and goats, this DNA demethylation is still controversial (Deshmukh et al., 2011; Fulka et al., 2006; Hou et al., 2005; Park et al., 2010; Reis e Silva et al., 2012) (see also **1.5.3**). It has been proposed that the loss of DNA methylation at the paternal genome is mediated by active DNA demethylation mechanisms as it is completed before the onset of DNA replication (Mayer et al., 2000; Oswald et al., 2000). The roles of 5hmC, TETs and BER in active DNA demethylation at the paternal genome have been described in **1.1.1.3**.
Removal of DNA methylation seems not to be restricted to CpG density or functional annotation (Smith et al., 2012; Wang et al., 2014). Moreover, the lowest DNA methylation level is reached within blastocyst stage (32-64 cells) (Messerschmidt et al., 2014). DNA demethylation in embryos differs from that in PGCs. First of all, PGCs become truly globally demethylated, with the exception of some resistant retroele-

ments, whereas during DNA demethylation in embryogenesis the imprinted genes and some transposable elements maintain the somatic pattern until later stage embryos (Borgel, 2010; Lane et al., 2003; Reik et al., 2001; Wang et al., 2014).

The reason for the asymmetric DNA methylation patterns in the different genomes in the zygote remains still unknown. Interestingly, an earlier work showed that the cellular machinery of the fertilized egg cannot demethylate the second maternal genome in parthenogenetic, gynogenetic and triploid digynic embryos (Barton et al., 2001). These results suggests that differential zygotic demethylation results from differences in the remodelling of paternal and maternal chromatin structures after fertilization, i.e. sperm nuclear decondensation and protamine-histone exchange. Consistent with these results, artificial fertilization using round spermatid, whose DNA is still associated with histones, revealed only slightly demethylated paternal DNA in zygotes, supporting a role of sperm nuclear decondensation and protamine-histone exchange in DNA demethylation process (Polanski et al., 2008). A similar conclusion was drawn through the analysis of the effect of interspecific oocytes on demethylation of sperm DNA (Beaujean et al., 2004b). This analysis was performed to understand why in sheep a lack of genome-wide demethylation of the paternal genome within the first cell cycle post-fertilization exists (Beaujean et al., 2004a). This difference was proposed to be due either to an absence of a sheep demethylase activity that is present in mouse ooplasm or to an increased protection of methylated cytosine residues in sheep sperm. However, injection of sheep sperm DNA in mouse oocytes led to a decrease of DNA methylation at the paternal genome (Beaujean et al., 2004b). Remarkably, it was also possible to observe demethylation of mouse sperm DNA in sheep oocytes. Thus, also in this case, it is probable that DNA demethylation in sperm is either dependent on a paternal sperm derived factor or the remodelling of the male chromatin.

It has been proposed that STELLA (also known as Dppa3, Pgc7) protects 5mC from Tet3-mediated conversion to 5hmC by binding to the maternal chromatin containing H3K9me2 in mice (Nakamura, 2012) (**Fig. 16**). Absence of STELLA led to a loss of 5mC on both pronuclei going along with the accumulation of 5hmC (Wossidlo, 2011). In addition, imprinted loci that are marked with H3K9me2 in mature sperm are protected by STELLA binding in early embryogenesis (Nakamura, 2012). A role of modifications at histones for the control of DNA methylation is also evident by experiments showing that overexpression of mutated H3.1 and H3.2 at either serine 10 or threonine 11 causes a decrease in H3K9me2 and 5mC and a concomitant increase in

5hmC in the maternal genome (Lan et al., 2017). STELLA is highly expressed in PGCs and counts as a maternal factor since *Stella*-deficient females displayed severely reduced fertility due to a lack of maternally inherited Stella-protein in their oocytes (Payer et al., 2003; Saitou et al., 2003). STELLA also plays a crucial role during bovine embryo development. STELLA was found in bovine oocytes and preimplantational embryos with a decrease in transcripts the closer the embryonic genome activation came. Knocking out STELLA in bovine germinal vesicles (GV) led to an increase of 5hmC on the mPN, while knockdown of STELLA in zygotes led to disturbances in early embryonic development and resulted in lower quality blastocysts (Bakhtari and Ross, 2014).

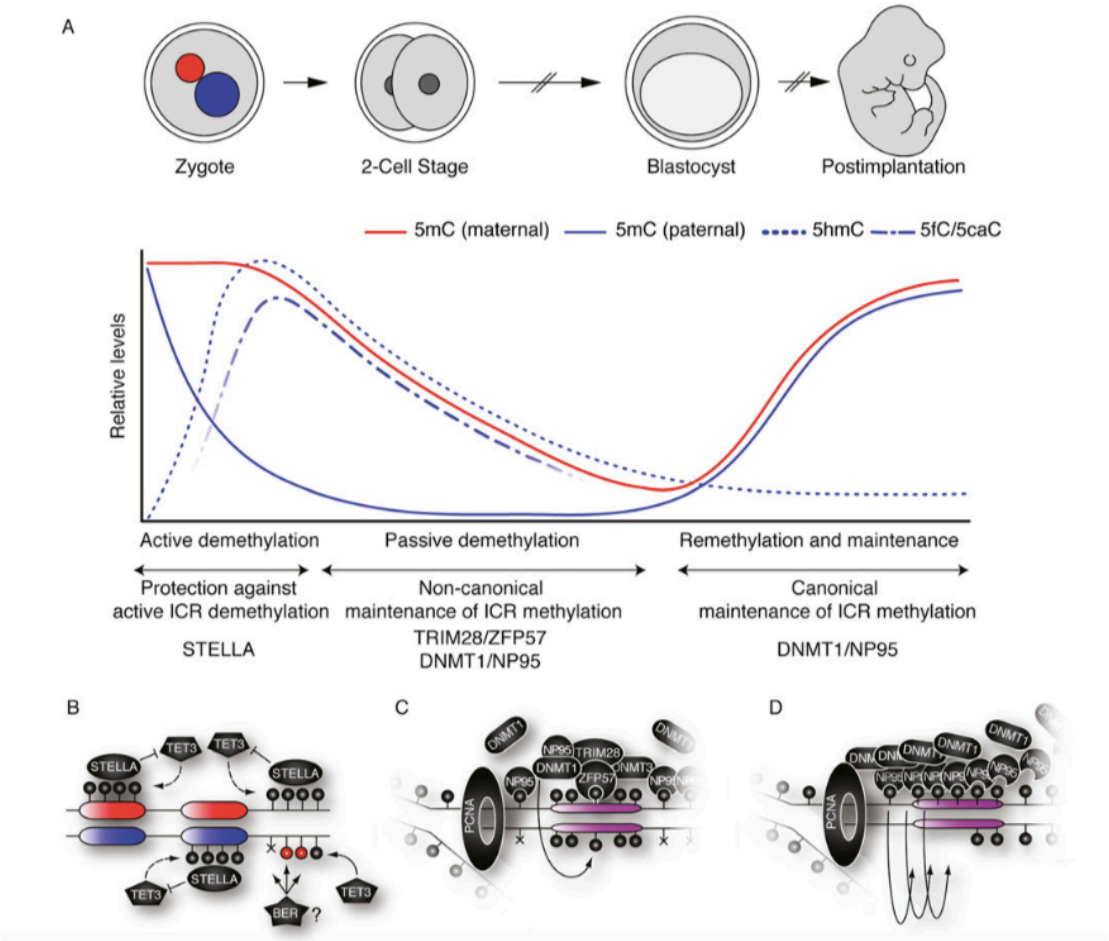

Figure 16. DNA demethylation dynamics and imprinting maintenance in preimplantation embryos.
A) 5mC and 5hmC dynamics during early embryonic development showing epigenetic asymmetry between the maternal (red) and paternal (blue) genomes in the zygote. Active DNA demethylation is taking place at the pPN whereas the maternal genome is demethylated throughout replication. B) In the zygote, STELLA prevents TET3-dependent oxidation of 5mC through binding to H3K9me2. C) Non-canonical targeting of DNMT1 that is excluded from the nucleus to the ICRs during early cleavage stages. D) In the later stage embryo and in adult tissues, DNMT1 is recruited to hemimethylated chromatin in a canonical manner since high DNMT1/NP95 levels during replication maintain DNA methylation. Taken from (Messerschmidt et al., 2014).

The biological function of DNA methylation parental asymmetry in zygotes is not understood. Strikingly, however, zygotes obtained after injection of round spermatids or injection of sperm heads, although impaired in the specific loss of DNA methylation at pPN, developed to term with similar rates. Thus, these results suggest that that hypomethylation of paternal DNA at the zygotic metaphase might not be essential for full development in mice (Polanski et al., 2008).

The maintenance of 5mC requires the activity of DNMT1 during early embryogenesis, whereby the shorter form that is inherited from the oocyte, DNMT1o, is responsible for maintaining the methylation at intracisternal A-particles (IAP) and the embryonic full-length variant takes over during later stages of embryonic development (Gaudet et al., 2004; Lei et al., 1996; Okano et al., 1999b). As mentioned above, imprinted control regions (ICRs) also maintain the DNA methylation throughout replication cycles. So far it is not completely understood why imprints withstand the multiple cell divisions during early embryo development. As for the IAPs, the maternal and zygotic DNMT1 seem to play a role in maintaining the DNA methylation within the ICRs. In contrast, DNMT3A (expressed in oocytes and early embryos) and DNMT3B (expressed in later stages of early embryogenesis) do not seem to be essential for this process (Borgel, 2010; Challen, 2012; Hirasawa, 2008; Kaneda, 2004; Okano et al., 1999b; Wu et al., 2010). Nuclear exclusion of DNMT1 seems to stand in contrast with the need of DNMT1 in maintaining imprints, since it was shown that zygotic deletion of DNMT1 causes a dramatic loss of global DNA methylation, including imprints, and was further shown to be embryonic-lethal (Li et al., 1993; Li et al., 1992b). Recently, it was shown that, although located to the cytoplasm, the oocyte-specific and the somatic DNMT1 isoforms drive imprint maintenance (Branco et al., 2008).
ZFP57 is a Krueppel-associated box (KRAB) domain zinc finger protein is another factor that has been implicated in imprinting maintenance since its loss led to hypomethylation at maternal and paternal ICRs (Li, 2008; Mackay et al., 2008; Quenneville et al., 2011; Zuo et al., 2012). KRAB zinc finger proteins often associate with epigenetic repressors like TRIM28 that is one component of a multifunctional repressor complex composed of the nucleosome remodelling and histone deacetylation (NuRD) complex, the H3K9me-catalyzing histone methyltransferase SETDB1, the HP1 and the DNA methyltransferases DNMT1, DNMT3A/B (Quenneville, 2011; Zuo et al., 2012). This pathway is referred to as the non-canonical DNA methylation

maintenance pathway that recruits the ZFP57-TRIM28 complex to the ICRs (Messerschmidt et al., 2014).

1.5.2 Histone modifications in embryonic reprogramming

Reprogramming in early embryos includes the incorporation of histones or histone variants, either provided by the oocyte or newly synthesized. Remarkably, the two parental genomes significantly differ in the chromatin composition. Immediately after fertilization, the protamines on the paternal genome are replaced by histones, even before the first S-phase of the cell cycle. Importantly, since all newly incorporated histones are hyperacetylated and hypomethylated, the paternal genome acquires a structure that is devoid of heterochromatic marks (Burton and Torres-Padilla, 2010). Concomitant with the replacement of protamines that occurs prior replication, the histone H3 variant H3.3 is rapidly incorporated into the paternal genome, in a replication-independent manner, a reaction that is most likely mediated by the histone chaperone HIRA (**Fig. 15**) (Santenard et al., 2010; Torres-Padilla et al., 2006; van der Heijden et al., 2005). The histone variant H3.3 differs within four and five amino acids, respectively, from the canonical histones H3.1 and H3.2. It remains elusive whether the H3.3 incorporation in the paternal genome is just a matter of gap filling until H3 can be incorporated during replication or if H3.3 incorporation facilitates opening of the chromatin on the pPN. Remarkably, data indicated that H3.3 seems to be important for the initial establishment of the paternal pericentric chromatin, since mutation of H3.3K27 had drastic effects on the embryo and resulted in an arrest of development (Santenard et al., 2010). This phenotype was rescued by the addition of major satellite transcripts, suggesting that H3.3 might be responsible for facilitating transcription within these regions (Santenard et al., 2010).

Another histone variant found to be specifically localized at the pPN was γH2A.X that usually marks double strand breaks (**Fig. 15**) (Wossidlo, 2010; Ziegler-Birling et al., 2009b). In this case, the recruitment to the chromatin appears to be DNA damage independent, since the co-factor tumour suppressor p53-binding protein 1 (TP53BP1) was not co-localized to the γH2A.X foci (Ziegler-Birling et al., 2009b). As described in a previous chapter (**1.1.1.3**), the presence of γH2A.X at pPN was associated with active DNA demethylation and the involvement of BER pathway.

Another relevant histone variant in embryogenesis is the H2A variant H2A.Z, which is lowly expressed in zygotes and become incorporated in euchromatic regions start-

ing from late 2-cell stage onwards (**Fig. 15**) (Bošković et al., 2012; Nashun et al., 2010; Rangasamy et al., 2003). The lack of H2A.Z results in a failure of development during implantation. Although, acetylated H2A.Z is a marker of active chromatin, it was surprisingly absent in the 2-cell stages during major EGA. Similarly, H3K36me3, another marker of active chromatin, was also not detectable in mice during EGA, whereas it was present during bovine EGA at around 4-8-cell stage (Bošković et al., 2012).

The pPN contains a specific pattern of histone modifications, showing H3K4me1, H3K9me1 and H3K27me1 directly at fertilization, whereas H3K4me3, H3K9me2, H3K27me3 first appear after replication (**Fig. 15**) (Arney et al., 2001; Lepikhov and Walter, 2004; Santos et al., 2005). This delay in establishing H3K27me3 at the pPN goes in line with the delayed recruitment of the polycomb repressive complex 2 (PRC2).

The maternal genome also undergoes epigenetic reprogramming such as the rapid loss of heterochromatic histone marks H4K20me3 and H3K64me3 before the first cell division even took place (**Fig. 15**) (Daujat et al., 2009; Kourmouli et al., 2004). H3K9me3, however, is passively diluted and its re-establishment is prevented for further two to three cell divisions (Liu et al., 2004b; Puschendorf et al., 2008). The mechanism of how constitutive heterochromatic marks are removed is not yet understood. However, due to its timing it is supposed that an active mechanism must take place. The loss of heterochromatic marks at the maternal genome goes along with the formation of an open chromatin necessary for regaining pluripotency in early embryos (Ahmed et al., 2010).

Investigating pre-implantation embryo development was long time limited due to the low amount of cells available. The recent establishment of micro-scale chromatin immunoprecipitation and sequencing (μChIP-seq, STAR ChIP-seq) method allowed to profile genome-wide H3K4me3, H3K27ac and H3K27me3 in mouse immature and metaphase II oocytes and in 2-cell and 8-cell embryos (Dahl et al., 2016; Liu et al., 2016; Wu et al., 2016; Zhang et al., 2016). These studies determined that in the oocyte genome H3K4me3 is enriched at low levels across large genomic regions, spanning more than 10 kilobases, and is mostly distant from transcription start sites. This pattern of 'non-canonical' H3K4me3 persists in the fertilized oocyte and in embryos at the early two-cell stage. In 2-cell embryos, the H3K4me3 signal becomes confined to transcriptional-start-site regions, concomitant with the onset of major zygotic genome

activation. The removal of non-canonical H3K4me3 requires zygotic transcription but is independent of DNA replication-mediated passive dilution. Remarkably, active removal of maternal inherited broad H3K4me3 domains was described to be mediated by the lysine demethylases KDM5A and KDM5B and this process is required for normal zygotic genome activation and essential for early embryo development. Moreover, parental differences in H3K4me3 distribution were found to be retained in the two sets of chromosomes in the early embryo, supporting the idea that some epigenetic information is inherited (Wu et al., 2016; Zhang et al., 2016). H3K27ac domains were found to be near genes associated with zygotic genome activation (Dahl et al., 2016). Re-establishment of H3K4me3, especially on promoter regions, occurs much faster than that of H3K27me3 following fertilization, which is consistent with the major wave of zygotic genome activation at the two-cell stage (Liu et al., 2016). Finally, compared to embryonic stem cells, the co-occurrence of H3K4me3 and H3K27me3 (bivalency) in early embryos was relatively infrequent and unstable. Interestingly, previous results using micro-ChIP for H3K4me3 and H3K9me3 levels on repetitive elements in 2- and 8-cell embryos revealed that long interspersed element 1 (LINE-1), short interspersed nuclear element (SINE) B2 and intracisternal A-particle (IAP) retrotransposons were enriched in H3K4me3 in 2-cell stage embryos at the time when they are transcriptionally reactivated after fertilization (Fadloun et al., 2013). This suggests that retrotransposons harbour a different chromatin pattern in embryonic cells compared to somatic cells (Burton and Torres-Padilla, 2014).

Major chromatin organization changes periodically occur during pre-implantational at defined time points. Chromocentres are DNA aggregates that consist of heterochromatic, centromeric and pericentromeric regions and can be visualized as DAPI-rich foci. These regions are also observed in mature oocytes and embryos, where they are arranged in ring-like structures surrounding nucleolar-like bodies (NLBs) (**Fig. 17**) (Aguirre-Lavin et al., 2012; Burns et al., 2003; Probst et al., 2007). NLBs are unique in pre-implantation embryos and are thought to be non-functional nucleoli pre-cursors that remain until late 2-cell stage. However, the function of NLB is not yet completely understood (Burton and Torres-Padilla, 2014; Jachowicz et al., 2013).

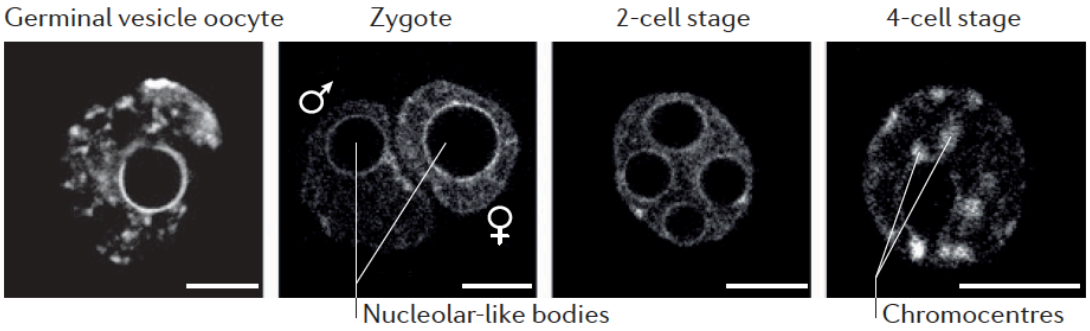

Figure 17. Global chromatin reorganization during early mouse development. DAPI staining in GV oocytes, zygotes, 2- and 4-cell stages displaying the A-T rich major satellite sequences that are arranged in ring-like structures around nucleolar-like bodies. The scale bar represents 10 µm. Taken from (Burton and Torres-Padilla, 2014).

1.5.3 Epigenetic reprogramming in early embryogenesis of different mammalian species

Epigenetic reprogramming during embryogenesis is most of the time exemplified in the mouse as the model organism standing for mammalian embryonic development. Mice are easy to keep, have a fast reproductive cycle and are easily available in large numbers. Nevertheless, it was shown that epigenetic reprogramming shows some species-specific differences within mammals and differences even occur between closer related species like species from the family of the ruminants (i.e. cattle vs. sheep).

The active DNA demethylation was first described in mice, when an asynchronous DNA demethylation prior to replication was detected (Mayer et al., 2000; Oswald, 2000; Wossidlo, 2010). DNA demethylation dynamics can also be seen in most other mammals, however, the exact dynamic seems to vary among species. Similarly to mouse, DNA demethylation in bovine embryos was detected at the pPN shortly after fertilization. However, the re-methylation in bovine embryos remains still controversial. One study observed that paternal DNA methylation was rapidly restored almost to the maternal methylation level even before the two-cell stage (Park et al., 2007). In another study, it was shown that embryos lose DNA methylation until they reach 8-cell stage, which might facilitate the EGA that starts between 4-cell and 8-cell stage, and *de novo* methylation takes place only at 16-cell stage (Dean et al., 2001). Reprogramming in rabbit zygotes somehow seems to differ from mice, but it is not yet completely understood. The rabbit zygote is very well investigated, since *in vivo* and *in vitro* derived zygotes are easily accessible. Evidence indicated that the mPN maintains its 5mC content throughout early embryonic development, whereas within the pPN a partial DNA demethylation, starting from 4-cell stage onwards, was visible (Reis e Silva et al., 2012; Reis Silva et al., 2011). DNA methylation and demethyla-

tion is also described in humans on a single cell level using a post-bisulfite adaptor tagging strategy (Zhu et al., 2018). In this study the authors traced DNA methylation through the whole embryonic development and showed that the process of methylation, demethylation and remethylation, is very dynamic. The 1st wave of demethylation occurs very early in the absence of replication, mainly in CpGs located at enhancers and gene bodies, the pPN loses around 30% of the 5mC whereas in contrast the mPN only loses 4%. The 2nd wave of demethylation was observed between late stage zygotes and the 4-cell stage, followed by the 3rd wave that was detected after 8-cell stage. Remarkably, two remethylation waves were detected, the 1st wave occurred in the pPN between early and mid-zygote stages and the 2nd *de novo* methylation wave occurred between 4- and 8-cell stages (Zhu et al., 2018). Interestingly, by IF analyses in ICSI derived human embryos the formation of 5hmC was detected on both parental pronuclei to the same extent, suggesting that either active DNA demethylation was also occurring on the mPN or 5hmC formation is not just occurring during DNA demethylation in early embryos (Guo et al., 2014b).

DNA methylation analysis of porcine "in vivo" produced embryos revealed drastic loss of 5mC at the pPN but not at the mPN (Fulka et al., 2006). Interestingly, methylation signal remains globally high until the late morula stage. H3K27 trimethylation was proposed to be an epigenetic marker of maternally derived chromatin that is globally remodelled during porcine embryogenesis (Park et al., 2009). H3K27me1 was detectable in the nuclei of oocytes and pronuclear, 2-cell, 4-cell, 8-cell, and blastocyst stage embryos. H3K27me3 was detectable in the nuclei of GV stage oocytes, the chromosome of MII stage oocytes and a single pronucleus of the pronuclear stage embryos produced by fertilization but was low or absent in nuclei of two-cell through blastocyst stage embryos.

DNA demethylation at the pPN of goat zygotes has not been detected. Global loss of DNA methylation was observed in in 2-cell embryos, with the lowest 5mC levels being seen in 4-cell embryos and increased *de novo* methylation during the 8-cell stage onwards (Park et al., 2010). Interestingly, the pPN in goats contain high H3K9me3 levels independent of replication, making this modification most likely responsible for the impairment of DNA demethylation (Kikyo and Wolffe, 2000; Park et al., 2010).

The analysis of epigenetic reprogramming in horses is rather difficult since *in vivo* derived horse embryos are rarely accessible and *in vitro* produced embryos can only be achieved by intracytoplasmatic sperm injection (ICSI). Therefore, examinations on

DNA methylation dynamics in horses were conducted in ICSI derived embryos, showing that 5mC was present in both parental pronuclei to the same extent throughout zygotic development. Interestingly, 5hmC levels were also detected to the same extent in both pronuclei but surprisingly the localization of the two cytosine analogues seemed different, 5mC tended to cluster at defined regions whereas 5hmC was homogenously distributed within the pronucleus (Heras et al., 2017).

Studies have also shown that *in vivo*-derived ovine zygotes do not show loss of DNA methylation (Beaujean et al., 2004a; Dean et al., 2001). Demethylation seemed to occur only at blastocyst stage, in the trophectoderm (Beaujean et al., 2004a). However, a recent study observed different patterns of methylation and hydroxymethylation between the two parental pronuclei, suggesting that male pronucleus undergoes active demethylation also in sheep (Masala et al., 2017).

1.6 DNA damage and DNA Repair pathways

All cells, whether post-mitotic or proliferating, are challenged by thousands of DNA-damaging events every day, and damage generally occurs irrespective of the underlying DNA sequence (Hauer and Gasser, 2017). DNA is constantly exposed to a variety of damaging factors such as genotoxic agents, environmental factors (e.g. UV light, irradiation) or normal metabolic activities (e.g. nucleotide misincorporation during DNA replication, reactive oxygen species) that causes a range of lesions (**Fig. 18**). If left unrepaired, such lesions pose a barrier to both DNA and RNA polymerases, causing the formation of single-stranded stretches of DNA and, occasionally, double strand breaks (DSBs). Damage in the cell leads to severe consequences for the cell, including cell death, mutations or even the formation of cancer. DNA repair pathways are constantly active in the cell to identify and correct all DNA damage that may occur.

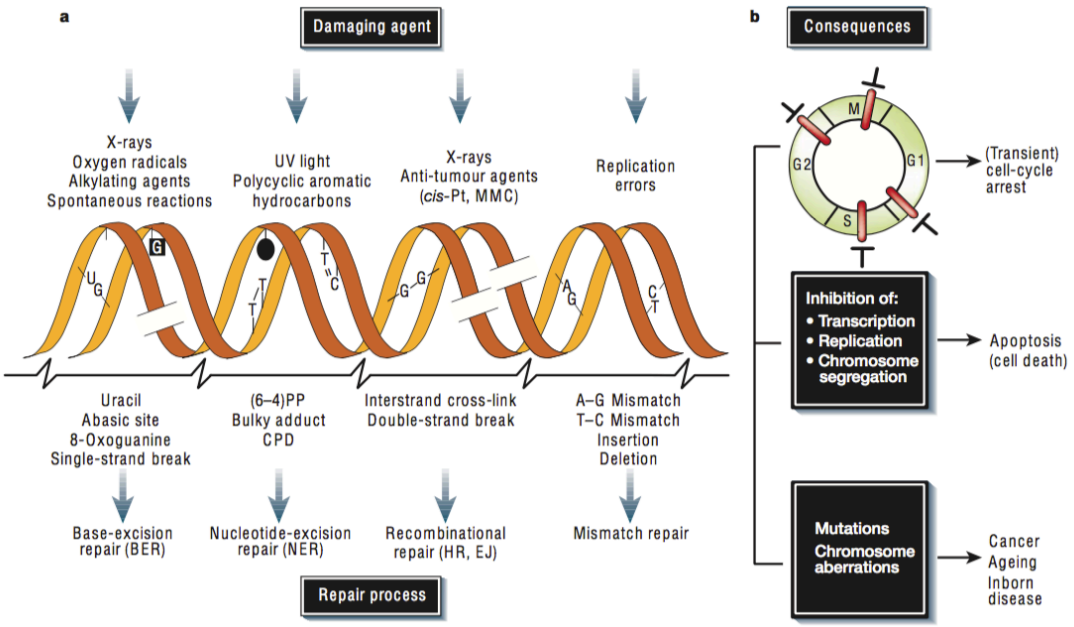

Figure 18. The five DNA repair pathways and the consequences for the cell resulting from DNA damage. A) Damaging agents damage the DNA. Depending on the kind of damage the respective DNA repair mechanism is activated and repairs the lesion. B) Cell cycle arrest in G1, S, G2 or M phase is induced that the cell has the chance to repair the DNA damage. In case of unsuccessful repair the cell can undergo programmed cell death or the damage leads to mutations or chromosome aberrations that further might lead to severe defects. Taken from (Hoeijmakers, 2001).

The wide diversity of DNA lesions requires multiple, largely distinct DNA repair processes. DNA repair pathways include the precise interplay of plenty of factors such as nucleases, helicases, polymerases, topoisomerases, recombinases, ligases, glycosylases, demethylases, kinases, and phosphatases. The DNA damage response (DDR) is

responsible for sensing the DNA damage and regulating several physiological and fateful decisions, including the decision of initiating apoptosis, activating an immune responses, entering senescence or activating DNA repair pathways (Cui et al., 2007; Gasser and Raulet, 2006; Zhou and Elledge, 2000).

Important factors that initiate and mediate the DDR are the phosphatidylinositol 3-kinase-like protein kinase (PIKK) family members Ataxia Telangiectasia Mutated (ATM), Ataxia Telangiectasia And Rad3 Related (ATR) and DNA-dependent protein kinase (DNA-PK) and the members of the Poly [ADP-ribose] polymerase (PARP) family. ATM senses hundreds of substrates and regulates a wide variety of proteins, whereas DNA-PK for example is more specialized in orchestrating a group of proteins involved in DSB end joining. Replication protein A (RPA) is the main factor binding preferentially to single stranded DNA (ssDNA) regions (e.g. at replication forks) but can also bind DSBs activating a complex consisting of ATR and ATR interacting protein (ATRIP) for further processing. The PARP family is a big family of proteins involved in several cellular processes, whereas mainly PARP1 and PARP2 are important for the DDR. PARPs catalyse the addition of poly [ADP-ribose] chains to sites of DNA damage in order to recruit the DDR machinery (Schreiber et al., 2006). DSBs or single strand breaks (SSBs) activate the PARP family members PARP1 and PARP2 that assemble PAR moieties on target proteins like histones H1 and H2B within seconds. PARP1 has additionally the ability to PARylate itself (Caldecott, 2008; Schreiber et al., 2006). Histone PARylation holds an important role in recruiting DNA repair factors and chromatin modifying complexes to damaged sites (Schreiber et al., 2006). Many DDR factors contain PAR binding motifs for example p53, X-ray repair cross-complementing protein 1 (XRCC1), DNA Ligase III (LIGIII), double-strand break repair protein MRE11 and ATM (Ciccia and Elledge). ATM/ATR kinases phosphorylate proteins that later recruit ATM/ATR substrates and activate the DDR. ATM/ATR signalling is needed for non-homologous end joining (NHEJ), homologous recombination (HR), and nucleotide excision repair (NER) and physiologically for stabilizing replication fork during DNA replication. The initiation of these processes is mediated through fast posttranslational modifications such as phosphorylation, ubiquitination, sumoylation, poly(ADP-ribosylation), acetylation, methylation later steps require transcriptional responses that generally take more time (Ciccia and Elledge). p53 is one of the best-studied DDR signalling factors that is regulated by ATM in response to DSBs, p53 responds to DNA damage by inducing

cell-cycle arrest, apoptosis or senescence. Additionally, p53 can also directly activate the NER pathway (Ciccia and Elledge).

γH2AX is often used as a marker of DNA damage in cells, since phosphorylation of Ser139 by PIKKs on histone H2AX (γH2AX) mediates the recruitment of DDR factors and is also responsible for maintaining the factors at the sites of damage (Celeste et al., 2002; Kuo and Yang, 2008). Tyr142 of H2AX is constantly phosphorylated in the cell this blocks the binding of mediator of DNA damage checkpoint protein 1 (MDC1). MDC1 binding to Ser139 of H2AX is important for the initiation of an adequate DDR therefore MDC1 binding goes in line with dephosphorylation of Tyr142 (Cook et al., 2009; Krishnan et al., 2009). γH2AX-dependent recruitments can be mediated by different posttranslational modifications like ubiquitination or SUMOylation, each modification recruits different factors to the damaged site in order to initiate different pathways or flexibly changing the recruitment of different factors in case one pathway is failing to repair the lesion (Ciccia and Elledge).

1.6.1 DNA repair pathways

DNA damaging agents are ubiquitous and the cell has to deal with DNA lesions arising. The different DNA damaging agents induce different lesions on the DNA that requires the initiation of an appropriate DDR. As shown in **Figure 18**, oxidative damage specifically induces single nucleotide lesions that initiate the base excision repair machinery, whereas UV-light induces bulky DNA damage including more than one nucleotide that needs to be repaired by the nucleotide excision repair pathway. Double strand breaks (DSBs) are fatal lesions of the DNA that need to be repaired immediately. The DDR of DSBs is mainly conducted by either NHEJ that does not depend on a homologous template and is therefore cell-cycle-independent or on HR that repairs the DNA lesion in the presence of a sister chromatid template. All repair mechanisms require a transient cell cycle arrest that gives the repair machinery the chance to repair the lesion. In case that the lesion cannot be repaired the cell undergoes programmed cell death. Cell cycle arrest leads to the inhibition of transcription, replication and chromosome segregation and bears therefore the risk for chromosome aberrations that consequently might lead to cancer or other disease. Unrepaired lesion that escaped the cellular control mechanisms can also result in mutation and the formation of cancer. The following paragraphs describe the different DNA repair pathways in more detail.

1.6.1.1 Base excision repair (BER)

The BER pathway is responsible for repairing single base lesions that do not distort the helical structure of the DNA. Damage arises from depurination, depyrimidation, oxidation, alkylation or deamination. Additionally, many of these lesions occur through spontaneous decay of the DNA (Lindahl, 1993).

Initiation of the BER pathway is catalysed by the activation of one out of at least eleven known human DNA glycosylases, which recognizes and excises the damaged base and paves the way for the activation of further protein complexes (Barnes and Lindahl, 2004; David and Williams, 1998; Fromme and Verdine, 2004). Functionally, four glycosylases are responsible for the removal of mispaired uracil or thymine, six are specifically devoted to the repair of oxidation induced lesions and the remaining last one is removing alkylated bases.

Six of these glycosylases are monofunctional glycosylases, being expressed in the nucleus (two of them are additionally expressed in mitochondria) and all of them participate in a substrate-specific manner in the repair of oxidative-induced DNA lesions (Almeida and Sobol, 2007). The substrates for monofunctional glycosylases are versatile. Alkyl guanine glycosylase/methyl purine glycosylase (AGG/MPG) recognize alkylated purines and ethenopurines, uracil glycosylases (UNG) recognizes uracil, 5-hydroxyuracil and other uracil intermediates. Single-strand-selective monofunctional uracil glycosylase 1 (SMUG1) recognizes the same substrates as UNG in single and double stranded DNA and additionally 5-hydroxymethyluracil. Thymine DNA glycosylase (TDG) removes mispaired bases (uracil, thymine and 5-hydroxymethyluracil) only in double stranded DNA when paired with guanine as is doing methyl CpG binding domain protein 4 (MBD4) that recognizes these lesions in CpG dinucleotides. MUYH recognises mispaired adenine opposite 7,8-dihydro-8-oxoguanine (8-oxoG) or 2,6-diamino-4-hydroxy-5-formamidopyrimidine (FapyG) (Wallace, 2014).

Monofunctional glycosylases cleave the *N*-glycosyl bond between the base and the sugar is hydrolysed and incised, creating the abasic site that has 3'-OH and a 5'-deoxyribose-phosphate (5'dRP) moiety in order to remove the wrongly incorporated or damaged base. End-processing is performed by apurinic endonuclease 1 (APE1) that cleaves the DNA strand, creating 5'OH and a 3'deoxyribose phosphate (5'dRP) and induces the "short-patch" BER (SP-BER) pathway (Almeida and Sobol, 2007; Gary et al., 1999; Svilar et al., 2011). Pol β itself has polymerase and dRP-lyase activ-

ity that removes the 5'dRP moiety, resulting in a 5' phosphate required for the following ligation step (Krokan and Bjoras, 2013) (**Fig. 19**, repair synthesis left arrow).

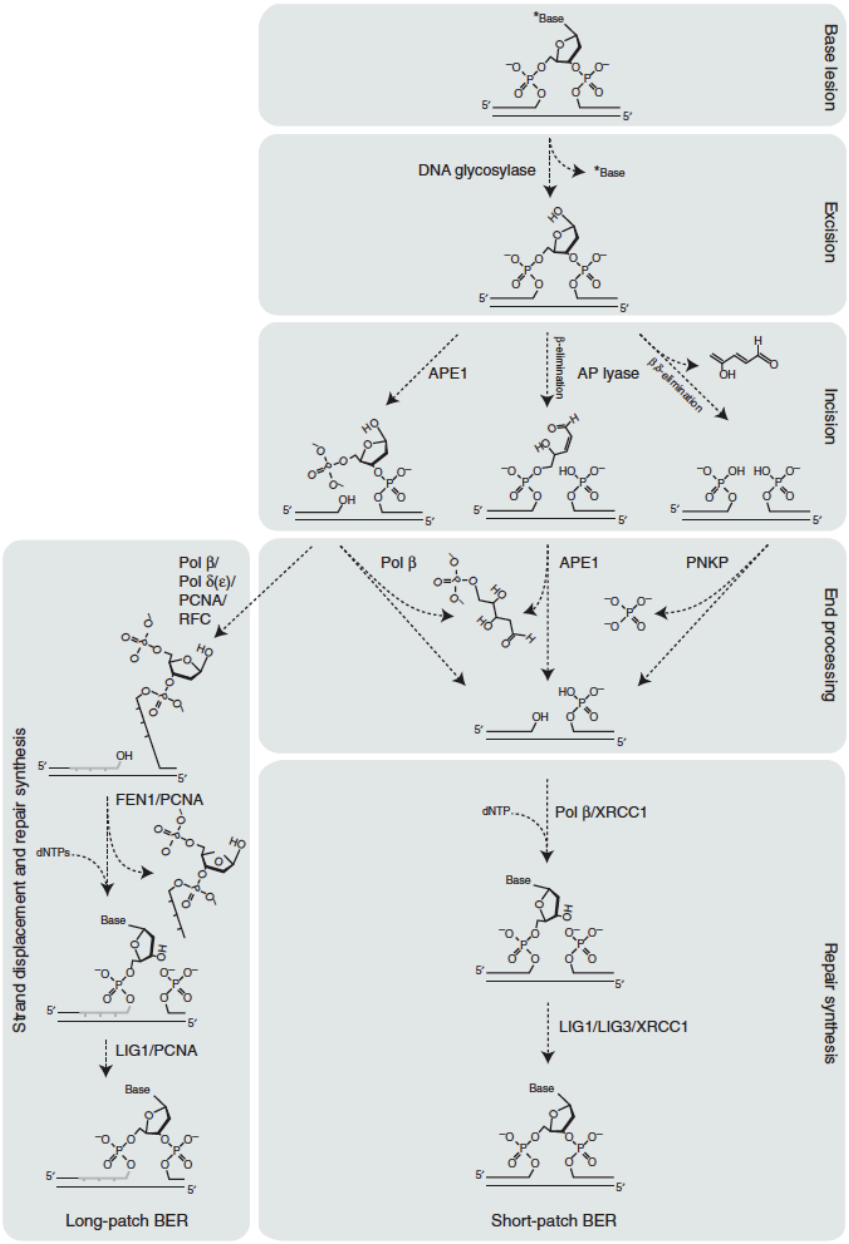

Figure 19. **Base excision repair pathway.** The classical short-patch BER pathway requires several steps starting with a base lesion that is excised and replaced by Pol β and the finale step of ligating the nick. Dependent on which glycosylase induced the excision of the base the end needs to be differentially processed. The impairment of excising the 5'dRP moiety induces the repair via the long-patch BER. Taken from (Krokan and Bjoras, 2013).

In case the base is removed by bi-functional glycosylases that contain β-lyase activity such as 8-Oxoguanine glycosylase (OGG1), β-elimination generates an unsaturated hydroxyaldehyde linked to the 3'dRP and a 5'phosphate by incising the DNA backbone (David et al., 2007; Svilar et al., 2011) (**Fig. 19**, "incision" middle arrow). The 3'dRP is also cleaved by APE1 resulting in a 3'OH that serves as a substrate for the

repair DNA polymerase β (Pol β) (**Fig. 19**, "end-processing" middle arrow). Bifunctional glycosylases like OGG1 or endonuclease III-like protein 1 (NTH1) play a crucial role in the repair of oxidative-induced DNA lesions (David et al., 2007). Substrates for OGG1 are mainly 8-oxoG and FapyG that pair with cytosine.
Glycosylases with β, δ-lyase activity release an unsaturated deoxyribose while cleaving, creating a one-nucleotide flap with 3' and 5' phosphate ends. The 3' phosphate is removed by polynucleotide kinase/phosphatase (PNKP) (**Fig. 19**, "incision"; right arrow) (Krokan and Bjoras, 2013). Followed by repair synthesis conducted by Pol β (**Fig. 19**, "end-processing")

Nonhistone protein high mobility group box 1 (HMGB1) regulates repair pathways and gene expression and binds to chromatin. HMGB1 promotes the binding of BER proteins APE1 and flap-endonuclease 1 (FEN1) and therefore promotes the LP-BER (Krokan and Bjoras, 2013). The LP-BER is mostly found in proliferating cells and uses the help of the replication machinery for repairing the lesion including Pol δ/ε, PCNA, FEN1 and LigI (Krokan and Bjoras, 2013; Svilar et al., 2011). In case of insufficient removal of the 5' end nick by Pol β, the long-patch BER (LP-BER) is initiated, including the activation of different DNA polymerases such as replicative polymerases or Pol λ. The initiation of this pathway remains the same as for the SP-BER. The LP-BER also needs the 3'OH moiety but the 5'dRP moiety is refractory to the Pol β dRP lyase activity (Gary et al., 1999). In this case Pols δ, ε and β form a complex with proliferating cell nuclear antigen (PCNA), FEN1, PARP1 and LigI. The whole machinery leads to DNA strand displacement through DNA synthesis by Pol β and an overhanging DNA flap of about 2-13 bases that is initiated by the presence of FEN1 and PARP1 (Fortini and Dogliotti, 2007; Nakamura et al., 1998; Prasad et al., 2000; Prasad et al., 2001; Stucki et al., 1998). FEN1 is an endonuclease responsible for the removing of the displaced DNA strand, creating a nick 2-13 bp further apart from the original DNA damage site, the resulting nick is then sealed by LigI (Almeida and Sobol, 2007) (**Fig. 19**, left panel).
Ligation of the nick is the last step in the BER pathway, whereby the binding of XRCC1 and LIG3, core components of the BER pathway, to SSBs is PARP1 dependent (Svilar et al., 2011; Wallace, 2014). Mammals own three different DNA ligases (LigI, LigII, LigIV). LigI interacts with PCNA and is the ligase ligating the nick in

LP-BER. LigIII is located in the nucleus and mitochondria and is the major ligase responsible in SP-BER through its association with XRCC1. Data have shown that LigI can fully replace LigIII in SP-BER, whereas the complex consisting of LigIII/XRCC1 can not replace LigI in LP-BER (Almeida and Sobol, 2007) (**Fig. 19**, "repair synthesis").

1.6.1.2 Nucleotide excision repair (NER)

The nucleotide excision repair (NER) pathway is responsible for repairing bulky or helix-distorting DNA lesions (**Fig. 20A**). These lesions are most likely photoproducts caused by UV-light or other chemicals.

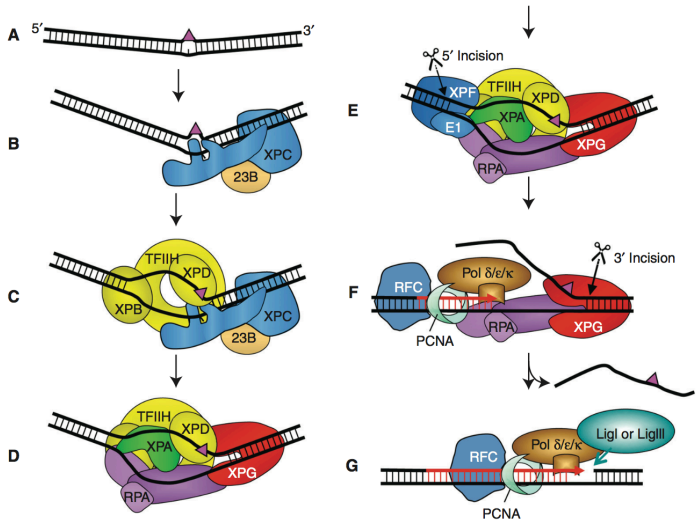

Figure 20. **Nucleotide excision repair pathway.** Bulky DNA A) lesions recruit specific NER factors B) unwinding the chromatin C). The damaged strand is excised (E,F) and newly synthesised with the help of Pol δ, Pol κ or Pol λ G). Taken from (Schärer, 2013).

NER plays a specific role in severe human diseases that harbour genetic mutations in the NER proteins, such as Xeroderma pigmentosum and Cockayne's syndrome. The proteins associated with NER are named after the diseases they induce, like the nine major NER proteins that are called Xeroderma pigmentosum A-F (XPA-XPF).

Several enzymes recognize a plethora of substrates (de Laat et al., 1999; Iyama and Wilson, 2013). All these NER substrates have one characteristic in common: they thermodynamically destabilize the DNA duplex and are therefore bulky. The repair complex has to reach the 22-30 bp long bulky lesion, that requires chromatin remodelling complexes to render the chromatin accessible for the repair machinery and recondense the chromatin after repairing the damage (Stadler and Richly, 2017). Two distinct NER sub-pathways exist. On one hand side the global genome NER (GG-

NER) being responsible for DNA damage throughout the entire genome and on the other hand the transcription-coupled NER, responsible for detecting lesions on the coding strand during transcription (Fagbemi et al., 2011; Iyama and Wilson, 2013; Menezo et al., 2010). For the initiation of GG-NER, the specific factor XPC-RAD23B binds the non-damaged strand opposite to the lesion with the help of UV-DDB (UV-damaged DNA-binding protein) (**Fig. 20B**) (Zhou and Elledge, 2000). Transcription factor II H (TFIIH) recognises and assembles to the complex and allows XPD to move along the DNA until it reaches and verifies the bulky lesion (**Fig. 20C**). This stalling of the complex leads to the initiation of the pre-incision complex consisting of XPA, RPA and the exonuclease XPG (**Fig. 20D**). Incision at the 5'end is initiated after the DNA excision repair protein (ERCC1)-XPF binds XPA (**Fig. 20E**). Repair synthesis is conducted by the Pols δ, κ or λ and is finished by an incision at the 3'end (**Fig. 20F**). The remaining nick is sealed by the DNA LIGIIIa/XRCC1 complex or by LIGI (**Fig. 20G**) (Schärer, 2013). In contrast, TC-NER is activated when RNA polymerases are stalled at DNA lesions. The initiation requires the different specific factors called Cockayne's syndrome A (CSA), CSB and XAB2. The following repair pathway requires the same core NER components as GG-NER.

1.6.1.3 Non-homologous end joining (NHEJ)

DNA double strand breaks (DSBs) are induced through ionizing radiation or X-rays, free radicals, chemicals or in a more physiological process during replication in S-phase of the cell cycle (Hoeijmakers, 2001). DSBs are severe damages to the chromatin that need to be repaired to prevent damage to future cell generations. Four known pathways are able to repair DSBs: Homologous recombination (HR), Non-homologous end-joining (NHEJ), alternative-NHEJ (alt-NHEJ) and single strand annealing (SSA). The repair pathway is chosen according to the necessary end processing at the break site. DNA DSBs are sensed by at least four different factors: PARP, Ku70/80, MRN and RPA that sense the DSBs within seconds.

NHEJ, as the name suggests, does not need a homologous DNA template and, consequentially, is independent of cell cycle progression. Like most DNA repair processes, there are three enzymatic activities required for repair of DSBs by the NHEJ pathway: (1) nucleases to remove damaged DNA, (2) polymerases to aid in the repair, and (3) a ligase to restore the phosphodiester backbone. Choosing the right DNA repair path-

way depends on the provided substrates present at the break site but also requires some regulatory factors such as tumour suppressor p53-binding protein 1 (TP53BP1) that promotes NHEJ by facilitating the ligation step of the two broken DNA ends (Difilippantonio et al., 2008; Dimitrova et al., 2008).

The initial step of NHEJ is the loading of the toroid structured Ku (Ku 70/80) heterodimer onto the ends of the DSBs. The classical NHEJ pathway (**Fig. 21A**) does not require end resection whereas the other pathways depend on end resection such as alt-NHEJ (**Fig. 21C**) that requires resection of about 5-25 nucleotides. Ku recruits DNA-PK that is loaded onto the DNA and its catalytic subunit (DNA-PKc) is activated. DNA-PKcs prevent DNA end resection during NHEJ by stabilizing the DNA ends and additionally recruit the XRCC4/LIG4 complex (Meek et al., 2008). The ends of the DSBs have to be prepared for further ligation steps, including resection of DNA ends, filling gaps and making them ligatable by removing blocking end groups. The final step contains the ligation of the DNA ends by Ligase IV (LigIV). So far it is not known what causes the release of the repair complex from the repaired DNA strand (Davis and Chen, 2013). The XRCC1/LIG4 complex initiates the ligation of the broken DNA ends (Mahaney et al., 2009). Recruitment can also be mediated by PARP1/2. PARPs induce the alt-NHEJ pathway (Hochegger et al., 2006). In DSB recognition PARP1 catalyses ATM activation and induces MRN (MRE11-RAD50-NBS1) complex recruitment in a γH2AX and MDC1- independent manner (Haince et al., 2007).

Physiologically, NHEJ plays an important role in the V(D)J recombination during maturation of pre-B cells (Hübscher, 2010). In yeast, Pol4 is the only polymerase implicated in NHEJ. In mammalian cells, the responsible polymerases are the Pols λ, μ and terminal deoxynucleotidyltransferase (TdT) (Benedict et al., 2000; Bertocci et al., 2006; Kawamoto et al., 2005; Maloisel et al., 2008; Sebesta et al., 2011; Sharma et al., 2012). All these polymerases contain the BRCA1 C-terminal (BRCT) domains. Pol μ and λ share the most homology with *Saccharomyces cerevisiae* Pol4, and both appear to be expressed in mammalian somatic cells. TdT is expressed only in pre-B and pre-T cells.

1.6.1.4 Homologous recombination (HR)

In contrast to NHEJ, the homologous recombination HR needs a homologous DNA template to repair the damaged DNA strand, which reduces the chances of errors (Hübscher, 2010). The need for a homologous DNA template results in cell cycle dependency, therefore HR is only taking place during late-S or G2 phase, when a daughter DNA duplex is present (Jackson and Bartek, 2009). When DSBs are recognized by the MRE11-RAD50-NBS1 (MRN) complex, ATM is activated and HR is initiated (Williams et al., 2007). The DNA repair protein RAD50 has ATPase domains interacting with MRE11 and associating with DNA ends (Williams et al., 2007). MRE11 acts as exo- and endonuclease initiating the first step of HR that requires end resection of the 5'end by exonucleases to generate 3' single stranded DNA. Following this end resection, the 3'ssDNA can directly be annealed to the homologous sequences (**Fig. 21D**). The third subunit of this complex is NBS1 that acts with MRE11 and recruits ATM. NSB1 function is not yet completely understood but most likely it forms ssDNA oligos involved in end resection (Jazayeri et al., 2008; Kanaar and Wyman, 2008; Lee and Paull, 2005). DNA end resection takes place during S and G2 phase of the cell cycle in the presence of sister chromatids that are needed for HR. The generated 3'ssDNA leads to RPA accumulation that in consequence leads to ATR activation. RPA is removed from the 3'ssDNA and RAD51 filaments are assembled resulting in RAD51-dependent strand invasion of the sister chromatid creating during S/G2-phase forming D loop structures that migrate following the DNA synthesis (West, 2003). The D-loop structures are either cleaved or displaced resulting in crossover or non-crossover events, respectively. RAD51 recombinase assembles to mediate strand invasion dependent on CDK phosphorylation of BRCA2 that is bound to the ssDNA. This is limited to S/G2 phase of the cell cycle and leads to the initiation of HR (Esashi et al., 2005; West, 2003). Alternatively, double holiday junctions (HJ) are formed capturing the second end by branch migration (West, 2003). Solving the HJs can result in crossover or non-crossover events (**Fig. 21B**).

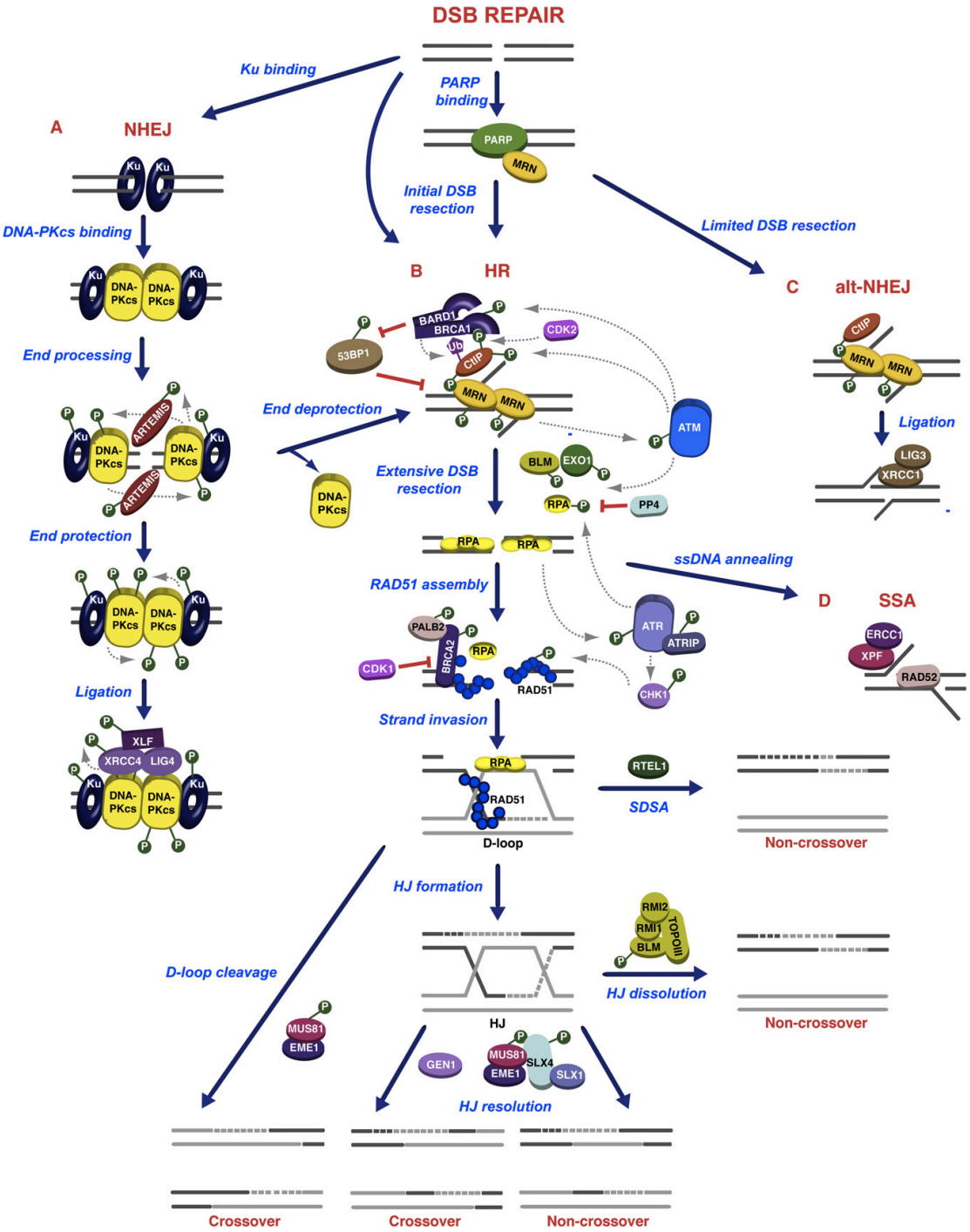

Figure 21. Alternative DNA Repair Pathways Involved in the Repair of Double-Strand Breaks
A) Ku associates to DSBs and recruits DNA-PKcs and promotes NHEJ. DNA ends assemble DNA end protection factors to facilitate the direct ligation of the ends. B) HR is initiated with the recruitment of MRN to DSBs by PARP. This mediates DSB resection to promote homologous recombination in S and G2. After DSB resection and formation of RPA-coated 3' ssDNA ends RPA is displaced from the 3' ssDNA ends strand invasion into homologous DNA sequences is started. The formed D loops can be cleaved displaced to generate crossover or noncrossover events, respectively. C) Limited DSB resection in G1 results in alternative NHEJ. D) Following DSB resection, 3' ssDNA ends with homologous sequences can be directly annealed by RAD52. Taken from (Ciccia and Elledge).

1.6.1.5 Mismatch repair (MMR)

The mismatch repair (MMR) pathway is highly conserved among species and can also be found in prokaryotes and yeast. The MMR is responsible for solving base-base mismatches or errors occurring during replication or recombination (insertions/deletions). These errors occur with a frequency of every 10^7 per inserted nucleotide (Baarends et al., 2001; Christmann et al., 2003; Kolas and Cohen, 2004; Modrich and Lahue, 1996). The MMR pathway in *E.coli* has been studied extensively and several MMR proteins are conserved among bacteria and humans.

The human ATPases hMutSα and hMutSβ are responsible for mismatch recognition and repair. Four hMutLs associate with hMutSs coordinating the initiation of the respective DNA repair machinery. hMutLα for example is responsible for initiating the MMR pathway whereas hMutLγ plays a role during meiosis. The first step in MMR is the binding of a MutS heterodimer to the mismatch. The sliding clamp PCNA helps with the recruitment ofMutSα/β to the newly synthesized DNA. The exonuclease EXO1 catalyses the 3'nick-directed repair. After the first step of recognizing the 3'nick and the mismatch, MutLα endonuclease incises the DNA 5' to the mismatch in a PCNA and RCF dependent manner. The next step includes EXO1 that excises the mismatch 5' → 3' starting from the MutLα-incision site until it reaches the mismatch. Pol δ is further recruited to the gapped single strand DNA and fills in the nucleotides and LigI seals the remaining nick (Hsieh and Zhang, 2017; Li, 2007).

1.7 Oxidative stress

Oxidative stress in cells is an imbalance of oxygen species content and the ability of the cell to neutralize those components. Oxidative stress is induced by exogenous sources like pollution, smoking, chemicals or radiation, but can also be induced by endogenous stressors like inflammation or metabolism. Oxidative stress is mostly caused by the formation of highly reactive oxygen species (ROS) that consist of oxygen or nitrogen molecules with one or more unpaired electrons.

ROS can be divided into three distinct groups. The first group contains the superoxide anion radical. Radicals are highly reactive due to their unpaired electron and cause severe damage by impacting cellular mechanisms that might consequently lead to cellular death (de Lamirande and Gagnon, 1993). The second group contains hydrogen peroxyde, hydroxyl and peroxyl radicals. The third group compromises all the nitrogen compounds (Agarwal et al., 2014b).

DNA is highly susceptible to oxidative stress. This might affect the DNA integrity by inducing alterations in the DNA sequence that can tremendously affect the physiology of the cell. The base guanine has a low redox potential, leading to oxidized DNA base products, such as 7,8-dihydro-8-oxoguanine (8-oxo-G) (Neeley and Essigmann, 2006). 8-oxo-G is induced upon oxidative stress in cells and is the best-investigated oxidized form of guanine, often used as a biomarker to quantify the amount of oxidative stress within cells (Burrows and Muller, 1998; Klaunig and Kamendulis, 2004; Neeley and Essigmann, 2006). The conformation of 8-oxo-G (addition of an oxo group and a nitrogen group) mimics the conformation of a thymine. Consequently, the G-to-T transversion has major consequences during the next replication cycle, when an adenosine at the opposite DNA strand is misincorporated (Neeley and Essigmann, 2006). The driving DDR for oxidation induced DNA damage is the BER pathway that specifically detects these lesions and repairs them.

1.7.1 Oxidative stress in gametes

1.7.1.1 Oxidative stress in sperm

Oxidative stress has been established as one of the main causes of male infertility and implicated in many diseases associated with infertile men (Agarwal et al., 2014b).

The formation of ROS induces oxidative stress and causes damage in sperm either through oxidation of the sperm membrane or through damaging the sperm DNA (**Fig.**

22) (Tremellen, 2008). The cell membrane of sperm harbours high levels of polyunsaturated fatty acids, which keep the sperm flexible and enable the fusion of the sperm membrane with that of the oocyte (Hwang and Lamb, 2012). Unfortunately, unsaturated fatty acids are highly susceptible to oxidative attacks and render sperm highly susceptible to oxidative damage. Moreover, the particularly susceptibility of sperm to DNA damage can also be ascribed to the lack of antioxidant protection, as a result of the restricted distribution and minimal volume of sperm cytoplasm, and a paucity of DNA repair mechanisms within a cell that possesses very little capacity for transcription or translation (Cocuzza et al., 2007; de Lamirande and Gagnon, 1995).

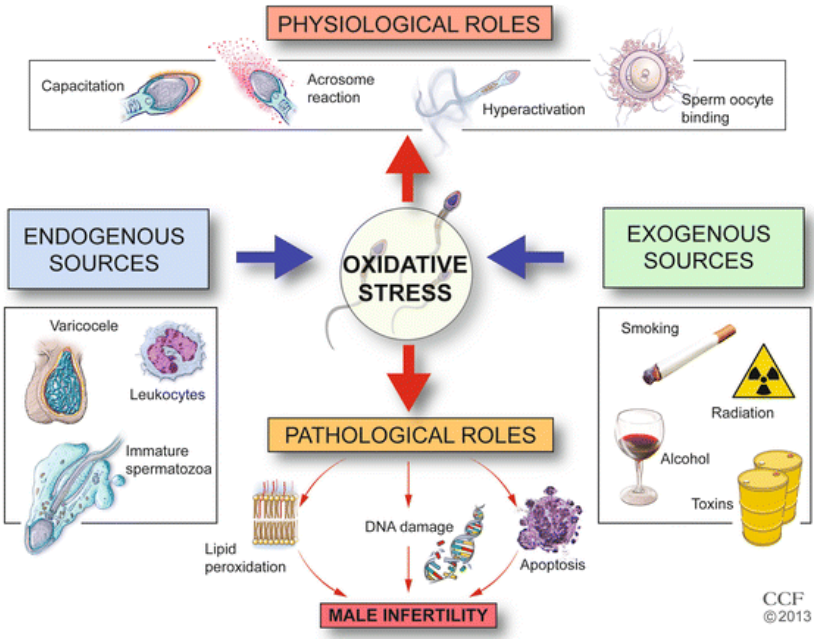

Figure 22. Sources and roles of oxidative stress in male infertility.
Taken from *https://obgynkey.com/compendium-of-oxidative-stress-related-research-from-cleveland-clinic-1993-2016/*

Oxidative DNA damage in sperm is frequently associated with errors in DNA compaction resulting from inadequate protamination of the sperm chromatin, which might increase the susceptibility to oxidative attack (Aitken and De Iuliis, 2010; De Iuliis et al., 2009). Errors during the protamination process were shown to be influenced by the paternal age, alterations in hormone levels (like FSH, LH), genetic mutations in the newly incorporated protamines or due chemotherapeutic treatment, all cases showing elevated DNA damage (Aleem et al., 2008; Plastira et al., 2007; Spermon et al., 2006).

Sources of oxidative stress in sperm are mainly described as endogenous sources like seminal leukocytes activated during infections or abnormal spermatozoa (Aitken and

Baker, 1995; Mazzilli et al., 1994). Additionally, several exogenous stressors are known to negatively influence the sperm integrity and/or function. Exogenous sources like radiation, chronic stress, air pollution or chemicals, such as herbicides, drugs, cigarette smoke or alcohol abuse were shown to drastically increase ROS concentrations in semen, resulting in DNA fragmentation, a higher number of leucocytes in the semen itself, decrease of conception rates, and increase the incidence of childhood cancer (**Fig. 22**) (Ji et al., 1997; Menezo et al., 2010; Mostafa et al., 2006; Saleh and Agarwal, 2002; Sepaniak et al., 2004; Trummer et al., 2002; Villalta et al., 1997; Zitzmann et al., 2003).

Spermatozoa are professional generators of reactive oxygen species (ROS), which appear to derive from three potential sources: sperm mitochondria, cytosolic L-amino acid oxidases, and plasma membrane nicotinamide adenine dinucleotide phosphate oxidases (NOX) (Aitken, 2017; Tremellen, 2008; Valko et al., 2007). The oxidative stress created via these sources appears to play a significant role in driving the physiological changes associated with sperm capacitation through the stimulation of a cyclic adenosine monophosphate/Protein kinase A phosphorylation cascade, including the activation of extracellular signal regulated kinase-like proteins, massive up-regulation of tyrosine phosphorylation in the sperm tail, as well as the induction of sterol oxidation (Aitken, 2017). Moreover, ROS are also essential requirements of spermatozoa for other sperm processes, such as hyperactivated motility and acrosomal reaction that lead to successful fertilization (Aitken, 2017; de Lamirande and Gagnon, 1995; de Lamirande and O'Flaherty, 2012). When generated in excess, however, ROS are detrimental for sperm hyperactivation and capacitation, reduce sperm motility, affect the fertilization potential and induce DNA damage or even cellular death (Agarwal et al., 2008; de Lamirande and Gagnon, 1995). Sperm contain high amounts of mitochondria in their midpiece, which provides the necessary energy for the progressive motility (Tremellen, 2008; Valko et al., 2007). Abnormal mitochondria function was shown to endogenously produce high levels of ROS (Sanocka and Kurpisz, 2004). Elevated ROS can induce lipid peroxidation, the generated lipid aldehydes bind to proteins in the mitochondrial electron transport chain, triggering yet more ROS generation in a self-perpetuating cycle, a process that is difficult to reverse (Bogenhagen, 1999; Liu et al., 2004a; Taylor and Turnbull, 2005).

All these results indicated that ROS are a two-edged sword in spermatozoa: a low level of ROS exposure is physiologically required to drive the signal transduction

processes associated with sperm capacitation and fertilization potential, whereas over-exposure to ROS leads to a state of oxidative stress that impairs the fertilizing potential as well as the capacity of these gametes to support the initiation of normal embryonic development (Aitken, 2017).

1.7.1.2 Oxidative stress in oocytes

In contrast to sperm, examining and quantifying oxidative stress in oocytes is more difficult since the oocyte is protected within the follicle and is surrounded with cumulus cells. Because of this, it has been proposed that the oocyte is well protected from oxygen-induced DNA damage. Additionally, the oxygen partial pressure in the female reproductive tract, also during pregnancy, is kept low (Fischer and Bavister, 1993). Nevertheless, as described for sperm, also in oocytes ROS represent the major source of DNA damaging agent, thereby inducing lipid peroxidation, inhibition of protein synthesis and depletion of the ATP pool (Ray et al., 2004). Moreover, ROS are described to negatively influence oocyte maturation, ovarian steroidogenesis, ovulation, implantation, blastocyst formation, luteolyses and luteal maintenance in pregnancy. Additionally, the age-dependent reduction in fertility in women might be also due to constant oxidative stress during meiotic arrest (de Bruin et al., 2002; Ishikawa, 1993; Jozwik et al., 1999; Sugino et al., 2000; Suzuki et al., 1999; Vega et al., 1998). DNA repair in the early embryonic development is described as a maternal trait, since DNA repair transcripts accumulated in the oocyte contribute to the repair of damaged DNA after fertilization, before the embryonic genome is activated (Menezo et al., 2007).

1.7.1.3 DNA damage response in gametes

In a physiological context, the DDR plays a key role in generating genetic diversity *via* sexual reproduction, in meiosis, the cell-division pathway that generates haploid gametes. Prior to MI, homologous chromosomes align and exchange genetic information by HR. DSB in meiosis occur in a coordinated manner through controlled breakage under the control of the specific topoisomerase II variant (SPO11) that is exclusively located to meiotic cells (Bergerat et al., 1997; Keeney et al., 1999; Keeney et al., 1997; Neale and Keeney, 2006; Romanienko and Camerini-Otero, 1999).

Alterations in DDR components have been frequently associated with infertility. For example, ATM knockout in mice leads to an arrest in meiotic pachytene stage (Xu et al., 1996). Interestingly, this arrest was also observed in many male factor infertility

cases, where sperm progenitors were shown to be arrested in development and, consequently, not able to fertilize the oocyte (Baarends et al., 2001). The NER core components, ERCC1, PCNA and RPA were found to be expressed in several stages during spermatogenesis some NER proteins were also detected in oocytes in rhesus monkeys (Hsia et al., 2003; Jaroudi and SenGupta, 2007; Shannon et al., 1999). So far, it is not known whether NER plays a role in spermatogonial cells. However, a study in 620 infertile men showed a significant association between xeroderma pigmentosum complementation group A protein (XPA) (-4) G/A polymorphism, a polymorphism affecting the promoter and altering gene transcription (Gu et al., 2010; Sugitani et al., 2016). Interestingly, *Xpa*-deficient male mice start to become infertile after 24 months due to a defect during spermatogenesis and diminished testis (Nakane et al., 2008). Mismatch repair in gametes is the most important pathway, since it detects the errors done by the replication machinery, during maturation. An oocyte undergoes approximately 20 replication cycles during its lifetime, whereas the sperm undergo about 1000 mitotic divisions until the men reaches 50 years of age. The mutation rate in the germline is estimated about 0.1%, nevertheless this rather small percentage of mutations accumulates during mitosis and is therefore thought to drive evolution within species (Agulnik et al., 1997; Hurst and Ellegren, 1998). Knockout mice for MMR components showed several symptoms, including male and female infertility, predisposition for hereditary colon cancer or defects in meiotic recombination (Arnheim and Shibata, 1997; Baker et al., 1996; Edelmann et al., 1996). Additionally, MMR KO animals showed severe defects in homologous recombination during meiosis, leading to the conclusion that MMR plays a major role in faithfully fulfilling homologous recombination during meiosis (Baarends et al., 2001). MMR activity declines during spermatogenesis since the cells become mitotically arrested. In the female germ cells, MMR becomes activated after finishing DNA replication interestingly, MMR-specific proteins were found in human MII oocytes and even blastocysts (Jaroudi et al., 2009).
Another important factor to be taken into consideration for male germ cells is that the apoptotic pathway that serves to eliminate defect stem cells is active only at the beginning of spermatogenesis whereas the ability to undergo apoptosis is lost later in spermatogenesis (Lewis and Aitken, 2005). Accordingly, sperm harbouring DNA damage are even able to fertilize oocytes, suggesting that the damage is recognized and repaired during early embryonic development with the help of the repair machinery stored in the oocyte (Aitken and Krausz, 2001; Brandriff and Pedersen, 1981).

Until recently, the DNA repair in mature spermatozoa has been considered to not take place due to the high level of DNA compaction observed in these cells. Interestingly, the first enzyme of the BER pathway, 8-oxoguanine DNA glycosylase 1 (OGG1), a DNA glycosylase that excises 8-oxo-G, has been identified in the chromatin of human spermatozoa (Smith et al., 2013). This sperm-derived OGG1 was not only found to be present at both the mRNA and protein level, but was also capable of cleaving 8-oxo-G adducts from sperm nuclear DNA to create the corresponding abasic sites. Despite the presence of OGG1 in sperm chromatin, the subsequent enzymes of the BER pathway, APE1 and XRCC1, could not be detected within human spermatozoa, suggesting that this repair pathway can only be driven to completion by the oocyte, post-fertilization (Smith et al., 2013). Interestingly, a recent study, utilizing the mouse model, determined a marked acceleration of 8-oxo-G repair in the mouse oocyte/zygote by the BER pathway following fertilization (Lord and Aitken, 2015). Specifically, it was shown that fertilization initiates post-translational modification to BER enzymes such as OGG1 and XRCC1, causing nuclear localization and accelerated 8-oxo-G excision. Remarkably, the expression of OGG1 in oocytes is relatively low whereas in the male germ line OGG1 is the only constituent of the BER pathway. These results proposed that the male and female germ lines collaborate in the repair of oxidative DNA damage, and highlight the necessity of OGG1 activity in the sperm cell prior to fertilization to lower the burden of 8-oxo-G repair on the oocyte (Lord and Aitken, 2015).

1.7.2 Oxidative stress in embryogenesis

Oxidative stress in embryogenesis is known to be detrimental for proper embryo development. Oxidative stress is mainly seen in *in vitro* derived embryos, since embryos developed *in utero* are kept at low oxygen pressure (2-7%), whereas *in vitro* derived counterparts have to deal with atmospheric oxygen partial pressure (20%). Many studies in different species demonstrated severe effects of oxidative stress on embryogenesis *in vitro* (Fischer and Bavister, 1993; Takahashi, 2012).

Oxidative stress in *in vivo* derived embryos mainly occurs due to the fast development of the embryo that requires high levels of energy or *via* the intake of xenobiotics or irradiation (Wells et al., 2009). The energy necessary for proper embryo development is generated by ATP production in mitochondria *via* oxidative phosphorylation and glycolysis. Unfortunately, during ATP synthesis ROS are built as a side product, and even more ROS production increases during high energetic processes that are particu-

larly susceptible to oxidative stress in embryogenesis such as embryonic genome activation, embryo compaction and hatching (Agarwal et al., 2003; Guerin et al., 2001). The exposure to high levels of ROS induce severe DNA damage and can influence the transcriptional program during embryogenesis, reduction in blastomere formation, reduction in blastocyst formation, apoptosis, and fragmentation of the embryo (Agarwal et al., 2014a; Agarwal et al., 2003; Rinaudo et al., 2006). Oxidative stress during embryogenesis may also have postnatal consequences like birth defects, postnatal functional deficits and disease (Wells et al., 2009).

Whereas oxidative stress during embryogenesis plays a minor role *per se*, the contribution of oxygen-induced DNA damage from the parental genomes however, does play a crucial role and is a major factor that zygotes have to deal with in order to ensure embryonic integrity.

1.7.2.1 DNA damage response in embryogenesis

Spermatozoa and oocyte accumulate oxidative DNA lesions that contribute to the zygote. The repair of these lesions prior zygotic S-phase is inevitable for ensuring embryonic integrity and healthy offspring. As described in the previous chapters, spermatozoa are highly susceptible to oxidative stress and contain reduced DNA damage response capacity (Aitken and Baker, 1995; O'Flaherty et al., 2006). Consequently, it is traditionally thought that repair is achieved after fertilization, in the zygote, using the repair factors provided by the oocyte (Menezo et al., 2007; Shimura et al., 2002). However, the embryonic cell cycle differs from the cell cycle described in somatic cells since it lacks a gap phase before and after replication (Newport and Kirschner, 1982a). This fast cell cycle progression facilitates the fast and synchronous cleavages that occur during early stages of development. Additionally, the embryonic cell cycle lacks the usual checkpoints, which arrest cell cycle due to incomplete replication, DNA damage or disrupted spindles (Conn et al., 2004). So far it is not completely understood how mammalian zygotes respond to DNA damage. Induced DNA damage revealed that zygotes lack the usual G1/S or G2/M checkpoints (Baart et al., 2004; Shimura et al., 2002). DNA damage is detected during sperm head decondendsation and induces p53 phosphorylation that is distributed in the male pronucleus and is further distributed across the cytoplasm to the maternal pronucleus ensuring a crosstalk between the two pronuclei (Shimura et al., 2002). p53 usually induces a cell cycle arrest at the G1/S border. Interestingly, in mouse zygotes the arrest did not occur at the

G1/S border but during S-phase and this process was p53-dependent, suggesting that this represents an embryonic specific checkpoint. (Shimura et al., 2002). p21 is another well known cyclin dependent kinase inhibitor that is activated either p53-dependently or independently and regulates G1/S and G2/M transition (Baus et al., 2003; Gartel and Tyner, 2002; Taylor and Stark, 2001). Mouse embryos that were obtained after fertilization with irradiated sperm surprisingly did not arrest at zygote stage but arrested only after 2.5 to 3.5 days after fertilization in a p21 dependent manner. These results suggest a hierarchy of the damage response during early embryogenesis where p53 acts from the beginning and p21 acts only after morula/blastocyst stage (Adiga et al., 2007).

Once the cell cycle is arrested an adequate DNA damage response has to occur. Prior S-phase the only available DNA repair enzymes are the ones inherited from the oocyte and indeed, the oocyte was shown to accumulate DNA repair mRNAs and proteins in their cytoplasm during oogenesis that were still present in the zygote (Menezo et al., 2007; Zheng et al., 2005). This is particularly important since transcription of new DNA repair genes is not available until 2-cell stage embryos in mice and 4-cell stage embryos in humans (Braude et al., 1988; Flach et al., 1982). Additionally, zygotes posses limited ability of 8-oxo-G repair that in consequence allows progression through S-phase in the presence of DNA damage (Aitken et al., 2009; Chabory et al., 2009; Lane et al., 2014; Ronen and Glickman, 2001; Takahashi, 2012; Vinson and Hales, 2002). Although, pre-S-phase zygotes harbour low amounts of OGG1, shortly after fertilization an increase in BER activity was detected that could not be attributed to gene expression since EGA is initiated only after 2-4 cell stage (Flach et al., 1982; Lord and Aitken, 2015). The increase in BER activity was shown to be PTM-dependent, phosphorylation on BER enzymes such as XRCC1 and OGG1 caused nuclear localisation and thus enhanced 8-oxo-G excision (Lord and Aitken, 2015). Surprisingly, when XRCC1 is lost DNA lesions on the paternal genome could anyways be repaired in a cohesin dependent manner, suggesting that HR, that requires the function of cohesion, can act redundantly to the BER pathway. Loss of cohesin in contrast, resulted in a delayed mitotic entry. This cohesin dependent pathway required the presence of the paternal genome and was shown to only act on TET3-induced damage during DNA demethylation (Ladstatter and Tachibana-Konwalski, 2016). The involved repair mechanisms driving DNA demethylation was described elsewhere (see **1.1.1.3**). Additionally, alternative DDR pathways (i.e. NHEJ and HR), have been pro-

posed to be implicated in the repair of DSBs in zygotes (Derijck et al., 2008; Generoso et al., 1979; Matsuda et al., 1989).

An alternative pathway of zygotes to react on DNA damage was recently postulated. In this regard, it was proposed that zygotes are generally defective of the ability to undergo apoptosis, but they are able to modulate embryonic development based on DNA damage in such a way that further progression is prohibited (Gawecka et al., 2013). Thereby, pronucleus formation seems not to be affected but the zygote sensed the DNA damage through phosphorylation of H2AX in the pPN. As consequence, replication on the pPN is delayed whereas the mPN progresses orderly. This somehow results in a delay in crossing the G2/M border, where some of the zygotes are arrested. Interestingly, the embryos that are able to pass the checkpoint eventually die at varies stages between 2-cell and blastocyst stage (Gawecka et al., 2013).

1.8 Assisted reproduction techniques (ART)

Assisted reproductive technologies encompass fertility treatments that handle the eggs, sperm or embryos outside the body, and provide a helpful approach to treat inhuman fertility (Canovas et al., 2017b). The first "test tube baby" was Louise Joy Brown, born in England on 25 July 1978. Her birth represents the cornerstone in the development of assisted reproduction. The use of ART has doubled during the last decade and makes up around 2% of the yearly born children (Canovas et al., 2017b). Reproductive biotechnologies are also widely used in large animal production. In 1981, the first calf after ART was born. Worldwide, more than 900,000 bovine embryos are produced yearly (Duranthon and Chavatte-Palmer, 2018). Cattle, together with small ruminants, account today for the largest part of the economy of large, medium or small farmers in developing countries worldwide. The use of reproductive biotechnologies has a clear economic impact since it allows shortening of generational intervals and propagation of genetic material among breeding animal populations. Although *in vitro* production has been achieved in farm animals, several existing limitations have led to varying degrees of success among different livestock. This is mostly due to differences in oocyte quality and experimental procedures for *in vitro* maturation and *in vitro* embryo developments, which are difficult to standardize between the different countries and laboratories (Perry, 2016).

1.8.1 Techniques

ART include a wide variety of techniques. The most commonly performed ART procedure is the *in vitro* fertilization (IVF), where oocytes and sperm are taken from the donors. Robert G. Edwards developed human IVF and for this work he was awarded in 2010 with the Nobel Prize in Physiology or Medicine (**Fig. 23**). Edwards' seminal achievements attracted many other researchers to the field of reproductive medicine, resulting in rapid technical development. The laparoscopic recovery of oocytes used in his study was replaced by a vaginal ultrasound-guided oocyte recovery method and cryopreservation of surplus human embryos was introduced (Trounson and Mohr, 1983). Successful IVF of *in vitro* matured human oocytes was reported in 1994 (Trounson et al., 1994), a method important to women that are sensitive to ovarian hormone stimulation protocols and to women that risk losing their ovarian pool of oocytes due to treatment of cancer. Further improvements in IVF have been made in all the stages of treatment, commencing from the initial stage of induction of ovulation to

the final step of transfer. In women, stimulation of follicles in the ovaries can be achieved through hormone therapy. As alternative to the induction of superovulation there is the possibility to recover immature oocytes from unstimulated ovaries and matured them *in vitro*. In cattle or other farm animals, oocytes are collected from slaughterhouse-derived ovaries or from live donors using ovum pick-up. Thus, in farm animals, successful IVF strongly depends on *in vitro* maturation of oocytes since they are still arrested in meiosis I. After that, IVF proceeds with the fertilization of matured oocytes with capacitated sperm followed by *in vitro* culture of zygotes until they reach the blastocyst stage. Usually, around 30-40% of blastocyst rate can be achieved by using IVF (Perry, 2016). Blastocysts formed during this period are then transferred to synchronized recipients or are frozen for future use. Because *in vitro* produced ruminant embryos are generally less cryotolerant than *in vivo* produced ones, blastocysts are mostly transferred fresh in sheep whereas in cattle, only a quarter are cryopreserved versus >60% of *in vivo* produced embryos (Dattena et al., 2000; Duranthon and Chavatte-Palmer, 2018; Papadopoulos et al., 2002; Perry, 2016).

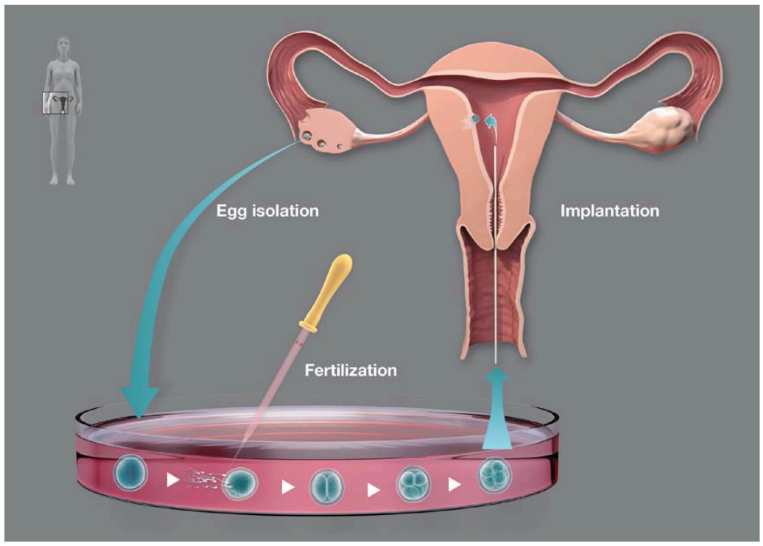

Figure 23. The principle for IVF as developed by Edwards. Oocytes arrested at the metaphase stage of meiosis II are retrieved prior to ovulation from the ovary by laparoscopy. The oocytes are placed in a culture dish and mixed with sperm in a medium that promotes sperm activation *in vitro*. The fertilization process results in the formation of an embryo that undergoes a number of cell divisions *in vitro*. The embryo is transferred back to the uterus at the 8-cell stage. The embryo will divide further in the uterus until it reaches the blastula stage and thereafter implant into the wall of the uterine lining, the endometrium. Taken from https://www.nobelprize.org.

Intracytoplasmatic sperm injection (ICSI) is a popular method used in assisted conception, and live offspring have been born from a variety of species, including humans. ICSI differs from IVF since it applies the mechanical injection of a single

sperm cell directly into the cytoplasm of a mature metaphase II oocyte bypassing natural process of sperm oocyte interaction (Salamone et al., 2017). The other steps (oocyte maturation and *in vitro* embryo development) are the same in ICSI and IVF. ICSI is an effective treatment for men with infertility and is usually applied in patients with very low sperm count, poor morphology and motility. However, the success of ICSI has been limited in farm animals (Salamone et al., 2017). The most extreme case is the cow, whose fertilization rates after ICSI are critically low (Arias et al., 2014; Chung et al., 2000; Devito et al., 2010). In sheep, although fertilization rates after ICSI can be improved by artificial activation treatments, development to blastocyst continues to be low (Shirazi et al., 2011). With regard to pigs, ICSI became an alternative fertilization technique for research purposes, since IVF produces high rates of polyspermia (Coy and Romar, 2002). In contrast to other species, the use of ICSI for elite horse reproduction has increased in recent years (Salamone et al., 2017). In this species, embryo production by IVF continues to be a challenge, since it has not been possible to obtain repeatable results (reviewed by (Leemans et al., 2016)). For this reason, the combination of ovum pick-up and ICSI followed by non-surgical embryo transfer to recipient mares is the current routine protocol for *in vitro* embryo production in horses. In recent years, surprising efficiency of this protocol ended in its inclusion in commercial breeding programs (Galli et al., 2014).

Somatic cell nuclear transfer (SCNT) is a technique in which the nucleus of a somatic cell is transferred into an enucleated metaphase-II oocyte for the generation of a new individual, genetically identical to the somatic cell donor. Dolly, the sheep, born in 1996, was the first mammal cloned using SCNT (Wilmut et al., 1997). Somatic cloning may be used to generate multiple copies of genetically elite farm animals, to produce transgenic animals for pharmaceutical protein production or xenotransplantation (Tian et al., 2003). SCNT is used commercially for a very limited number of animals. Among livestock, cattle have been cloned in the greatest number because of the potential commercial interests of the cattle industry and breeders (Galli et al., 2014).

1.8.2 Epigenetic impact of ART

As discussed in the previous chapters, early stages of mammalian embryonic development have been shown to be very sensitive to their microenvironment, with long term effects on fetal, postnatal and adult health. ARTs are conducted under different

conditions than natural conception and chemical and physical variants in the environment of gametes and embryos substantially differ from physiological conditions (Duranthon and Chavatte-Palmer, 2018).

Epigenetic risks in ART born children are often a matter of concern. Examples of this are the Angelman and Beckwith-Wiedemann syndromes, which present defects of genomic imprinting. It was reported 71% of the Angelman's Syndrome patients among IVF/ICSI born children versus 5% after natural conception, and 90% of the Beckwith-Wiedemann cases in IVF/ ICSI born children versus 40–50% after natural conception (Manipalviratn et al., 2009). Evidence also indicated DNA methylation differences at specific imprinted loci in cord blood, placenta or mouth cells of IVF/ICSI conceived children compared to naturally conceived controls (reviewed in (Duranthon and Chavatte-Palmer, 2018)). Large scale analyses have also provided further evidences that ART or associated subfertility may be associated with genome-wide changes in DNA methylation, and these changes appear to be, at least in part, due to epigenetic instability in ART pregnancies (Melamed et al., 2015). However, since ART procedures are most often applied in a context of couple infertility/subfertility, confounding effects are always difficult to exclude. Thus, results obtained in animals using fertile males and females may help discriminate effects linked to infertility/subfertility and effects due to ART procedures *per se* (Duranthon and Chavatte-Palmer, 2018). However, also in this case, difference in species and ART techniques and procedures need also to be carefully taken into consideration.

In cattle *in vitro* production (IVP), fetal overgrowth phenomenon, most often referred to as the large offspring syndrome (LOS), has been described in late gestation, inducing parturition difficulties, and neonatal mortality (Bertolini et al., 2004). In sheep, IVP has been reported to delay development around the time of implantation (Ptak et al., 2013). As in the case of cattle, placental vascularization together with the expression of genes involved in angiogenesis and steroid receptors were shown to be affected by IVP in early gestation (Fidanza et al., 2014). These effects were associated with abnormalities in global DNA methylation in the placenta, most probably related to the reduced DNMT1 expression and enzyme activity observed at the time of implantation (Ptak et al., 2013). Interestingly, embryos for which DNMT1 expression was most affected did not survive implantation whereas those where DNMT1 expression was less affected developed to term, indicating that implantation is an important bottle-

neck for the development of IVP embryos (Duranthon and Chavatte-Palmer, 2018; Ptak et al., 2013).

Several studies have shown that ART affects DNA methylation patterns, genomic imprinting status, and imprinted gene expression in mouse, pig and cow embryos, among other species (Canovas et al., 2017a; Chen et al., 2015; de Waal et al., 2014; Salilew-Wondim et al., 2015). It has been proposed that DNA methylation might act as a sensor of the *in vitro* culture modifications and other perturbations. For example, the kinetics of DNA methylation and hydroxymethylation in rabbit embryos, as assessed by immunofluorescence, were altered by modifications in the *in vitro* culture system ("one-step" vs. "sequential") (Salvaing et al., 2016). A recent analysis observed alterations of methylation at ICRs of *H19*, *KCNQ1OT1*, and *SNRPN,* indicating that ART human preimplantation embryos possess a high frequency of imprinted methylation errors (White et al., 2015). Another study revealed alterations in expression and DNA methylation at genes related to lipid and cholesterol metabolism in ICSI-conceived fetus compared to the IVF and control groups (Lou et al., 2014). In case of humans, however, these analyses remain quite complex in their interpretation. Indeed, the patients who receive ART may differ both demographically and genetically from the general population at reproductive age. Moreover, patients requesting ART have a low fertility rate, an increased reproductive loss rate and are often of advanced age, all of which are associated with various fetal and neonatal abnormalities (Duranthon and Chavatte-Palmer, 2018).

Because of the higher frequency of defects been reported among ART-conceived infants, a recent study performed a whole-genome DNA methylation analysis from single pig blastocysts in order to detect differences between *in vivo* and *in vitro* produced embryos (Canovas et al., 2017a). This work analysed expression and DNA methylation of blastocysts produced *in vitro* either without (C-IVF) or in the presence of natural reproductive fluids (Natur-IVF). The results revealed that Natur-IVF embryos were of higher quality than C-IVF in terms of cell number and hatching ability. Moreover, Natur-IVF embryos had expression and DNA methylation patterns closer to *in vivo* blastocysts. Finally, genes involved in reprogramming, imprinting and development were affected by culture, with fewer aberrations in Natur-IVF embryos. These results clearly indicated that culture conditions in ART might affect embryo quality and opened the possibility of exploring the use of natural fluids in the human clinic in order to imitate, as far as possible, *in vivo* conditions.

Another factor that can affect ART is the building of ROS. *In vitro* produced embryos have to deal with atmospheric oxygen pressure (21%), while oxygen partial pressure in the oviduct is between 5-7% (Fischer and Bavister, 1993; Harvey, 2007). A recent study analysed expression and DNA methylation of bovine blastocysts produced *in vitro* at high (20%) or low (5%) oxygen partial pressure and found that embryos under high oxygen partial pressure possessed elevated ROS abundance and presented altered expression of the epigenetic-associated transcripts *DNMT3A*, *H2AFZ*, *H3F3B*, *HDAC2*, *MORF4L2*, *REST*, and *PAF1*. In addition, these embryos have increased global DNA methylation, suggesting that DNA hypermethylation is mediated by the deregulation of epigenetic-related enzymes due to oxidative stress (Bomfim et al., 2017). A clear readout of this study is the necessity to optimize devices that avoid the exposure of the embryos to even subtle variations in their environmental conditions.

As described in the previous chapters, preimplantation embryo development experiences a highly controlled dynamic DNA methylation. The impact of ARTs on the DNA methylation profile and consequently gene expression highlights the importance to understand health risks that may be associated with ART by increasing the safety of these technologies. Research on ART procedures, deciphering their consequences on DNA methylation, as well as establishing alternative, improved or complementary methods to minimize the risks, are more than ever necessary, considering the increasing numbers of people who will be using ART in the coming years (Canovas et al., 2017a).

2. Aims

Infertility affects around 15% of all couples of reproductive age, with about 50% being associated with abnormalities in the male. Most of the cases of male infertility are caused by abnormal spermatogenesis and failure in sperm function. Reactive oxygen species (ROS)-induced oxidative stress is well-known to play a major role in male factor infertility. Sperm are particularly susceptible to the damaging effects of ROS since their cell membrane is composed of large amounts of unsaturated fatty acids, which can be oxidized, and contain few amounts of scavenging enzymes able to neutralize ROS. These factors can affect membrane integrity, motility as well as the ability to fertilize oocytes. Furthermore, DNA fragmentation may harm the paternal genetic contribution to the developing embryo. The post-meiotic phase of mouse spermatogenesis is very sensitive to the genomic effects of environmental mutagens because as soon as male germ cells form mature sperm they progressively lose the ability to repair DNA damage. To a certain extent the maternal repair machinery in the zygote can repair DNA damage of the incoming paternal genome, however extensive DNA damage in sperm can exceed the maternal repair capacities and have a direct impact on subsequent development. To this point, how oxidative stress in sperm affects early development is not fully understood.

The aim of my PhD work was to determine the impact of oxidative stress in sperm in early embryonic development and understand whether and how oxidative DNA lesions in sperm affect the epigenetic reprogramming of parental genome in zygotes.

3. Results

3.1 Research articles

3.1.1 Oxidative stress in sperm affects epigenetic reprogramming in early embryonic development

Authors: **Sarah Wyck**, Carolina Herrera, Cristina Requena-Torres, Lilli Bittner, Petra Hajkova, Heinrich Bollwein & Raffaella Santoro

Abstract Reactive oxygen species (ROS)-induced oxidative stress is well known to play a major role in male infertility. However, how oxidative DNA lesions in sperm affects early development remains elusive. Using cattle as model, we show that oxidative stress induces DNA damage in sperm and causes an arrest at later stages of embryo development, close to the onset of embryonic genome activation. Quantitative immunofluorescence analysis and ultrasensitive LC-MS-based measurements revealed that oxidative DNA lesions in sperm impair active DNA demethylation at paternal pronuclei, without affecting 5-hydroxymethylcytosine (5hmC), a Tet3-mediated modified cytosine that has been linked to DNA demethylation pathways in mouse embryos. Thus, active DNA demethylation in bovine embryos does not necessarily depend on the 5hmC pathway. Sequestration of the base excision repair (BER) component X-ray repair cross-complementing protein 1 (XRCC1) from maternal pronuclei to damaged paternal pronuclei indicates that oxidative DNA lesions are repaired by BER-mediated pathways and support a role of BER in active DNA demethylation. Finally, we provide direct evidence that cytosines are incorporated into pre-replicative zygotes, suggesting that active DNA demethylation is mediated by nucleotide replacement activities. Together, the data demonstrate that oxidative stress in sperm has an impact not only on DNA integrity but also on the dynamics of epigenetic reprogramming, which may harm the paternal genetic and epigenetic contribution to the developing embryo and affect embryo development and embryo quality.

Journal Submitted for publication

Contribution S.W. contributes to Figures 1B, 1C, 2, 3A, 3B, 4 and 5 and wrote the manuscript with RS.

3.1.2 Pramel7 mediates ground-state pluripotency through proteasomal–epigenetic combined pathways

Authors: Urs Graf, Elisa A. Casanova, **Sarah Wyck**, Damian Dalcher, Marco Gatti, Eva Vollenweider, Michal J. Okoniewski, Fabienne A.Weber, Sameera S. Patel, MarcW. Schmid, Jiwen Li, Jafar Sharif, Guido A.Wanner, Haruhiko Koseki, JieminWong, Pawel Pelczar, Lorenza Penengo, Raffaella Santoro and Paolo Cinelli

Abstract Naive pluripotency is established in preimplantation epiblast. Embryonic stem cells (ESCs) represent the immortalization of naive pluripotency. 2i culture has optimized this state, leading to a gene signature and DNA hypomethylation closely comparable to preimplantation epiblast, the developmental ground state. Here we show that Pramel7 (PRAME-like 7), a protein highly expressed in the inner cell mass (ICM) but expressed at low levels in ESCs, targets for proteasomal degradation UHRF1, a key factor for DNA methylation maintenance. Increasing Pramel7 expression in serum-cultured ESCs promotes a preimplantation epiblast-like gene signature, reduces UHRF1 levels and causes global DNA hypomethylation. Pramel7 is required for blastocyst formation and its forced expression locks ESCs in pluripotency. Pramel7/UHRF1 expression is mutually exclusive in ICMs whereas Pramel7-knockout embryos express high levels of UHRF1. Our data reveal an as-yet-unappreciated dynamic nature of DNA methylation through proteasome pathways and offer insights that might help to improve ESC culture to reproduce in vitro the in vivo ground-state pluripotency.

Journal Nature Cell Biology

DOI 10.1038/ncb3554.

External link: https://www.nature.com/articles/ncb3554

Contribution S.W. contributes to Figures 2E and 2F, Supplementary Figures 3A and 3B.

Oxidative stress in sperm affects the epigenetic reprogramming in early embryonic development

Sarah Wyck[1,2,3], Carolina Herrera[1], Cristina E. Requena[4,5], Lilli Bittner[1], Petra Hajkova[4,5], Heinrich Bollwein[1#], Raffaella Santoro[2#]

1. Clinic of Reproductive Medicine, Department for Farm Animals, University of Zurich, 8057 Zurich, Switzerland
2. Department of Molecular Mechanisms of Disease, DMMD, University of Zurich, 8057 Zurich, Switzerland
3. Molecular Life Science Program, Life Science Zurich Graduate School, University of Zurich, 8057 Zurich, Switzerland
4. MRC London Institute of Medical Sciences (LMS), London W12 0NN, UK
5. Institute of Clinical Sciences (ICS), Faculty of Medicine, Imperial College London, London W12 0NN, UK

Corresponding authors: hbollwein@vetclinics.uzh.ch; raffaella.santoro@dmmd.uzh.ch

Abstract

Reactive oxygen species (ROS)-induced oxidative stress is well known to play a major role in male infertility. However, how oxidative DNA lesions in sperm affects early development remains elusive. Using cattle as model, we show that oxidative stress induces DNA damage in sperm and causes an arrest at later stages of embryo development, close to the onset of embryonic genome activation. The levels of DNA damage response did not directly correlate with the degree of developmental defects. Instead, paternal genome harbouring oxidative lesions showed an impairment of zygotic active DNA demethylation, a process that has previously been linked with the base excision repair (BER) pathway. Quantitative immunofluorescence analysis and ultrasensitive LC-MS-based measurements revealed that oxidative DNA lesions in sperm impair active DNA demethylation at paternal pronuclei, without affecting 5-hydroxymethylcytosine (5hmC), a TET3-mediated 5-methylcytosine modification that has been linked to paternal DNA demethylation in mouse embryos. Thus, active DNA demethylation in bovine embryos does not necessarily depend on the 5hmC pathway. Recruitment of the BER component X-ray repair cross-complementing protein 1 (XRCC1) to damaged paternal pronuclei indicates that oxidative DNA lesions are repaired by BER-mediated pathways and that this process occurs at the expense of DNA demethylation. Together, the data demonstrate that oxidative stress in sperm has an impact not only on DNA integrity but also on the dynamics of epigenetic reprogramming, which may harm the paternal genetic and epigenetic contribution to the developing embryo and affect embryo development and embryo quality.

Introduction

Infertility affects around 15% of all couples of reproductive age, with about 50% being associated with abnormalities in the male (Agarwal et al., 2014b; Walczak-Jedrzejowska et al., 2013). Most of the cases of male infertility are caused by abnormal spermatogenesis and failure in sperm function. Decrease of male fertility has been associated with environmental factors (i.e. exposure to certain chemicals, heavy metals, pesticides, and heat), smoking, alcohol abuse, chronic stress, obesity, urogenital trauma, and inflammation in the male reproductive system (Esteves, 2002; Gharagozloo and Aitken, 2011; Sikka et al., 1995).

Reactive oxygen species (ROS)-induced oxidative stress is well-known to play a major role in male factor infertility (Tremellen, 2008). Oxidative stress occurs when the production of potentially destructive ROS exceeds the body's own natural antioxidant defences, resulting in cellular damage. Oxygen is important for the aerobic metabolism of spermatogenic cells (Sabeti et al., 2016; Sikka et al., 1995). In physiological amounts, ROS are essential requirements of spermatozoa for sperm processes that lead to successful fertilization, such as capacitation, hyperactivated motility and acrosomal reaction (Aitken, 2017; de Lamirande and O'Flaherty, 2012). However, sperm are particularly susceptible to the damaging effects of ROS since their cell membrane is composed of large amounts of unsaturated fatty acids, which can be oxidized, and contain few amounts of scavenging enzymes able to neutralize ROS (Cocuzza et al., 2007; de Lamirande and Gagnon, 1995). These factors can affect membrane integrity, motility as well as the ability to fertilize oocytes (Agarwal and Saleh, 2002; Aitken et al., 1989). Furthermore, DNA fragmentation may harm the paternal genetic contribution to the developing embryo (Tremellen, 2008). The post-meiotic phase of mouse spermatogenesis is very sensitive to the genomic effects of environmental mutagens because as soon as male germ cells form mature sperm they progressively lose the ability to repair DNA damage (Marchetti and Wyrobek, 2008; Olsen et al., 2005). Consequentially, it is believed that DNA damage in sperm can be repaired only post-fertilization by the maternal base excision repair (BER) machinery. However extensive DNA damage in sperm can exceed the maternal repair capacities and have a direct impact on subsequent development (Marchetti et al., 2007; Schulte et al., 2010). To this point, how oxidative stress in sperm affects early development is not fully understood.

DNA methylation is a crucial element in the epigenetic regulation of mammalian embryonic development (Messerschmidt et al., 2014). After fertilization, the two specialized and highly differentiated cells, the oocyte and the sperm, fuse to form the zygote. In order to reset the gamete's epigenome into a totipotent state, both parental and maternal genomes undergo epigenetic reprogramming. In early embryos, DNA methylation is reprogrammed genome-wide. Shortly after zygote formation, the mature sperm genome is globally demethylated, with exception of a limited number of loci including parental imprints and active retrotransposons,

which are protected from demethylation to ensure embryonic viability (Mayer et al., 2000; Oswald et al., 2000; Seisenberger et al., 2012).

It has been proposed that loss of DNA methylation at paternal genome is mediated by active DNA demethylation mechanisms as it is completed before the onset of DNA replication (Mayer et al., 2000; Oswald et al., 2000). Conversely, the maternal genome undergoes replication-dependent DNA demethylation (passive demethylation), further adding to a parental epigenetic asymmetry in the zygote. Similar DNA demethylation pattern was detected in several other mammals (i.e. human, mouse, rat and cattle) whereas in other species, such as pigs and goats, DNA demethylation is still controversial (Deshmukh et al., 2011; Fulka et al., 2006; Hou et al., 2005; Park et al., 2010; Reis e Silva et al., 2012). The mechanism of active DNA demethylation utilized in zygotes is poorly understood.

Active DNA demethylation has been proposed to be a multistep process that is initiated by modifications of the methylated cytosine or methyl group, followed by replication based dilution or removal of the modified base via a DNA repair mechanism. In the mouse zygotes, pharmacological inactivation of components of the BER pathway resulted in zygotes with significantly higher levels of paternal DNA methylation, suggesting that BER might play an important role in active DNA demethylation (Hajkova et al., 2010; Wossidlo et al., 2010). A pathway recently suggested for active DNA demethylation in the early mouse embryo involves the conversion of 5-methylcytosine (5mC) to 5-hydroxymethylcytosine (5hmC) mediated by TET3, a member of the Ten-eleven translocation (Tet) family of DNA dioxygenases that is expressed at high levels in oocytes and zygotes (Iqbal et al., 2011). In the mouse zygotes the paternal pronucleus (pPN) contains substantial amounts of 5hmC but lacks 5mC; furthermore the depletion of *Tet3* affects both 5hmC and 5mC patterns (Gu, 2011; Iqbal et al., 2011; Wossidlo, 2011).

In this study, we set out to analyse how oxidative stress affects early embryo development using the bovine system due to its similarity to early human embryo development (Santos et al., 2014; Simmet et al., 2018). Fertilization using sperm exposed to oxidative stress caused a developmental arrest at the time of embryonic genome activation. Remarkably, the levels of DNA damage response did not directly correlate with the degree of developmental defects as zygotes that progress normally in development already contained high levels of γH2AX, an

early cellular response to the induction of DNA double- and single-strand breaks (Thiriet and Hayes, 2005). On the contrary, the DNA demethylation of paternal genome harbouring oxidative lesions was impaired. The recruitment of XRCC1, a factor involved in the final step of BER pathway, to the paternal genome containing oxidative DNA lesions indicates that the zygotic BER pathway recognizes and repairs DNA lesions at the expense of DNA demethylation. Remarkably, this impairment of active DNA demethylation did not affect 5hmC levels in zygotes, indicating that other 5hmC independent processes are implicated in active DNA demethylation in bovine embryos. Together, our study demonstrates that next to the impact on DNA integrity, oxidative stress in sperm has a direct effect on the dynamics of epigenetic reprogramming. This in turn may harm the paternal genetic and epigenetic contribution to the developing embryo and affect embryo development and embryo quality. Last, but not least our results reveal species-specific epigenetic differences between bovine and mouse embryos and gametes that will facilitate the understanding of the dynamics of DNA methylation in early development.

Results

Oxidative stress in sperm affects early embryonic development

To determine whether and how oxidative stress in sperm affects early embryonic development, we aimed to use conditions that induce DNA damage in sperm without harming its fertilization capacity. We treated cryopreserved sperm of a fertile bull from an approved artificial insemination (AI)-station with 100 μm H_2O_2 for one hour and analysed the effects of this treatment on sperm motility, morphology and DNA integrity. Higher concentrations of H_2O_2 induced cell death (data not shown). We performed sperm chromatin structure assay (SCSA), which yields information on strand breaks but also reveals the presence of DNA adducts or abasic sites. As expected, the DNA fragmentation index (DFI) in sperm significantly increased upon H_2O_2 treatment (Control: 3% DFI; H_2O_2: 7% DFI) (**Fig. 1A**). Next, we measured the effects of oxidative stress on progressive motility and morphology by performing computer assisted sperm analysis (CASA) that is routinely used in sperm quality control. Progressive motility of the sperm was reduced in the group treated with H_2O_2 (Control: 79.5% motile sperm; H_2O_2: 24.2% motile sperm) (**Fig. 1B**). In contrast, the overall morphology was not greatly af-

fected upon H_2O_2 treatment (normal morphology: control, 99.5%; H_2O_2, 87.1%) (**Fig. 1C**). Finally, to determine whether these oxidative stress conditions affect the penetration of sperm into the oocyte, we measured the fertilization rate by performing *in vitro* fertilization (IVF) using slaughterhouse oocytes and H_2O_2-treated and untreated bovine sperm. After H_2O_2 treatment, sperm were extensively washed to ensure that the oxidative stress was only limited to sperm itself without affecting oocyte integrity. Fertilization rate was measured by staining the pronuclei of the presumptive zygotes with DAPI and quantifying the number of obtained zygotes relative to the total number of oocytes used for each IVF cycle (**Fig. 2A**). Using these conditions, we did not observe remarkable changes in the fertilization rate (Control: 75.0 ± 1.5 %; +H_2O_2: 69.0 ± 1.9%) (**Fig. 2A**). These results indicate that the conditions used for oxidative stress induces DNA damage without impacting the fertilisation capacity of the sperm.

To determine whether and how oxidative stress in sperm affects the early steps of embryo development, we performed IVF and measured cleavage rate and blastocyst formation of embryos derived from sperm of control and H_2O_2-treated groups. A first critical checkpoint in early embryonic development is the capability of the growing embryos to undergo the first cell divisions. We quantified the first cell division of embryos 24 hours after IVF by calculating the number of cleaved embryos (2-cell stage and further) vs. the total number of oocytes used in each IVF experiment (**Fig. 2B**). In control samples, we obtained a cleavage rate of 57.0 ± 2.4% whereas the cleavage rate after IVF with sperm treated with H_2O_2 was 42.3 ± 3.2%, indicating that oxidative stress in sperm induces some defects in this early stage of development.

Next, we analysed the impact of oxidative stress in sperm on further developmental progression. Blastocyst formation was measured by calculating the number of blastocysts obtained 8 days after IVF vs. the number of cleaved embryos obtained 24 hours after IVF (2-cell stage and further) (**Fig. 2C**). Blastocyst formation in the control group was 40.3 ± 4.4%. Remarkably, the number of blastocysts originated from fertilization with sperm treated with H_2O_2 was drastically reduced (9.0 ± 2.7%). These results indicate that H_2O_2 treatment of sperm induces major defects after the first cleavage. Embryonic genome activation (EGA) in bovine embryos starts at 4-cell stage and this is considered another important checkpoint of early embryonic development (Graf et al., 2014). Therefore, we asked whether embryos fertilized with H_2O_2-

treated sperm were arrested at this time point. We monitored the number of embryos of control and H_2O_2 groups 36 hours after fertilization and found that 49.3 ± 0.7% of embryos derived from fertilization with sperm treated with H_2O_2 were still at 2- or 4-cell stages while the majority of embryos of the control group reached further developmental stages (**Fig. 2D**).

Taken together, these results indicate that oxidative stress in sperm affects early embryonic development and that the major defects occur in later phase of development, closed to embryonic genome activation.

The BER machinery is recruited to the paternal genome of zygotes generated from sperm harbouring oxidative DNA lesions

To determine the extent of DNA damage at the paternal pronucleus of zygotes generated with sperm harbouring oxidative DNA lesions, we measured γH2AX, an early cellular response to the induction of DNA double- and single-strand breaks (Thiriet and Hayes, 2005). Surprisingly, γH2AX was abundantly present at both maternal and paternal pronuclei of the control zygotes, which however progress normally through early development (**Fig. 3A**). As it will be discussed later, the presence of γH2AX at both pronuclei of bovine zygotes differs from the exclusive localization of γH2AX at the pre-replicative paternal pronuclear stage described in mouse zygotes (Wossidlo et al., 2010; Ziegler-Birling et al., 2009a). The abundance of γH2AX signal under unperturbed conditions did not allow detecting a significant increase at paternal genome that underwent oxidative damage prior fertilization. These results indicated that the levels of γH2AX did not directly correlate with the arrest in early embryo development observed in embryo obtained with sperm containing oxidative DNA lesions.

Since all major DNA repair pathways are less functional in late spermatids and sperm (Marchetti and Wyrobek, 2008), we asked whether the BER machinery in zygotes has the potential to repair the paternal genome harbouring oxidative DNA lesions. We measured the localization of XRCC1 (X-ray repair cross-complementing protein 1), a factor involved in the final step of BER pathway that serves as scaffold for DNA ligases in the ligation of the DNA strand nick (Marsin et al., 2003; Vidal et al., 2001) (**Fig. 3B**). In control zygotes, XRCC1 was equally distributed between paternal and maternal pronuclei. In contrast, in zygotes obtained with sperm that underwent oxidative stress, a large portion of XRCC1 was recruited to the

paternal pronucleus. These results indicated that oxidative lesions induced in the sperm prior to fertilization can be repaired in zygotes and that the BER pathway is implicated in this DNA damage response. Together these data suggest that DNA damage response cannot be the only reason for embryo developmental arrest since zygotes that progress normally in development already contain high level of DNA damage and have the potential to repair sperm DNA lesions through BER pathway.

Oxidative stress in sperm impairs active DNA demethylation in the paternal pronucleus

The results described above implicated the BER pathway in the repair of oxidative DNA lesions of the paternal genome in zygotes. However, the BER pathway has also been implicated in the active DNA demethylation of the paternal genome in the mouse zygotes (Hajkova, 2010; Wossidlo, 2010). Pharmacological inactivation of the BER core components - APE1 (apurinic/apyrimidinic endonuclease) and PARP1 (poly(ADP-ribose) polymerase family, member 1) - resulted in zygotes with significantly higher levels of DNA methylation in the paternal pronucleus (Hajkova et al., 2010). Moreover, XRCC1 was shown to have a pronounced chromatin association in the paternal pronucleus of mouse zygotes (Hajkova et al., 2010). The implication of BER in both DNA repair and active DNA demethylation activities at the paternal genome prompted us to ask whether the paternal genome containing DNA lesions could be efficiently DNA demethylated.

To test whether oxidative stress in sperm affects DNA demethylation, we measured 5mC in bovine zygotes by immunofluorescence (IF) using anti-5mC specific antibodies. 24 hours after IVF most of the pronuclei in the zygotes reached late pronuclear stage 3 or 4 (PN3/4). The size of the two pronuclei was informative of the parental origin: the paternal pronucleus (pPN) displays a more enlarged structure, which reflects the level of chromatin decondensation, compared to the maternal pronucleus (mPN). As shown in **Figure 4A**, 24 h post IVF the pPN in control zygotes shows a dramatically reduced 5mC signal compared to the mPN, which still retained DNA methylation. These results are consistent with previous reports showing that also the paternal genome in bovine embryos undergoes DNA demethylation (de Montera et al., 2013; Lepikhov et al., 2008; Wossidlo, 2011). Remarkably, zygotes fertilized with sperm treated with H_2O_2 retained higher levels of DNA methylation, indicating that the active DNA

demethylation process in the pPN is compromised (**Fig. 4A**). The pPN volume of H_2O_2-treated group was similar to the control, suggesting that impairment of DNA demethylation was not due to defects in chromatin decondensation (**Supplementary Fig. 1**). In mice, DNA demethylation of the paternal genome is accompanied by the establishment of cytosine hydroxymethylation (5hmC), a reaction that has been implicated in the loss of DNA methylation (Kriaucionis and Heintz, 2009; Tahiliani, 2009). To test whether the impairment of DNA demethylation correlated with changes in 5hmC levels in the paternal pronuclei, we analysed 5hmC content by IF using specific 5hmC antibodies. Interestingly, IF analyses revealed that both paternal and maternal pronuclei at PN3/4 contain equal amounts of 5hmC (average mean intensity of 5hmC pPN vs mPN equal to 1.01, **Fig. 4B**). This pattern observed in bovine zygotes is similar to the 5hmC localization observed in human zygotes but differs from what has been described in mouse zygotes where 5hmC is present only in the pPN (Guo et al., 2014b; Wossidlo et al., 2010). These results indicated that 5hmC in bovine zygotes as well as in human is not only restricted to the paternal genome. Remarkably, 5hmC levels were not considerably affected in zygotes obtained with sperm containing oxidative DNA lesions, indicating that oxidative stress in sperm impairs DNA demethylation without altering global 5hmC levels (**Fig. 4B**). Recent results have revealed that in mouse zygotes the loss of paternal 5mC and accumulation of 5hmC are temporally disconnected, with a first wave of DNA demethylation that is independent of 5hmC followed by zygotic *de novo* DNA methylation activities that trigger TET3-driven methylcytosine hydroxylation (Amouroux et al., 2016). Thus, our results showing that oxidative stress in sperm impairs active DNA demethylation without altering 5hmC suggest that these paternal oxidative DNA lesions impair the first, 5hmC independent wave of active DNA demethylation. It is also important to note that 5mC and 5hmC signals cannot be directly compared since 5hmC antibody shows about 10,000 fold greater sensitivity than the 5mC antibody (Amouroux et al., 2016). To provide quantitative measurements and to further support our results obtained by IF analyses, we quantified DNA methylation content of isolated 2-cell stage embryos using liquid-chromatography tandem mass spectrometry (LC-MS/MS), a highly quantitative method to measure DNA methylation (**Fig. 4C**). Consistent with the IF analysis in zygotes, 2-cell stage embryos obtained using H_2O_2 treated sperm retained higher 5mC levels than control embryos (**Fig. 4C**). Importantly, 5mC content was similar in

control and H_2O_2-treated sperm, indicating that oxidative stress has no impact on DNA methylation prior to fertilization (**Fig. 4B**). These measurements also showed that the majority of cytosine hydroxylation occurs after fertilisation as 5hmC levels were higher in 2-cell embryos than in sperm and oocyte. Interestingly, 5hmC was lower in 2-cell stage embryos generated with H_2O_2-treated sperm compared to control embryos (0.21% vs. 0.07%) (**Fig. 4C**). Considering that our IF measurements did not detect any changes in 5hmC levels in zygotes, these results suggest that oxidative stress in sperm might also have an effect on methylcytosine hydroxylation activities during/after the first zygotic replication. Accordingly, recent genome-scale DNA methylation maps for both the paternal and maternal genomes suggested that TET3 might facilitate DNA demethylation largely by coupling with DNA replication (Shen et al., 2014). Together these results indicated that oxidative DNA lesions in sperm impair active DNA demethylation of the paternal genome in zygotes, leading to alterations in the epigenetic reprogramming during early development. Moreover, the data highlighted substantial differences in the dynamic of cytosine hydroxymethylation between species, showing higher similarity between bovine and human embryos respect to mouse embryos.

Unmodified cytosines are incorporated in pre-replicative bovine zygotes

The results described above showed that the pattern of γH2AX and 5hmC differs between bovine and mouse zygotes. Both modifications have been linked to active DNA demethylation in zygote and found to be exclusively located at paternal pronuclei in mouse zygotes whereas in bovine zygotes are present at both pronuclei (**Fig. 3A, 4B**). The presence of γH2AX at mouse paternal genome supports a repair-coupled pathway of active DNA demethylation since the replacement of 5mC or its derivatives with unmodified cytosine should create DNA strand breaks and as such it should induce DNA damage response including γH2AX. The detection of 5hmC and γH2AX at both pronuclei of bovine zygotes raised the question whether also the maternal genome can undergo some minor waves of active DNA demethylation. To do so, we analysed the incorporation of unmodified cytosines in the paternal and maternal pronuclei of prereplicative zygotes by performing IVF in the presence of nucleotide analogues (EdU or EdC) and monitored their incorporation by click-chemistry 12 hour after IVF (**Fig. 5A**). The incorporation of EdU will be indicative of DNA replication, whereas the incorporation of

EdC will correspond to either DNA replication or to the replacement of an unmodified cytosine. Our pilot experiments indicated that 12 hours after IVF the majority of zygotes is in a pre-replicative state. Accordingly, only few zygotes (3 out of 14) incorporated EdU, indicating that only a small number of zygotes have already entered S phase. In contrast, 10 out of 21 analysed zygotes incorporated EdC, suggesting that unmodified cytosines are incorporated at both pronuclei in the absence of replication. To further support these results, IVF was performed in the presence of BrdU and EdC and 12 hours after IVF their incorporation was measured by double staining using anti-BrdU and click-chemistry for EdC (**Fig. 5B**). As control, we analysed zygotes that had already accomplished the first cell cycle (24 hours after IVF) and were therefore positive for both BrdU and EdC. None of the zygotes analysed 12 hours after IVF incorporated BrdU, indicating a pre-replicative state at this time point. Remarkably, 22 out of the 27 analysed zygotes showed EdC signals at both paternal and maternal pronuclei. These two different experimental approaches unequivocally demonstrated that cytosines are incorporated into the DNA of pre-replicative zygotes and further support a mechanism by which active DNA demethylation might occur via excision of 5mC or its oxidative forms followed by replacement with unmodified cytosines. Furthermore, the incorporation of unmodified cytosines at both paternal and maternal pronuclei in pre-replicative bovine eygotes is consistent with the presence of 5hmC and γH2AX at both pronuclei and suggests the occurrence of some zygotic DNA demethylation activities also at maternal genome. Locus-specific active DNA demethylation of the maternal genome was already described in mouse zygotes (Guo et al., 2014a; Wang et al., 2014). Our results thus raise the possibility that also in bovine embryos active DNA demethylation might not be exclusively restricted to the paternal genome.

Discussion

DNA damage in the male germ line is mainly caused by the presence of unbalanced reactive oxygen species, which might contribute to infertility, miscarriage and birth defects in the offspring (Aitken and De Iuliis, 2010). In this study, we evaluated how oxidative stress in sperm affects early embryo development using conditions that induced DNA damage without affecting the fertilization rate. Enhanced recruitment of the BER core component XRCC1 at pPN of

zygotes generated with sperm exposed to oxidative stress indicates that the BER pathway might be implicated in this zygotic DNA damage response. It has been suggested that early-stage embryos have a different DNA damage response compared to somatic cells, which normally activate cell cycle checkpoints (Adiga et al., 2007; Gawecka et al., 2013; Tubbs and Nussenzweig, 2017). Accordingly, the major defects of embryos obtained with H_2O_2-treated sperm were identified in later time points of development - at 2-4 cell stages - with a 78% reduction in the formation of blastocysts from embryos that progress beyond the 2-cell stage. Similar observations have been described in previous studies in cattle and primates showing that DNA fragmentation has an impact in later phase of development (Burruel et al., 2013; de Castro et al., 2016; Fatehi et al., 2006; Tesarik et al., 2004).

Why does oxidative stress in sperm induce an arrest in early embryo development only after the first cell division, at the 2-4 cell stage? We can envision several possible scenarios. In the first case, the oxidative DNA lesions present in the paternal genome cannot be properly repaired in the zygotes and consequently embryonic DNA damage response can promote, for yet unknown reasons, cell cycle arrest only after the first cell division. However, the fact that the BER machinery was recruited to damaged pPN indicates that zygotes can repair, at least in part, these lesions. Moreover, the presence of high γH2AX signal at both paternal and maternal genome of control zygotes suggests that DNA lesions alone cannot be responsible for embryo developmental arrest. Although we cannot exclude that sperm exposed to an oxidative environment may carry toxic metabolites that would then impair embryo development, it is notable that embryonic arrest occurs at the onset of bovine embryonic genome activation. Thus, a possible further explanation is that the impairment of active DNA demethylation at paternal genome might affect the expression of genes critical to development due to failure in zygotic epigenetic reprogramming.

The finding that active DNA demethylation is impaired in zygotes obtained with sperm exposed to oxidative damage provides a strong indication that this process is likely linked to DNA repair pathways. Moreover, we provide direct evidence that cytosines are incorporated into pre-replicative zygotes, further supporting a mechanism by which DNA demethylation might occur via excision of 5mC or its oxidative forms and replacement with unmodified cytosines. The accumulation of BER components at pPN of zygotes originating from sperm with

oxidative DNA lesions suggests a competition model between repair and DNA demethylation activities, where oxidative lesions at paternal DNA are repaired at the expense of DNA demethylation (**Fig. 6**). A switch in BER activity that favours the repair of oxidative lesions (e.g. 8-oxoguanine, 8-oxoG) over the replacement of 5mC or 5mC oxidized products can be explained by the different activities between DNA glycosylases, which recognize specific base modifications and generate an abasic site product (Kim and Wilson, 2012). In humans, there are six glycosylases that repair mainly oxidized DNA lesions. Interestingly, 8-oxo-guanine glycosylase 1 (OGG1) has been identified in the chromatin of human spermatozoa (Lord and Aitken, 2015; Smith et al., 2013). OGG1 can cleave 8-oxoG adducts from sperm nuclear DNA to create the corresponding abasic sites that, however, cannot be repaired in sperm due to the lack of AP endonucleases and XRCC1. Thus, the presence of already established abasic sites at pPN might explain the sequestration of BER components such as XRCC1 at the expense of DNA demethylation activities, where recognition and excision of 5mC or its derivative is initiated only post-fertilization. Another possibility is that DNA lesions inhibit the activity of the DNA glycosylase(s) responsible for the DNA demethylation (**Fig. 6**). Thymine DNA glycosylase (TDG) was implicated in DNA demethylation due to its ability to recognize and remove the oxidized forms of 5mC, 5fC and 5caC (He et al., 2011; Kohli and Zhang, 2013; Maiti and Drohat, 2011). *In vitro* biochemical analyses indicated that the removal of symmetrically methylated CpGs by TDG/TET1 complex occurs in a sequential manner and that the presence of the DNA lesions on one strand delays the nucleotide removal of the opposite strand (Weber et al., 2016). Although this can represent a possible scenario occurring at the paternal genome harbouring DNA lesions in the zygote, the factors implicated in DNA demethylation in the zygotes remain still elusive. Indeed, TET1 is present only in later stages of early embryonic development and *Tdg* deletion from the zygote has not effect on DNA demethylation (Guo et al., 2014a; He et al., 2011; Kohli and Zhang, 2013). Thus, the identification of glycosylases implicated in the excision of 5mC or its modified derivatives will be important in order to understand not only the dynamics of DNA demethylation but also the impact of DNA damage on the early embryo epigenetic reprogramming. Finally, our results excluded the possibility that DNA damage might affect protamine-histone exchange and chromatin decondensation of the paternal genome, which have been thought to be necessary for active DNA demethylation

(Lin et al., 2013; Polanski et al., 2008), as we did not observe any apparent defects in decondensation of paternal pronuclei as well as the incorporation of the early embryo epigenetic mark H3K27me3 (Santenard et al., 2010) (**Supplementary Fig. 1** and data not shown).

Importantly, our study also revealed several differences between bovine and mouse embryos. Although DNA demethylation of the paternal genome was conserved, factors previously linked to active DNA demethylation in the mouse zygotes, namely γH2AX and 5hmC, displayed a distinct localization (Iqbal et al., 2011; Wossidlo, 2010, 2011). In the mouse zygotes, γH2AX and 5hmC were shown to be present only in the pPN whereas in bovine they were equally present at both paternal and maternal pronuclei. Interestingly, a recent study showed that 5hmC in human embryos is also localized at both paternal and maternal pronuclei (Guo et al., 2014b). Thus, the similar 5hmC pattern between bovine and human embryos makes the bovine model an interesting system to better understand epigenetic remodelling in human embryo, which for ethical issues cannot be easily studied. Remarkably, the impairment of active DNA demethylation in bovine zygotes obtained with sperm exposed to oxidative stress was not accompanied by alterations in 5hmC content. These results indicated that the active DNA demethylation in bovine embryos might not completely depend on the 5hmC pathway. Remarkably, recent studies using mouse models showed that in the zygotes the loss of paternal 5mC and accumulation of 5hmC are temporally disconnected and proposed that TET3 might play a major role in preventing aberrant d*e novo* methylation from the abundant DNMT3A inherited from the oocyte (Amouroux et al., 2016). Along the same lines, it was recently shown that in the gonadal mouse primordial germ cells 5hmC was not a prerequisite for the 5mC loss and that TET1 played a role in maintaining but not driving DNA demethylation (Hill et al., 2018). Thus, the detection of 5hmC in the bovine paternal pronuclei with impaired DNA demethylation suggests that H_2O_2-mediated DNA lesions in sperm affect the first wave of active DNA demethylation that is 5hmC independent. We want also to highlight here that the setting of our experiment in the context of DNA demethylation analysis in the zygote is unique of its kind. Indeed, all the studies so far have used strategies to impair 5hmC (i.e. *Tet3* deletion) whereas the impairment of DNA demethylation was never used since it is not know how this process occurs. Therefore, our study represents the first analysis of 5hmC under conditions where DNA demethylation is impaired.

The equal presence of 5hmC in the maternal pronuclei, which do not undergo a global active demethylation, suggests that some events of pre-replicative TET3-mediated DNA demethylation can also occur in the maternal genome. This result is also consistent with the pre-replicative replacement of unmodified cytosines in the maternal pronuclei detected in this work and with previous studies showing locus-specific active DNA demethylation in the maternal genome (Guo et al., 2014a; Wang et al., 2014). Alternatively, the conversion of 5mC to 5hmC is not implicit to active DNA demethylation but more linked to passive demethylation as previously proposed (Shen et al., 2014).

Quantification of total 5mC and 5hmC content in bovine gametes revealed another peculiar epigenetic species-specific feature. 5mC and meCpG levels in mouse and human gametes were reported to be higher in the sperm than in the oocytes (Amouroux et al., 2016; Guo et al., 2014a; Zhu et al., 2018). In contrast, our measurements in bovine gametes revealed that the oocytes contain higher global 5mC compared to sperm. Thus, the different 5mC content between bovine female and male gametes underlies a novel species-specific epigenetic feature.

In a clinical context, this study has relevance in assisted reproductive techniques (ARTs) that are commonly used in human medicine and livestock breeding. Nowadays children conceived using ART account for 2% of all births, which has brought the society a growing interest in their long-term health (Canovas et al., 2017b). Moreover, *in vitro* production of bovine embryos is used worldwide for commercial purposes. Meta-analysis in human and veterinary medicine has correlated increased ROS levels in sperm to a reduction of success when using ARTs (Agarwal et al., 2005). The fact that oxidative stress in sperm induces not only DNA lesions but also epigenetic alterations strongly indicates the importance to identify sub-fertile patients that potentially harbour high levels of oxidative DNA damage within their spermatozoa. Indeed, the use of ARTs with these patients will undoubtedly increase the likelihood that a spermatozoon harbouring genetic/epigenetic lesions will achieve fertilization by bypassing a number of natural selection strategies that would normally be operating *in vivo* (Lord and Aitken, 2015). *In vitro* production of bovine embryos with frozen/thawed semen is a standard method. Exposure of sperm to high levels of ROS in the sperm freezing/thawing process was indicated as a potential inducer of DNA damage and decrease of sperm fertility (Amirat et al.,

2005; Bansal and Bilaspuri, 2010; Gurler et al., 2016). Accordingly, the supplementation of a cryopreservation extender with antioxidant has been shown to provide a cryoprotective effect on mammalian sperm quality (Bansal and Bilaspuri, 2010; Korkmaz et al., 2017). Our work has shown that oxidative stress compromises not only the integrity of sperm DNA but also its post-fertilization epigenetic reprogramming with consequent defects in early embryo development. Considering the increase use of ART in human medicine and livestock breeding in the upcoming years, optimization of the ART procedures and understanding of their effect on epigenetic reprogramming in the early embryo is a necessary step to determine health risks that may be associated with these reproductive technologies.

Acknowledgements

Work in Santoro lab is supported by the Swiss National Science Foundation (310003A-152854 and 31003A_173056). Work in Hajkova lab is supported by the MRC funding (MC_US_A652_5PY70) and by an ERC grant (ERC-CoG- 648879 – dynamicmodifications). We thank SBZ Schlachtbetriebe Zürich AG and BVN Besamungsverein Neustadt an der Aisch for the collection of oocytes and semen.

Material and Methods

Sperm chromatin structure assay

Cryopreserved semen from a bull with proven fertility from an approved artificial insemination (AI)-station was used for subsequent experiments (Besamungsverein Neustadt an der Aisch, Germany). Two 0.25 ml straws containing 15 million sperm cells/ml in an egg yolk extender were thawed in a waterbath at 37°C for 30 seconds. Separation of the sperm was performed with a gradient centrifugation (600 x g for 15 minutes) with 90% Percoll (Sigma). The sperm pellet was collected, separated into two groups (untreated and H_2O_2) and transferred in H-Talp (1 M NaCl, 32 mM KCl, 4 mM $NaH_2PO_4 \bullet H_2O$, 1U Penicillin G Na salt, 250 mM $NaHCO_3$, 250 mM Hepes, 170 mM $CaCl_2$, 49 mM $MgCl_2 \bullet 6H_2O$, 330 mM Na Lactate, 33 mM Na pyruvate, 1% (v/v) NEAAs, 2% (v/v) EAAs). Sperm in the H_2O_2 group were treated with 100 μM H_2O_2 (Sigma) for 1 hour at 37°C prior to IVF. The control group (untreated) was kept in H-

Talp without H_2O_2. Samples were centrifuged (600 x g for 3 minutes) and washed several time with H-Talp to eliminate H_2O_2 traces.

Sperm chromatin structure assay (SCSA) was performed by diluting sperm samples to a concentration of 2 x 10^6 sperm/mL with TNE buffer (0.01 M Tris-HCl, pH 7.4, 0.15 M NaCl, 1 mM EDTA). 200 µl of the sperm suspension were mixed with 400 µl of an acid-detergent solution (pH 1.2, 0.08 N HCl, 0.15 M NaCl, 0.1 % Triton X-100) and vortexed for 30 sec. 1.2 ml of acridine orange solution (6 mg/mL) in a phosphate-citrate buffer (0.2 M Na_2HPO_4, 0.1 M citric acid, 0.15 M NaCl, 1 mM EDTA, pH 6.0) were added to the sample and incubated for 3 min. Sperm chromatin structure was measured using an Epics XL-MCL flow cytometer (Beckman Coulter, Fullerton, CA, USA). Cells were exposed to a laser beam generated by a 488 nm argon laser (Laser Components, Olching, Germany). Fluorescence detectors 1 and 3 (FL1 and FL3) were used for detection of green (515-530 nm) and red fluorescence (> 630 nm), respectively. Flow cytometric data were acquired using EXPO 32 ADC XL4 Colour software (Beckman Coulter, Fullerton, CA, USA). Ten thousand events were counted per sample with a flow rate of 200-400 events per sec. Debris, which are non-sperm events, were gated out based on the forward scatter and sideward scatter dot plot by drawing a region enclosing the cell population of interest. The number of sperm showing a high degree of DNA fragmentation were determined by SCSA™ (Evenson and Jost, 2001). Cell gating and quantification of the percentage of sperm cells with high DNA fragmentation index (%DFI) was performed as previously described (Evenson and Jost, 2001) and analysed using FCS express 4 FLOW research edition (De Novo Software, Glendale, USA).

Computer assisted sperm analysis (CASA)

To assess sperm motility and morphological analysis, we used the Hamilton Thorne IVOS II CASA driven by the software version 14 (Hamilton-Thorne Research, Beverly, MA, USA) according to the manufacturer's guidelines. The sperm were Percoll centrifuged and H_2O_2 treated the same way as for the SCSA. Six µl of semen was placed in a chamber of a Leja 20-mm 2-chamber slide (Leja Products BV, Nieuw Vennep, Netherlands). The percentage of progressively motile sperm at 37 °C was assessed in a minimum of 1000 cells in no less than eight randomly selected fields, with 30 frames acquired per field at a frame rate of 60 Hz.

***In vitro* production of bovine embryos**

Bovine ovaries were retrieved from the nearby slaughterhouse and transported in 0.9% NaCl (Braun) at 38°C within 2 hours. Cumulus-oocyte-complexes (COCs) were isolated using the slicing method from Eckert and Niemann (Eckert and Niemann, 1995). Under a stereomicroscope with a warming plate at 38°C, COCs with several layers of compact cumulus cells and a homogeneous cytoplasma were selected and transferred to holding medium (Hepes-buffered TCM-199 supplemented with 10 % (v/v) fetal bovine serum).

In vitro maturation (IVM) was performed by grouping 10 COCs in 50 µl microdroplets covered with oil in BO-IVM medium (IVF Bioscience) for 18 to 22 hours with 5% CO_2 in air, saturated humidity and 38.2°C.

Sperm were treated with H_2O_2 as described above. The sperm pellet was transferred into 100 µl BO-IVF medium (IVF Bioscience) and centrifuged for 3 minutes at 600 x g. Twenty COCs were transferred into a 100 µl droplet of BO-IVF medium under mineral oil. Sperm samples were added to the IVF droplets to obtain a final concentration of 2 x 10^6 sperm/ml and cultures were performed with 5% CO_2 in air and saturated humidity at 38.2°C.

Presumptive zygotes were denuded from their cumulus cells 24 hours after IVF using a capillary (Stripper, 135 µm, Origio) and transferred in groups of ten to 40 µl microdroplets of BO-IVC (IVF Bioscience) under mineral oil (Sigma). 48 hours after IVF the cleavage rate was evaluated and the cleaved embryos were separated from the non-cleaved ones and further cultured with 5% CO_2, 5% O_2 at 38.2°C and saturated humidity.

Fluorescence microscopy and image analysis

Bovine zygotes were collected 20 hours post *in vitro* fertilization (pIVF) and incubated in 0.1% Hyuloronidase solution (w/v) (Sigma) followed by the denudation with a capillary (Stripper, 135 µm, Origio). The zona pellucida was removed by incubating zygotes with Pronase (Sigma, 5mg/ml in H_2O) for 3 minutes at 37°C. Zygotes were washed three times with PBS buffer (Sigma), fixed with 4% Paraformaldehyde (PFA) for 1 hour at room temperature (RT) and washed three times with PBS buffer. Permeabilization was performed by incubating zygotes with 0.5% Triton-X 100 (Thermo Scientific) in PBS for 15 minutes at RT followed by three washes with PBS buffer.

5mC and 5hmC immunostaining. After fixation, zygotes were incubated with 4 M HCl for 10 minutes at RT, followed by a neutralization step with 100 mM Tris-HCl (pH 8) for 10 minutes. After three times washing with PBS buffer, embryos were incubated with a blocking buffer (3% BSA, in PBS, Sigma) for 1 hour at 4°C followed by incubation with antibodies 5mC (Diagenode/C15200081-100, diluted to 1:5000) or 5hmC (Active Motif/39769, diluted to 1:500) in PBS buffer containing 1.5% BSA and 0.25% Triton-X 100) overnight at 4°C. Samples were washed three times with PBS and incubated with secondary antibodies FITC or Cy3 diluted 1:100 with PBS, 1.5% BSA and 0.25% Triton-X 100 for 2 hours at RT. After washing three times with PBS buffer samples were mounted on glass slides in mounting medium (Vectashield containing DAPI, Vector Laboratories) and analysed using an inverted Leica CTR6000 microscope (software: Leica Microsystems LAS-AF6000; Leica Microsystems, Bensheim, Germany).

γH2AX immunostaining. After fixation, embryos were incubated with a blocking buffer (PBS containing 1.5% BSA and 0.25% Triton-X-100) for 1 hour at 4°C. Samples were transferred to a 500 μl droplet containing gH2AX antibodies (Biolegend/613402) diluted 1:1000 in 1.5% BSA in PBS buffer for 2 hours at RT. Embryos were washed with 0.5% Triton X-100 in PBS for 10 minutes at RT and incubated with secondary antibodies (FITC mouse, 1:100) overnight at 4°C. After washing with PBS, samples were mounted on glass slides in mounting medium (Vectashield containing DAPI, Vector Laboratories) and analysed using a Leica microscope.

XRCC1 immunostaining. After fixation, embryos were incubated with a blocking buffer (PBS containing 3% BSA) for 1hour at 4°C. Samples were transferred to a 40 μl droplet of XRCC1 (XRCC1 Thermo Fischer/MS-1393-P0; dilution 1:500) in 1.5% BSA in PBS and covered with oil. 5μl of 0.5% Triton-X-100 were added to the droplet and samples were incubated for 2 hours at room temperature. After washing with PBS, samples were incubated with FITC-conjugated secondary antibodies diluted 1:100 with PBS buffer containing 1.5% BSA and 0.25% Triton X-100 for 2 hours at room temperature. After washing with PBS, samples were mounted on glass slides in mounting medium (Vectashield containing DAPI, Vector laboratories) and analysed using a Leica microscope.

Quantification of the immunofluorescence pictures. The images were analysed using Image J Software (ImageJ 1.48v, National Institute of Health, USA). Each pronucleus was measured

individually. The equal staining of the cytoplasmic area was subtracted (staining background). The microscope settings (exposure time and gain) within each individual experiment remained the same, to ensure comparability. Statistical analysis was performed using Graph Pad Prism (Prism for Mac OS X, Version 5.0a; two-tailed Student's *t*-test).

Mass spectrometry

Genomic DNA (gDNA) of 50 to 150 2-cell embryos or MII oocytes cleaned from cumulus cells was extracted using ZR-Duet DNA/RNA Miniprep kit (Zymo Research) following manufacturer instructions and eluted in LC/MS grade water. MII oocytes were obtained by placing the processed oocytes into maturation for 22 hours (in accordance with the maturation for the IVF procedure). gDNA extraction of sperm was performed according to a modified protocol from (Walsh and Bestor, 1999). The sperm were treated with H_2O_2 as described above (SCSA), subsequently washed in 750 µl H-Talp and centrifuged for 3 minutes at 600 x g. After centrifugation, pellet was transferred into a 200 µl of lysis buffer (10 mM Tris-HCl pH 8, 10 mM EDTA, 2% SDS and 80 mM DTT) and inverted gently. 100 µg/ml RNase A (Thermo Fisher) was added and incubated overnight at 37°C. Upon Proteinase K digestion (200 µg/ml at 55°C overnight), gDNA was purified by a phenol/chloroform/isoamyl alcohol extraction, followed by ethanol precipitation. The obtained gDNA was resuspended in 50 µl H_2O. DNA was digested to nucleosides for a minimum of 9 hours at 37°C using a digestion enzymatic mix (kind gift from NEB). All samples and standard curve points were spiked with a similar amount of isotope-labelled synthetic nucleosides: 50 fmol of dC* and dG* purchased from Silantes, 2.5 fmol of 5mdC* and 250 amol of 5hmdC* obtained from T. Carell (Center for Integrated Protein Science at the Department of Chemistry, Ludwig-Maximilians-Universität München, München, Germany). Standard curves were set up for dC and dG (Berry & ass.) from 5 pmol to 0.1 fmol, and for 5mdC (Carbosynth) and 5hmdC (Berry & ass.) from 250 fmol to 5 amol. The nucleosides were separated on an Agilent RRHD Eclipse Plus C18 2.1 × 100 mm 1.8u column by using the HPLC 1290 system (Agilent) and analysed using an Agilent 6490 triple quadrupole mass spectrometer. To calculate the concentrations of individual nucleosides, standard curves representing the ratio of unlabelled over isotope-labelled nucleoside peak responses were generated and used to convert the peak-area values to corresponding concentrations.

The threshold for peak detection was a signal-to-noise ratio (calculated with a peak-to-peak method) above 10, and the limit of quantification was 25 amol for 5mdC and 5hmdC. Final measurements were normalized by dividing by the dG level measured for the same sample.

EdU/EdC labelling

IVF medium was supplemented with either EdC (200 mM, Sigma-Aldrich/T511307) or EdU (200 mM, Invitrogen/C10337). 12 hours after fertilization, zygotes were denuded and the zona pellucida was removed. Fixation was performed with 4% PFA for 30 minutes at room temperature (protected from light). Zygotes were washed with PBS and permeabilized with PBS buffer containing 0.5% Triton X-100 for 15 minutes at room temperature. Zygotes were washed twice with PBS**,** transferred into 40 μl droplets of Click-it reaction cocktail (Invitrogen), covered with oil and incubated for 30 minutes at room temperature protected from light. Zygotes were washed with PBS and mounted on slides with Vectashield containing DAPI.

BrdU/EdC labelling

Embryos were fertilized in IVF medium supplemented with nucleotide analogues BrdU (100 μM, Roche/10280879001) and EdC (200 μM, Sigma-Aldrich/ T511307). 12 hours after IVF, zygotes were denuded and the zona pellucida was removed. Control zygotes were stained 24 hours pIVF. Zygotes were incubated with PBS and fixed with 4% PFA for 30 minutes at room temperature (protected from light). Zygotes were washed with PBS and permeabilisation was performed with 0.5% Triton-X100 in PBS for 15 minutes at room temperature. Zygotes were washed with PBS followed by denaturation with 3 M HCl for 10 minutes and a neutralization step with 100 mM Tris-HCl (pH 7.5) for 10 minutes. After washing, zygotes were transferred into 40 μl droplets of Click-it® reaction cocktail covered with oil and incubate for 50 minutes at room temperature protected from light. Samples were then washed and incubated with a solution containing anti-BrdU antibody (Roche/11170376001; 6ng/μl in 1.5% BSA and PBS) for 1 hour at RT. Zygotes were washed PBS, incubated with Cy3-conjugated secondary antibodies for 1 hour at RT, washed again with PBS and mounted on slides with Vectashield containing DAPI.

Figure legends

Figure 1

Oxidative stress reduces motility and increases DNA damage in sperm.

A. Sperm chromatin structure measurements (%DFI) of sperm treated without (control) and with H_2O_2 (+H_2O_2) were performed using the sperm chromatin structure assay (SCSA). Mean and values of two independent experiments are shown.

Progressive motility (**B**) and morphology (**C**) of sperm treated without and with H_2O_2 were analysed by computer assisted sperm analysis (CASA). Mean and values of two independent experiments are shown.

Figure 2

The developmental capacity of embryos is drastically reduced upon oxidative stress in sperm.

A. Fertilization rates of sperm treated without (control) or with H_2O_2 (+H_2O_2) were evaluated 20 hours after IVF by staining the pronuclei with DAPI. Images were acquired with an inverted Leica CTR6000 microscope (software: Leica Microsystems LAS-AF6000; Leica Microsystems, Bensheim, Germany). The fertilization capacity (%) was quantified by calculating the number of obtained zygotes vs. the total number of oocytes used in each IVF experiment. Each data point represents the mean of one of four independent experiments. Total amount of oocytes: 225 (control) and 209 (+H_2O_2).

B. Cleavage rate (%) was quantified by calculating the number of cleaved embryos (2-cell stage and further) obtained 24 hours after IVF vs. the total number of oocytes used in each IVF experiment. Each data point represents the mean of one of the four independent experiments. Total amount of oocytes: 100 (control), 123 (+H_2O_2). Arrows indicate the cleaved embryo stages.

C. Blastocyst rate (%) was quantified by calculating the number of blastocysts obtained 8 days after IVF vs. the number of embryos that reached the cleavage stage 24 hours after IVF. Each data point represents the mean of one of the four independent experiments. Total amount of oocytes: 148 (control) and 165 (+H_2O_2). Arrows indicate the blastocyst stage embryos.

D. Arrested embryos were evaluated 36 hours after IVF. Quantifications were assessed by counting the number of embryos that were arrested at 2-4 cell stages 36 h after IVF vs. the number of embryos that already reached 2-4 cell stage 24 hours after IVF. Each data point represents the mean of one of three independent experiments. Total amount of oocytes: 127 (control) and 141 (+H_2O_2).

Statistical analyses were performed using Student's *t*-test (two-tailed). Error bars indicate s.d. ns: non-significant and refers to *P*=0.091; * *P* < 0.05; ** *P* < 0.01; *** *P* < 0.0001. Maternal pronucleus: mPN/♀/continuous line; paternal pronucleus: pPN/♂/dashed line. Scale bars, 50 μm.

Figure 3

The BER machinery is sequestered to paternal pronuclei of zygotes derived from sperm exposed to oxidative stress

A. γH2AX (green) levels were assessed by immunofluorescence of zygotes 20 hours after IVF using γH2AX antibodies. Representative images of PN3/4 zygotes are shown. Quantification of γH2AX is represented as a ratio of the mean signal intensity between the two pronuclei signal (mean γH2AX intensities pPN/mPN). (*n* = 24 zygotes control and *n* = 17 H_2O_2 treated zygotes; experiment replicated three times independently.) Each data point represents the mean signal of the ratio (pPN/mPN) within an independent zygote.

B. Representative immunofluorescence images of PN3/4 zygotes 20 hours after IVF stained with XRCC1 antibody (green) are shown. Quantifications of XRCC1 are shown as ratio of the mean signal intensity between the two pronuclei signal (pPN/mPN). Each data point represents the value of four independent experiments, using 120 zygotes for the control group and 85 zygotes from +H_2O_2 groups.

Statistical analysis was performed using Student's *t*-test (two-tailed). Error bars indicate s.d.; **P* < 0.01; ns: non-significant and refers to *P*=0.075. Maternal pronucleus: mPN/♀/continuous line; paternal pronucleus: pPN/♂/dashed line. Scale bars, 50 μm.

Figure 4

Oxidative stress in sperm impairs active DNA demethylation on the paternal pronucleus.

Levels of 5mC (green) (**A**) and 5hmC (red) (**B**) in PN3/4 zygotes were assessed by immunofluorescence using 5mC- and 5hmC-specific antibodies. Representative images are shown and correspond to the 5mC (**A**) and 5hmC (**B**) signal quantification shown in the lower panels. Zygotes were analysed 20 hours after IVF. Quantification of 5mC and 5hmC are shown as ratio of the signal of the mean intensity of the paternal pronucleus (pPN) over the mean intensity signal of the maternal pronucleus (mPN) after background subtraction. Each data point represents an independent zygote (5mC control n = 27 zygotes and 5mC +H_2O_2 = 21 zygotes, three independent experiments; 5hmC control n = 52 and 5hmC +H_2O_2 n = 48, three independent experiments). Statistical analysis was performed using Student's *t*-test (two-tailed). Error bars indicate s.d., ns: non-significant **$P < 0.01$. Maternal pronucleus: mPN/♀/continuous line; paternal pronucleus: pPN/♂/dashed line. Scale bars, 50 μm.

C. Quantification of 5mC/dG by LC-MS of 2-cell embryos obtained upon IVF with control sperm and sperm treated with H_2O_2. Data are from two independent experiments. Each data point represents the mean of two technical replicates of a pool of 50 embryos.

D. Quantification of 5mC and 5hmC by LC-MS of bovine sperm untreated or treated with H_2O_2 and MII oocytes. Data are from three independent experiments. Each data point represents the mean of two technical replicates.

Figure 5

Replacement of cytosines in pre-replicative zygotes

A. Schema describes the strategy to measure replication and DNA demethylation via the incorporation of EdU and EdC in zygotes and its readout. Representative images showing zygotes with EdU (green) and EdC (green) incorporation 12 hours after IVF. Numbers refer to zygotes showing EdU or EdC incorporation relative to the total number of analysed zygotes, respectively.

B. Schema describes the strategy to measure replication and DNA demethylation via the incorporation of BrdU and EdC in zygotes and its readout. Representative images showing zygotes stained for BrdU (red) and EdC (green) incorporation 12 hours after IVF. Numbers refer

to zygotes positive for EdC signal and negative for BrdU signal relative to the total number of analysed zygotes. Zygotes 24 hours pIVF were stained and used as post-replicative control zygotes. Scale bars, 50 μm.

Figure 6

Oxidative lesions in sperm impair active DNA demethylation at the paternal genome in zygotes. The model shows the link of BER to DNA damage and active DNA demethylation. On the left, it is shown how a putative DNA glycosylase recognizes 5mC or its modified forms, giving rise to abasic sites that via the subsequent enzymes of the BER pathway (i.e. APE1 and XRCC1) allows the incorporation of unmodified cytosines. On the right, it is shown how oxidative lesions in sperm can impair DNA demethylation. Two models are here shown. In the first case, the presence of abasic sites that are established by OGG1 prior fertilization in sperm sequester XRCC1 at the expense of DNA demethylation activities, where recognition and excision of 5mC or its derivative is initiated only post-fertilization. The second model suggests that DNA lesions inhibit the activity of the DNA glycosylase(s) responsible for the DNA demethylation. In both cases, the final product is a DNA that is repaired but still contains methylated cytosines.

Supplementary Figure 1

Oxidative stress in sperm does not affect paternal genome decondensation in zygotes

Quantification of the DAPI signal of paternal and maternal pronuclei in zygotes from control and H_2O_2-treated groups.

References

Adiga, S.K., Toyoshima, M., Shiraishi, K., Shimura, T., Takeda, J., Taga, M., Nagai, H., Kumar, P., and Niwa, O. (2007). p21 provides stage specific DNA damage control to preimplantation embryos. Oncogene *26*, 6141-6149.
Agarwal, A., Allamaneni, S.S., Nallella, K.P., George, A.T., and Mascha, E. (2005). Correlation of reactive oxygen species levels with the fertilization rate after in vitro fertilization: a qualified meta-analysis. Fertility and sterility *84*, 228-231.
Agarwal, A., Durairajanayagam, D., Halabi, J., Peng, J., and Vazquez-Levin, M. (2014). Proteomics, oxidative stress and male infertility. Reproductive biomedicine online *29*, 32-58.
Agarwal, A., and Saleh, R.A. (2002). Role of oxidants in male infertility: rationale, significance, and treatment. Urol Clin North Am *29*, 817-827.
Aitken, R.J. (2017). Reactive oxygen species as mediators of sperm capacitation and pathological damage. Mol Reprod Dev *84*, 1039-1052.
Aitken, R.J., Clarkson, J.S., and Fishel, S. (1989). Generation of reactive oxygen species, lipid peroxidation, and human sperm function. Biology of reproduction *41*, 183-197.
Aitken, R.J., and De Iuliis, G.N. (2010). On the possible origins of DNA damage in human spermatozoa. Mol Hum Reprod *16*, 3-13.
Amirat, L., Anton, M., Tainturier, D., Chatagnon, G., Battut, I., and Courtens, J.L. (2005). Modifications of bull spermatozoa induced by three extenders: Biociphos, low density lipoprotein and Triladyl, before, during and after freezing and thawing. Reproduction *129*, 535-543.
Amouroux, R., Nashun, B., Shirane, K., Nakagawa, S., Hill, P.W., D'Souza, Z., Nakayama, M., Matsuda, M., Turp, A., Ndjetehe, E.*, et al.* (2016). De novo DNA methylation drives 5hmC accumulation in mouse zygotes. Nat Cell Biol *18*, 225-233.
Bansal, A.K., and Bilaspuri, G.S. (2010). Impacts of oxidative stress and antioxidants on semen functions. Vet Med Int *2010*.
Burruel, V., Klooster, K.L., Chitwood, J., Ross, P.J., and Meyers, S.A. (2013). Oxidative damage to rhesus macaque spermatozoa results in mitotic arrest and transcript abundance changes in early embryos. Biology of reproduction *89*, 72.
Canovas, S., Ross, P.J., Kelsey, G., and Coy, P. (2017). DNA Methylation in Embryo Development: Epigenetic Impact of ART (Assisted Reproductive Technologies). Bioessays *39*.
Cocuzza, M., Sikka, S.C., Athayde, K.S., and Agarwal, A. (2007). Clinical relevance of oxidative stress and sperm chromatin damage in male infertility: an evidence based analysis. International braz j urol : official journal of the Brazilian Society of Urology *33*, 603-621.
de Castro, L.S., de Assis, P.M., Siqueira, A.F., Hamilton, T.R., Mendes, C.M., Losano, J.D., Nichi, M., Visintin, J.A., and Assumpcao, M.E. (2016). Sperm Oxidative Stress Is Detrimental to Embryo Development: A Dose-Dependent Study Model and a New and More Sensitive Oxidative Status Evaluation. Oxid Med Cell Longev *2016*, 8213071.
de Lamirande, E., and Gagnon, C. (1995). Impact of reactive oxygen species on spermatozoa: a balancing act between beneficial and detrimental effects. Human reproduction *10 Suppl 1*, 15-21.
de Lamirande, E., and O'Flaherty, C. (2012). Sperm Capacitation as an Oxidative Event. Oxid Stress Appl Bas, 57-94.
de Montera, B., Fournier, E., Shojaei Saadi, H.A., Gagne, D., Laflamme, I., Blondin, P., Sirard, M.A., and Robert, C. (2013). Combined methylation mapping of 5mC and 5hmC during early embryonic stages in bovine. BMC genomics *14*, 406.
Deshmukh, R.S., Ostrup, O., Ostrup, E., Vejlsted, M., Niemann, H., Lucas-Hahn, A., Petersen, B., Li, J., Callesen, H., and Hyttel, P. (2011). DNA methylation in porcine preimplantation embryos developed in vivo and produced by in vitro fertilization, parthenogenetic activation and somatic cell nuclear transfer. Epigenetics *6*, 177-187.
Eckert, J., and Niemann, H. (1995). In vitro maturation, fertilization and culture to blastocysts of bovine oocytes in protein-free media. Theriogenology *43*, 1211-1225.
Esteves, S.C. (2002). Effect of cigarette smoking on levels of seminal oxidative stress in infertile men: a prospective study. International braz j urol : official journal of the Brazilian Society of Urology *28*, 484-485.
Evenson, D., and Jost, L. (2001). Sperm chromatin structure assay for fertility assessment. Current protocols in cytometry *Chapter 7*, Unit 7 13.
Fatehi, A.N., Bevers, M.M., Schoevers, E., Roelen, B.A., Colenbrander, B., and Gadella, B.M. (2006). DNA damage in bovine sperm does not block fertilization and early embryonic development but induces apoptosis after the first cleavages. Journal of andrology *27*, 176-188.
Fulka, J., Fulka, H., Slavik, T., Okada, K., and Fulka, J., Jr. (2006). DNA methylation pattern in pig in vivo produced embryos. Histochem Cell Biol *126*, 213-217.
Gawecka, J.E., Marh, J., Ortega, M., Yamauchi, Y., Ward, M.A., and Ward, W.S. (2013). Mouse zygotes respond to severe sperm DNA damage by delaying paternal DNA replication and embryonic development. PLoS One *8*, e56385.
Gharagozloo, P., and Aitken, R.J. (2011). The role of sperm oxidative stress in male infertility and the significance of oral antioxidant therapy. Human reproduction *26*, 1628-1640.
Graf, A., Krebs, S., Zakhartchenko, V., Schwalb, B., Blum, H., and Wolf, E. (2014). Fine mapping of genome activation in bovine embryos by RNA sequencing. Proc Natl Acad Sci U S A *111*, 4139-4144.

Gu, T.P. (2011). The role of Tet3 DNA dioxygenase in epigenetic reprogramming by oocytes. Nature *477*, 606-610.
Guo, F., Li, X., Liang, D., Li, T., Zhu, P., Guo, H., Wu, X., Wen, L., Gu, T.P., Hu, B.*, et al.* (2014a). Active and passive demethylation of male and female pronuclear DNA in the mammalian zygote. Cell Stem Cell *15*, 447-458.
Guo, H., Zhu, P., Yan, L., Li, R., Hu, B., Lian, Y., Yan, J., Ren, X., Lin, S., Li, J.*, et al.* (2014b). The DNA methylation landscape of human early embryos. Nature *511*, 606-610.
Gurler, H., Malama, E., Heppelmann, M., Calisici, O., Leiding, C., Kastelic, J.P., and Bollwein, H. (2016). Effects of cryopreservation on sperm viability, synthesis of reactive oxygen species, and DNA damage of bovine sperm. Theriogenology *86*, 562-571.
Hajkova, P., Jeffries, S.J., Lee, C., Miller, N., Jackson, S.P., and Surani, M.A. (2010). Genome-wide reprogramming in the mouse germ line entails the base excision repair pathway. Science *329*, 78-82.
He, Y.F., Li, B.Z., Li, Z., Liu, P., Wang, Y., Tang, Q., Ding, J., Jia, Y., Chen, Z., Li, L.*, et al.* (2011). Tet-mediated formation of 5-carboxylcytosine and its excision by TDG in mammalian DNA. Science *333*, 1303-1307.
Hill, P.W.S., Leitch, H.G., Requena, C.E., Sun, Z., Amouroux, R., Roman-Trufero, M., Borkowska, M., Terragni, J., Vaisvila, R., Linnett, S.*, et al.* (2018). Epigenetic reprogramming enables the transition from primordial germ cell to gonocyte. Nature *555*, 392-396.
Hou, J., Lei, T.H., Liu, L., Cui, X.H., An, X.R., and Chen, Y.F. (2005). DNA methylation patterns in in vitro-fertilised goat zygotes. Reproduction, fertility, and development *17*, 809-813.
Iqbal, K., Jin, S.G., Pfeifer, G.P., and Szabo, P.E. (2011). Reprogramming of the paternal genome upon fertilization involves genome-wide oxidation of 5-methylcytosine. Proc Natl Acad Sci U S A *108*, 3642-3647.
Kim, Y.J., and Wilson, D.M., 3rd (2012). Overview of base excision repair biochemistry. Curr Mol Pharmacol *5*, 3-13.
Kohli, R.M., and Zhang, Y. (2013). TET enzymes, TDG and the dynamics of DNA demethylation. Nature *502*, 472-479.
Korkmaz, F., Malama, E., Siuda, M., Leiding, C., and Bollwein, H. (2017). Effects of sodium pyruvate on viability, synthesis of reactive oxygen species, lipid peroxidation and DNA integrity of cryopreserved bovine sperm. Animal reproduction science *185*, 18-27.
Kriaucionis, S., and Heintz, N. (2009). The nuclear DNA base 5-hydroxymethylcytosine is present in Purkinje neurons and the brain. Science *324*, 929-930.
Lepikhov, K., Zakhartchenko, V., Hao, R., Yang, F., Wrenzycki, C., Niemann, H., Wolf, E., and Walter, J. (2008). Evidence for conserved DNA and histone H3 methylation reprogramming in mouse, bovine and rabbit zygotes. Epigenetics Chromatin *1*, 8.
Lin, C.J., Conti, M., and Ramalho-Santos, M. (2013). Histone variant H3.3 maintains a decondensed chromatin state essential for mouse preimplantation development. Development *140*, 3624-3634.
Lord, T., and Aitken, R.J. (2015). Fertilization stimulates 8-hydroxy-2'-deoxyguanosine repair and antioxidant activity to prevent mutagenesis in the embryo. Dev Biol *406*, 1-13.
Maiti, A., and Drohat, A.C. (2011). Thymine DNA glycosylase can rapidly excise 5-formylcytosine and 5-carboxylcytosine: potential implications for active demethylation of CpG sites. J Biol Chem *286*, 35334-35338.
Marchetti, F., Essers, J., Kanaar, R., and Wyrobek, A.J. (2007). Disruption of maternal DNA repair increases sperm-derived chromosomal aberrations. Proc Natl Acad Sci U S A *104*, 17725-17729.
Marchetti, F., and Wyrobek, A.J. (2008). DNA repair decline during mouse spermiogenesis results in the accumulation of heritable DNA damage. DNA Repair (Amst) *7*, 572-581.
Marsin, S., Vidal, A.E., Sossou, M., Menissier-de Murcia, J., Le Page, F., Boiteux, S., de Murcia, G., and Radicella, J.P. (2003). Role of XRCC1 in the coordination and stimulation of oxidative DNA damage repair initiated by the DNA glycosylase hOGG1. J Biol Chem *278*, 44068-44074.
Mayer, W., Niveleau, A., Walter, J., Fundele, R., and Haaf, T. (2000). Demethylation of the zygotic paternal genome. Nature *403*, 501-502.
Messerschmidt, D.M., Knowles, B.B., and Solter, D. (2014). DNA methylation dynamics during epigenetic reprogramming in the germline and preimplantation embryos. Genes Dev *28*, 812-828.
Olsen, A.K., Lindeman, B., Wiger, R., Duale, N., and Brunborg, G. (2005). How do male germ cells handle DNA damage? Toxicol Appl Pharmacol *207*, 521-531.
Oswald, J., Engemann, S., Lane, N., Mayer, W., Olek, A., Fundele, R., Dean, W., Reik, W., and Walter, J. (2000). Active demethylation of the paternal genome in the mouse zygote. Curr Biol *10*, 475-478.
Park, J.S., Lee, D., Cho, S., Shin, S.T., and Kang, Y.K. (2010). Active loss of DNA methylation in two-cell stage goat embryos. Int J Dev Biol *54*, 1323-1328.
Polanski, Z., Motosugi, N., Tsurumi, C., Hiiragi, T., and Hoffmann, S. (2008). Hypomethylation of paternal DNA in the late mouse zygote is not essential for development. Int J Dev Biol *52*, 295-298.
Reis e Silva, A.R., Bruno, C., Fleurot, R., Daniel, N., Archilla, C., Peynot, N., Lucci, C.M., Beaujean, N., and Duranthon, V. (2012). Alteration of DNA demethylation dynamics by in vitro culture conditions in rabbit pre-implantation embryos. Epigenetics *7*, 440-446.
Sabeti, P., Pourmasumi, S., Rahiminia, T., Akyash, F., and Talebi, A.R. (2016). Etiologies of sperm oxidative stress. Int J Reprod Biomed (Yazd) *14*, 231-240.
Santenard, A., Ziegler-Birling, C., Koch, M., Tora, L., Bannister, A.J., and Torres-Padilla, M.E. (2010). Heterochromatin formation in the mouse embryo requires critical residues of the histone variant H3.3. Nat Cell Biol *12*, 853-862.
Santos, R.R., Schoevers, E.J., and Roelen, B.A. (2014). Usefulness of bovine and porcine IVM/IVF models for reproductive toxicology. Reprod Biol Endocrinol *12*, 117.

Schulte, R.T., Ohl, D.A., Sigman, M., and Smith, G.D. (2010). Sperm DNA damage in male infertility: etiologies, assays, and outcomes. Journal of assisted reproduction and genetics *27*, 3-12.
Seisenberger, S., Andrews, S., Krueger, F., Arand, J., Walter, J., Santos, F., Popp, C., Thienpont, B., Dean, W., and Reik, W. (2012). The dynamics of genome-wide DNA methylation reprogramming in mouse primordial germ cells. Mol Cell *48*, 849-862.
Shen, L., Inoue, A., He, J., Liu, Y., Lu, F., and Zhang, Y. (2014). Tet3 and DNA replication mediate demethylation of both the maternal and paternal genomes in mouse zygotes. Cell Stem Cell *15*, 459-471.
Sikka, S.C., Rajasekaran, M., and Hellstrom, W.J. (1995). Role of oxidative stress and antioxidants in male infertility. Journal of andrology *16*, 464-468.
Simmet, K., Zakhartchenko, V., Philippou-Massier, J., Blum, H., Klymiuk, N., and Wolf, E. (2018). OCT4/POU5F1 is required for NANOG expression in bovine blastocysts. Proc Natl Acad Sci U S A *115*, 2770-2775.
Smith, T.B., Dun, M.D., Smith, N.D., Curry, B.J., Connaughton, H.S., and Aitken, R.J. (2013). The presence of a truncated base excision repair pathway in human spermatozoa that is mediated by OGG1. J Cell Sci *126*, 1488-1497.
Tahiliani, M. (2009). Conversion of 5-methylcytosine to 5-hydroxymethylcytosine in mammalian DNA by MLL partner TET1. Science *324*, 930-935.
Tesarik, J., Greco, E., and Mendoza, C. (2004). Late, but not early, paternal effect on human embryo development is related to sperm DNA fragmentation. Human reproduction *19*, 611-615.
Thiriet, C., and Hayes, J.J. (2005). Chromatin in need of a fix: phosphorylation of H2AX connects chromatin to DNA repair. Mol Cell *18*, 617-622.
Tremellen, K. (2008). Oxidative stress and male infertility--a clinical perspective. Hum Reprod Update *14*, 243-258.
Tubbs, A., and Nussenzweig, A. (2017). Endogenous DNA Damage as a Source of Genomic Instability in Cancer. Cell *168*, 644-656.
Vidal, A.E., Boiteux, S., Hickson, I.D., and Radicella, J.P. (2001). XRCC1 coordinates the initial and late stages of DNA abasic site repair through protein-protein interactions. EMBO J *20*, 6530-6539.
Walczak-Jedrzejowska, R., Wolski, J.K., and Slowikowska-Hilczer, J. (2013). The role of oxidative stress and antioxidants in male fertility. Cent European J Urol *66*, 60-67.
Walsh, C.P., and Bestor, T.H. (1999). Cytosine methylation and mammalian development. Genes & development *13*, 26-34.
Wang, L., Zhang, J., Duan, J., Gao, X., Zhu, W., Lu, X., Yang, L., Zhang, J., Li, G., Ci, W*., et al.* (2014). Programming and inheritance of parental DNA methylomes in mammals. Cell *157*, 979-991.
Weber, A.R., Krawczyk, C., Robertson, A.B., Kusnierczyk, A., Vagbo, C.B., Schuermann, D., Klungland, A., and Schar, P. (2016). Biochemical reconstitution of TET1-TDG-BER-dependent active DNA demethylation reveals a highly coordinated mechanism. Nat Commun *7*, 10806.
Wossidlo, M. (2011). 5-hydroxymethylcytosine in the mammalian zygote is linked with epigenetic reprogramming. Nature Commun *2*, 241.
Wossidlo, M., Arand, J., Sebastiano, V., Lepikhov, K., Boiani, M., Reinhardt, R., Scholer, H., and Walter, J. (2010). Dynamic link of DNA demethylation, DNA strand breaks and repair in mouse zygotes. The EMBO journal *29*, 1877-1888.
Zhu, P., Guo, H., Ren, Y., Hou, Y., Dong, J., Li, R., Lian, Y., Fan, X., Hu, B., Gao, Y*., et al.* (2018). Single-cell DNA methylome sequencing of human preimplantation embryos. Nat Genet *50*, 12-19.
Ziegler-Birling, C., Helmrich, A., Tora, L., and Torres-Padilla, M.E. (2009). Distribution of p53 binding protein 1 (53BP1) and phosphorylated H2A.X during mouse preimplantation development in the absence of DNA damage. Int J Dev Biol *53*, 1003-1011.

Figure 1

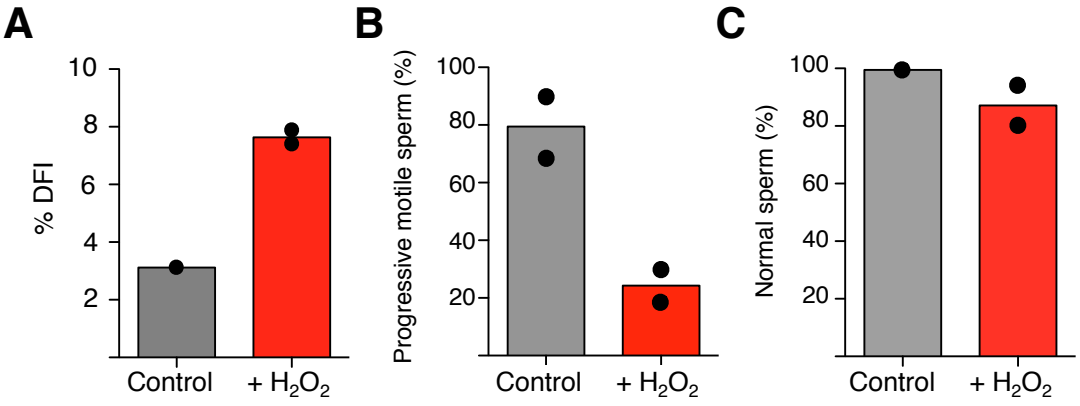
A
% DFI
10
8
6
4
2
Control
+ H2O2
B
Progressive motile sperm (%)
100
80
60
40
20
Control
+ H2O2
C
Normal sperm (%)
100
80
60
40
20
Control
+ H2O2

Figure 2

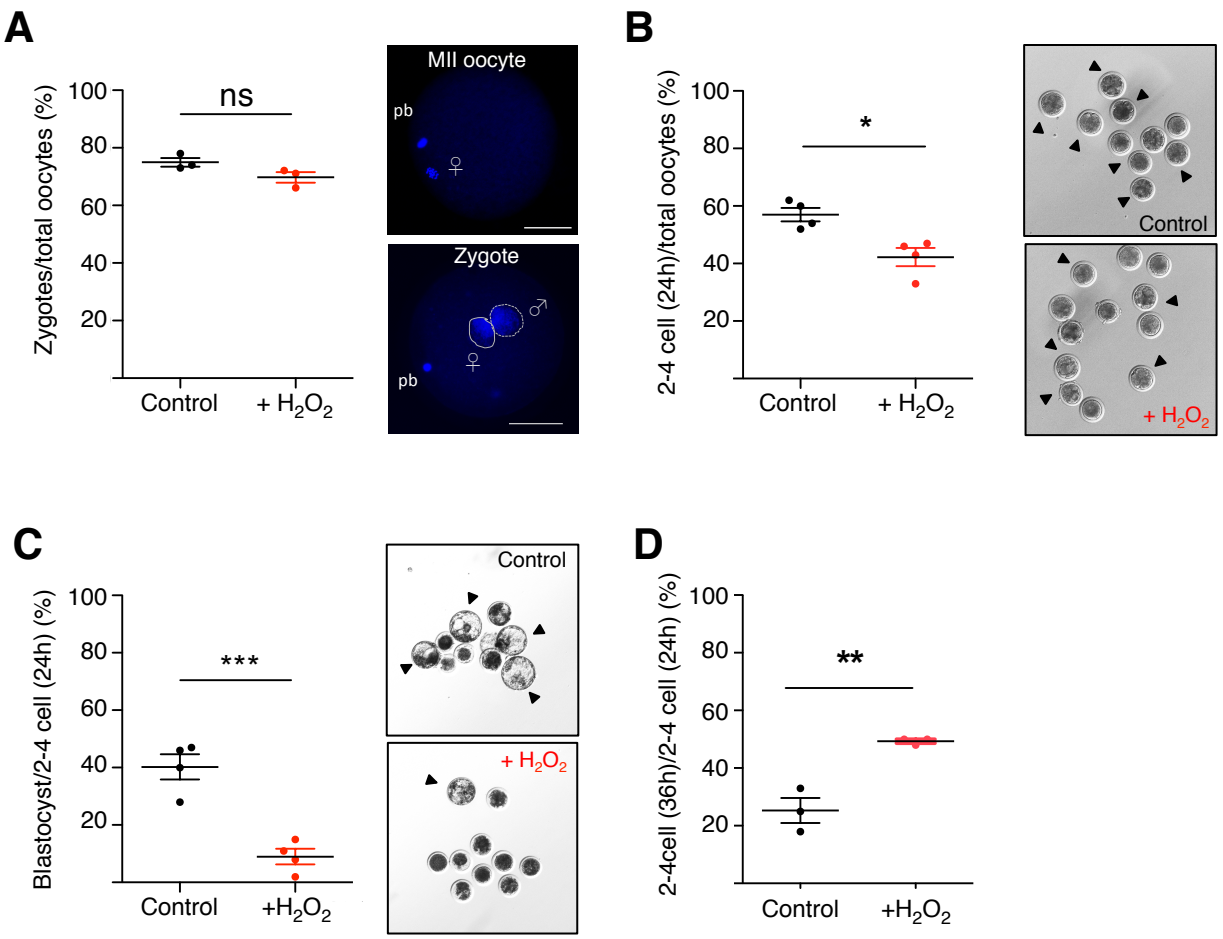
A
Zygotes/total oocytes (%)
100
80
60
40
20
ns
Control
+ H2O2
MII oocyte
pb
♀
Zygote
♂
♀
pb
B
2-4 cell (24h)/total oocytes (%)
100
80
60
40
20
*
Control
+ H2O2
Control
+ H2O2
C
Blastocyst/2-4 cell (24h) (%)
100
80
60
40
20
***
Control
+H2O2
Control
+ H2O2
D
2-4cell (36h)/2-4 cell (24h) (%)
100
80
60
40
20
**
Control
+H2O2

Figure 3

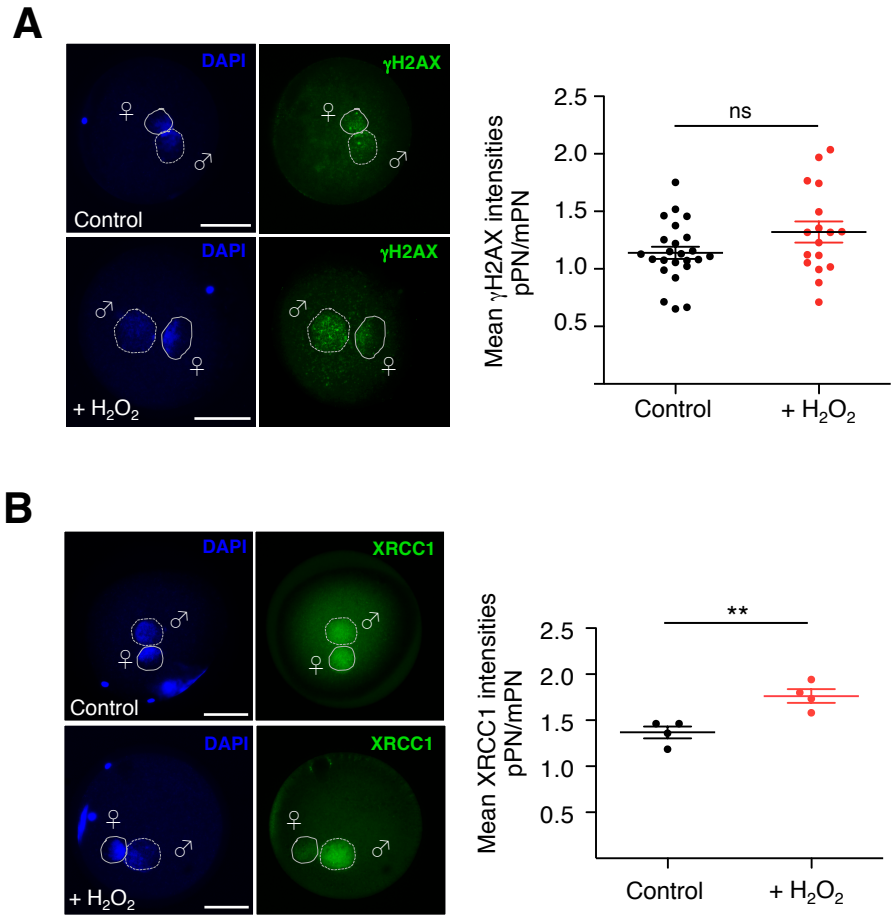
A
DAPI
γH2AX
Control
DAPI
γH2AX
+ H2O2
Mean γH2AX intensities pPN/mPN
2.5
2.0
1.5
1.0
0.5
ns
Control
+ H2O2
B
DAPI
XRCC1
Control
DAPI
XRCC1
+ H2O2
Mean XRCC1 intensities pPN/mPN
2.5
2.0
1.5
1.0
0.5
**
Control
+ H2O2

Figure 4

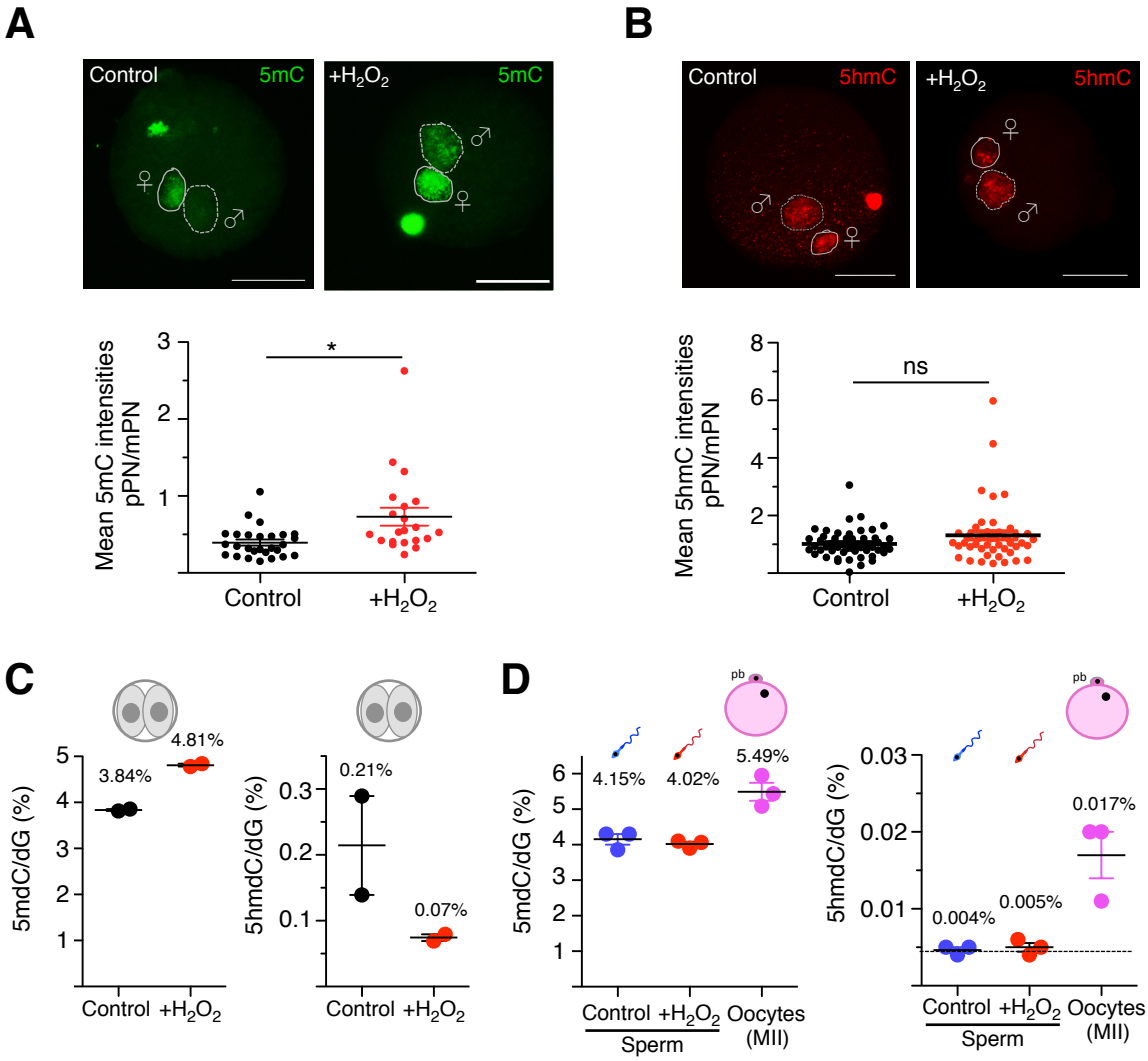
A
Control
5mC
+H2O2
5mC
Mean 5mC intensities pPN/mPN
*
Control
+H2O2
B
Control
5hmC
+H2O2
5hmC
Mean 5hmC intensities pPN/mPN
ns
Control
+H2O2
C
5mdC/dG (%)
3.84%
4.81%
Control
+H2O2
5hmdC/dG (%)
0.21%
0.07%
Control
+H2O2
D
5mdC/dG (%)
pb
4.15%
4.02%
5.49%
Control
+H2O2
Sperm
Oocytes (MII)
5hmdC/dG (%)
pb
0.004%
0.005%
0.017%
Control
+H2O2
Sperm
Oocytes (MII)

Figure 5

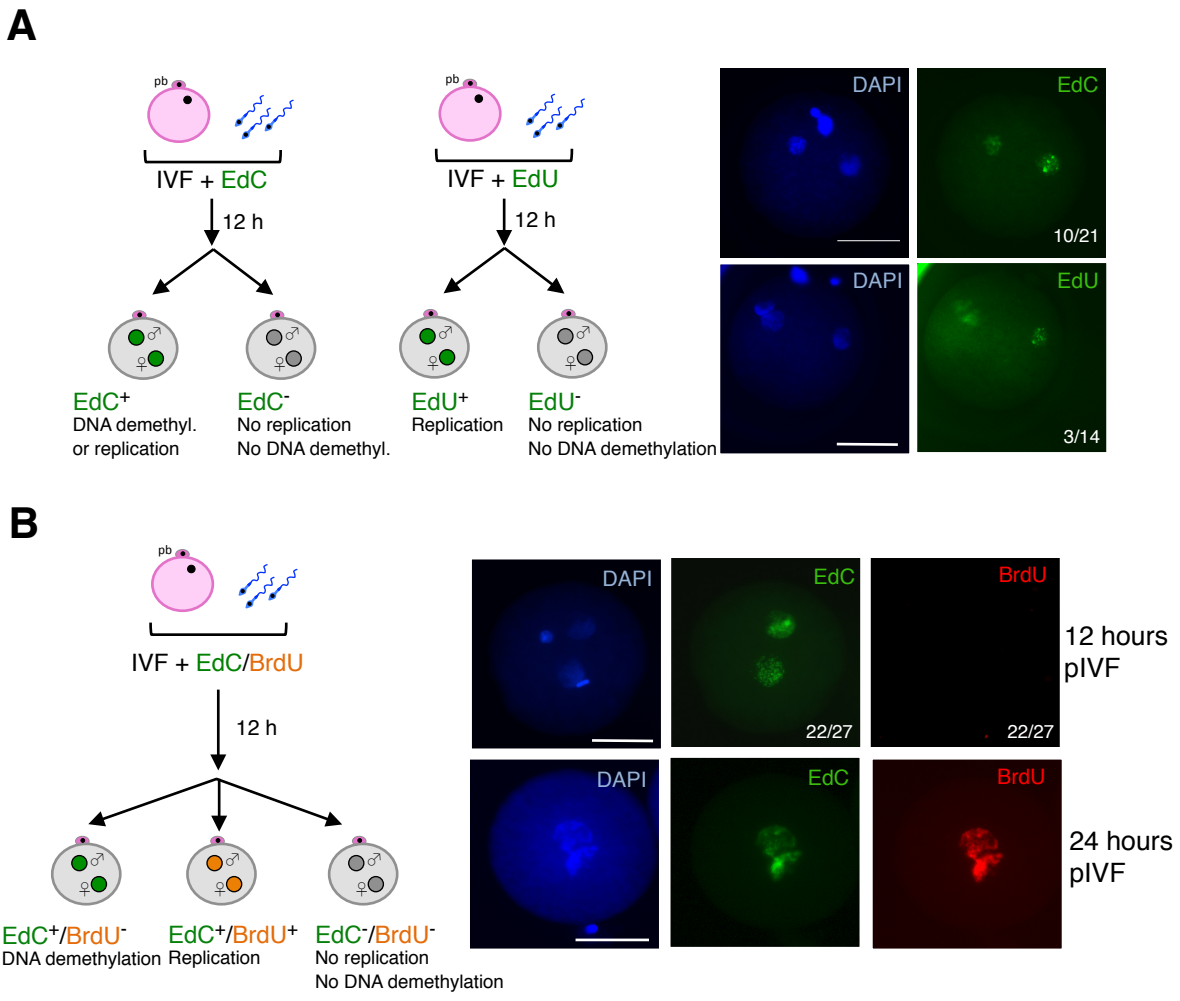
A
pb
IVF + EdC
12 h
EdC+
DNA demethyl.
or replication
EdC-
No replication
No DNA demethyl.
pb
IVF + EdU
12 h
EdU+
Replication
EdU-
No replication
No DNA demethylation
DAPI
EdC
10/21
DAPI
EdU
3/14
B
pb
IVF + EdC/BrdU
12 h
EdC+/BrdU-
DNA demethylation
EdC+/BrdU+
Replication
EdC-/BrdU-
No replication
No DNA demethylation
DAPI
EdC
22/27
BrdU
22/27
12 hours
pIVF
DAPI
EdC
BrdU
24 hours
pIVF

Figure 6

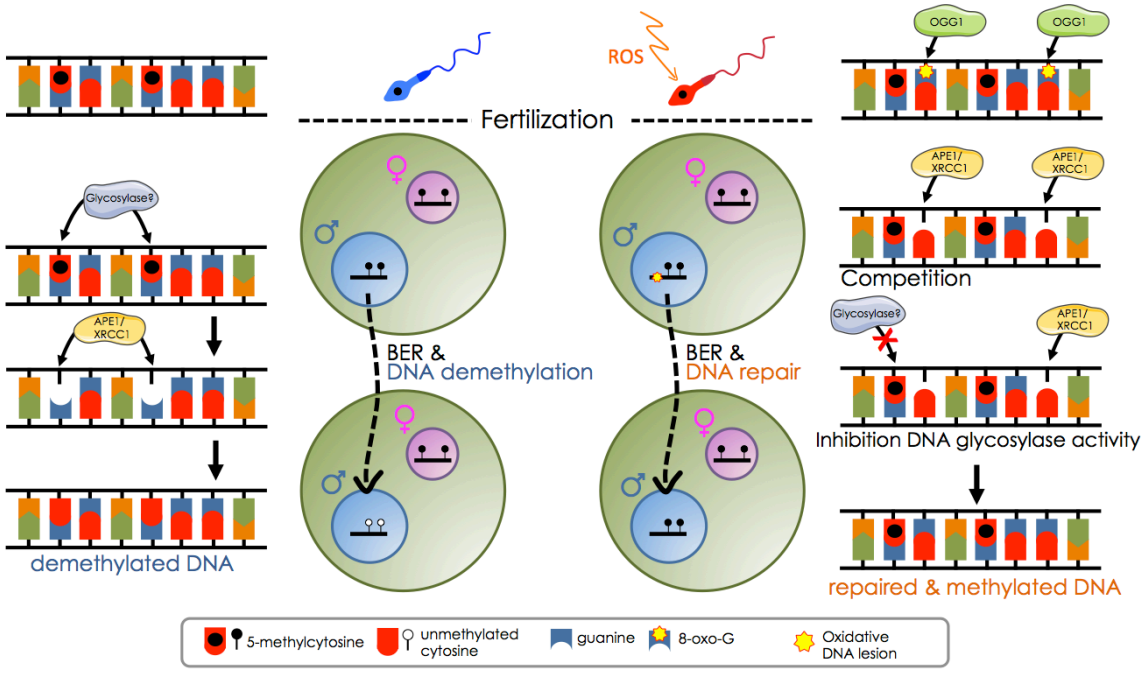
Glycosylase?
APE1/ XRCC1
demethylated DNA
Fertilization
ROS
BER & DNA demethylation
BER & DNA repair
OGG1
OGG1
APE1/ XRCC1
APE1/ XRCC1
Competition
Glycosylase?
APE1/ XRCC1
Inhibition DNA glycosylase activity
repaired & methylated DNA
5-methylcytosine
unmethylated cytosine
guanine
8-oxo-G
Oxidative DNA lesion

Supplementary Figure 1

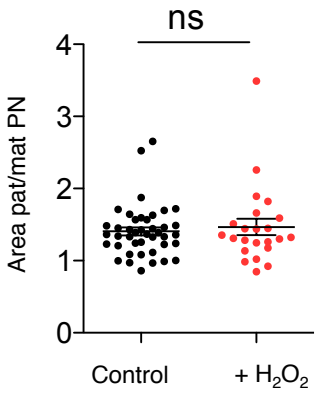

nature cell biology

ARTICLES

Pramel7 mediates ground-state pluripotency through proteasomal–epigenetic combined pathways

Urs Graf[1,2,3], Elisa A. Casanova[1], Sarah Wyck[3,4,5], Damian Dalcher[3,4], Marco Gatti[6], Eva Vollenweider[3,4], Michal J. Okoniewski[7], Fabienne A. Weber[2,3], Sameera S. Patel[2,3], Marc W. Schmid[8], Jiwen Li[9], Jafar Sharif[10], Guido A. Wanner[1], Haruhiko Koseki[10], Jiemin Wong[9], Pawel Pelczar[11], Lorenza Penengo[6], Raffaella Santoro[4,12,13] and Paolo Cinelli[1,2,12,13]

Naive pluripotency is established in preimplantation epiblast. Embryonic stem cells (ESCs) represent the immortalization of naive pluripotency. 2i culture has optimized this state, leading to a gene signature and DNA hypomethylation closely comparable to preimplantation epiblast, the developmental ground state. Here we show that Pramel7 (PRAME-like 7), a protein highly expressed in the inner cell mass (ICM) but expressed at low levels in ESCs, targets for proteasomal degradation UHRF1, a key factor for DNA methylation maintenance. Increasing Pramel7 expression in serum-cultured ESCs promotes a preimplantation epiblast-like gene signature, reduces UHRF1 levels and causes global DNA hypomethylation. Pramel7 is required for blastocyst formation and its forced expression locks ESCs in pluripotency. Pramel7/UHRF1 expression is mutually exclusive in ICMs whereas Pramel7-knockout embryos express high levels of UHRF1. Our data reveal an as-yet-unappreciated dynamic nature of DNA methylation through proteasome pathways and offer insights that might help to improve ESC culture to reproduce *in vitro* the *in vivo* ground-state pluripotency.

Embryonic stem cells (ESCs) are derived from the inner cell mass (ICM) of blastocysts and can be expanded indefinitely *in vitro*[1,2]. However, only ESCs have the capacity for unlimited self-renewal while ICM cells only briefly proliferate before acquiring a more restricted developmental potential[3,4]. Consequently, during the conversion of ICM cells to ESCs, there is an evident arrest of a normal developmental program, which *in vitro* is subverted in favour of a potential for unrestricted self-renewal while retaining pluripotency[5].

Depending on culture conditions, pluripotent ESCs can acquire molecular features that are distinct from those characterizing the developmental ground state of epiblast cells. Cultivation of ESCs in the presence of either serum/leukaemia inhibitory factor (LIF) or MEK/ERK and GSK3β inhibitors (2i, PD0325901 and CHIR99021) is conducive for maintenance of naive pluripotency. Most ESCs in serum/LIF (ESCs+serum) exhibit an altered transcriptional and epigenetic profile relative to preimplantation epiblast cells and are considered to be functionally naive but not ground state[6]. When compared to ICM, ESCs+serum have a globally more repressive epigenetic status as evident by a higher DNA methylation content and elevated expression of epigenetic regulators linked to transcriptional repression[5,7,8]. Conversely, a large proportion of epigenetic modifiers known to confer an active epigenetic state show higher expression in ICM.

Gene expression and DNA methylation analyses have shown that ESCs grown in 2i (ESCs+2i) are in an optimized state of naive pluripotency that closely resembles the developmental ground state *in vivo*[9–13]. Compared with ESCs+serum, ESCs+2i exhibit a permissive epigenetic landscape, including a hypomethylated genome that also characterizes ICM[7,8,10–12]. Thus, until now, the 2i-culture system represents the best available approach to model the developmental state of preimplantation epiblast cells in ESCs.

[1]Department of Trauma Surgery, Center for Clinical Research, University Hospital Zurich, University of Zurich, Sternwartstrasse 14, CH-8091 Zurich, Switzerland. [2]Institute of Laboratory Animal Science, University of Zurich, Winterthurerstrasse 190, CH-8057 Zurich, Switzerland. [3]Life Science Zurich Graduate School, University of Zurich, Winterthurerstrasse 190, CH-8057 Zurich, Switzerland. [4]Department of Molecular Mechanisms of Disease, University of Zurich, Winterthurerstrasse 190, CH-8057 Zurich, Switzerland. [5]Clinic of Reproductive Medicine, University of Zurich, Winterthurerstrasse 260, CH-8057 Zurich, Switzerland. [6]Institute of Molecular Cancer Research, University of Zurich, Winterthurerstrasse 190, CH-8057 Zurich, Switzerland. [7]Scientific IT Services, ETH Zurich, Weinbergstrasse 11, CH-8092 Zurich, Switzerland. [8]Service and Support for Science IT, University of Zurich, Winterthurerstrasse 190, CH-8057 Zurich, Switzerland. [9]Shanghai Key Laboratory of Regulatory Biology, Institute of Biomedical Sciences and School of Life Sciences, East China Normal University, Shanghai 200241, China. [10]Developmental Genetics Laboratory, RIKEN Center for Integrative Medical Sciences, 1-7-22 Suehiuro-cho, Tsurumi-ku, Yokohama City, Kanagawa 230-0045, Japan. [11]Center for Transgenic Models, University of Basel, Mattenstrasse 22, CH-4002 Basel, Switzerland. [12]Center for Applied Biotechnology and Molecular Medicine, University of Zurich, Winterthurerstrasse 190, CH-8057 Zurich, Switzerland.
[13]Correspondence should be addressed to R.S. or P.C. (e-mail: raffaella.santoro@dmmd.uzh.ch or paolo.cinelli@usz.ch)

Received 9 November 2016; accepted 11 May 2017; published online 12 June 2017; corrected after print 21 June 2017; DOI: 10.1038/ncb3554

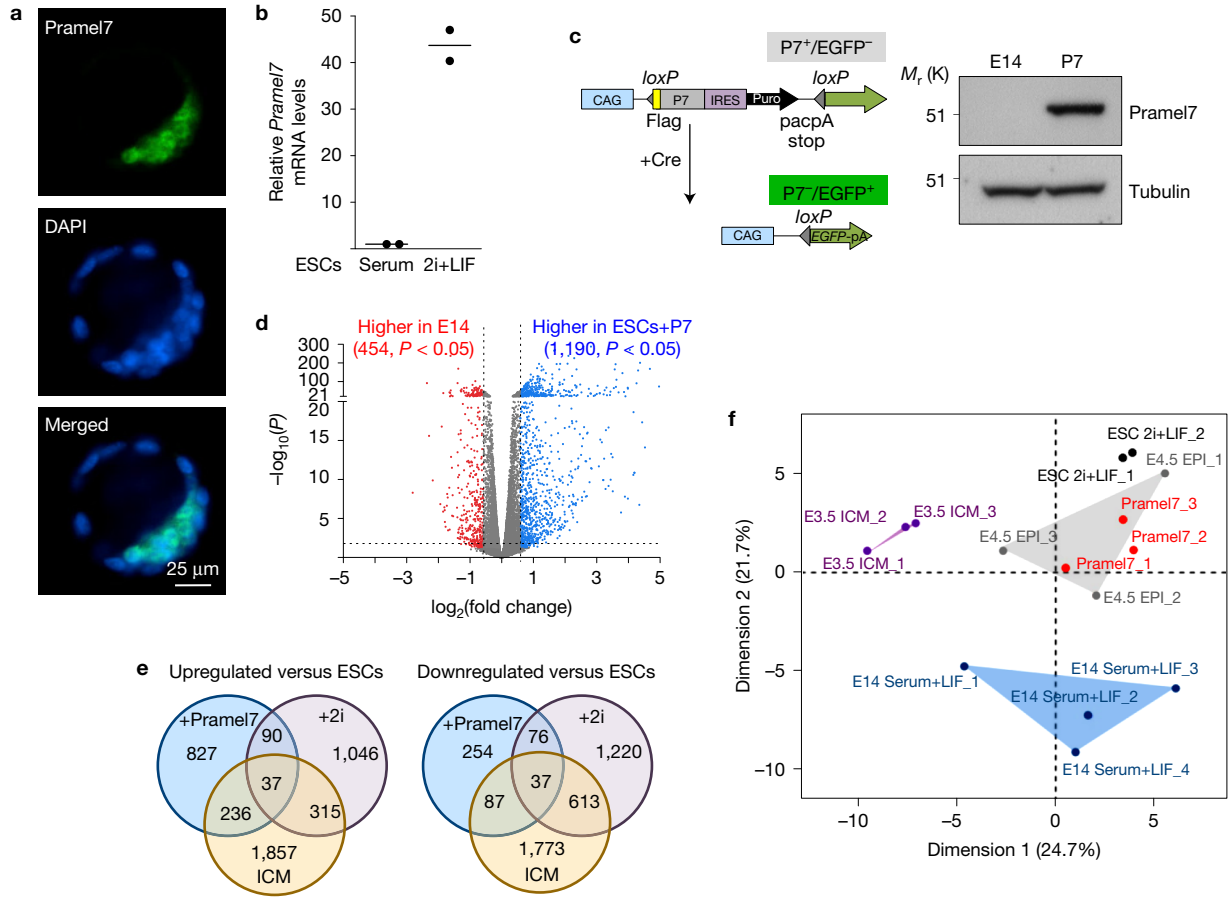

Figure 1 Expression of Pramel7 in ESCs induces a gene signature similar to ICM. (**a**) Pramel7 is expressed in ICM. Immunofluorescence analysis of a blastocyst showing expression of Pramel7 in ICM but not in trophoblast cells. (**b**) *Pramel7* gene expression in ESCs+2i compared with ESCs+serum. *Pramel7* mRNA levels were measured by qRT–PCR and normalized to actin mRNA and to ESCs+serum. Average values of two independent experiments; lines represent means. (**c**) Scheme displaying the construct used to establish P7 ESCs, which expresses FLAG-Pramel7 under the control of the CAG promoter and contains a Pramel7-IRES-Puro cassette flanked by *loxP* sites followed by *EGFP* sequences (P7 ESCs). Western blot indicates expression levels of Pramel7 in E14 ESCs and P7 ESCs (P7) detected with Pramel7 antibodies. Tubulin is shown as a loading control. (**d**) Volcano plot showing fold change ($\log_2$ values) in transcript level of all coding genes in ESCs+Pramel7 (P7) versus control ESCs (E14). Gene expression values of three replicates were averaged and selected for $P < 0.05$. A 1.5-fold change is indicated by the dotted line. (**e**) Venn diagrams showing transcript level changes detected in ESCs grown in serum compared with ESCs+Pramel7, ICM (ref. 5) and ESCs grown in 2i (ref. 12). (**f**) Correlation of P7 ESC gene expression to the early embryo stages. PCA analysis of P7 ESCs, embryonic stages E3.5 and E4.5, ESCs cultured in serum/LIF or 2i from the data set published in ref. 9. The image shown in **a** is representative of three independent stainings. Unprocessed original scans of immunoblots are shown in Supplementary Fig. 6.

We and others have recently found that Pramel7 (PRAME-like 7), a member of the Preferentially Expressed Antigen in Melanoma (PRAME) family, is expressed at high levels at the morula stage and in ICM, at lower levels in ESCs, but is completely absent in post-implantation embryos and in somatic tissues[14,15]. Correct dosage of Pramel7 levels is critical in early development. In ESCs, *Pramel7* knockdown induces differentiation, whereas its overexpression is sufficient to suppress differentiation in the absence of exogenous LIF, impairs teratoma formation and leads to embryonic lethality[15,16]. Moreover, expression of Pramel7 in combination with the GSK3β-inhibitor CHIR99021 is sufficient to maintain ESCs undifferentiated even in the absence of LIF, indicating that the presence of Pramel7 can compensate for the need of MEK/ERK inhibition (PD0325901) (ref. 15). The considerably higher expression level of Pramel7 in ICM compared with ESCs and its requirement to sustain pluripotency suggested an important role in naive pluripotency.

RESULTS

Expression of Pramel7 in ESCs induces a gene signature similar to preimplantation naive epiblast cells

Analysis of Pramel7 protein levels in blastocysts revealed specific expression in ICM cells and absence in trophectoderm[15,16] (Fig. 1a). Interestingly, *Pramel7* expression was also higher in ESCs+2i than in ESCs+serum (Fig. 1b and Supplementary Fig. 1a). However, Pramel7 levels in ESCs+2i were still very low and could not be detected by immunofluorescence, as done for ICM, or western blot with Pramel7 antibodies (Fig. 1c and Supplementary Fig. 1a,b). The elevated Pramel7 expression in ICM and its strong reduction during ICM–ESC transition[5] prompted us to investigate whether increasing the Pramel7 expression might induce ESCs+serum to acquire a molecular signature similar to naive preimplantation epiblast cells. We made use of a previously established E14 ESC line that expresses elevated levels of FLAG-Pramel7 (P7 ESCs) under the control of the

CAG promoter (Fig. 1c)[15]. We performed transcriptomic analysis and compared P7 ESCs versus E14 ESCs and found 1,190 genes displaying more than 1.5× higher transcript abundance in P7 ESCs ($P < 0.05$) whereas only 454 genes exhibited more than 1.5× higher expression in E14 ESCs (Fig. 1d and Supplementary Table 1). Transcription of the majority of categorized stem cell maintenance genes (Gene Ontology (GO): 0019827) including the core pluripotency factors *Oct4* and *Nanog* was not affected.

Since E14 ESCs and P7 ESCs are grown in serum, we analysed the RNA-seq results with published transcriptomic data comparing ICM or ESCs+2i versus ESCs+serum[5,12]. Of the 1,190 genes upregulated in P7 ESCs, 273 genes (23%) are upregulated in ICM versus ESCs (Fig. 1e). A similar number of ICM-specific genes are upregulated in ESCs+2i (352 out of 1,488 genes, 23%). In contrast, the number of genes downregulated was less in P7 ESCs (454) than in ESCs+2i (1,946), of which 124 and 650, respectively, were downregulated in ICM versus ESCs.

Functional annotation clustering of differentially expressed genes by GO revealed that P7 ESCs, ESCs+2i and ICM share similar biological processes (Supplementary Tables 2 and 3). The top 10 GO terms of genes with altered transcription are the same and all refer to developmental processes. Genes upregulated in P7 ESCs are highly enriched for terms associated with developmental process and the majority of them coincide with the top 10 GO terms of ICM-specific genes (Supplementary Table 4). In contrast, pathways associated with upregulated genes in ESCs+2i differ from ICM and P7 ESCs and, as previously reported, are highly enriched for terms associated with metabolic processes[12]. Downregulated genes in P7 ESCs are enriched for terms associated with ion transport and differ from GO terms associated with downregulated genes in ICM and ESCs+2i, which in turn are very similar to each other and implicated in developmental processes (Supplementary Table 5). Of note, *Fgf4*, a factor known to stimulate the ERK pathway that primes ESCs for lineage specification, is downregulated in P7 ESCs[17–19]. To assess how P7 ESCs are related to embryonic stages E3.5 and E4.5, and ESCs+serum or ESCs+2i, we performed principal component analysis (PCA) using recently published gene expression profiles[9]. Two-dimensional PCA analysis grouped ESCs+2i close to E4.5 epiblast cells (Fig. 1f)[9]. Remarkably, P7 ESCs were closer to ESCs+2i than to ESCs+serum and grouped with the greatest similarity to E4.5 epiblast cells. Dimensions 2 and 3 of the PCA analysis suggest that P7 ESCs also recapitulate certain aspects seen in epiblast cells (E3.5–4.5) (Supplementary Fig. 2).

Expression of Pramel7 induces hypomethylation of embryonic stem cells

The genome of ICM and ESCs+2i has a low content of DNA methylation compared with ESCs+serum and to later developmental stages[7,8,10,12]. To determine whether expression of Pramel7 affects the epigenetic state of ESCs+serum, we analysed the DNA methylation content of P7 ESCs. Intense 5-methylcytosine staining at 4′,6-diamidino-2-phenylindole (DAPI)-dense heterochromatic regions observed in control ESCs was significantly reduced in P7 ESCs (Fig. 2a). Measurement of global DNA methylation with the methylation-sensitive restriction enzyme HpaII indicated that CpG methylation was substantially reduced in P7 ESCs (Fig. 2b). We obtained similar results with McrBC digestion, an endonuclease that cleaves DNA containing only methylcytosine on one or both strands (Fig. 2c). Next, we deleted the *Pramel7* transgene with Cre-recombinase (P7^{-}) and found that HpaII or McrBC DNA digestion resistance reverted to levels found in control cells, indicating that the DNA methylation content depends on Pramel7 expression levels (Figs 1b and 2d).

Despite the low DNA methylation, ICM cells and ESCs+2i retain DNA methylation at imprinting control regions (ICRs)[8,10]. We examined the methylation of two ICRs, KvDMR1 and *Igf2/H19*, using bisulfite sequencing, COBRA and GlucMS-qPCR (glucosylation followed by methylation-sensitive quantitative PCR) and found that their methylation is drastically reduced in P7 ESCs (Fig. 2e,f and Supplementary Fig. 3a,b). This loss of methylation is also consistent with the upregulation of *H19* and *Kcnq1ot1* and silencing of the adjacent imprinted transcripts within the clusters (*Cdkn1c*) (Supplementary Table 1 and Supplementary Fig. 3c). A similar relationship between DNA methylation and gene expression was obtained through the analysis of methylation profiles of ESCs+serum[8], which revealed that genes upregulated following expression of Pramel7 display a higher methylation content at the transcription start site than average. As previously reported, genes upregulated following ESC transition from serum to 2i conditions do not show this correlation (Fig. 2g)[10]. These results indicate that expression of Pramel7 in ESCs+serum induces global hypomethylation and suggest a link between high Pramel7 expression levels and the hypomethylated state characterizing preimplantation embryos and ESCs+2i. Nevertheless, the methylation content of P7 ESCs is not identical to ICM and ESCs+2i since ICRs do not retain methylation.

Pramel7 interacts with UHRF1 and the Cullin 2 RING E3 ubiquitin ligase complex

P7 ESCs and E14 ESCs express similar levels of the DNA methyltransferases Dnmt1, Dnmt3a and Dnmt3b and the Ten-eleven translocation enzymes Tet1, Tet2 and Tet3 (Supplementary Fig. 4), indicating that Pramel7-mediated DNA hypomethylation is not due to altered expression of regulators of DNA methylation. To identify factors interacting with Pramel7, we performed a yeast two-hybrid screen using a Pramel7-LexA fusion protein as a bait to screen an E14 ESC complementary DNA library (Fig. 3a). Three out of five isolated clones displayed a strong LacZ signal, all expressing the protein UHRF1 (Ubiquitin-like, with PHD and RING finger domains 1). UHRF1 specifically recognizes and binds to hemimethylated DNA and is crucial for the transmission of DNA methylation marks during cell division[20–22]. Indeed, *Uhrf1*$^{-/-}$ ESCs display a drastic global reduction of DNA methylation content, including ICRs[20]. Anti-FLAG co-immunoprecipitation analysis in P7 ESCs confirmed the interaction of Pramel7 with UHRF1 (Fig. 3b). Pramel7–UHRF1 association was also detected in HEK293T cells, which do not express Pramel7, after anti-FLAG co-immunoprecipitation of cells transfected with plasmids expressing FLAG-Pramel7 (Fig. 3c,d). Additionally, we detected the association with histones, suggesting a role of Pramel7 that is linked to chromatin. We also identified Elongin C (TCEB1) and polyubiquitin as Pramel7-interacting proteins, both components of the Cullin 2 RING E3 ubiquitin ligase (CRL) complex that is involved in polyubiquitylation and subsequent proteasomal degradation of target substrates[23] (Fig. 3d). Interestingly, we found ubiquitin

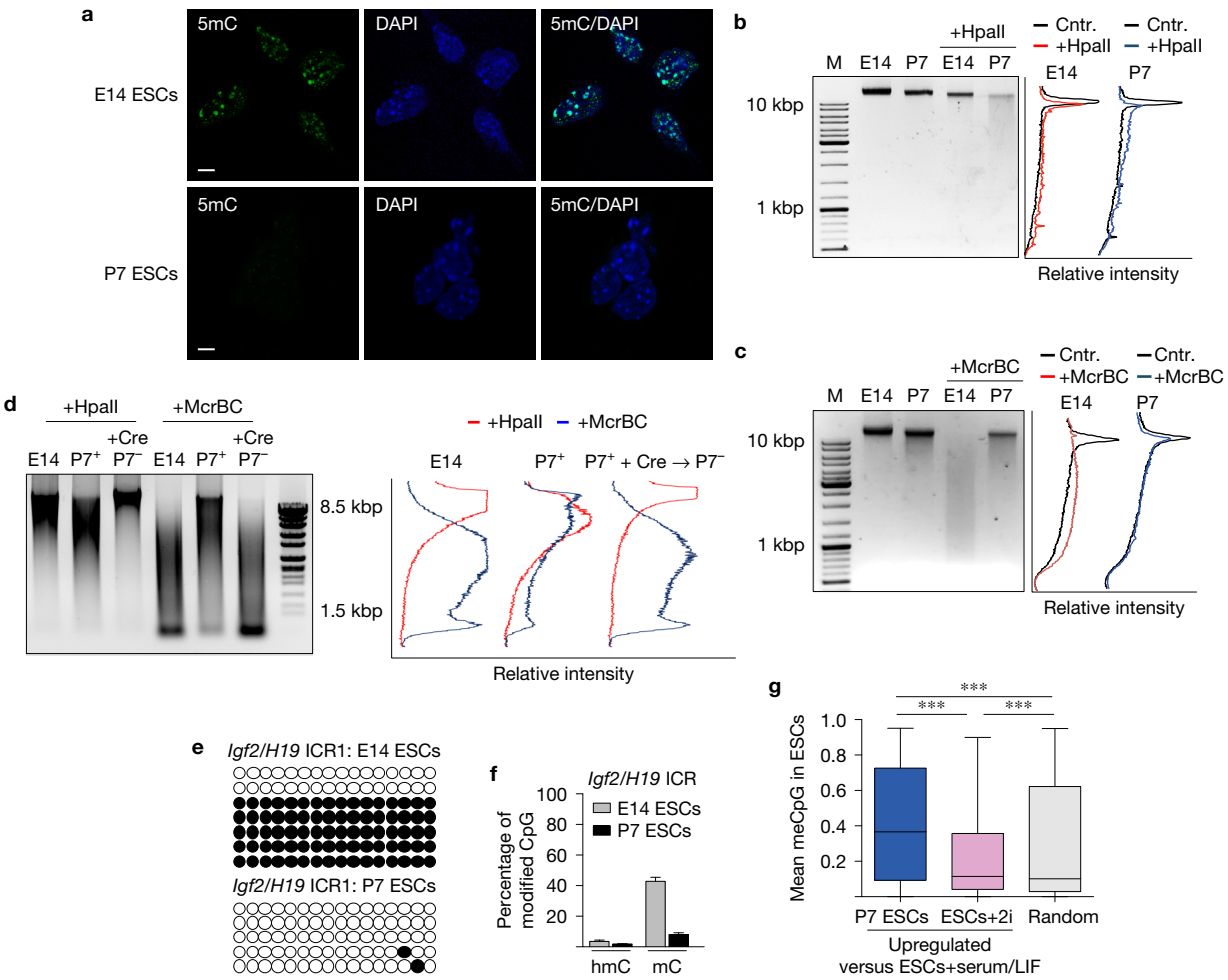

Figure 2 Expression of Pramel7 induces hypomethylation of embryonic stem cells. (**a**) DNA methylation defects in P7 ESCs in comparison with control E14 ESCs as revealed by immunofluorescent staining using anti-5mC antibody. Scale bars, 10 μm. The image is representative of three independent stainings. (**b**,**c**) CpG methylation levels measured by digestion of genomic DNA from E14 ESCs and P7 ESCs with the methylation-sensitive restriction enzymes HpaII and McrBC. Quantification of DNA signal was measured using Fiji image analysis software. M, DNA ladder. The image shown in **b** is representative of four independent experiments and in **c** of three independent experiments. (**d**) Defects in DNA methylation depend on Pramel7 expression levels. CpG methylation levels in E14, Cre-recombined (+Cre, $P7^-$) and non-recombined ($P7^+$) ESC clones were measured by HpaII and McrBC digestion. The image shown in **d** is representative of three independent experiments. (**e**) Bisulfite sequencing showing extensive demethylation of *Igf2/H19* ICR in P7 ESCs. (**f**) Analysis of methylation levels at one single MspI site (CCGG) by GlucMS-qPCR confirmed that *Igf2/H19* ICR underwent substantial demethylation without affecting hmC (hydroxy-methyl cytosine) levels in P7 ESCs. $n=3$ independent experiments performed in triplicates, error bars represent s.d. (**g**) CpG methylation levels at the transcription start site (+/− 1 kb) of RefSeq RNAs from differently expressed genes in P7 ESCs versus E14 ECSs and randomly picked (same number of transcripts as upregulated + downregulated) genes (data are from ref. 8). Box plot with median bar, first–third quantile box and 5th–95th percentile whiskers. ($^{***}P<0.001$, two-tailed Student's *t*-test.)

associated with UHRF1 whereas the interaction with Elongin C was detected only in the presence of Pramel7 (Supplementary Table 6). Finally, analyses in *Uhrf1*$^{-/-}$ ESCs revealed that Pramel7 association with the CRL complex does not depend on UHRF1 (Fig. 3e,f).

Pramel7 mediates the proteasomal degradation of UHRF1

The above findings prompted us to investigate whether Pramel7 targets UHRF1 for proteasomal degradation. We measured UHRF1 levels by immunofluorescence and western blot analysis and found a significant reduction of UHRF1 in P7 ESCs (Fig. 4a,b). Similarly, UHRF1 levels were drastically reduced in HEK293T cells after 48 h of ectopic expression of Pramel7 (Fig. 4b). The reduction in UHRF1 was not mediated through the inhibition of *Uhrf1* gene expression, as *Uhrf1* messenger RNA levels in P7 ESCs were comparable to those of control ESCs (Fig. 4c). This is also consistent with a previous analysis showing no remarkable alterations of *Uhrf1* mRNA levels in ICM, where Pramel7 is highly expressed, and ESCs[5]. Remarkably, UHRF1 levels were also reduced in ESCs+2i when compared with ESCs+serum, a result that is consistent with a recent report[24] (Supplementary Fig. 1b).

To get insight into the Pramel7-mediated degradation of UHRF1, we excised the *Pramel7* cassette in P7 ESCs by Cre-recombinase, simultaneously bringing *EGFP* under the control of the CAG promoter (Fig. 1b). Clones were selected for EGFP-positive ($P7^-$/$EGFP^+$) and -negative ($P7^+$/$EGFP^-$) signal. The dependency of UHRF1 moieties on Pramel7 expression was evident by the reduction of UHRF1

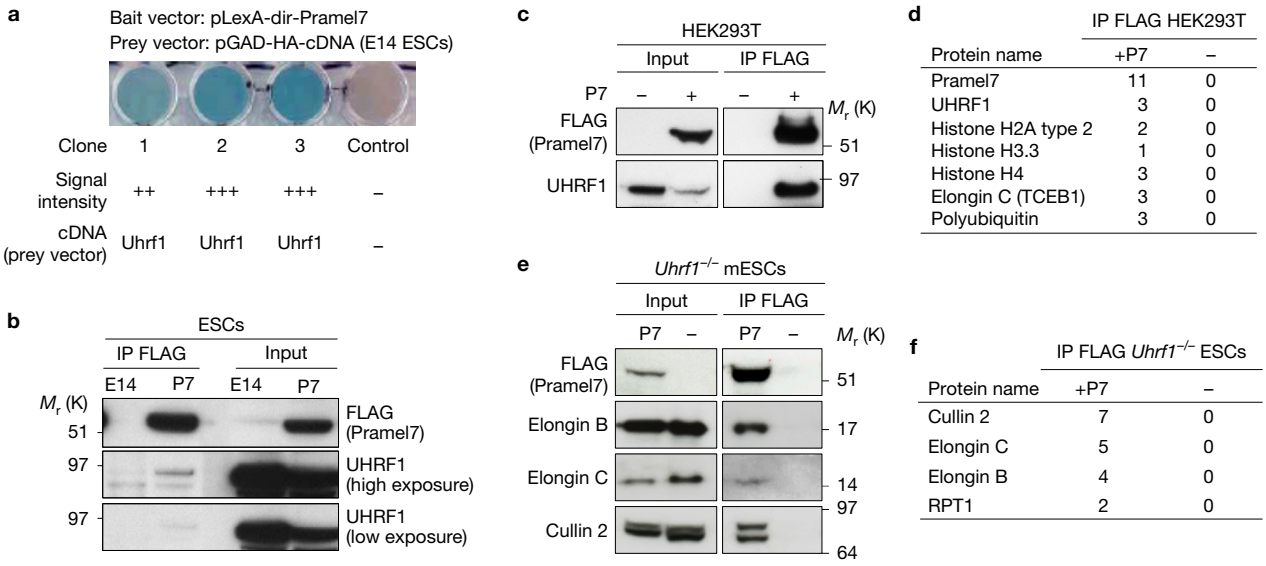

Figure 3 Pramel7 associates with UHRF1 and components of the Cullin 2 RING E3 ubiquitin ligase (CRL) complex. (**a**) Yeast two-hybrid assay using Pramel7 as a bait and a whole transcriptome cDNA library of E14 ESCs as prey. Three clones displayed a strong LacZ signal and all expressed UHRF1. (**b**,**c**) FLAG-immunoprecipitation from P7 ESCs and HEK293T cells transfected with FLAG-Pramel7 (P7)-expressing plasmids. Immunoblots show association of Pramel7 with UHRF1. Images are representative of five independent experiments. (**d**) Mass-spectrometry analysis of proteins co-immunoprecipitated with FLAG-Pramel7 (P7) in HEK293T cells. Values represent peptide hits. (**e**) FLAG co-immunoprecipitation of components of the Cullin 2 RING E3 ubiquitin ligase (CRL) complex (Elongin B, Elongin C, Cullin 2) in *Uhrf1*$^{-/-}$ ESCs expressing FLAG-Pramel7 (P7). The image is representative of three independent experiments. mESC, mouse ESC. (**f**) Mass-spectrometry analysis of proteins FLAG-immunoprecipitated in *Uhrf1*$^{-/-}$ ESCs expressing FLAG-Pramel7 (P7). Values represent peptide hits. Unprocessed original scans of immunoblots are shown in Supplementary Fig. 6.

expression in P7^{+}/EGFP^{-} cells as measured by immunofluorescence and western blotting (Fig. 4d,e). Finally, we monitored UHRF1 levels in HEK293T cells after transfection of FLAG-Pramel7 expression plasmid (Fig. 4f). Pramel7 expression was first detected 24 h post-transfection, which coincides with the initial UHRF1 reduction. After 72 h, when Pramel7 expression started to decline, UHRF1 again increased and, concomitant with the disappearance of Pramel7 (96 h and 120 h), UHRF1 levels were restored to similar amounts found in control cells.

The 26S-proteasome mediates the final step in the degradation of polyubiquitin-tagged proteins. We evaluated endogenous ubiquitylation of UHRF1 and found that ectopic Pramel7 expression increases polyubiquitylated UHRF1 (Fig. 4g). Next, we analysed whether UHRF1 is modified with Lys48-linked polyubiquitin chains, the canonical signal for proteasomal degradation[25]. We co-expressed UHRF1 together with the FLAG-tagged ubiquitin wild-type (WT) and the mutants Lys0, which can only monoubiquitylate target proteins, and Lys48-only, which can generate only Lys48-ubiquitin chains. We found that UHRF1 polyubiquitylation is largely due to Lys48-linkage of ubiquitin (Fig. 4h) and that the presence of Pramel7 further increased UHRF1 Lys48-polyubiquitylation. Finally, we tested the effect of proteasomal inhibition on the stability of UHRF1. Treatment with the proteasome inhibitor MG132 increases UHRF1 amounts and blocked Pramel7-mediated UHRF1 degradation (Fig. 4i), indicating that Pramel7 targets UHRF1 for degradation via the 26S-proteasome pathway. Thus, genome hypomethylation observed in P7 ESCs correlates well with the degradation of UHRF1 (ref. 20). Furthermore, the data suggest that the reduction of DNA methylation following Pramel7 expression occurs via a passive demethylation process, which includes the loss of methylation at ICRs as previously reported in the case of *Uhrf1*$^{-/-}$ ESCs[20].

The Pramel7-LRR and UHRF1-SRA and RING domains are necessary for the Pramel7–UHRF1 interaction and UHRF1 degradation

We next analysed whether the interaction of Pramel7 with UHRF1 is required for UHRF1 degradation. Pramel7 contains 3 leucine-rich repeat (LRR) motifs, which in general are implicated in the formation of protein–protein interactions[26]. Analysis of Pramel7-LRR deletion mutants indicated that deletion of the first LRR (ΔLRR1) was sufficient to impair Pramel7-mediated degradation of UHRF1 and the association of Pramel7 with UHRF1 (Fig. 5a–c). Similar results were obtained with further deletions of the second (ΔLRR1/2) and third LRR (ΔLRR1/2/3). Thus, Pramel7-mediated degradation of UHRF1 requires the association of UHRF1 with the Pramel7-LRR motif. Next, we analysed the degradation and Pramel7 association with UHRF1 mutants lacking the carboxy-terminal region, including all PHD, SRA and RING (ΔPSR) domains or only SRA and RING motifs (ΔSR) (Fig. 5d–f). These regions were previously implicated in hemimethylated DNA recognition, ubiquitylation of histone H3K23 and association with the histone methyltransferase G9a (refs 27–29). Deletion of SRA and RING regions was sufficient to impair UHRF1 degradation and Pramel7 interaction with both ΔPSR and ΔSR UHRF1 mutants was strongly reduced (Fig. 5e,f). UHRF1 associates with histones and, consistent with previous reports[30], this interaction is abolished following deletion of PSR domains, whereas the ΔSR mutant still associates with histones (Fig. 5g). Similar to UHRF1, Pramel7 in ESCs also associated with histones (Figs 3d and 5h) and

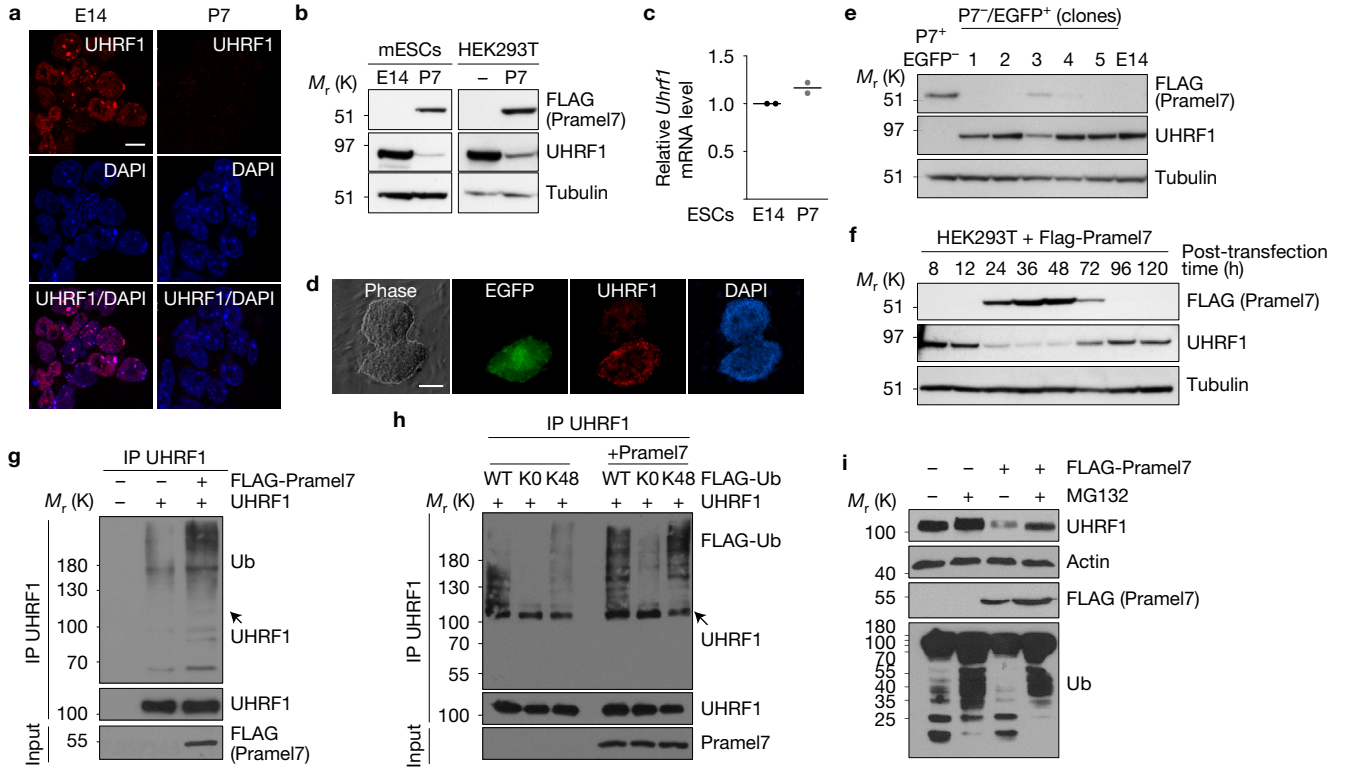

Figure 4 Pramel7 expression affects UHRF1 stability and leads to UHRF1 degradation via the 26S-proteasome pathway. (**a**) Immunofluorescent labelling of UHRF1 protein in E14 ESCs and P7 ESCs (P7). Scale bar, 10 μm. (**b**) Western blot for Pramel7 and UHRF1 in whole-cell lysates of E14 ESCs and P7 ESCs and in HEK293T cells 48 h after transient transfection with FLAG-Pramel7 plasmid (P7). Tubulin is shown as a loading control. (**c**) *Uhrf1* gene expression in E14 ESCs and P7 ESCs. *Uhrf1* mRNA levels were measured by qRT–PCR and normalized to actin mRNA. Average values of two independent experiments; lines represent means. (**d**) Immunofluorescence showing mutually exclusive UHRF1 and EGFP expression in P7$^-$/EGFP$^+$ (Cre-recombined) and P7$^+$/EGFP$^-$ (non-recombined) ESC colonies; scale bar, 200 μm. (**e**) UHRF1 and Pramel7 levels measured by western blotting analysis of cell lysates from five P7$^-$/EGFP$^+$ ESC clones and one P7$^+$/EGFP$^-$ ESC clone. (**f**) UHRF1 levels in HEK293T cells were monitored during the 5 days after transient transfection of FLAG-Pramel7 plasmid DNA (8 h to 120 h post-transfection). (**g**) Pramel7 increases polyubiquitylation of UHRF1. Endogenous ubiquitin levels of UHRF were monitored following immunoprecipitation of UHRF1 from HEK293T cells transfected with plasmid expressing UHRF1 and/or FLAG-Pramel7. (**h**) UHRF1 is modified through Lys48-linked polyubiquitin chains. Ubiquitin levels of UHRF1 were measured following immunoprecipitation of UHRF1 from HEK293T cells transfected with plasmid expressing UHRF1 and WT, Lys0 (K0) or Lys48 (K48) Flag-ubiquitin as indicated. (**i**) Pramel7-mediated UHRF1 degradation in HEK293T cells was monitored after addition of the proteasome inhibitor MG132 (20 μM). Images in **a**,**b**,**d**–**i** are representative of three independent experiments. Unprocessed original scans of immunoblots are shown in Supplementary Fig. 6.

exhibited a preferential association with chromatin, which as expected was also enriched in UHRF1 (Fig. 5i). We conclude that Pramel7-LRR and UHRF1-SRA and RING domains mediate Pramel7–UHRF1 interaction, which is required to target UHRF1 to the 26S-proteasome. Furthermore, this association is most likely occurring on chromatin.

Lack of Pramel7 increases UHRF1 protein levels in embryos and impairs blastocyst formation

Our attempts to obtain Pramel7-null mice and blastocysts have failed so far, suggesting an important role of Pramel7 in the late stages of preimplantation development. To better understand the *in vivo* function of Pramel7 we made use of the CRISPR/Cas9 technology to target the coding region of Pramel7 by using a single guide RNA (sgRNA-P7). As a control, we used sgRNA targeting the *Rosa26* locus[31]. sgRNA-P7 and sgRNA-Rosa26 were microinjected into the pronuclei of C57Bl/6J zygotes. The surviving zygotes (E0.5) were cultured for 4 days (until E4.5) and the development of the embryos was checked daily. Embryos developed normally until E3.5 (Fig. 6a). At E4.5 the number of sgRNA-P7 embryos that reached the blastocyst stage drastically reduced compared with the controls and was mirrored in an increase of developmentally arrested morula. Arrested sgRNA-P7 embryos showed an aberrant morphology and lacked expression of Pramel7 (Pramel7-KO) (Fig. 6b,c). sgRNA-P7 embryos that reached blastocyst stage were still expressing Pramel7, indicating that only a successful Pramel7 deletion causes a developmental arrest and that Pramel7 is required for the establishment of the blastocyst. Correctly developed embryos displayed a mutually exclusive expression of Pramel7 and UHRF1 in ICM whereas Pramel7-KO embryos expressed high UHRF1 (Fig. 6c). These results support a role of Pramel7 in regulating UHRF1 stability in ICM.

Pramel7 maintains the pluripotency state by repressing DNA methylation through regulation of UHRF1 stability

Following differentiation, ESC chromatin remodels into a condensed and repressed structure and DNA methylation was shown to be crucial for permanent restriction of developmental fate during

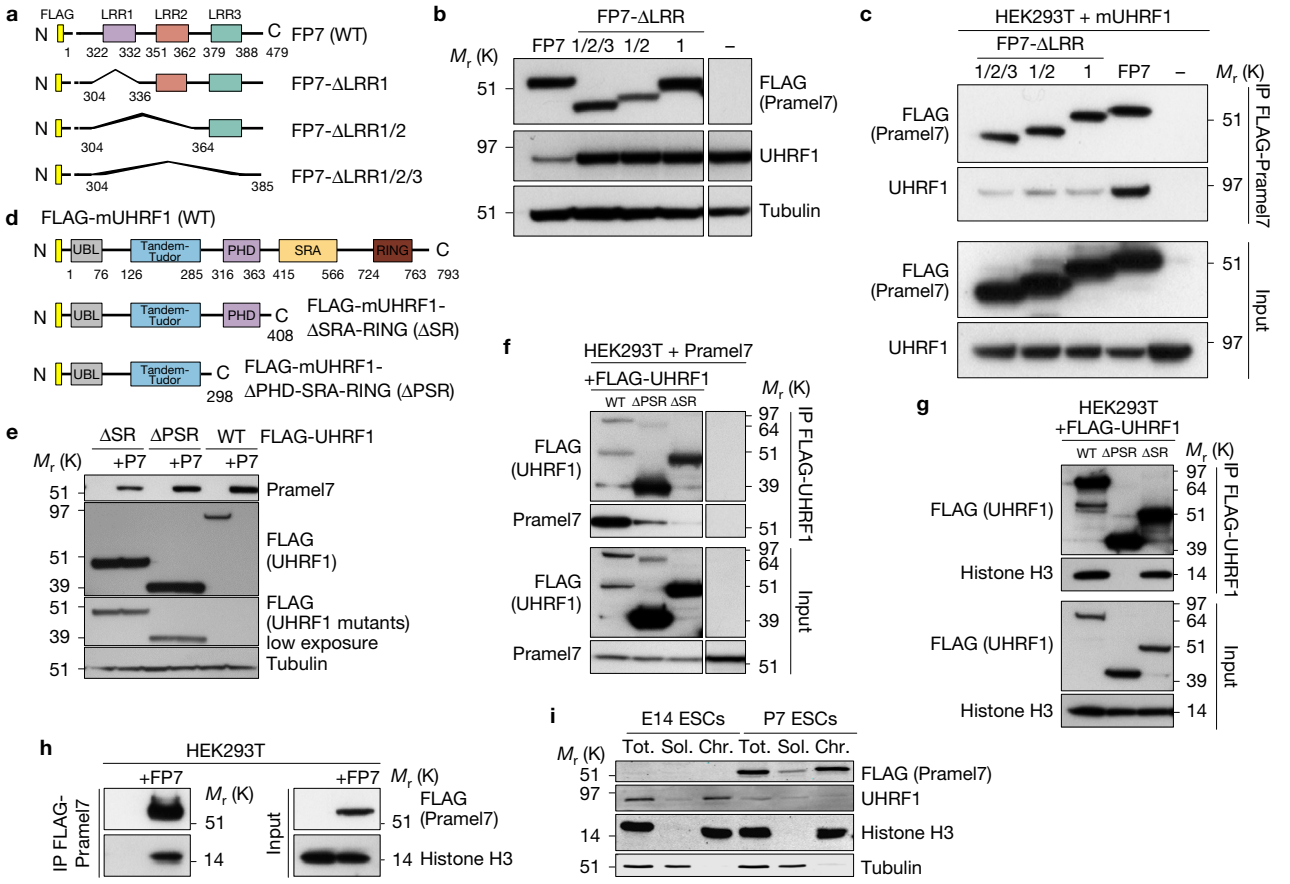

Figure 5 Pramel7 LRRs and UHRF1-SRA and RING domains are implicated in Pramel7–UHRF1 interaction and UHRF1 stability. (**a**) Schema representing the domain organization of Pramel7 and the analysed ΔLRR mutants. LRR, leucine-rich repeat. (**b**) Western blot of UHRF1 in HEK293T cells 48 h after transfection of FLAG-Pramel7 (FP7) and FP7-ΔLRR mutants; tubulin is shown as a loading control. (**c**) FLAG immunoprecipitation from HEK293T cells expressing FP7-ΔLRR mutants and mouse UHRF1 (mUHRF1). Overexpression of mUHRF1 was intended to increase the UHRF1 signal and achieve better detection of the UHRF1–Pramel7 interaction. (**d**) Schematic representation of FLAG-UHRF1 and UHRF1 mutant constructs: ΔSR (deletion of SRA and RING domains) and ΔPSR (deletion of PHD, SRA and RING domains). (**e**) Western blot of UHRF1 WT and mutants in HEK293T cells 48 h post-transfection of UHRF1 and Pramel7 expression plasmids. (**f**) FLAG-immunoprecipitation from HEK293T cells transfected with FLAG-UHRF1 WT and mutants and Pramel7 expression plasmids. (**g**,**h**) Association of UHRF1 and Pramel7 with histone H3 shown by FLAG-immunoprecipitation from HEK293T expressing FLAG-UHRF1 WT or FLAG-UHRF1 mutants (**g**) and FLAG-Pramel7 (**h**). (**i**) UHRF1 and Pramel7 associate with chromatin of ESCs. Chromatin-bound (Chr.) and soluble (Sol.) fractions of equivalent cell number of E14 ESCs and P7 ESCs were analysed by western blot for UHRF1 and Pramel7 levels. Tot., total. Tubulin and histones are shown as loading and fractionation control. Images in **b**,**c**,**e**–**h** are representative of three independent experiments. Unprocessed original scans of immunoblots are shown in Supplementary Fig. 6.

differentiation[32–34]. To determine whether the expression of Pramel7 following ESC differentiation impairs terminal differentiation, we tested the ability of P7 ESCs to differentiate into a stable state. We differentiated P7 ESCs following withdrawal of LIF and feeders for 14 days and observed that E14 ESCs developed into a homogeneous cell layer whereas P7 ESCs formed less differentiated and more compact colonies (Fig. 7a). As expected, UHRF1 levels were lower in differentiated cells than in ESCs reflecting a lower cell proliferation rate of the differentiated state[35] (Fig. 7b). Pramel7-mediated UHRF1 degradation was still active during differentiation as evident by low UHRF1 and DNA methylation content (Fig. 7b,c). In differentiated P7 cells the pluripotency genes *Oct4*, *Nanog* and *Rex1* and the pluripotency marker stage-specific embryonic antigen 1 (SSEA1) were expressed at high levels, suggesting that transcriptional silencing was not as efficient as in differentiated control ESCs (Fig. 7a,d). Consistent with the hypomethylated state of P7 ESC genome, methylation of the *Oct4* promoter was lower in differentiated P7 cells than in control-differentiated cells (Fig. 7e). *Uhrf1*$^{-/-}$ ESCs shared several similarities with P7 ESCs. After 26 days of differentiation, *Uhrf1*$^{-/-}$ ESCs were also defective in transcriptional silencing of pluripotency genes and formed less differentiated and more compact colonies, a phenotype that we also observed in DNMT-TKO cells (Fig. 7f and Supplementary Fig. 5a). Finally, to determine whether expression of Pramel7 affects the stable terminally differentiated state, we tested the ability of 14-day differentiated P7 cells to reconvert to a pluripotent state (Fig. 8a). Differentiated cells were seeded at a density of 10 cells per well in 96-well plates, cultured for 7 days in conditions supporting pluripotency (+LIF) and screened for the expression of the pluripotency marker alkaline phosphatase (AP). AP-positive (AP$^+$) colonies were found in only 2.7% of E14 ESC wells (5/182) whereas 80.8% (147/182) of wells with P7 ESCs contained AP$^+$ colonies. P7 ESC reconverted clones maintained Pramel7 expression and low

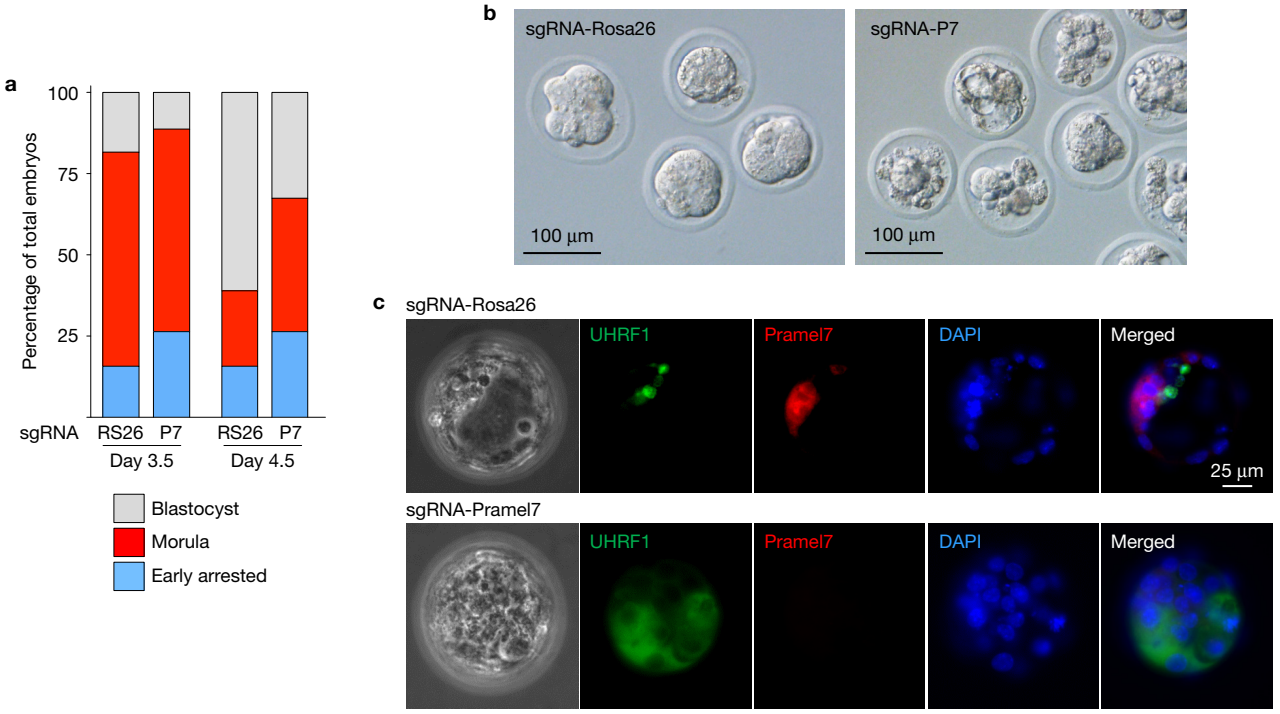

Figure 6 Pramel7 is required for ICM. (**a**) Stacked bar plots showing the fraction of embryos at different developmental stages at day 3.5 and day 4.5, after injection with sgRNA-Rosa26 and sgRNA-P7. Data are from two independent microinjections. In experiment 1, 114 embryos were microinjected with sgRNA-Rosa26 and 110 embryos with sgRNA-P7. In experiment 2, 87 embryos were microinjected with sgRNA-Rosa26 and 91 embryos with sgRNA-P7. Source data for this experiment are available in Supplementary Table 8. (**b**) Representative images of embryos at the morula stage obtained at day 4.5 showing aberrant morphology of sgRNA-P7-injected embryos compared with sgRNA-Rosa26 control embryos. (**c**) Immunofluorescence analysis of a blastocyst from a sgRNA-Rosa26 control embryo showing mutually exclusive expression of UHRF1 and Pramel7 in ICM cells. sgRNA-Pramel7 embryos lacked Pramel7 expression and expressed UHRF1.

UHRF1 levels (Fig. 8b) and expressed pluripotency markers (Fig. 8c and Supplementary Fig. 5b). We conclude that increased expression of Pramel7 in ESCs impairs exit from pluripotency by repressing DNA methylation through regulation of UHRF1 stability.

DISCUSSION

ESCs need to be shielded from extrinsic signals to indefinitely retain pluripotency in culture and serum/LIF and 2i conditions have both been proposed to be conducive for maintenance of naive pluripotency. Additionally, 2i optimizes the state of naive pluripotency, inducing a gene signature and DNA hypomethylation state that resembles naive epiblast cells[36]. Here we show that expression levels of Pramel7 correlate with ground-state pluripotency, high in ICM and ESCs+2i and low in ESCs+serum (Fig. 8d). Increasing Pramel7 expression in ESCs+serum causes global DNA hypomethylation and induces a naive pluripotency state closely comparable to the developmental ground state *in vivo*.

ESCs+2i or P7 ESCs have similar properties, for example, robust pluripotency, hypomethylated genome and activated pathways, all similar to ICM. Nevertheless, it is likely that they achieved these features using different mechanisms. Genes upregulated in P7 ESCs are strongly linked to developmental processes and coincide with ICM-specific genes whereas genes downregulated in ESCs+2i share more similarity with ICM. Additionally, P7 ESCs are characterized by elevated expression of genes involved in sustaining self-renewal and retention of pluripotency such as *Gbx2* and *Lef1*[37,38] and reduced expression of genes implicated in controlling exit from pluripotency such as *Fgf4* and *Tbx3*[17–19,39]. Therefore, an inducible system that modulates expression of Pramel7 in cultured pluripotent ESCs might represent an attractive and physiological alternative to *in vitro* reproduce the *in vivo* ground-state pluripotency.

DNA hypomethylation has been considered an epigenetic trait of ground-state pluripotency. Downregulation of both the *de novo* DNA methyltransferases Dnmt3a and Dnmt3b has been proposed as a way to maintain genome hypomethylation in ICM[11]. A similar mechanism has been observed in ESCs+2i (refs 8,11). The post-translational control of UHRF1 levels through Pramel7 might represent an additional regulatory pathway to establish a hypomethylated genome, creating greater epigenetic flexibility required by preimplantation epiblasts to undergo rapid and transient developmental changes. Interestingly, during the revision of this work, it was reported that ESCs+2i have lower UHRF1 protein levels compared with ESCs+serum[24]. Our data support these results. Moreover, we showed that Pramel7 levels are higher in ESCs+2i than in ESCs+serum. Although the role of Pramel7 in ESCs+2i still requires further investigation, these results are consistent with our *in vivo* analyses determining a mutually exclusive expression of Pramel7 and UHRF1 in ICM cells. The phenotype of P7 ESCs and *Uhrf1*$^{-/-}$ ESCs is very similar, including the loss of methylation at ICRs and their corresponding transcriptional changes[20]. However, ICM and ESCs+2i

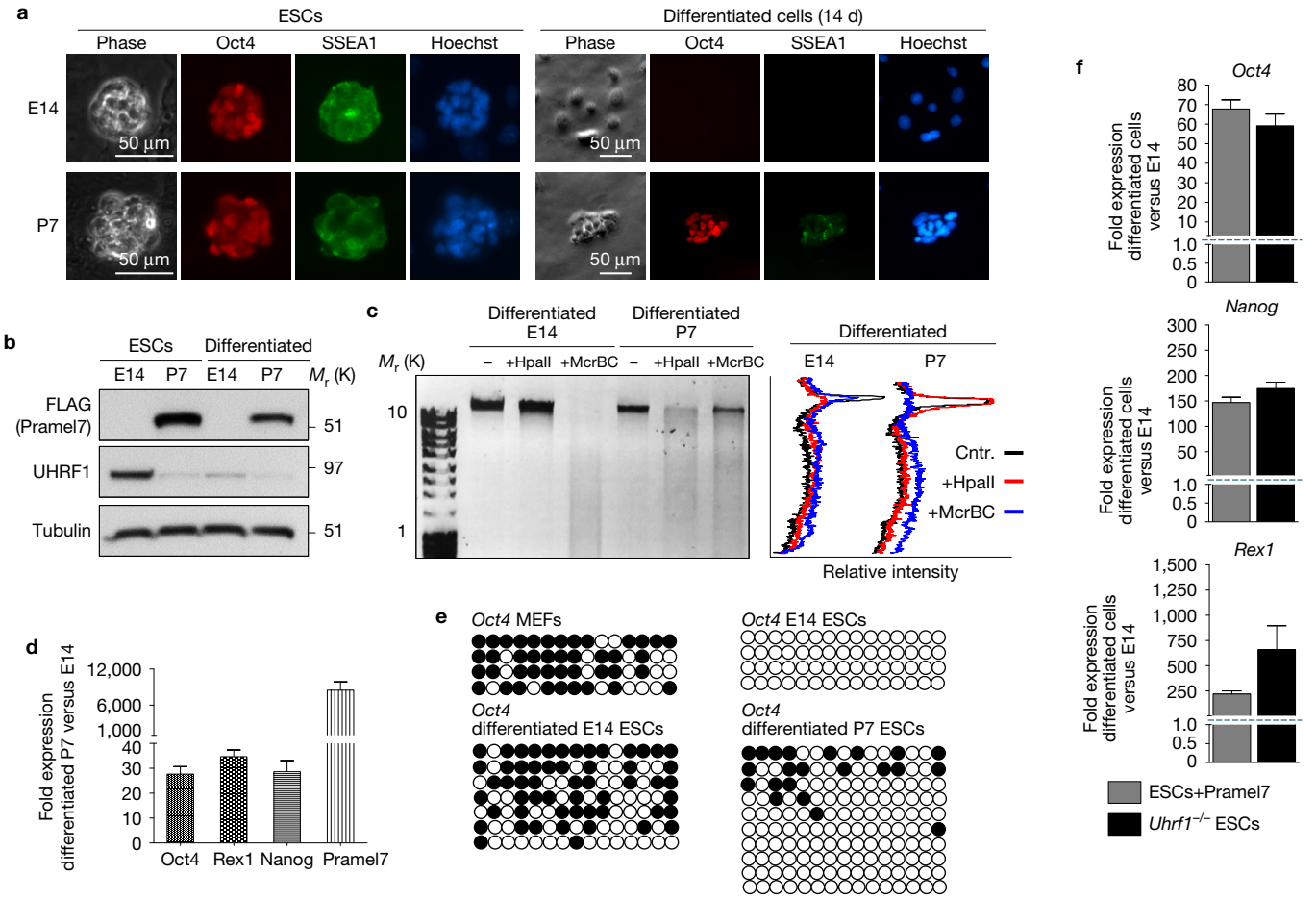

Figure 7 Pramel7 maintains the pluripotent state by repressing DNA methylation through regulation of UHRF1 stability. (**a**) Immunofluorescence analysis of the pluripotency markers Oct4 and SSEA1 in E14 ESCs and P7 ESCs and after 14 days of differentiation. Images are representative of four independent stainings. (**b**) UHRF1 and Pramel7 protein levels from whole-cell lysates of E14 ESCs and P7 ESCs in self-renewing conditions (+LIF) and after 14 days of differentiation. Representative of three independent experiments. (**c**) DNA methylation levels of 14-day differentiated E14 ESCs and P7 ESCs measured by digestion with HpaII and McrBC. Representative of three independent experiments. (**d**) Expression of the pluripotency-associated genes *Oct4*, *Nanog* and *Rex1* in differentiated cells measured by qRT–PCR and normalized to actin mRNA. Data are represented as fold expression in differentiated P7 cells compared with differentiated E14 ESCs. Values represent the average of $n=3$ independent experiments performed in triplicates; error bars represent s.d. (**e**) Bisulfite genomic sequencing analysis of the *Oct4* promoter in MEFs, E14 ESCs and differentiated E14 and P7 cells. Open and filled circles indicate unmethylated and methylated CpGs, respectively. (**f**) *Oct4*, *Rex1* and *Nanog* expression levels in P7 ESCs and *Uhrf1*$^{-/-}$ ESCs after 26 days of differentiation. Values were measured by qRT–PCR, normalized to actin mRNA and represented as fold change relative to the expression of differentiated E14 ESCs. Values represent the average of $n=3$ independent experiments performed in triplicates, error bars represent s.d. Unprocessed original scans of immunoblots are shown in Supplementary Fig. 6.

maintain the parental methylation pattern at imprinted loci[7,10,11]. There are several reasons that might explain the loss of methylation at ICRs in P7 ESCs. Compared with ICM, which undergoes only a few rounds of duplication, P7 ESCs have divided for a much longer time and thus are more prone to lose methylation, including methylation at ICRs (as in the case of *Uhrf1*$^{-/-}$ ESCs[20]). Moreover, UHRF1 in ESCs+2i is only modestly reduced while the elevated expression of Pramel7 in P7 ESCs (under the control of CAG promoter) induced a strong UHRF1 downregulation. Alternatively, ICM cells might modulate the activity of Pramel7 at defined gene loci (that is, at ICRs) whereas the elevated expression of Pramel7 in P7 ESCs might not allow this tight regulation.

Our results suggest that controlling the maintenance of DNA methylation through modulation of UHRF1 stability has the potential to regulate cell fate and might represent an as-yet-unappreciated dynamic nature of DNA methylation. Our data imply that maintenance of DNA methylation has a role for stable exit from pluripotency, as evident by differentiation defects observed in ESCs with deletion of *Dnmt1* (ref. 32) or *Uhrf1* or Pramel7-mediated degradation of UHRF1. Importantly, demethylation of ESCs following knockout of all *Dnmt* or *Uhrf1* genes or following culture in 2i conditions did not result in a proper activation of methylated genes[10,40,41], which suggests that either transcription factors are not present or compensatory mechanisms can replace the repressive effect of DNA methylation. The fact that increased expression of Pramel7 induced global demethylation and changes in transcription at genes with high methylation content indicates that Pramel7 might have additional functions not limited to DNA methylation pathways.

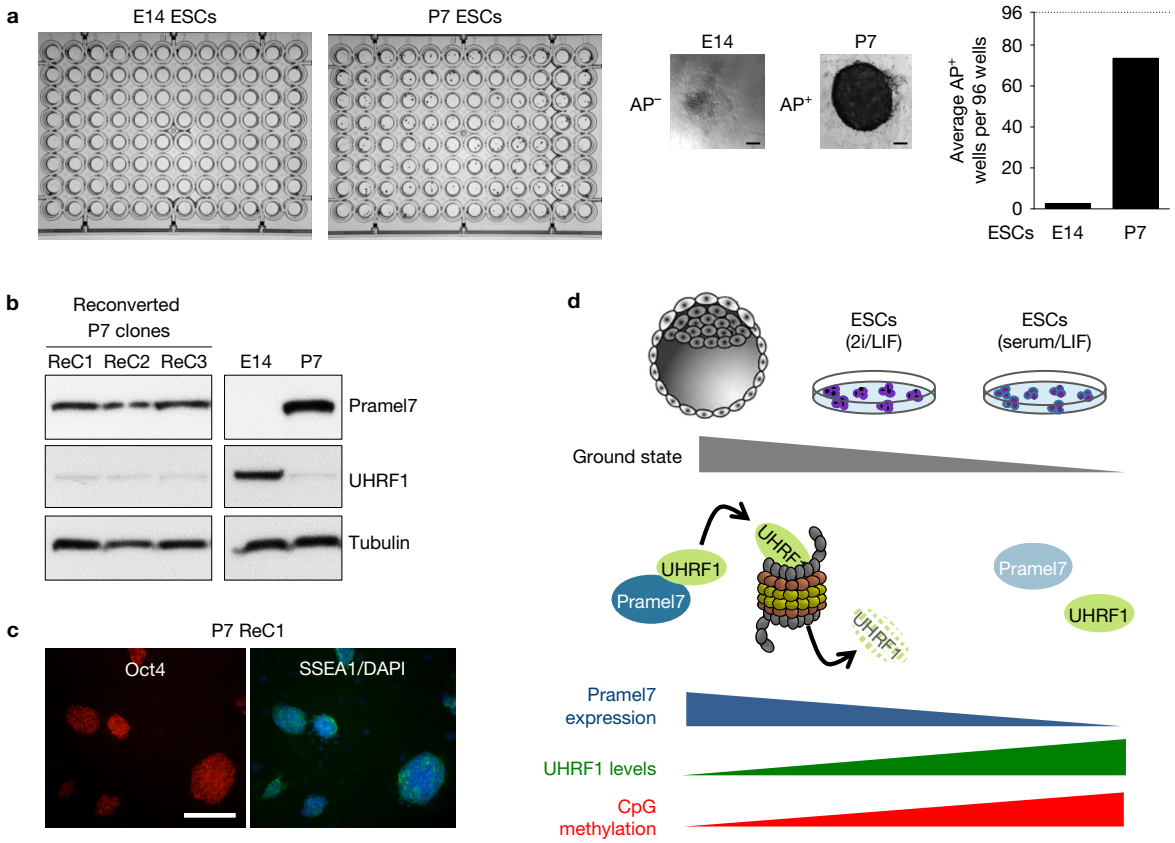

Figure 8 Forced expression of Pramel7 affects the stable terminally differentiated state. (**a**) Alkaline phosphatase (AP) staining assay of 14-day differentiated E14 ESCs and P7 ESCs re-exposed to self-renewing conditions (+LIF) for 7 days. Representative images of AP-stained 96-well plates and of an AP⁻ colony typical for E14 ESCs and an AP⁺ colony characteristic for P7 ESCs are shown. Scale bars, 100 μm. The right panel shows average numbers of wells containing AP⁺ colonies. The experiment was repeated $n=2$ independent times. (**b**) Differentiated P7 cells reconverted into ESCs (ReCs) still exhibit decreased levels of UHRF1. Western blot indicated UHRF1 protein levels of three P7 reconverted clones expanded in self-renewing conditions (+LIF). Western blot representative of two independent experiments. (**c**) Representative immunofluorescence of a P7 reconverted clone (P7-ReC1) showing expression of the pluripotency markers Oct4 and SSEA1. Scale bar, 200 μm. The image is representative of three independent experiments. (**d**) Model showing how Pramel7 contributes to ground-state pluripotency. Expression levels of Pramel7 correlate with ground-state pluripotency, high in ICM and ESCs+2i and low in ESCs in serum/LIF. Pramel7 induces global hypomethylation by targeting UHRF1 for proteasomal degradation and establishes an active epigenetic state that might be required by ICM to undergo rapid and transient developmental changes. Unprocessed original scans of immunoblots are shown in Supplementary Fig. 6.

The post-transcriptional control of UHRF1 levels mediated by Pramel7 joins two pathways, proteasome and epigenetics, which have been independently implicated in the maintenance of pluripotency. We showed that controlling UHRF1 levels through Pramel7-mediated targeting for proteasome degradation is an important molecular pathway for the regulation of epigenetic states linked to ground-state pluripotency (Fig. 8d). Since PRAME and PRAME family members are expressed in a wide range of human tumours and are often correlated with poor clinical outcome[42–44], our data also offer important insights into how developmental programs might be undermined, leading to the formation of diseased tissues, including cancers. □

METHODS

Methods, including statements of data availability and any associated accession codes and references, are available in the online version of this paper.

Note: Supplementary Information is available in the online version of the paper

ACKNOWLEDGEMENTS

The authors thank D. Bär for technical assistance, W. Piwko and O. Shakhova for discussions and reagents and J. vom Berg, D. Korkmaz and M. Tarnowska for embryo isolation. We acknowledge assistance provided by the Functional Genomic Center Zurich, especially C. Aquino and L. Opitz. This work was supported by the Olga Mayenfisch Foundation (to P.C. and R.S.), Julius Müller Stiftung (to R.S.), the Novartis Foundation for Medical-Biological Research (to P.C.), the Theodor und lda Herzog-Egli Foundation (to P.C. and R.S.), the Sassella Stiftung (P.C.), the Stiftung für Wissenschaftliche Forschung an der Universität Zürich (to P.C. and R.S.), the Helmut Horten Stiftung (to L.P.), Krebsliga Schweiz (KFS-3497-08-2014 to R.S.), the Swiss National Science Foundation (31003A_173056 and 31003A-152854 to R.S., 323530-133905 to F.A.W., 31003A-166370 to L.P.), the UBS-Promedica Stiftung (to R.S.) and the Forschungskredit of the University of Zurich (to U.G., E.V. and D.D.).

AUTHOR CONTRIBUTIONS

U.G. performed most of the experiments, contributed to experimental design and data analysis and wrote the manuscript. E.A.C. performed yeast two-hybrid screening. S.W., D.D. and E.V. performed methylation analysis. R.S., D.D. and M.W.S. analysed transcriptome and methylation data. M.J.O. performed RNA-seq and PCA analysis. E.A.C., F.A.W. and S.S.P. generated and analysed Pramel7 ESCs. J.L., J.S., H.K. and J.W. contributed to UHRF1 plasmids and UHRF1-KO ESCs. G.A.W. contributed to data analysis. M.G. and L.P. performed the ubiquitylation analysis. P.C. and P.P. generated and analysed Pramel7 knockout embryos; P.C. designed most of the experiments; R.S. and P.C. jointly directed the study and wrote the manuscript.

COMPETING FINANCIAL INTERESTS

The authors declare no competing financial interests.

Published online at http://dx.doi.org/10.1038/ncb3554

1. Martin, G. R. Isolation of a pluripotent cell line from early mouse embryos cultured in medium conditioned by teratocarcinoma stem cells. *Proc. Natl Acad. Sci. USA* **78,** 7634–7638 (1981).
2. Evans, M. J. & Kaufman, M. H. Establishment in culture of pluripotential cells from mouse embryos. *Nature* **292,** 154–156 (1981).
3. Zwaka, T. P. & Thomson, J. A. A germ cell origin of embryonic stem cells? *Development* **132,** 227–233 (2005).
4. Niwa, H. How is pluripotency determined and maintained? *Development* **134,** 635–646 (2007).
5. Tang, F. *et al.* Tracing the derivation of embryonic stem cells from the inner cell mass by single-cell RNA-Seq analysis. *Cell Stem Cell* **6,** 468–478 (2010).
6. Hackett, J. A. & Surani, M. A. Regulatory principles of pluripotency: from the ground state up. *Cell Stem Cell* **15,** 416–430 (2014).
7. Smith, Z. D. *et al.* A unique regulatory phase of DNA methylation in the early mammalian embryo. *Nature* **484,** 339–344 (2012).
8. Habibi, E. *et al.* Whole-genome bisulfite sequencing of two distinct interconvertible DNA methylomes of mouse embryonic stem cells. *Cell Stem Cell* **13,** 360–369 (2013).
9. Boroviak, T., Loos, R., Bertone, P., Smith, A. & Nichols, J. The ability of inner-cell-mass cells to self-renew as embryonic stem cells is acquired following epiblast specification. *Nat. Cell Biol.* **16,** 516–528 (2014).
10. Ficz, G. *et al.* FGF signaling inhibition in ESCs drives rapid genome-wide demethylation to the epigenetic ground state of pluripotency. *Cell Stem Cell* **13,** 351–359 (2013).
11. Leitch, H. G. *et al.* Naive pluripotency is associated with global DNA hypomethylation. *Nat. Struct. Mol. Biol.* **20,** 311–316 (2013).
12. Marks, H. *et al.* The transcriptional and epigenomic foundations of ground state pluripotency. *Cell* **149,** 590–604 (2012).
13. Ying, Q. L. *et al.* The ground state of embryonic stem cell self-renewal. *Nature* **453,** 519–523 (2008).
14. Bortvin, A. *et al.* Incomplete reactivation of Oct4-related genes in mouse embryos cloned from somatic nuclei. *Development* **130,** 1673–1680 (2003).
15. Casanova, E. *et al.* Pramel7 mediates LIF/STAT3-dependent self-renewal in embryonic stem cells. *Stem Cells* **29,** 474–485 (2011).
16. Cinelli, P. *et al.* Expression profiling in transgenic FVB/N embryonic stem cells overexpressing STAT3. *BMC Dev. Biol.* **8,** 57 (2008).
17. Burdon, T., Stracey, C., Chambers, I., Nichols, J. & Smith, A. Suppression of SHP-2 and ERK signalling promotes self-renewal of mouse embryonic stem cells. *Dev. Biol.* **210,** 30–43 (1999).
18. Kunath, T. *et al.* FGF stimulation of the Erk1/2 signalling cascade triggers transition of pluripotent embryonic stem cells from self-renewal to lineage commitment. *Development* **134,** 2895–2902 (2007).
19. Stavridis, M. P., Lunn, J. S., Collins, B. J. & Storey, K. G. A discrete period of FGF-induced Erk1/2 signalling is required for vertebrate neural specification. *Development* **134,** 2889–2894 (2007).
20. Sharif, J. *et al.* The SRA protein Np95 mediates epigenetic inheritance by recruiting Dnmt1 to methylated DNA. *Nature* **450,** 908–912 (2007).
21. Bostick, M. *et al.* UHRF1 plays a role in maintaining DNA methylation in mammalian cells. *Science* **317,** 1760–1764 (2007).
22. Liu, X. *et al.* UHRF1 targets DNMT1 for DNA methylation through cooperative binding of hemi-methylated DNA and methylated H3K9. *Nat. Commun.* **4,** 1563 (2013).
23. Hotton, S. K. & Callis, J. Regulation of cullin RING ligases. *Annu. Rev. Plant Biol.* **59,** 467–489 (2008).
24. von Meyenn, F. *et al.* Impairment of DNA methylation maintenance is the main cause of global demethylation in naive embryonic stem cells. *Mol. Cell* **62,** 848–861 (2016).
25. Grice, G. L. & Nathan, J. A. The recognition of ubiquitinated proteins by the proteasome. *Cell. Mol. Life Sci.* **73,** 3497–3506 (2016).
26. Kobe, B. & Kajava, A. V. The leucine-rich repeat as a protein recognition motif. *Curr. Opin. Struct. Biol.* **11,** 725–732 (2001).
27. Nishiyama, A. *et al.* Uhrf1-dependent H3K23 ubiquitylation couples maintenance DNA methylation and replication. *Nature* **502,** 249–253 (2013).
28. Arita, K., Ariyoshi, M., Tochio, H., Nakamura, Y. & Shirakawa, M. Recognition of hemi-methylated DNA by the SRA protein UHRF1 by a base-flipping mechanism. *Nature* **455,** 818–821 (2008).
29. Achour, M. *et al.* UHRF1 recruits the histone acetyltransferase Tip60 and controls its expression and activity. *Biochem. Biophys. Res. Commun.* **390,** 523–528 (2009).
30. Gelato, K. A. *et al.* Accessibility of different histone H3-binding domains of UHRF1 is allosterically regulated by phosphatidylinositol 5-phosphate. *Mol. Cell* **54,** 905–919 (2014).
31. Chu, V. T. *et al.* Efficient generation of Rosa26 knock-in mice using CRISPR/Cas9 in C57BL/6 zygotes. *BMC Biotechnol.* **16,** 4 (2016).
32. Schmidt, C. S. *et al.* Global DNA hypomethylation prevents consolidation of differentiation programs and allows reversion to the embryonic stem cell state. *PLoS ONE* **7,** e52629 (2012).
33. Sakaue, M. *et al.* DNA methylation is dispensable for the growth and survival of the extraembryonic lineages. *Curr. Biol.* **20,** 1452–1457 (2010).
34. Savic, N. *et al.* lncRNA maturation to initiate heterochromatin formation in the nucleolus is required for exit from pluripotency in ESCs. *Cell Stem Cell* **15,** 720–734 (2014).
35. Bonapace, I. M. *et al.* Np95 is regulated by E1A during mitotic reactivation of terminally differentiated cells and is essential for S phase entry. *J. Cell Biol.* **157,** 909–914 (2002).
36. Kalkan, T. & Smith, A. Mapping the route from naive pluripotency to lineage specification. *Phil. Trans. R Soc. B* **369,** 20130540 (2014).
37. Tai, C. I. & Ying, Q. L. Gbx2, a LIF/Stat3 target, promotes reprogramming to and retention of the pluripotent ground state. *J. Cell Sci.* **126,** 1093–1098 (2013).
38. Huang, C. & Qin, D. Role of Lef1 in sustaining self-renewal in mouse embryonic stem cells. *J. Genet. Genomics* **37,** 441–449 (2010).
39. Weidgang, C. E. *et al.* TBX3 directs cell-fate decision toward mesendoderm. *Stem Cell Rep.* **1,** 248–265 (2013).
40. Fouse, S. D. *et al.* Promoter CpG methylation contributes to ES cell gene regulation in parallel with Oct4/Nanog, PcG complex, and histone H3 K4/K27 trimethylation. *Cell Stem Cell* **2,** 160–169 (2008).
41. Sharif, J. *et al.* Activation of endogenous retroviruses in Dnmt1$^{-/-}$ ESCs involves disruption of SETDB1-mediated repression by NP95 binding to hemimethylated DNA. *Cell Stem Cell* **19,** 81–94 (2016).
42. van Baren, N. *et al.* PRAME, a gene encoding an antigen recognized on a human melanoma by cytolytic T cells, is expressed in acute leukaemia cells. *Br. J. Haematol.* **102,** 1376–1379 (1998).
43. Ikeda, H. *et al.* Characterization of an antigen that is recognized on a melanoma showing partial HLA loss by CTL expressing an NK inhibitory receptor. *Immunity* **6,** 199–208 (1997).
44. van 't Veer, L. J. *et al.* Gene expression profiling predicts clinical outcome of breast cancer. *Nature* **415,** 530–536 (2002).

DOI: 10.1038/ncb3554

METHODS

Animals. All experiments were performed with C57BL/6J mice. Fertilized eggs were obtained from superovulated 3–4-week-old females. Animals were housed under controlled lighting (lights on at 6:00–18:00), temperature (23 ± 2 °C) and humidity (50 ± 5%), with free access to food and water. The Veterinary Offices of the Canton of Zurich, Switzerland (license no. 165/2014 to P.C.) and Basel, Switzerland (license no. 1023G1 to P.P.) approved all animal experiments. Housing and experimental procedures were in accordance with the Swiss animal protection law and conformed to the European Convention for the protection of vertebrate animals used for experimental and other scientific purposes (Council of Europe no. 123, Strasbourg 1985).

Cell lines and culture media. No cell lines used in this study were found in the database of commonly misidentified cell lines that is maintained by ICLAC and NCBI Biosample. All of the cell lines generated for this study were derived from E14 129/Ola, karyotyped, tested for mycoplasma and their identity authenticated by several means including resistance to drug selection, PCR and sequencing of specific genomic regions.

ESCs were routinely cultivated on mitotically inactivated mouse embryonic fibroblasts (MEFs) in complete medium (Serum +LIF: GMEM (Sigma), 10% FCS, 10 mM sodium pyruvate, 1× NEAA, 1× Pen/Strep/Glu, 0.1 mM 2-mercaptoethanol) supplemented with 1,000 U ml^{-1} leukaemia inhibitory factor (LIF). HEK293T cells and MEFs were grown in DMEM (Life Technologies) supplemented with 10% FCS, 1× Pen/Strep/Glu and 10 mM sodium pyruvate. Establishment of Pramel7 ESCs (P7 ESC) was described in ref. 15. *Uhrf1*$^{-/-}$ ESCs were previously described[20]. DNMT-TKO ESCs were kindly provided by M. Okano[45] (Laboratory for Mammalian Epigenetic Studies, Center for Developmental Biology, RIKEN, Kobe, Japan).

Immunofluorescent detection and alkaline phosphatase staining. Cells were fixed in 4% formalin. For confocal analysis formalin was supplemented with 1:555 100% Triton X-100 (Sigma). Primary antibodies were diluted in PBST (PBS + 0.1% Tween-20) and 4% horse serum and cells were incubated either overnight at 4 °C or at room temperature for 2–4 h. Nuclei were stained with DAPI (Roche) or Hoechst for 60 s. Wide-field images were taken on a Zeiss Axiovert 40 CFL and processed using AxioVision 4.6 software (Zeiss) and Adobe Photoshop CS6. Confocal pictures were taken in the Center for Microscopy and Image Analysis (ZMB) of the University of Zurich and processed with IMARIS 7.6 software. For alkaline phosphatase staining, cells were fixed in 4% formalin, washed 2× with AP buffer (0.1 M Tris-HCl, 0.1 M NaCl, 20 mM $MgCl_2$, pH 9.5) and incubated with AP staining solution (AP Buffer +0.5 µl ml^{-1} NBT (Roche) and 3.5 µl ml^{-1} BCIP (Roche)). The staining reaction was stopped with 1× Tris-EDTA (20 mM Tris-HCl, 5 mM EDTA).

Isolation of genomic DNA and DNA methylation analysis. Cells were incubated with Proteinase K overnight at 50 °C followed by treatment with RNAseA (Fermentas) for 30 min at 37 °C. Genomic DNA (gDNA) was purified with 25:24:1 phenol/chloroform/isoamyl alcohol and subsequently precipitated by addition of NH_4Ac/ethanol. Four micrograms of gDNA was digested overnight with 20 U HpaII or McrBC in 20 µl total reaction volume containing 0.5 ng of pBluescript plasmid DNA for testing the efficiency of the HpaII digest. Digested gDNA was loaded on a 0.8% agarose gel and gDNA fragments were separated by electrophoresis. Quantification of DNA signal was measured using Fiji image analysis software. To verify HpaII digestion efficiency, pBluescript KS(+) plasmid was analysed by qPCR using one forward primer that is complementary to sequences upstream of the CCGG site of the β-lactamase gene (at 2580) and two different reverse primers that map upstream and downstream the HpaII sites. All analysed samples displayed 96–98% digestion efficiency. Bisulfite conversion was performed using the EpiTect Bisulfite Kit (Qiagen) according to the manufacturer's protocol. Amplification was performed with a nested touchdown PCR program with a 0.5 °C decrease in the annealing temperature after each cycle. Bisulfite primers are listed in Supplementary Table 7. Amplified sequences were cloned in pCR II-TOPO (Life Technologies) and sequenced. For COBRA assay, PCR products were digested with BstUI (New England Biolabs) followed by agarose gel electrophoresis. GlucMS-qPCR assay was performed using the EpiMark 5-hmC and 5mC-Analysis Kit (NEB). Briefly, genomic DNA was treated with T4 Phage β-glucosyltransferase. Glucosylated DNA was digested with HpaII or MspI or no enzyme (mock digestion) at 37 °C for 2 h and inactivated for 20 min at 80 °C. The HpaII- and MspI-resistant fraction was quantified by qPCR using primers designed around a single HpaII/MspI site, normalizing to the mock digestion control (Supplementary Table 7).

For promoter methylation analyses of Pramel7-regulated genes and ESCs versus 2i (ref. 12), WGBS data of E14 serum ESCs from ref. 8 were used. A minimum CpG coverage of 10 was set as a threshold. Average promoter methylation (+1 kb and −1 kb relative to the transcription start site) was calculated using deepTools[46] for all RefSeq RNA genes—retrieved through BioMart—taking each CpG into consideration (no binning). Random promoters from all RefSeq RNA genes were taken as a reference for average genome-wide promoter methylation using the same number of promoter regions as for upregulated gene sets together. Median promoter methylations with interquartile ranges are plotted for the indicated gene sets.

Yeast two-hybrid assay. Pramel7 was used as bait and a cDNA library of E14 ESCs as a pool of prey proteins. The bait was cloned into a lexA-expression vector and tested for self-activation and successful expression. cDNA library was transformed and co-expressed with the bait plasmid. Positive clones were selected and library plasmids were isolated. Finally positive clones were sequenced and BLAST analysis was performed.

Co-immunoprecipitation and proteomic analysis. Cell pellets were resuspended in IP buffer (50 mM Tris-HCl pH 7.5, 150 mM KCl, 5 mM $MgCl_2$, 0.2 mM EDTA, 20% (v/v) glycerol, 0.5 mM dithiothreitol, 0.1% (v/v) NP-40, Proteinase inhibitor cocktail (Roche)), sonicated and DNase treated. One milligram of nuclear protein was subjected to immunoprecipitation overnight at 4 °C using ANTI-FLAG M2 affinity gel (Sigma). Precipitates were washed three times with IP buffer, separated on a 6% SDS-polyacrylamide gel and analysed by immunoblot. For proteomic analysis, immunoprecipitated proteins were eluted twice using 100 µl M2 FLAG-peptide (Sigma). Eluates were precipitated with trichloro-acetic acid (TCA), washed 4–6× with cold acetone and then dried at 95 °C. Proteomic analysis was carried out at the Functional Genomics Centre Zurich (University and ETH Zurich).

RNA extraction, reverse transcription and quantitative real-time PCR and RNA-seq. RNA was extracted using the RNeasy Mini Kit (Qiagen). Five hundred nanograms or 1 microgram of RNA was reverse transcribed using Oligo(dT)12–18 Primer (Life Technologies), 10 mM dNTP Mix (Life Technologies), RNAsin Plus RNAse Inhibitor (Promega) and SuperscriptIII Reverse Transcriptase (Life Technologies). Real-Time PCR was performed with the Rotor-Gene SYBR Green PCR Kit (FAST) (Qiagen). Primer sequences are listed in Supplementary Table 7.

Illumina RNA-sequencing. Data were deposited to the European Nucleotide Archive (ENA) under the accession number: PRJEB12665.

Library preparation. The quality of the isolated RNA was determined with a Qubit (1.0) Fluorometer (Life Technologies) and a Bioanalyzer 2100 (Agilent). Only those samples with a 260 nm/280 nm ratio between 1.8–2.1 and a 28S/18S ratio within 1.5–2 were further processed. The TruSeq RNA Sample Prep Kit v2 (Illumina) was used in the succeeding steps. Briefly, total RNA samples (100–1,000 ng) were ribo-depleted using Ribo Zero Gold(Epicentre) and then fragmented. The fragmented samples were reversed transcribed to cDNA, end-repaired and polyadenylated before ligation of TruSeq adapters containing the index for multiplexing. Fragments containing TruSeq adapters on both ends were selectively enriched with PCR. The quality and quantity of the enriched libraries were validated using Qubit (1.0) Fluorometer and the Caliper GX LabChip GX (Caliper Life Sciences). The product is a smear with an average fragment size of approximately 260 bp. The libraries were normalized to 10 nM in Tris-Cl 10 mM, pH 8.5 with 0.1% Tween-20.

Cluster generation and sequencing. The TruSeq PE Cluster Kit v4-cBot-HS or TruSeq SR Cluster Kit v4-cBot-HS (Illumina) was used for cluster generation using 10 pM of pooled normalized libraries on the cBOT. Sequencing was performed on the Illumina HiSeq 2500 paired end at 2 X101 bp or single end 100 bp using the TruSeq SBS Kit v4-HS (Illumina).

Data analysis. The raw reads were first cleaned by removing adapter sequences, trimming low-quality ends, and filtering reads with low quality (phred quality <20) using Trimmomatic[47]. Sequence alignment of the resulting high-quality reads to the *Mus musculus* reference genome (build GRCm38) was performed with STAR (version 2.4.2a) (ref. 48). The aligned reads were counted using the featureCount method of the R-package Rsubread (version 1.18.0). To detect differentially expressed genes we applied a count-based negative binomial model implemented in the software package edgeR (version: 3.10.2) (ref. 49), in which the normalization factor was calculated by the trimmed mean of M values (TMM) method[49]. The gene-wise dispersions were estimated by conditional maximum likelihood and an empirical Bayes procedure was used to shrink the dispersions towards a consensus value. The differential expression was assessed using an exact test adapted for over-dispersed data. Genes showing altered expression with adjusted (Benjamini and Hochberg method) P value < 0.05 were considered as differentially expressed.

Principal component analysis (PCA). The principal component analysis has been performed on the qRT–PCR data set combined with the RNA-seq data set described in ref. 9. The $\log_2$ counts in RNA-seq have been selected and normalized to mean. The data set taken for PCA and hierarchical clustering was created as a projection of

96 genes used in ref. 9 onto the Pramel7 ESCs RNA-seq experiment. The data sets of Borowiak *et al.* (ref. 9) and our own RNA-seq were combined and batch correction was applied using the ComBat function from the sva Bioconductor package[50]. PCA has been calculated using the FactoMineR[51] R library.

Transfection of HEK293T cells and electroporation of ESCs. Transfection of HEK293T with plasmid DNA was performed using either $CaCl_2$ and BES solution (50 mM BES, 280 mM NaCl, 1.5 mM Na_2HPO_4, pH 7.0) or Xtremegene HP (Roche) transfection reagent. For stable integration of the plasmid pCAG-FLAG-Pramel7-PGK-puro in E14 ESCs, the cells were first separated from the feeder layer by trypsinization, incubated with plasmid DNA and electroporated at 500 µF capacitance and 240 V using a Bio Rad Gene Pulser II. Antibiotic selection was started 24–48 h after electroporation and continued for 4 subsequent days (puromycin, 1 µg ml^{-1}). After the selection medium was changed to standard conditions (serum +LIF), the selected colonies were grown and clonally expanded.

For the time course experiment in HEK293T cells, HEK293T cells were transfected with FLAG-Pramel7 expression plasmid. Samples were collected 8, 12, 24, 36, 48, 72, 96 and 120 h after transfection and analysed for FLAG-Pramel7 and UHRF1 protein levels by western blotting. Endogenous ubiquitylation on UHRF1 was determined by anti-UHRF1 immunoprecipitation of HEK293 cells 36 h after transfection with UHRF1 and FLAG-Pramel7 expression plasmid. When indicated, plasmids expressing WT, Lys0 or Lys48 mutant FLAG-ubiquitin were co-transfected and ubiquitin was detected with FLAG antibodies. Proteasomal degradation of endogenous UHRF1 was monitored in 28 h post-transfection HEK293 cells treated with MG132 (20 µM) for 8 h.

Differentiation and reconversion of control E14 ESCs and P7 ESCs. E14 ESCs and P7 ESCs were separated from the feeder layer and seeded on gelatinized feeder-free culture dishes in complete medium without LIF. To avoid confluence, cells were passaged after 6 and 10 days. After 14 days, the cells were seeded on two 96-well plates containing feeder cells and LIF in a dilution of 10 cells per well and cultured for a further 7 days. Fourteen-day differentiated cells and cells cultured in the presence of LIF were harvested and analysed for the expression of Pramel7 and UHRF1 and of the pluripotency factors Oct4, Nanog, Rex1 and SSEA1 (immunofluorescence and qPCR).

CRISPR/CAS9 targeting of Pramel7 in preimplantation embryo. The Cas9 target sequence GCCTAAGAAGCAAATAGTGG in the Pramel7 gene was selected using the CRISPOR search algorithm http://crispor.tefor.net. The target sequence was incorporated into a dsDNA GenBlock fragment (IDT) 5′-GCGCGCTAATACGACTCACTATAGCCTAAGAAGCAAATAGTGGGTTTAAGAGCTATGCTGGAAACAGCATAGCAAGTTTAAATAAGGCTAGTCCGTTATCAACTTGAAAAAGTGGCACCGAGTCGGTGCTTT-3′ containing a 5′ proximal T7 promoter and a 3′ proximal sgRNA sequence shown to promote optimal assembly of Cas9 RNPs[52]. The sgRNA RNA was synthesized using the T7 transcription kit (NEB) following the manufacturer's instructions and the resulting transcripts were purified using the NuclAway gel filtration spin columns (Ambion). The Cas9 RNPs were assembled by heating the solution of 300 ng µl^{-1} sgRNA at 70 °C for 5 min, cooling to room temperature and incubating with 67 ng µl^{-1} of Cas9 protein (Toolgene) at room temperature for 20 min in a final volume of 30 µl. For the control Rosa26 RNP the procedure was repeated using a similar sgRNA targeting the XbaI site of the Rosa26 locus[31]. The Cas9 RNPs targeting the Pramel7 and Rosa26 were microinjected into the pronuclei of C57Bl/6J zygotes essentially as described in ref. 53.

We performed two independent injection rounds. The first round was performed with 224 embryos (Rosa26 = 114 embryos, P7 = 110 embryos), the second with 178 embryos (Rosa26 = 87 embryos, P7 = 91 embryos). Based on our experience, this number of embryos is sufficient to assess an effect. The surviving zygotes were cultured for 4 days in KSOM medium (Millipore). The development of the embryos was checked daily using an inverted microscope equipped with Nomarski optics. No statistical method was used to predetermine sample size and the experiments were not randomized. The investigators were not blinded to allocation during experiments and outcome assessment.

Antibodies. For immunofluorescence analysis, the following antibodies were used: anti-5mC (1:1,000: Diagenode C15200081), anti-OCT-3/4 (1:500: Santa Cruz sc-9081), anti-SSEA1 (1:200: Developmental Studies Hybridoma Bank, University of Iowa), anti-UHRF1 (1:200: Santa Cruz sc-98817).

For western blotting and immunoprecipitation analyses the following antibodies were used: anti-H3 (1:15,000: Abcam ab1791), anti-Tubulin (1:10,000: Sigma T8203), anti-FLAG (1:15,000: Sigma F7425), anti-UHRF1 (1:3,000: Santa Cruz sc-98817), anti-Elongin B (1:1,000: Santa Cruz sc-11447), anti-Elongin C (1:1,000: Santa Cruz sc-1559), anti-Cullin 2 (1:2,000: Invitrogen 51-1800), anti-ubiquitin (1:1,000: Santa Cruz sc-8017). Pramel7 antibodies were produced in rabbit through immunization with a specific Pramel7 peptide (mPRAMEL7-5: NH2-CRDYLVGTLPKKQIVEDHSR-COOH, Pineda Antikörper Services). Serum was purified by Protein A Sepharose followed by affinity chromatography and used with a dilution of 1:5,000 for western blotting and 1:200 for embryo staining.

Statistics and reproducibility. For animal experiments no statistical method was used to predetermine sample size and the experiments were not randomized. The investigators were not blinded to allocation during experiments and outcome assessment. RNA-Seq analysis was performed in triplicates: genes showing altered expression with adjusted (Benjamini and Hochberg method) P value < 0.05 were considered as differentially expressed. Bar graphs represent mean ± s.d.

Data availability. RNA-seq data that support the findings in Fig. 1e,f and Supplementary Fig. 2 and Supplementary Tables 1–4 have been deposited in the European Nucleotide Archive (ENA) under the accession code PRJEB12665. Previously published RNA-seq and Bisulfite-seq data that were reanalysed here are available under accession codes GSE20187, GSE23943 and GSE41923 at the Gene Expression Omnibus (Figs 1e and 2g and Supplementary Tables 2–4), in the ArrayExpress repository under accession number E-MTAB-2555 (Fig. 1f and Supplementary Fig. 2) and in the European Nucleotide Archive as study ERP005749 (Fig. 1f and Supplementary Fig. 2). Source data for Figs 1b, 4c, 6 and 8a; and Supplementary Figs 1a, 4b and 5b have been provided as Supplementary Table 8. All other data supporting the findings of this study are available from the corresponding authors on reasonable request.

45. Tsumura, A. *et al.* Maintenance of self-renewal ability of mouse embryonic stem cells in the absence of DNA methyltransferases Dnmt1, Dnmt3a and Dnmt3b. *Genes Cells* **11,** 805–814 (2006).
46. Ramirez, F., Dundar, F., Diehl, S., Gruning, B. A. & Manke, T. deepTools: a flexible platform for exploring deep-sequencing data. *Nucleic Acids Res.* **42,** W187–W191 (2014).
47. Bolger, A. M., Lohse, M. & Usadel, B. Trimmomatic: a flexible trimmer for Illumina sequence data. *Bioinformatics* **30,** 2114–2120 (2014).
48. Dobin, A. *et al.* STAR: ultrafast universal RNA-seq aligner. *Bioinformatics* **29,** 15–21 (2013).
49. Robinson, M. D. & Oshlack, A. A scaling normalization method for differential expression analysis of RNA-seq data. *Genome Biol.* **11,** R25 (2010).
50. Johnson, W. E., Li, C. & Rabinovic, A. Adjusting batch effects in microarray expression data using empirical Bayes methods. *Biostatistics* **8,** 118–127 (2007).
51. Le, S., Josse, J. & Husson, F. FactoMineR: an R package for multivariate analysis. *J. Stat. Softw.* **25,** 1–18 (2008).
52. Chen, B. *et al.* Dynamic imaging of genomic loci in living human cells by an optimized CRISPR/Cas system. *Cell* **155,** 1479–1491 (2013).
53. Hermann, M., Cermak, T., Voytas, D. F. & Pelczar, P. Mouse genome engineering using designer nucleases. *J. Vis. Exp.* **86,** 50930 (2014).

nature cell biology

DOI: 10.1038/ncb3554

In the format provided by the authors and unedited.

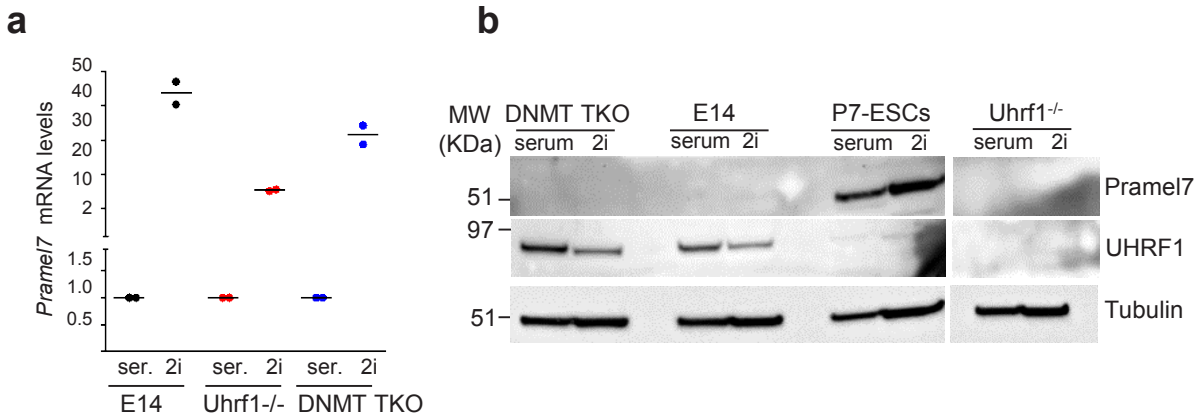

Supplementary Figure 1 (Related to Fig. 1) **a**, Expression of Pramel7 in E14, *Uhrf1*$^{-/-}$ and DNMT-TKO ESCs grown in serum/LIF or 2i conditions. Pramel7 mRNA levels were measured by qRT-PCR and normalized to Actin mRNA. Average values of two independent experiments, lines represent means. **b**, Western blot showing expression levels of Pramel7 and UHRF1 in E14, DNMT-TKO, *Uhrf1*$^{-/-}$ ESCs and P7-ESCs cultured in serum/LIF and 2i conditions detected with Pramel7 and UHRF1 antibodies. Tubulin is shown as loading control. Representative of 3 independent experiments. Unprocessed original scans of immunoblots are shown in Supplementary Figure 6.

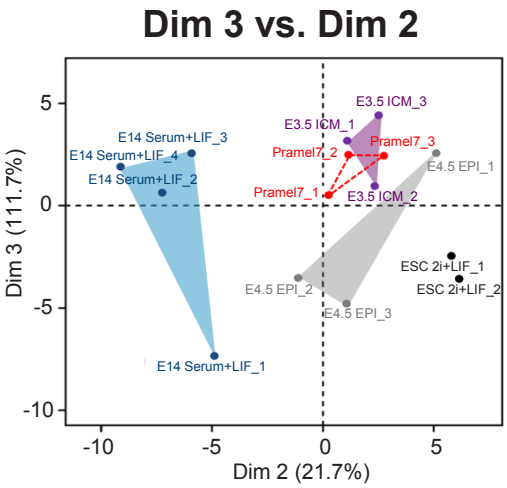

Supplementary Figure 2 (Related to Fig. 1) Correlation of P7-ESC gene expression to the early embryo stages. PCA analysis (dimensions 2 and 3) of P7-ESCs, embryonic stages E3.5 and E4.5, ESCs cultured in serum/LIF or 2i from data set published in [9].

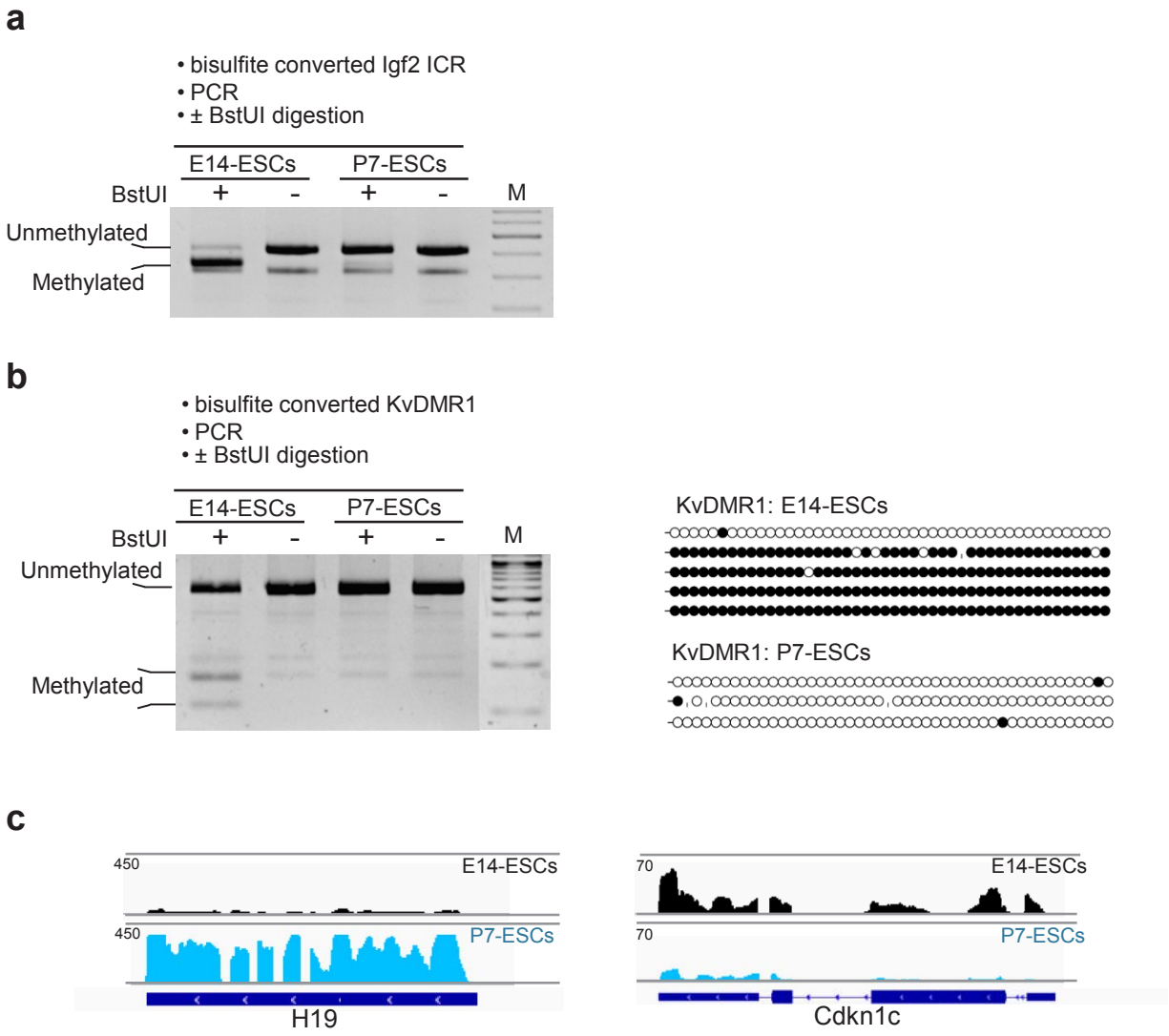

Supplementary Figure 3 (Related to Fig. 2) **a, b,** COBRA analysis showing extensive demethylation of *H19/Igf2* ICR and KvDMR1 (an intronic CpG island within the *KCNQ1* gene) in P7-ESCs. Bisulfite converted DNA was amplified with bisulfite specific primers and methylation content was assessed by digestion with BstUI that recognizes CGCG sequences. Digestion of BstUI serves as indicator of the presence of methylated sequences which were resistant to C to U conversion. Bisulfite sequencing of KvDMR1 (**b**) supports the lack of DNA methylation measured by COBRA assay. **c,** Example of changes in transcription of two imprinting regulated genes in P7-ESCs. Experiments in **a** and **b** were repeated independently twice.

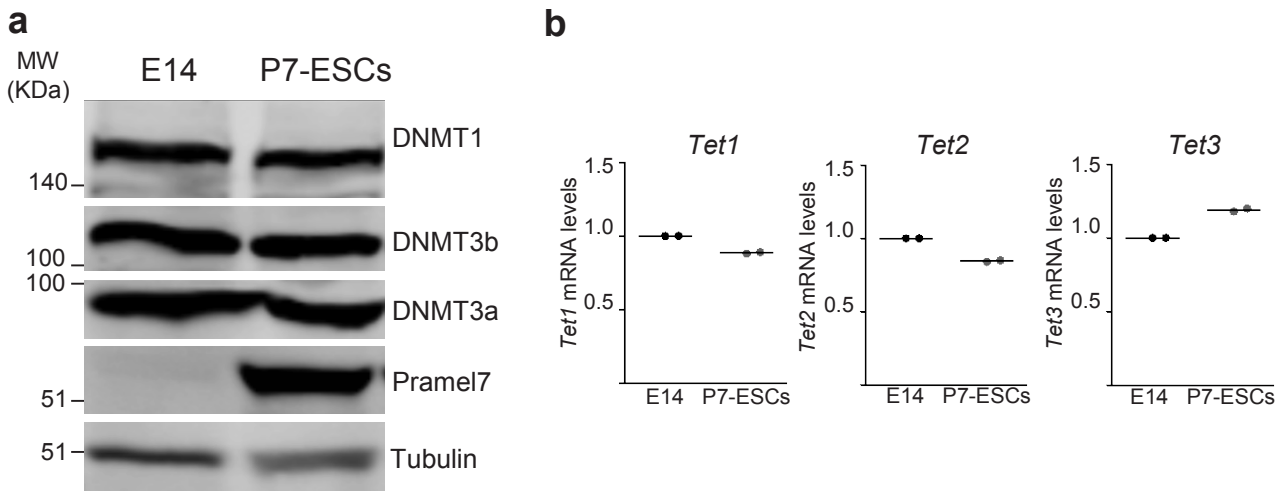

Supplementary Figure 4 (Related to Fig. 2) **a,** Western blot showing expression levels of DNMT1, 3a and 3b in E14 and P7-ESCs cultured in serum/LIF. Tubulin is shown as loading control. **b,** *Tet*1, *Tet2* and *Tet3* expression levels measured by RT-qPCR. Values were normalized to Actin mRNA and represent the average of two independent experiments. Average values of two independent experiments. Unprocessed original scans of immunoblots are shown in Supplementary Figure 6.

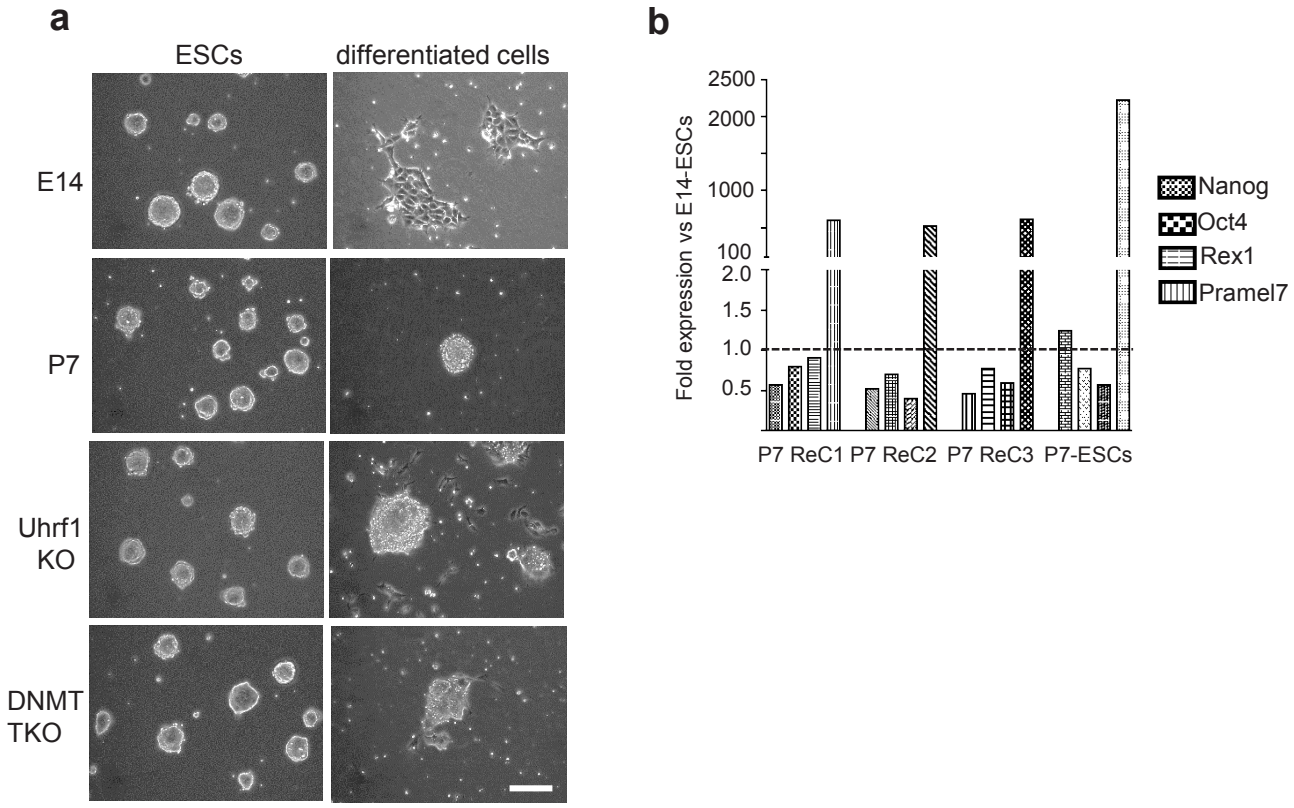

Supplementary Figure 5 (Related to Fig. 7 and 8) **a**, Representative images of ESCs grown in 2i condition and upon 5 days of differentiation. Upon differentiation methylation defective *Uhrf1*$^{-/-}$ and DNMT-TKO ESCs formed less differentiated and more compact colonies as in the case of P7-ESCs. Scale bar: 200μm. Representative of 2 independent experiments. **b**, Expression of pluripotency-associated genes *Nanog*, *Oct4* and *Rex1* in three P7 reconverted clones. Values were measured by qRT-PCR, normalized to *actin* mRNA and represented as fold change relative to the expression in E14-ESCs. Average values of two independent experiments.

4. Discussion

Oxidative stress in sperm is considered one of the major factor of male infertility. However, the contribution of oxidative DNA lesions in sperm during embryonic development remains elusive. The results of this study revealed that next to the impact on DNA integrity, oxidative stress in sperm has a direct effect on the epigenetic reprogramming. Thus, our results indicate that oxidative stress in sperm may harm both paternal genetic and epigenetic contribution to the developing embryo, affecting embryo development and embryo quality. This work also provides further evidence supporting a mechanism where active DNA demethylation in zygotes is mediated by nucleotide replacement and that the BER pathway is implicated in this process. Last, but not least our results reveal species-specific epigenetic differences between bovine and mouse embryos and gametes that will facilitate the understanding of the dynamics of DNA methylation in early development.

4.1 Contribution of paternal DNA damage in early embryonic development

In order to better define the effects of oxidative stress during early embryonic development, we used conditions (i.e. treatment with H_2O_2) that induced DNA damage without affecting the fertilization rate. We reason that the use of IVF overcame the reduction in progressive motility of sperm treated with H_2O_2 that *in vivo* would clearly have played a role. These results are also consistent with previous works showing that sperm harbouring DNA damage are able to fertilize oocytes where they can repair the DNA lesions using the repair machinery stored in the oocyte (Aitken et al., 2009; Chabory et al., 2009; Lane et al., 2014; Ronen and Glickman, 2001; Takahashi, 2012; Vinson and Hales, 2002). Accordingly, we observed enhanced recruitment of the BER core component XRCC1 to the paternal pronucleus of zygotes obtained with sperm treated with H_2O_2, suggesting that BER pathway might be implicated in this zygotic DNA damage response. We also want to point out that the analysis of XRCC1 was performed without pre-extraction, which was used in a previous study to show the stronger association of XRCC1 with paternal pronucleus in mouse zygotes (Amouroux et al., 2016). Consistent with this work our IF analyses, performed without pre-extraction showed that XRCC1 is localized at both paternal and maternal pronuclei of control zygotes. The recruitment of XRCC1 to the paternal pronuclei de-

rived from sperm treated with H_2O_2 also indicated that oxidative DNA lesions in sperm activate a DDR in the zygote and that DNA damage in sperm can be repaired post-fertilization. However, quantifying to which extent DNA damage can be repaired in the zygote is technically challenging. We were unable to detect 8-oxo-G using specific 8-oxo-G antibodies for immunofluorescence analyses in zygotes. Although we cannot exclude a technical issue, there is always the possibility that this oxidized DNA base product cannot be detected in zygotes since it was already removed in sperm by OGG1 glycosylase. Accordingly, a previous work reported that OGG1 is not only expressed in human spermatozoa but is also able to cleave 8-oxo-G adducts from sperm nuclear DNA and create the corresponding abasic sites (Smith et al., 2013). OGG1 is the only constituent of the BER pathway in sperm and given the absence of the subsequent enzymes of the BER pathway, APE1 and XRCC1, it is plausible that the paternal genome in zygotes contains abasic sites. A similar result was also reported in a study that used mouse model system (Lord and Aitken, 2015).

An important question of this work was to understand how DNA damage response to oxidative lesion of paternal genome affects early embryonic development. The DDR in embryos is distinct from what is described in somatic cells. Elementary differences exist between the embryonic and somatic cell cycle progression since the respective gap phase before and after replication is missing, resulting in a faster embryonic cell cycle progression that is in favour of the fast dividing embryos during early embryogenesis (Newport and Kirschner, 1982a). Early embryos lack the somatic cell cycle checkpoints this clearly renders the initiation of cell cycle arrest different. Additionally, early stage embryos have lost the ability to undergo apoptosis (Adiga et al., 2007; Gawecka et al., 2013; Tubbs and Nussenzweig, 2017). Our quantifications of developmental progression of embryos obtained with sperm harbouring oxidative DNA lesions showed that the major defects were in later phase of development, closed to embryonic genome activation. We observed only a moderate reduction (25%) in the completion of the first cell division (from zygote to 2-cell stage) of embryos obtained with H_2O_2-treated sperm compared to control group. In contrast, we observed a 78% reduction in the formation of blastocysts from embryos that progress beyond the 2-cell stage. Similar observations have been described in previous studies in cattle and primates showing that DNA fragmentation has an impact on later phases of development (Burruel et al., 2013; de Castro et al., 2016; Fatehi et al., 2006; Tesarik et al., 2004).

Why does oxidative stress in sperm induce an arrest in early embryonic development only later in development? We can envision several possible scenarios. In the first case, the oxidative DNA lesions present in the paternal genome cannot be properly repaired in zygotes and consequently embryonic DDR can promote, for yet unknown reasons, cell cycle arrest only after the first cell division. A possible explanation might be a p21-induced arrest of early embryos that was shown to occur only in later stages of pre-implantation embryo development after DNA damage in sperm, without affecting pronuclei formation (Adiga et al., 2007; Shimura et al., 2002). However, the fact that the BER machinery was recruited to the damaged pPN indicates that zygotes are able to conduct DNA repair, at least to some extent. Moreover, we observed that γH2AX, an early cellular response to the induction of DNA double- and single-strand breaks, is abundantly present at both the paternal and the maternal genome in control zygotes which develop normally (Thiriet and Hayes, 2005). Thus, these results indicated the presence of DNA damage in zygotes under unperturbed conditions and suggested that DNA lesions alone cannot be responsible for embryo developmental arrest. Although we cannot exclude that sperm exposed to an oxidative environment may carry toxic metabolites that would then impair embryo development, it is notable that embryonic arrest occurs at the onset of bovine embryonic genome activation (EGA, 4-cell stage). Thus, a possible further explanation is that the observed impairment of active DNA demethylation at the paternal genome might affect the expression of genes critical to development due to failure in zygotic epigenetic reprogramming.

4.2 Contribution of the paternal DNA damage to the zygotic epigenetic reprogramming

Previous studies have implicated BER in the active DNA demethylation of the paternal genome in mouse zygotes (Hajkova, 2010; Wossidlo, 2010). Pharmacological inactivation of the BER core components - APE1 and PARP1 - resulted in zygotes with significantly higher levels of DNA methylation in the paternal pronucleus (Hajkova et al., 2010). The finding that active DNA demethylation is impaired in zygotes obtained with sperm exposed to oxidative damage provides a further strong indication that this process is likely linked to DNA repair pathways. The implication of BER in DNA demethylation process suggests that the loss of 5mC is potentially driven by nucleotide replacement. Although there is a certain consensus that active DNA demethylation likely occurs through the removal of 5mC or 5mC oxidized products in pre-

replicative zygotes, this mechanism has not yet been formally proven since, to our knowledge, the incorporation of unmodified cytosines in the paternal or maternal pronuclei of pre-replicative zygotes has never been demonstrated. This work provided direct evidence of the incorporation of unmodified cytosines in the absence of DNA replication and supports a model where active DNA demethylation is mediated by nucleotide replacement activities.

We showed an enhanced recruitment of the BER core component XRCC1 from the mPN to the pPN of zygotes generated with sperm exposed to oxidative stress. Thus, as discussed above, zygotes can initiate a DDR at paternal genome harbouring DNA lesions. The fact that DNA demethylation is impaired in the damaged paternal genome suggests that oxidative lesions are repaired by BER at the expense of DNA demethylation. This impairment of DNA demethylation can be explained with two mechanisms, which are not mutually exclusive. In the first case, it can occur a competition between repair and DNA demethylation activities, where oxidative DNA lesions at paternal genome sequester BER components and make the replacement of 5mC or its derivatives less efficient. A switch in BER activity that favours the repair of oxidative lesions (i.e 8-oxoG) over the replacement of 5mC or 5mC oxidized products can be probably explained by the different activities between DNA glycosylases, which recognize specific base modifications and generate an abasic site product (Kim and Wilson, 2012). Although the glycosylase(s) implicated in active DNA demethylation in zygotes is still under debate, the glycosylases implicated in oxidative DNA lesions have been well characterized. Among them, OGG1 cleaves 8-oxo-G producing an abasic site and it is important for the recruitment of XRCC1 to damaged site that is required for successful repair (Campalans et al., 2015). Importantly, previous studies have shown that OGG1 can cleave 8-oxo-G adducts from sperm nuclear DNA to create the corresponding abasic sites that, however, cannot be repaired in sperm due to the lack of AP endonucleases and XRCC1 (Lord and Aitken, 2015; Smith et al., 2013). Thus, the presence of already established abasic sites at the paternal genome might explain the sequestration of XRCC1 at the expense of DNA demethylation activities, where recognition and excision of 5mC or its derivative is initiated only post-fertilization (**Fig. 24**).

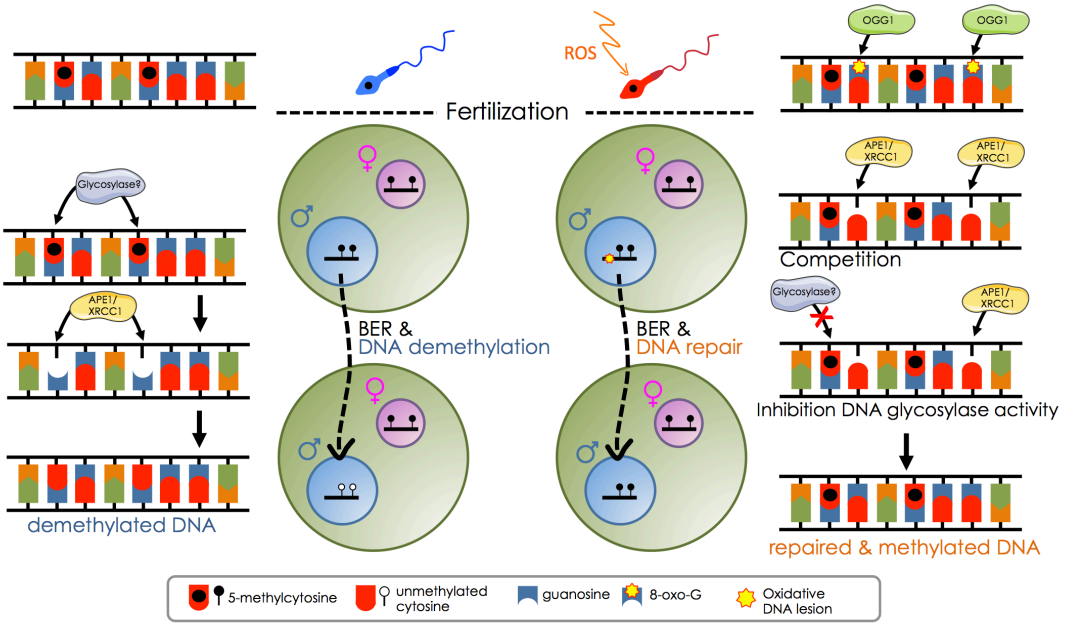

Figure 24. Oxidative lesions in sperm impair active DNA demethylation at paternal genome in zygotes. The model shows the link of BER to DNA damage and active DNA demethylation. On the left, it is shown how a putative DNA glycosylase recognizes 5mC or its modified forms, giving rise to abasic sites that via the subsequent enzymes of the BER pathway (i.e. APE1 and XRCC1) allows the incorporation of unmodified cytosines. On the right, it is shown how oxidative lesions in sperm can impair DNA demethylation. Two models are shown here. In the first case, the presence of abasic site that are established by OGG1 prior fertilization in sperm sequester XRCC1 at the expense of DNA demethylation activities, where recognition and excision of 5mC or its derivative is initiated only post-fertilization. The second model suggests that DNA lesions inhibit the activity of the DNA glycosylase(s) responsible for the DNA demethylation. In both cases, the final product is a DNA that is repaired but still contains methylated cytosines.

Another possibility is that DNA lesions inhibit the activity of the DNA glycosylase(s) responsible for the DNA demethylation (**Fig. 24**). Thymine DNA glycosylase (TDG) was implicated in DNA demethylation due to its ability to recognize and remove the oxidized forms of 5mC, 5fC and 5caC. *In vitro* biochemical analyses indicated that the removal of symmetrically methylated CpGs by TDG/TET1 complex occurs in a sequential manner and that the presence of the abasic site on one strand delays the nucleotide removal of the opposite strand (Weber et al., 2016). Although this can represent a possible scenario occurring at the paternal genome harbouring DNA lesions in the zygote, it is still possible that the factors implicated in DNA demethylation in the zygotes are different. Indeed, TET1 is present only in later stages of early embryonic development and *Tdg* deletion from the zygote has not effect on DNA demethylation (Guo et al., 2014a; He et al., 2011; Kohli and Zhang, 2013). Thus, the identification of glycosylases implicated in the excision of 5mC or its modified derivatives will be necessary to understand not only the dynamics of DNA demethylation but also the impact of DNA damage in early embryonic epigenetic reprogramming. An important

point that we took into consideration during the progression of our study was the possibility that DNA damage could affect protamine-histone exchange and chromatin decondensation of the paternal genome, which have been thought to be necessary for active DNA demethylation (Lin et al., 2013; Polanski et al., 2008). However, we did not observe any apparent defects in decondensation of the paternal pronuclei as well as in the incorporation of the early embryonic epigenetic mark H3K27me3 (Santenard et al., 2010) (data not shown). Thus, our results suggest that the impairment of DNA demethylation by oxidative lesions in sperm acts either through competition of BER or via inhibition of DNA glycosylase activity that mediate DNA demethylation.

4.3 Active DNA demethylation in bovine zygotes

This study also revealed several differences between bovine and mouse embryos. Although DNA demethylation at the paternal genome was conserved, factors previously linked to active DNA demethylation in mouse zygotes, namely γH2AX and 5hmC, displayed a distinct localization (Iqbal et al., 2011; Wossidlo, 2010, 2011). In mouse zygotes, γH2AX and 5hmC were shown to be present only in the paternal pronucleus whereas in bovine zygotes they were equally present at both paternal and maternal pronuclei. Interestingly, a recent study showed that 5hmC in human ICSI derived embryos is also localized at both paternal and maternal pronuclei (Guo et al., 2014b). Thus, the similar 5hmC pattern between bovine and human embryos makes the bovine model an interesting system to better understand epigenetic remodelling in human embryo, which for ethical issues cannot be easily accessed.

Remarkably, impairment of active DNA demethylation in bovine zygotes obtained with sperm exposed to oxidative stress was not accompanied by alterations of 5hmC content. These results indicated that active DNA demethylation in bovine embryos might not completely depend on the 5hmC pathway. Our results are consistent with recent studies showing that in mouse zygotes the loss of paternal 5mC and accumulation of 5hmC are temporally disconnected and proposed that TET3 might play a major role in preventing aberrant *de novo* methylation from the abundant DNMT3A inherited from the oocyte (Amouroux et al., 2016). Along the same line, it was recently shown that in mouse primordial germ cells 5hmC was not a prerequisite for 5mC loss and that TET1 played a role in maintaining but not driving DNA demethylation (Hill et al., 2018). Thus, the detection of 5hmC at bovine paternal pronuclei with impaired DNA demethylation suggests that H_2O_2-mediated DNA lesions in sperm impair the

first wave of DNA demethylation that is 5hmC independent. We want also to highlight here that the setting of our experiment in the context of DNA demethylation analysis in the zygote is unique of its kind. Indeed, all the studies so far have used strategies to impair 5-hmC (i.e. *Tet3* deletion) whereas the impairment of DNA demethylation was never used since it is not know how this process occurs. Therefore, our study represents the first analysis of 5hmC under conditions where DNA demethylation is impaired.

The equal presence of 5hmC at maternal pronuclei, which do not undergo a global active demethylation, suggests that some events of pre-replicative Tet3-mediated DNA demethylation can also occur at the maternal genome. This result is also consistent with the pre-replicative replacement of unmodified cytosines detected in this work and with previous studies showing loci-specific active DNA demethylation of the maternal genome (Guo et al., 2014a; Wang et al., 2014). Alternatively, the conversion of 5mC to 5hmC is not implicit to active DNA demethylation. Of note is that global 5hmC levels were lower in 2-cell stage embryos generated with H_2O_2-treated sperm compared to control embryos. Considering that our IF measurements did not detect any changes in 5hmC levels in zygotes, these results suggest that oxidative DNA lesions in sperm might also have an effect on methylcytosine hydroxylation activities during/after the first zygotic replication. Accordingly, recent genome-scale DNA methylation maps for both the paternal and maternal genomes suggested that TET3 might facilitate DNA demethylation largely by coupling with DNA replication (Shen et al., 2014).

Quantification of total 5mC and 5hmC content in bovine gametes revealed another peculiar epigenetic species-specific feature. Global 5mC and meCpG levels in mouse and human germ cells were reported to be higher in sperm than in oocytes (Amouroux et al., 2016; Guo et al., 2014a; Zhu et al., 2018). In contrast, our measurements in bovine gametes revealed that 5mC was higher in oocytes than in sperm. To our knowledge this is the first comparative analysis in bovine sperm and oocytes for global 5mC and 5hmC levels. Thus, the different 5mC content between female and male gametes underlies a novel species-specific epigenetic feature.

4.4 Oxidative stress in sperm and its implication in the success of ARTs

In a clinical context, this study has relevance in assisted reproductive techniques (ARTs) that are commonly used in human medicine and livestock breeding. Nowadays children conceived using ART account for 2% of all births, which has brought to the society a growing interest in their long-term health to the society (Canovas et al., 2017b). The fact that oxidative stress in sperm induces not only DNA lesions but also epigenetic alterations that can be transmitted to offsprings strongly indicates the necessity to identify sub-fertile patients that potentially harbour high levels of oxidative DNA damage within their spermatozoa. Accordingly, meta-analysis in human and veterinary medicine correlates increased ROS levels in sperm to a reduction of success when using ARTs (Agarwal et al., 2005). Moreover, ART constitute substantial chemical and physical variations in the environment of gametes and embryos in comparison to normal physiological conditions (Canovas et al., 2017b). For example, early embryonic development *in utero* takes place in the oviduct under physiological oxygen partial pressure (5-7%) whereas ARTs, like IVF, are performed under atmospheric oxygen partial pressure (Fischer and Bavister, 1993). *In vitro* production of bovine embryos with frozen/thawed semen is used worldwide for commercial purposes. Exposure of sperm to high levels of ROS during freezing and thawing was indicated as a potential inducer of DNA damage and decrease of sperm fertility (Amirat et al., 2005; Bansal and Bilaspuri, 2010). Accordingly, the supplementation of a cryopreservation extender with antioxidants, such as sodium pyruvate, has been shown to provide a cryoprotective effect on mammalian sperm quality (Bansal and Bilaspuri, 2010; Korkmaz et al., 2017). Additionally, the feeding of saturated as well as non-saturated fatty acids increased the quality of bull semen after cryopreservation (Gurler et al., 2015). Our work has shown that oxidative stress compromises not only the integrity of sperm DNA but also its post-fertilization epigenetic reprogramming with consequence defects in early embryo development. Considering the increasing numbers of people who will be using ART in the upcoming years, optimization of ART procedures and understanding their effect in epigenetic reprogramming in early embryo is a necessary step to determine health risks that may be associated with ART.

5. Curriculum Vitae

Personal Data

Name	Wyck Sarah Luisa
Address	Bahnhofstrasse 5
	CH-5430 Wettingen
Telephone	+41 79 248 34 27
Email	sarahwyck@aol.com
Date of birth	24 July1986
Nationality	Germany

Education

Since 5/2014	**Molecular Life Science PhD program, Zurich** **MD-PhD program, Zurich** University of Zurich, Switzerland *"Analysis of Oxidative Stress in Sperm in Early Embryonic Development"*
5/2014	**Diploma Doctor of Veterinary Medicine (Dr.med.vet.)** Vetsuisse-Faculty, University of Zurich, Switzerland
01/2014	**Diploma Veterinary Medicine (mark 5.0)** Vetsuisse-Faculty, University of Zurich, Switzerland
08/2013-01/2014	**Doctoral Thesis in Veterinary Medicine** Vetsuisse-Faculty, University of Zurich, Switzerland "*Regulation of Human DNA Polymerase β by Protein Kinase C mediated Phosphorylation"*
08/2011-08/2013	**Master of Veterinary Medicine (mark 5.3)** Vetsuisse-Faculty, University of Zurich, Switzerland "*Phosphorylation of Human DNA Polymerase β by Protein Kinase C"*
08/2008-08/2011	**Bachelor of Veterinary Medicine (mark 4.3)** Vetsuisse-Faculty, University of Zurich, Switzerland
06/2006	**Abitur (mark 2.3)** Theodor-Heuss-Gymnasium, Schopfheim, Deutschland

Publications

Graf, U., Casanova, E.A., **Wyck, S.**, Dalcher, D., Gatti, M., Vollenweider, E., Okoniewski, M.J., Weber, F.A., Patel, S.S., Schmid, M.W.*, et al.* (2017). Pramel7 mediates ground-state pluripotency through proteasomal-epigenetic combined pathways. **Nature cell biology** *19*, 763-773.

6. Acknowledgements

I would like to acknowledge all the many people that supported me throughout the period of my MD-PhD.

First of all, I would like to state extraordinary thank to my MD-PhD supervisors PD Dr. Raffaella Santoro and Prof. Dr. Heiner Bollwein for giving me the chance to be part of their group and clinic, respectively, and to perform my MD-PhD within such a fantastic scientific environment.

Un ringraziamento speciale va alla PD Dr. Raffaella Santoro che mi ha supportato sotto tutti i punti di vista durante il mio MD-PhD con incredibile passione ed entusiasmo, nonostante il mio progetto fosse cosí diverso da tutti gli altri del laboratorio. Lei ha sempre creduto nelle potenzialità del progetto e, con la sua eccezionale competenza e il suo supporto, il progetto è stato completato con successo (e cosí Viktorinox e gli altri diventarono famosi).

I mechd am Prof. Dr. Heiner Bollwein dankschee sogn, weil dank eam hob I des Ganze, wo a rechts Ausmass hod, bei eam in der Gruppn mocha kenna. Und weil er ois zur Verfügung gstellt hod, wo‘s braucht hed, daß des Ganze hod sauba obgschlossn wern kenna.

Additionally, I would like to thank my MD-PhD committee members Prof. Dr. Hanspeter Nägeli, PD Dr. Paolo Cinelli and Prof. Dr. Petra Hajkova for providing great input and having great discussions during my yearly committee meetings. Especially, I am very thankful for the collaboration with Prof. Dr. Petra Hajkova’s lab, especially thanking Dr. Cristina Requena who performed the LC-MS analyses.

Performing a MD-PhD would not have been possible without a lot of people and the great atmosphere within the group, institute and clinic. I would like to highlight the people of the Santoro lab that always supported me and kept me as an adequate group member, although I was not often physically present. Thanks to Dominik Bär, Damian Dalcher, Rodrigo Peña-Hernandez, Karolina Pietrzak, Marcin Roganowicz, Dr. Isabella Zanini, Cristiana Bersaglieri, Giorgia Rizzari, Meneka Ruvi Rupasinghe, Juliana Bizzarro and the alumni Seraina Steiger, Julia Kuhn, Erik Slabber, Dr. Natasa Savic, Dr. Eva Vollenweider and Dr. Sergio Leone for all the support and the nice

time in this group. Bsunders möcht ich mich au bi de Dr. Sandra Frommel bedanke, sie isch im wahrschte Sinn vom Wort eifach e Fründin zum Pferd stehle.

I would also like to thank the people of the Clinic of Reproductive Medicine. En primer lugar, gracias a Carolina Herrera, quien me enseñó los secretos sobre cómo tener éxito en construir una vaca. Y quien, cuando mis embriones no se comportaban como esperaba, me recordaba que esto es lo normal «trabajas con embriones, no simples células, es diferente» y que tenía que aprender a ser paciente.

Additionally, I would like to thank Dr. Elise Jeannerat, Julia Traversari and Mubbashar Hasan. Ozancan Arslan, Esin Keles ve Muhittin Tekin'e teşekkür ederim. Ayrıca, Fırat Korkmaz'a, isthmuslu ve kontralı geçen bu süre için teşekkür etmek istiyorum.

Ich würde ebenfalls gerne den Leuten vom „Alten Strickhof" danken.

Sco prüm less eu manzunar a signur prof. dr. Fredi Janett. El es adüna stat cun tuots fich serviziaivel, pront per dar üna man e güdar a chi chi d'eira aint il'ogna. Ed uschè nu staiva'l da las jadas lönch a stübgiar e pigliava sainza far lungas per mans il problem cun ün telefon spontan.

Zudem würi gärn im Hanspeter Müller für siini Unterstützig, bi welem Problem au immer, und siini Lektione in schwiizerischer Geographie danke.

Ganz speziell möchte ich mich bei Christin Oehler für ihre ständige Unterstützung und ihre Freundschaft danken. Ohne ihren täglichen Support wäre die Zeit während des PhDs nur halb so lustig und aushaltbar geworden. Vielen Dank für unvergesslichen Dienstagabende und dafür, dass ich jederzeit auf dem Sofa übernachten durfte, wenn die Embryonen mal wieder mitten in der Nacht geerntet werden wollten.

Ein af mikilvægustum persónum á meðan ég skrifaði mína doktorsritgerð í heimspeki var Andreas Fleisch, sem var alltaf til staðar, þegar mig vantaði einhvern til að tala við eða hlusta á mig, og með sinni ró og yfirvegun kom hann alltaf í veg fyrir það að ég fríkaði út. Einnig sýndi hann mér að sem liðsheild getur maður náð næstum því öllu og það er alltaf hurð sem opnast!

Επιπρόσθετα θα ήθελα να αναφέρω την Δρ Ελένη Μάλαμα. Το μαύρο χιούμορ της και οι συζητήσεις μας για επιστημονικά και μη θέματα ομόρφυναν την καθημερινότητα μας. Δεν γίνετε να ξεχάσουμε την Εμμέλεια η οποία έκανε τα «απογεύματα της Τρίτης» αξέχαστα και θα θυμάμαι για πάντα τους στίχους από το «Frozen» και το «Pumuckl»

Furthermore, I have benefited from the great scientific environment of the University of Zurich, the Vetsuisse-Faculty and the MD-PhD and the Life Science Graduate School Zurich program.

Während des Schreibens meiner Thesis habe ich Asyl im Exil bei Marina Klawitter, Dr. Laura Frese, Dr. Izaskun Mallona und Dr. Silke Kalchofner erhalten und möchte mich bei ihnen für die nette Aufnahme und die vielen aufmunternden Worte bedanken.

Ohni diä großi und bedingungslosi Unterstützig vo minere Familiä, wär dä PhD mit allä sinä guetä und schlechtä Zite net in derä Wies umsetzbar gsi. Deshalb möcht ich mich gern bi mienä Eltere Ingrid Wagner und Manfred Wyck und miem Brueder Raphael Wyck, ganz speziell bedanke. Ihr sind großartig!

Speziell möcht ich mi au bim Dario Zimmerli bedanke, er het mich während dere Ziit immer unterstützt und het net nur einmal miini diverse Gfühlusbrüch ertrage müesse. Au siini Biiträg zu minere wüsseschaftliche Arbet sin vu unschätzbarem Wert und hän mich immer wiedr agregt d'Dinge vu verschiednige Perspektive z'betrachte.

Zuedem möcht ich gärn mine liebe Vetis (Saskia Keller, Rebekka Romer und Ursina Renggli) für die lang und guet Fründschaft, d'Unterstützig und die viele tolle gmeinsame Erläbnis danke.

En bsundere Dank goht au a d'Denise Stein, defür dass ich jederziit uf ihre Unterstützig zähle chan und sie mier immer mit Rat und Tat zur Siite stoht und das siit fascht 25 Johr.

And thanks to all the people who helped out with translating the acknwoledgment paragraphs: Ingrid Wagner (alemannisch), Sabine Boetius (bayrisch), Prof. Dr. Rico Thun (rätoromanisch), Eva Tesche (isländisch), Dr. Izaskun Mallona (spanisch), Cristiana Bersaglieri (italienisch), Dr. Nick Doumpas (griechisch) and Dr. Firat Korkmaz (türkisch).

7. References

Adiga, S.K., Toyoshima, M., Shiraishi, K., Shimura, T., Takeda, J., Taga, M., Nagai, H., Kumar, P., and Niwa, O. (2007). p21 provides stage specific DNA damage control to preimplantation embryos. Oncogene *26*, 6141-6149.

Agarwal, A., Allamaneni, S.S., Nallella, K.P., George, A.T., and Mascha, E. (2005). Correlation of reactive oxygen species levels with the fertilization rate after in vitro fertilization: a qualified meta-analysis. Fertility and sterility *84*, 228-231.

Agarwal, A., Durairajanayagam, D., and du Plessis, S.S. (2014a). Utility of antioxidants during assisted reproductive techniques: an evidence based review. Reproductive biology and endocrinology : RB&E *12*, 112.

Agarwal, A., Durairajanayagam, D., Halabi, J., Peng, J., and Vazquez-Levin, M. (2014b). Proteomics, oxidative stress and male infertility. Reproductive biomedicine online *29*, 32-58.

Agarwal, A., Makker, K., and Sharma, R. (2008). Clinical relevance of oxidative stress in male factor infertility: an update. American journal of reproductive immunology (New York, NY : 1989) *59*, 2-11.

Agarwal, A., and Saleh, R.A. (2002). Role of oxidants in male infertility: rationale, significance, and treatment. Urol Clin North Am *29*, 817-827.

Agarwal, A., Saleh, R.A., and Bedaiwy, M.A. (2003). Role of reactive oxygen species in the pathophysiology of human reproduction. Fertility and sterility *79*, 829-843.

Aguirre-Lavin, T., Adenot, P., Bonnet-Garnier, A., Lehmann, G., Fleurot, R., Boulesteix, C., Debey, P., and Beaujean, N. (2012). 3D-FISH analysis of embryonic nuclei in mouse highlights several abrupt changes of nuclear organization during preimplantation development. BMC developmental biology *12*, 30.

Agulnik, A.I., Bishop, C.E., Lerner, J.L., Agulnik, S.I., and Solovyev, V.V. (1997). Analysis of mutation rates in the SMCY/SMCX genes shows that mammalian evolution is male driven. Mammalian genome : official journal of the International Mammalian Genome Society *8*, 134-138.

Ahmed, K., Dehghani, H., Rugg-Gunn, P., Fussner, E., Rossant, J., and Bazett-Jones, D.P. (2010). Global Chromatin Architecture Reflects Pluripotency and Lineage Commitment in the Early Mouse Embryo. PloS one *5*, e10531.

Aiken, C.E., Swoboda, P.P., Skepper, J.N., and Johnson, M.H. (2004). The direct measurement of embryogenic volume and nucleo-cytoplasmic ratio during mouse pre-implantation development. Reproduction *128*, 527-535.

Aitken, R.J. (2017). Reactive oxygen species as mediators of sperm capacitation and pathological damage. Mol Reprod Dev *84*, 1039-1052.

Aitken, R.J., and Baker, H.W. (1995). Seminal leukocytes: passengers, terrorists or good samaritans? Human reproduction *10*, 1736-1739.

Aitken, R.J., Clarkson, J.S., and Fishel, S. (1989). Generation of reactive oxygen species, lipid peroxidation, and human sperm function. Biology of reproduction *41*, 183-197.

Aitken, R.J., and De Iuliis, G.N. (2010). On the possible origins of DNA damage in human spermatozoa. Mol Hum Reprod *16*, 3-13.

Aitken, R.J., De Iuliis, G.N., and McLachlan, R.I. (2009). Biological and clinical significance of DNA damage in the male germ line. International journal of andrology *32*, 46-56.

Aitken, R.J., and Krausz, C. (2001). Oxidative stress, DNA damage and the Y chromosome. Reproduction *122*, 497-506.

Alberts, B., Johnson, A., Lewis, J., Raff, M., Roberts, K., and Walter, P. (2008). Molecular Biology of the Cell, Vol 5 (Garland Science).

Aleem, M., Padwal, V., Choudhari, J., Balasinor, N., and Gill-Sharma, M.K. (2008). Sperm protamine levels as indicators of fertilising potential in sexually mature male rats. Andrologia *40*, 29-37.

Allis, C.D., and Jenuwein, T. (2016). The molecular hallmarks of epigenetic control. Nat Rev Genet *17*, 487-500.

Almeida, K.H., and Sobol, R.W. (2007). A unified view of base excision repair: lesion-dependent protein complexes regulated by post-translational modification. DNA repair *6*, 695-711.

Ambrosi, C., Manzo, M., and Baubec, T. (2017). Dynamics and Context-Dependent Roles of DNA Methylation. Journal of molecular biology *429*, 1459-1475.

Amirat, L., Anton, M., Tainturier, D., Chatagnon, G., Battut, I., and Courtens, J.L. (2005). Modifications of bull spermatozoa induced by three extenders: Biociphos, low density lipoprotein and Triladyl, before, during and after freezing and thawing. Reproduction *129*, 535-543.

Amouroux, R., Nashun, B., Shirane, K., Nakagawa, S., Hill, P.W., D'Souza, Z., Nakayama, M., Matsuda, M., Turp, A., Ndjetehe, E.*, et al.* (2016). De novo DNA methylation drives 5hmC accumulation in mouse zygotes. Nature cell biology *18*, 225-233.

Aravin, A.A., Sachidanandam, R., Bourc'his, D., Schaefer, C., Pezic, D., Toth, K.F., Bestor, T., and Hannon, G.J. (2008). A piRNA pathway primed by individual transposons is linked to de novo DNA methylation in mice. Mol Cell *31*, 785-799.

Arias, M.E., Sanchez, R., Risopatron, J., Perez, L., and Felmer, R. (2014). Effect of sperm pretreatment with sodium hydroxide and dithiothreitol on the efficiency of bovine intracytoplasmic sperm injection. Reproduction, fertility, and development *26*, 847-854.

Arita, K., Ariyoshi, M., Tochio, H., Nakamura, Y., and Shirakawa, M. (2008). Recognition of hemi-methylated DNA by the SRA protein UHRF1 by a base-flipping mechanism. In Nature, pp. 818-821.

Arney, K.L., Erhardt, S., Drewell, R.A., and Surani, M.A. (2001). Epigenetic reprogramming of the genome--from the germ line to the embryo and back again. Int J Dev Biol *45*, 533-540.

Arnheim, N., and Shibata, D. (1997). DNA mismatch repair in mammals: role in disease and meiosis. Current opinion in genetics & development *7*, 364-370.

Awe, S., and Renkawitz-Pohl, R. (2010). Histone H4 Acetylation is Essential to Proceed from a Histone- to a Protamine-based Chromatin Structure in Spermatid Nuclei of Drosophila melanogaster. Systems biology in reproductive medicine *56*, 44-61.

Baarends, W.M., Hoogerbrugge, J.W., Roest, H.P., Ooms, M., Vreeburg, J., Hoeijmakers, J.H., and Grootegoed, J.A. (1999). Histone ubiquitination and chromatin remodeling in mouse spermatogenesis. Dev Biol *207*, 322-333.

Baarends, W.M., van der Laan, R., and Grootegoed, J.A. (2001). DNA repair mechanisms and gametogenesis. Reproduction *121*, 31-39.

Baart, E.B., van der Heijden, G.W., van der Hoeven, F.A., Bakker, R., Cooper, T.G., and de Boer, P. (2004). Reduced oocyte activation and first cleavage rate after ICSI with spermatozoa from a sterile mouse chromosome mutant. Human reproduction *19*, 1140-1147.

Baker, S.M., Plug, A.W., Prolla, T.A., Bronner, C.E., Harris, A.C., Yao, X., Christie, D.M., Monell, C., Arnheim, N., Bradley, A.*, et al.* (1996). Involvement of mouse Mlh1 in DNA mismatch repair and meiotic crossing over. Nature genetics *13*, 336-342.

Bakhtari, A., and Ross, P.J. (2014). DPPA3 prevents cytosine hydroxymethylation of the maternal pronucleus and is required for normal development in bovine embryos. Epigenetics *9*, 1271-1279.

Balhorn, R. (2007). The protamine family of sperm nuclear proteins. Genome Biol *8*, 227.

Bansal, A.K., and Bilaspuri, G.S. (2010). Impacts of oxidative stress and antioxidants on semen functions. Vet Med Int *2010*.

Bao, J., and Bedford, M.T. (2016). Epigenetic regulation of the histone-to-protamine transition during spermiogenesis. Reproduction *151*, R55-70.

Barau, J., Teissandier, A., Zamudio, N., Roy, S., Nalesso, V., Herault, Y., Guillou, F., and Bourc'his, D. (2016). The DNA methyltransferase DNMT3C protects male germ cells from transposon activity. Science *354*, 909-912.

Barnes, D.E., and Lindahl, T. (2004). Repair and genetic consequences of endogenous DNA base damage in mammalian cells. Annual review of genetics *38*, 445-476.

Barton, S.C., Arney, K.L., Shi, W., Niveleau, A., Fundele, R., Surani, M.A., and Haaf, T. (2001). Genome-wide methylation patterns in normal and uniparental early mouse embryos. Human molecular genetics *10*, 2983-2987.

Baubec, T., Colombo, D.F., Wirbelauer, C., Schmidt, J., Burger, L., Krebs, A.R., Akalin, A., and Schubeler, D. (2015). Genomic profiling of DNA methyltransferases reveals a role for DNMT3B in genic methylation. Nature *520*, 243-247.

Baus, F., Gire, V., Fisher, D., Piette, J., and Dulic, V. (2003). Permanent cell cycle exit in G2 phase after DNA damage in normal human fibroblasts. Embo J *22*, 3992-4002.

Beaujean, N., Hartshorne, G., Cavilla, J., Taylor, J., Gardner, J., Wilmut, I., Meehan, R., and Young, L. (2004a). Non-conservation of mammalian preimplantation methylation dynamics. Curr Biol *14*, R266-267.

Beaujean, N., Taylor, J.E., McGarry, M., Gardner, J.O., Wilmut, I., Loi, P., Ptak, G., Galli, C., Lazzari, G., Bird, A.*, et al.* (2004b). The effect of interspecific oocytes on demethylation of sperm DNA. Proc Natl Acad Sci U S A *101*, 7636-7640.

Benedict, C.L., Gilfillan, S., Thai, T.H., and Kearney, J.F. (2000). Terminal deoxynucleotidyl transferase and repertoire development. Immunological reviews *175*, 150-157.

Bergerat, A., de Massy, B., Gadelle, D., Varoutas, P.C., Nicolas, A., and Forterre, P. (1997). An atypical topoisomerase II from Archaea with implications for meiotic recombination. Nature *386*, 414-417.

Bertocci, B., De Smet, A., Weill, J.C., and Reynaud, C.A. (2006). Nonoverlapping functions of DNA polymerases mu, lambda, and terminal deoxynucleotidyltransferase during immunoglobulin V(D)J recombination in vivo. Immunity *25*, 31-41.

Bertolini, M., Moyer, A.L., Mason, J.B., Batchelder, C.A., Hoffert, K.A., Bertolini, L.R., Carneiro, G.F., Cargill, S.L., Famula, T.R., Calvert, C.C.*, et al.* (2004). Evidence of increased substrate availability to in vitro-derived bovine foetuses and association with accelerated conceptus growth. Reproduction *128*, 341-354.

Bjerregaard, B., Pedersen, H.G., Jakobsen, A.S., Rickords, L.F., Lai, L., Cheong, H.T., Samuel, M., Prather, R.S., Strejcek, F., Rasmussen, Z.R.*, et al.* (2007). Activation of ribosomal RNA genes in porcine embryos produced in vitro or by somatic cell nuclear transfer. Molecular reproduction and development *74*, 35-41.

Bogenhagen, D.F. (1999). Repair of mtDNA in vertebrates. American Journal of Human Genetics *64*, 1276-1281.

Bomfim, M.M., Andrade, G.M., Del Collado, M., Sangalli, J.R., Fontes, P.K., Nogueira, M.F.G., Meirelles, F.V., da Silveira, J.C., and Perecin, F. (2017). Antioxidant responses and deregulation of epigenetic writers and erasers link oxidative stress and DNA methylation in bovine blastocysts. Molecular reproduction and development.

Borgel, J. (2010). Targets and dynamics of promoter DNA methylation during early mouse development. Nature Genet *42*, 1093-1100.

Bošković, A., Bender, A., Gall, L., Ziegler-Birling, C., Beaujean, N., and Torres-Padilla, M.-E. (2012). Analysis of active chromatin modifications in early mammalian embryos reveals uncoupling of H2A.Z acetylation and H3K36 trimethylation from embryonic genome activation. Epigenetics *7*, 747-757.

Bostick, M. (2007). UHRF1 plays a role in maintaining DNA methylation in mammalian cells. Science *317*, 1760-1764.

Bowles, J., and Koopman, P. (2010). Sex determination in mammalian germ cells: extrinsic versus intrinsic factors. Reproduction *139*, 943-958.

Branco, M.R., Oda, M., and Reik, W. (2008). Safeguarding parental identity: Dnmt1 maintains imprints during epigenetic reprogramming in early embryogenesis. Genes & development *22*, 1567-1571.

Brandriff, B., and Pedersen, R.A. (1981). Repair of the ultraviolet-irradiated male genome in fertilized mouse eggs. Science *211*, 1431-1433.

Braude, P., Bolton, V., and Moore, S. (1988). Human gene expression first occurs between the four- and eight-cell stages of preimplantation development. Nature *332*, 459-461.

Brykczynska, U., Hisano, M., Erkek, S., Ramos, L., Oakeley, E.J., Roloff, T.C., Beisel, C., Schubeler, D., Stadler, M.B., and Peters, A.H. (2010). Repressive and active histone methylation mark distinct promoters in human and mouse spermatozoa. Nature structural & molecular biology *17*, 679-687.

Burns, K.H., Viveiros, M.M., Ren, Y., Wang, P., DeMayo, F.J., Frail, D.E., Eppig, J.J., and Matzuk, M.M. (2003). Roles of NPM2 in chromatin and nucleolar organization in oocytes and embryos. Science *300*, 633-636.

Burrows, C.J., and Muller, J.G. (1998). Oxidative Nucleobase Modifications Leading to Strand Scission. Chemical reviews *98*, 1109-1152.

Burruel, V., Klooster, K.L., Chitwood, J., Ross, P.J., and Meyers, S.A. (2013). Oxidative damage to rhesus macaque spermatozoa results in mitotic arrest and transcript abundance changes in early embryos. Biology of reproduction *89*, 72.

Burton, A., and Torres-Padilla, M.E. (2010). Epigenetic reprogramming and development: a unique heterochromatin organization in the preimplantation mouse embryo. Brief Funct Genom *9*, 444-454.

Burton, A., and Torres-Padilla, M.E. (2014). Chromatin dynamics in the regulation of cell fate allocation during early embryogenesis. Nat Rev Mol Cell Biol *15*, 723-734.

Caldecott, K.W. (2008). Single-strand break repair and genetic disease. Nature reviews Genetics *9*, 619-631.

Campalans, A., Moritz, E., Kortulewski, T., Biard, D., Epe, B., and Radicella, J.P. (2015). Interaction with OGG1 Is Required for Efficient Recruitment of XRCC1 to Base Excision Repair and Maintenance of Genetic Stability after Exposure to Oxidative Stress. Molecular and cellular biology *35*, 1648-1658.

Canovas, S., Ivanova, E., Romar, R., Garcia-Martinez, S., Soriano-Ubeda, C., Garcia-Vazquez, F.A., Saadeh, H., Andrews, S., Kelsey, G., and Coy, P. (2017a). DNA methylation and gene expression changes derived from assisted reproductive technologies can be decreased by reproductive fluids. Elife *6*.

Canovas, S., Ross, P.J., Kelsey, G., and Coy, P. (2017b). DNA Methylation in Embryo Development: Epigenetic Impact of ART (Assisted Reproductive Technologies). Bioessays *39*.

Cantley, L.C. (2002). The phosphoinositide 3-kinase pathway. Science *296*, 1655-1657.

Castrillon, D.H., Miao, L., Kollipara, R., Horner, J.W., and DePinho, R.A. (2003). Suppression of ovarian follicle activation in mice by the transcription factor Foxo3a. Science *301*, 215-218.

Celeste, A., Petersen, S., Romanienko, P.J., Fernandez-Capetillo, O., Chen, H.T., Sedelnikova, O.A., Reina-San-Martin, B., Coppola, V., Meffre, E., Difilippantonio, M.J.*, et al.* (2002). Genomic instability in mice lacking histone H2AX. Science *296*, 922-927.

Chabory, E., Damon, C., Lenoir, A., Kauselmann, G., Kern, H., Zevnik, B., Garrel, C., Saez, F., Cadet, R., Henry-Berger, J.*, et al.* (2009). Epididymis seleno-independent glutathione peroxidase 5 maintains sperm DNA integrity in mice. The Journal of clinical investigation *119*, 2074-2085.

Challen, G.A. (2012). DNMT3A is essential for hematopoietic stem cell differentiation. Nature Genet *44*, 23-31.

Chen, C.C., Wang, K.Y., and Shen, C.K. (2012). The mammalian de novo DNA methyltransferases DNMT3A and DNMT3B are also DNA 5-hydroxymethylcytosine dehydroxymethylases. The Journal of biological chemistry *287*, 33116-33121.

Chen, T., Tsujimoto, N., and Li, E. (2004). The PWWP domain of Dnmt3a and Dnmt3b is required for directing DNA methylation to the major satellite repeats at pericentric heterochromatin. Mol Cell Biol *24*, 9048-9058.

Chen, T., Ueda, Y., Dodge, J.E., Wang, Z., and Li, E. (2003). Establishment and maintenance of genomic methylation patterns in mouse embryonic stem cells by DNMT3A and DNMT3B. Mol Cell Biol *23*, 5594-5605.

Chen, T., Ueda, Y., Xie, S., and Li, E. (2002). A novel Dnmt3a isoform produced from an alternative promoter localizes to euchromatin and its expression correlates with active de novo methylation. J Biol Chem *277*, 38746-38754.

Chen, Z., Hagen, D.E., Elsik, C.G., Ji, T., Morris, C.J., Moon, L.E., and Rivera, R.M. (2015). Characterization of global loss of imprinting in fetal overgrowth syndrome induced by assisted reproduction. Proceedings of the National Academy of Sciences of the United States of America *112*, 4618-4623.

Chen, Z.X., and Riggs, A.D. (2011). DNA methylation and demethylation in mammals. J Biol Chem *286*, 18347-18353.

Cho, C., Willis, W.D., Goulding, E.H., Jung-Ha, H., Choi, Y.C., Hecht, N.B., and Eddy, E.M. (2001). Haploinsufficiency of protamine-1 or -2 causes infertility in mice. Nat Genet *28*, 82-86.

Chocu, S., Calvel, P., Rolland, A.D., and Pineau, C. (2012). Spermatogenesis in mammals: proteomic insights. Systems biology in reproductive medicine *58*, 179-190.

Christmann, M., Tomicic, M.T., Roos, W.P., and Kaina, B. (2003). Mechanisms of human DNA repair: an update. Toxicology *193*, 3-34.

Chuang, L.S., Ian, H.I., Koh, T.W., Ng, H.H., Xu, G., and Li, B.F. (1997). Human DNA-(cytosine-5) methyltransferase-PCNA complex as a target for p21WAF1. Science *277*, 1996-2000.

Chung, J.T., Keefer, C.L., and Downey, B.R. (2000). Activation of bovine oocytes following intracytoplasmic sperm injection (ICSI). Theriogenology *53*, 1273-1284.

Ciccia, A., and Elledge, S.J. (2010). The DNA Damage Response: Making It Safe to Play with Knives. Molecular cell *40*, 179-204.

Cocuzza, M., Sikka, S.C., Athayde, K.S., and Agarwal, A. (2007). Clinical relevance of oxidative stress and sperm chromatin damage in male infertility: an evidence based analysis. International braz j urol : official journal of the Brazilian Society of Urology *33*, 603-621.

Conn, C.W., Lewellyn, A.L., and Maller, J.L. (2004). The DNA Damage Checkpoint in Embryonic Cell Cycles Is Dependent on the DNA-to-Cytoplasmic Ratio. Developmental Cell *7*, 275-281.

Cook, P.J., Ju, B.G., Telese, F., Wang, X., Glass, C.K., and Rosenfeld, M.G. (2009). Tyrosine dephosphorylation of H2AX modulates apoptosis and survival decisions. Nature *458*, 591-596.

Cortazar, D., Kunz, C., Selfridge, J., Lettieri, T., Saito, Y., MacDougall, E., Wirz, A., Schuermann, D., Jacobs, A.L., Siegrist, F.*, et al.* (2011). Embryonic lethal phenotype reveals a function of TDG in maintaining epigenetic stability. Nature *470*, 419-423.

Cortellino, S. (2011). Thymine DNA glycosylase is essential for active DNA demethylation by linked deamination-base excision repair. Cell *146*, 67-79.

Cortellino, S., Xu, J., Sannai, M., Moore, R., Caretti, E., Cigliano, A., Le Coz, M., Devarajan, K., Wessels, A., Soprano, D.*, et al.* (2011). Thymine DNA glycosylase is essential for active DNA demethylation by linked deamination-base excision repair. Cell *146*, 67-79.

Cowell, I.G., Aucott, R., Mahadevaiah, S.K., Burgoyne, P.S., Huskisson, N., Bongiorni, S., Prantera, G., Fanti, L., Pimpinelli, S., Wu, R.*, et al.* (2002). Heterochromatin, HP1 and methylation at lysine 9 of histone H3 in animals. Chromosoma *111*, 22-36.

Coy, P., and Romar, R. (2002). In vitro production of pig embryos: a point of view. Reproduction, fertility, and development *14*, 275-286.

Crosby, I.M., Gandolfi, F., and Moor, R.M. (1988). Control of protein synthesis during early cleavage of sheep embryos. Journal of reproduction and fertility *82*, 769-775.

Cui, R., Widlund, H.R., Feige, E., Lin, J.Y., Wilensky, D.L., Igras, V.E., D'Orazio, J., Fung, C.Y., Schanbacher, C.F., Granter, S.R.*, et al.* (2007). Central role of p53 in the suntan response and pathologic hyperpigmentation. Cell *128*, 853-864.

Dada, R., Kumar, M., Jesudasan, R., Fernandez, J.L., Gosalvez, J., and Agarwal, A. (2012). Epigenetics and its role in male infertility. Journal of assisted reproduction and genetics *29*, 213-223.

Dahl, J.A., Jung, I., Aanes, H., Greggains, G.D., Manaf, A., Lerdrup, M., Li, G., Kuan, S., Li, B., Lee, A.Y.*, et al.* (2016). Broad histone H3K4me3 domains in mouse oocytes modulate maternal-to-zygotic transition. Nature *537*, 548-552.

Dalton, S.R., and Bellacosa, A. (2012). DNA demethylation by TDG. Epigenomics *4*, 459-467.

Dattena, M., Ptak, G., Loi, P., and Cappai, P. (2000). Survival and viability of vitrified in vitro and in vivo produced ovine blastocysts. Theriogenology *53*, 1511-1519.

Daujat, S., Weiss, T., Mohn, F., Lange, U.C., Ziegler-Birling, C., Zeissler, U., Lappe, M., Schubeler, D., Torres-Padilla, M.E., and Schneider, R. (2009). H3K64 trimethylation marks heterochromatin and is dynamically remodeled during developmental reprogramming. Nature structural & molecular biology *16*, 777-781.

David, S.S., O'Shea, V.L., and Kundu, S. (2007). Base-excision repair of oxidative DNA damage. Nature *447*, 941-950.

David, S.S., and Williams, S.D. (1998). Chemistry of Glycosylases and Endonucleases Involved in Base-Excision Repair. Chemical reviews *98*, 1221-1262.

Davis, A.J., and Chen, D.J. (2013). DNA double strand break repair via non-homologous end-joining. Translational cancer research *2*, 130-143.

Davis, T.L., Yang, G.J., McCarrey, J.R., and Bartolomei, M.S. (2000). The H19 methylation imprint is erased and re-established differentially on the parental alleles during male germ cell development. Hum Mol Genet *9*, 2885-2894.

Dawlaty, M.M., Ganz, K., Powell, B.E., Hu, Y.C., Markoulaki, S., Cheng, A.W., Gao, Q., Kim, J., Choi, S.W., Page, D.C.*, et al.* (2011). Tet1 is dispensable for maintaining pluripotency and its loss is compatible with embryonic and postnatal development. Cell stem cell *9*, 166-175.

de Bruin, J.P., Dorland, M., Spek, E.R., Posthuma, G., van Haaften, M., Looman, C.W., and te Velde, E.R. (2002). Ultrastructure of the resting ovarian follicle pool in healthy young women. Biol Reprod *66*, 1151-1160.

de Castro, L.S., de Assis, P.M., Siqueira, A.F., Hamilton, T.R., Mendes, C.M., Losano, J.D., Nichi, M., Visintin, J.A., and Assumpcao, M.E. (2016). Sperm Oxidative Stress Is Detrimental to Embryo Development: A Dose-Dependent Study Model and a New and More Sensitive Oxidative Status Evaluation. Oxid Med Cell Longev *2016*, 8213071.

De Iuliis, G.N., Thomson, L.K., Mitchell, L.A., Finnie, J.M., Koppers, A.J., Hedges, A., Nixon, B., and Aitken, R.J. (2009). DNA damage in human spermatozoa is highly correlated with the efficiency of chromatin remodeling and the formation of 8-hydroxy-2'-deoxyguanosine, a marker of oxidative stress. Biology of reproduction *81*, 517-524.

de Laat, W.L., Jaspers, N.G., and Hoeijmakers, J.H. (1999). Molecular mechanism of nucleotide excision repair. Genes & development *13*, 768-785.

de Lamirande, E., and Gagnon, C. (1993). Human sperm hyperactivation in whole semen and its association with low superoxide scavenging capacity in seminal plasma. Fertility and sterility *59*, 1291-1295.

de Lamirande, E., and Gagnon, C. (1995). Impact of reactive oxygen species on spermatozoa: a balancing act between beneficial and detrimental effects. Human reproduction *10 Suppl 1*, 15-21.

de Lamirande, E., and O'Flaherty, C. (2012). Sperm Capacitation as an Oxidative Event. Oxid Stress Appl Bas, 57-94.

De Lucia, F., Faraone-Mennella, M.R., D'Erme, M., Quesada, P., Caiafa, P., and Farina, B. (1994). Histone-induced condensation of rat testis chromatin: testis-specific H1t versus somatic H1 variants. Biochemical and biophysical research communications *198*, 32-39.

de Montera, B., Fournier, E., Shojaei Saadi, H.A., Gagne, D., Laflamme, I., Blondin, P., Sirard, M.A., and Robert, C. (2013). Combined methylation mapping of 5mC and 5hmC during early embryonic stages in bovine. BMC genomics *14*, 406.

de Waal, E., Mak, W., Calhoun, S., Stein, P., Ord, T., Krapp, C., Coutifaris, C., Schultz, R.M., and Bartolomei, M.S. (2014). In vitro culture increases the frequency of stochastic epigenetic errors at imprinted genes in placental tissues from mouse concepti produced through assisted reproductive technologies. Biol Reprod *90*, 22.

Dean, W. (2014). DNA methylation and demethylation: a pathway to gametogenesis and development. Mol Reprod Dev *81*, 113-125.

Dean, W., Santos, F., Stojkovic, M., Zakhartchenko, V., Walter, J., Wolf, E., and Reik, W. (2001). Conservation of methylation reprogramming in mammalian development: aberrant reprogramming in cloned embryos. Proc Natl Acad Sci U S A *98*, 13734-13738.

Derijck, A., van der Heijden, G., Giele, M., Philippens, M., and de Boer, P. (2008). DNA double-strand break repair in parental chromatin of mouse zygotes, the first cell cycle as an origin of de novo mutation. Human molecular genetics *17*, 1922-1937.

Deshmukh, R.S., Ostrup, O., Ostrup, E., Vejlsted, M., Niemann, H., Lucas-Hahn, A., Petersen, B., Li, J., Callesen, H., and Hyttel, P. (2011). DNA methylation in porcine preimplantation embryos developed in vivo and produced by in vitro fertilization, parthenogenetic activation and somatic cell nuclear transfer. Epigenetics *6*, 177-187.

Devito, L.G., Fernandes, C.B., Blanco, I.D., Tsuribe, P.M., and Landim-Alvarenga, F.C. (2010). Use of a Piezo drill for intracytoplasmic sperm injection into cattle oocytes activated with ionomycin associated with roscovitine. Reproduction in domestic animals = Zuchthygiene *45*, 654-658.

Dhayalan, A., Rajavelu, A., Rathert, P., Tamas, R., Jurkowska, R.Z., Ragozin, S., and Jeltsch, A. (2010). The Dnmt3a PWWP domain reads histone 3 lysine 36 trimethylation and guides DNA methylation. J Biol Chem *285*, 26114-26120.

Difilippantonio, S., Gapud, E., Wong, N., Huang, C.Y., Mahowald, G., Chen, H.T., Kruhlak, M.J., Callen, E., Livak, F., Nussenzweig, M.C.*, et al.* (2008). 53BP1 facilitates long-range DNA end-joining during V(D)J recombination. Nature *456*, 529-533.

Dimitrova, N., Chen, Y.C., Spector, D.L., and de Lange, T. (2008). 53BP1 promotes non-homologous end joining of telomeres by increasing chromatin mobility. Nature *456*, 524-528.

Dokshin, G.A., Baltus, A.E., Eppig, J.J., and Page, D.C. (2013). Oocyte differentiation is genetically dissociable from meiosis in mice. Nat Genet *45*, 877-883.

Dottermusch-Heidel, C., Gartner, S.M., Tegeder, I., Rathke, C., Barckmann, B., Bartkuhn, M., Bhushan, S., Steger, K., Meinhardt, A., and Renkawitz-Pohl, R. (2014). H3K79 methylation: a new conserved mark that accompanies H4 hyperacetylation prior to histone-to-protamine transition in Drosophila and rat. Biology open *3*, 444-452.

Drabent, B., Bode, C., Miosge, N., Herken, R., and Doenecke, D. (1998). Expression of the mouse histone gene H1t begins at premeiotic stages of spermatogenesis. Cell and tissue research *291*, 127-132.

Duranthon, V., and Chavatte-Palmer, P. (2018). Long term effects of ART: What do animals tell us? Mol Reprod Dev *85*, 348-368.

Eckert, J., and Niemann, H. (1995). In vitro maturation, fertilization and culture to blastocysts of bovine oocytes in protein-free media. Theriogenology *43*, 1211-1225.

Edelmann, W., Cohen, P.E., Kane, M., Lau, K., Morrow, B., Bennett, S., Umar, A., Kunkel, T., Cattoretti, G., Chaganti, R.*, et al.* (1996). Meiotic pachytene arrest in MLH1-deficient mice. Cell *85*, 1125-1134.

Edwards, J.R., Yarychkivska, O., Boulard, M., and Bestor, T.H. (2017). DNA methylation and DNA methyltransferases. Epigenetics & Chromatin *10*, 23.

Eitoku, M., Sato, L., Senda, T., and Horikoshi, M. (2008). Histone chaperones: 30 years from isolation to elucidation of the mechanisms of nucleosome assembly and disassembly. Cellular and molecular life sciences : CMLS *65*, 414-444.

Erkek, S., Hisano, M., Liang, C.Y., Gill, M., Murr, R., Dieker, J., Schubeler, D., van der Vlag, J., Stadler, M.B., and Peters, A.H. (2013). Molecular determinants of nucleosome retention at CpG-rich sequences in mouse spermatozoa. Nature structural & molecular biology *20*, 868-875.

Esashi, F., Christ, N., Gannon, J., Liu, Y., Hunt, T., Jasin, M., and West, S.C. (2005). CDK-dependent phosphorylation of BRCA2 as a regulatory mechanism for recombinational repair. Nature *434*, 598-604.

Esteves, S.C. (2002). Effect of cigarette smoking on levels of seminal oxidative stress in infertile men: a prospective study. International braz j urol : official journal of the Brazilian Society of Urology *28*, 484-485.

Evenson, D., and Jost, L. (2001). Sperm chromatin structure assay for fertility assessment. Current protocols in cytometry *Chapter 7*, Unit 7 13.

Fadloun, A., Le Gras, S., Jost, B., Ziegler-Birling, C., Takahashi, H., Gorab, E., Carninci, P., and Torres-Padilla, M.E. (2013). Chromatin signatures and retrotransposon profiling in mouse embryos reveal regulation of LINE-1 by RNA. Nature structural & molecular biology *20*, 332-338.

Fagbemi, A.F., Orelli, B., and Scharer, O.D. (2011). Regulation of endonuclease activity in human nucleotide excision repair. DNA repair *10*, 722-729.

Fatehi, A.N., Bevers, M.M., Schoevers, E., Roelen, B.A., Colenbrander, B., and Gadella, B.M. (2006). DNA damage in bovine sperm does not block fertilization and early embryonic development but induces apoptosis after the first cleavages. Journal of andrology *27*, 176-188.

Fidanza, A., Toschi, P., Zacchini, F., Czernik, M., Palmieri, C., Scapolo, P., Modlinski, J.A., Loi, P., and Ptak, G.E. (2014). Impaired placental vasculogenesis compromises the growth of sheep embryos developed in vitro. Biology of reproduction *91*, 21.

Fischer, B., and Bavister, B.D. (1993). Oxygen tension in the oviduct and uterus of rhesus monkeys, hamsters and rabbits. Journal of reproduction and fertility *99*, 673-679.

Flach, G., Johnson, M.H., Braude, P.R., Taylor, R.A., and Bolton, V.N. (1982). The transition from maternal to embryonic control in the 2-cell mouse embryo. Embo J *1*, 681-686.

Fortini, P., and Dogliotti, E. (2007). Base damage and single-strand break repair: mechanisms and functional significance of short- and long-patch repair subpathways. DNA repair *6*, 398-409.

Frauer, C., Rottach, A., Meilinger, D., Bultmann, S., Fellinger, K., Hasenöder, S., Wang, M., Qin, W., Söding, J., Spada, F., *et al.* (2011). Different Binding Properties and Function of CXXC Zinc Finger Domains in Dnmt1 and Tet1. PloS one *6*, e16627.

Fromme, J.C., and Verdine, G.L. (2004). Base excision repair. Advances in protein chemistry *69*, 1-41.

Fulka, J., Fulka, H., Slavik, T., Okada, K., and Fulka, J., Jr. (2006). DNA methylation pattern in pig in vivo produced embryos. Histochemistry and cell biology *126*, 213-217.

Galli, C., Duchi, R., Colleoni, S., Lagutina, I., and Lazzari, G. (2014). Ovum pick up, intracytoplasmic sperm injection and somatic cell nuclear transfer in cattle, buffalo and horses: from the research laboratory to clinical practice. Theriogenology *81*, 138-151.

Gartel, A.L., and Tyner, A.L. (2002). The role of the cyclin-dependent kinase inhibitor p21 in apoptosis. Molecular cancer therapeutics *1*, 639-649.

Gary, R., Kim, K., Cornelius, H.L., Park, M.S., and Matsumoto, Y. (1999). Proliferating cell nuclear antigen facilitates excision in long-patch base excision repair. The Journal of biological chemistry *274*, 4354-4363.

Gasser, S., and Raulet, D.H. (2006). The DNA damage response arouses the immune system. Cancer research *66*, 3959-3962.

Gaudet, F., Rideout, W.M., 3rd, Meissner, A., Dausman, J., Leonhardt, H., and Jaenisch, R. (2004). Dnmt1 expression in pre- and postimplantation embryogenesis and the maintenance of IAP silencing. Molecular and cellular biology *24*, 1640-1648.

Gaudet, F., Talbot, D., Leonhardt, H., and Jaenisch, R. (1998). A short DNA methyltransferase isoform restores methylation in vivo. J Biol Chem *273*, 32725-32729.

Gawecka, J.E., Marh, J., Ortega, M., Yamauchi, Y., Ward, M.A., and Ward, W.S. (2013). Mouse zygotes respond to severe sperm DNA damage by delaying paternal DNA replication and embryonic development. PloS one *8*, e56385.

Generoso, W.M., Cain, K.T., Krishna, M., and Huff, S.W. (1979). Genetic lesions induced by chemicals in spermatozoa and spermatids of mice are repaired in the egg. Proceedings of the National Academy of Sciences of the United States of America *76*, 435-437.

Gharagozloo, P., and Aitken, R.J. (2011). The role of sperm oxidative stress in male infertility and the significance of oral antioxidant therapy. Human reproduction *26*, 1628-1640.

Ginsburg, M., Snow, M.H., and McLaren, A. (1990). Primordial germ cells in the mouse embryo during gastrulation. Development *110*, 521-528.

Goll, M.G., and Bestor, T.H. (2005). Eukaryotic cytosine methyltransferases. Annual review of biochemistry *74*, 481-514.

Govin, J., Caron, C., Lestrat, C., Rousseaux, S., and Khochbin, S. (2004). The role of histones in chromatin remodelling during mammalian spermiogenesis. Eur J Biochem *271*, 3459-3469.

Govin, J., Dorsey, J., Gaucher, J., Rousseaux, S., Khochbin, S., and Berger, S.L. (2010). Systematic screen reveals new functional dynamics of histones H3 and H4 during gametogenesis. Genes & development *24*, 1772-1786.

Govin, J., Escoffier, E., Rousseaux, S., Kuhn, L., Ferro, M., Thevenon, J., Catena, R., Davidson, I., Garin, J., Khochbin, S*., et al.* (2007). Pericentric heterochromatin reprogramming by new histone variants during mouse spermiogenesis. The Journal of cell biology *176*, 283-294.

Graf, A., Krebs, S., Zakhartchenko, V., Schwalb, B., Blum, H., and Wolf, E. (2014). Fine mapping of genome activation in bovine embryos by RNA sequencing. Proceedings of the National Academy of Sciences of the United States of America *111*, 4139-4144.

Gu, A., Ji, G., Zhou, Y., Long, Y., Shi, X., Fu, G., Wang, S., Song, L., and Wang, X. (2010). Polymorphisms of nucleotide-excision repair genes may contribute to sperm DNA fragmentation and male infertility. Reproductive biomedicine online *21*, 602-609.

Gu, T.P. (2011). The role of Tet3 DNA dioxygenase in epigenetic reprogramming by oocytes. Nature *477*, 606-610.

Guerin, P., El Mouatassim, S., and Menezo, Y. (2001). Oxidative stress and protection against reactive oxygen species in the pre-implantation embryo and its surroundings. Human reproduction update *7*, 175-189.

Guibert, S., Forne, T., and Weber, M. (2012). Global profiling of DNA methylation erasure in mouse primordial germ cells. Genome research *22*, 633-641.

Gunes, S., Al-Sadaan, M., and Agarwal, A. (2015). Spermatogenesis, DNA damage and DNA repair mechanisms in male infertility. Reproductive biomedicine online *31*, 309-319.

Guo, F., Li, X., Liang, D., Li, T., Zhu, P., Guo, H., Wu, X., Wen, L., Gu, T.P., Hu, B*., et al.* (2014a). Active and passive demethylation of male and female pronuclear DNA in the mammalian zygote. Cell Stem Cell *15*, 447-458.

Guo, H., Zhu, P., Yan, L., Li, R., Hu, B., Lian, Y., Yan, J., Ren, X., Lin, S., Li, J*., et al.* (2014b). The DNA methylation landscape of human early embryos. Nature *511*, 606-610.

Guo, J.U., Su, Y., Zhong, C., Ming, G.L., and Song, H. (2011). Hydroxylation of 5-methylcytosine by TET1 promotes active DNA demethylation in the adult brain. Cell *145*, 423-434.

Gurler, H., Calisici, O., Calisici, D., and Bollwein, H. (2015). Effects of feeding omega-3-fatty acids on fatty acid composition and quality of bovine sperm and on antioxidative capacity of bovine seminal plasma. Anim Reprod Sci *160*, 97-104.

Gurler, H., Malama, E., Heppelmann, M., Calisici, O., Leiding, C., Kastelic, J.P., and Bollwein, H. (2016). Effects of cryopreservation on sperm viability, synthesis of reactive oxygen species, and DNA damage of bovine sperm. Theriogenology *86*, 562-571.

Haince, J.F., Kozlov, S., Dawson, V.L., Dawson, T.M., Hendzel, M.J., Lavin, M.F., and Poirier, G.G. (2007). Ataxia telangiectasia mutated (ATM) signaling network is modulated by a novel poly(ADP-ribose)-dependent pathway in the early response to DNA-damaging agents. The Journal of biological chemistry *282*, 16441-16453.

Hajkova, P. (2002). Epigenetic reprogramming in mouse primordial germ cells. Mech Dev *117*, 15-23.

Hajkova, P. (2010). Genome-wide reprogramming in the mouse germ line entails the base excision repair pathway. Science *329*, 78-82.

Hajkova, P. (2011). Epigenetic reprogramming in the germline: towards the ground state of the epigenome. Philos Trans R Soc Lond B Biol Sci *366*, 2266-2273.

Hajkova, P., Ancelin, K., Waldmann, T., Lacoste, N., Lange, U.C., Cesari, F., Lee, C., Almouzni, G., Schneider, R., and Surani, M.A. (2008). Chromatin dynamics during epigenetic reprogramming in the mouse germ line. Nature *452*, 877-881.

Hajkova, P., Erhardt, S., Lane, N., Haaf, T., El-Maarri, O., Reik, W., Walter, J., and Surani, M.A. (2002). Epigenetic reprogramming in mouse primordial germ cells. Mech Dev *117*, 15-23.

Hajkova, P., Jeffries, S.J., Lee, C., Miller, N., Jackson, S.P., and Surani, M.A. (2010). Genome-wide reprogramming in the mouse germ line entails the base excision repair pathway. Science *329*, 78-82.

Hamatani, T., Carter, M.G., Sharov, A.A., and Ko, M.S. (2004). Dynamics of global gene expression changes during mouse preimplantation development. Dev Cell *6*, 117-131.

Hammoud, S.S., Nix, D.A., Zhang, H., Purwar, J., Carrell, D.T., and Cairns, B.R. (2009). Distinctive chromatin in human sperm packages genes for embryo development. Nature *460*, 473-478.

Handel, M.A. (2004). The XY body: a specialized meiotic chromatin domain. Exp Cell Res *296*, 57-63.

Handel, M.A., and Schimenti, J.C. (2010). Genetics of mammalian meiosis: regulation, dynamics and impact on fertility. Nature reviews Genetics *11*, 124-136.

Hann, M.C., Lau, P.E., and Tempest, H.G. (2011). Meiotic recombination and male infertility: from basic science to clinical reality? Asian J Androl *13*, 212-218.

Hardeland, U., Bentele, M., Lettieri, T., Steinacher, R., Jiricny, J., and Schar, P. (2001). Thymine DNA glycosylase. Progress in nucleic acid research and molecular biology *68*, 235-253.

Harvey, A.J. (2007). The role of oxygen in ruminant preimplantation embryo development and metabolism. Anim Reprod Sci *98*, 113-128.

Hashimoto, H., Horton, J.R., Zhang, X., Bostick, M., Jacobsen, S.E., and Cheng, X. (2008). The SRA domain of UHRF1 flips 5-methylcytosine out of the DNA helix. In Nature, pp. 826-829.

Hashimoto, H., Pais, J.E., Zhang, X., Saleh, L., Fu, Z.Q., Dai, N., Correa, I.R., Jr., Zheng, Y., and Cheng, X. (2014). Structure of a Naegleria Tet-like dioxygenase in complex with 5-methylcytosine DNA. Nature *506*, 391-395.

Hata, K., Okano, M., Lei, H., and Li, E. (2002). Dnmt3L cooperates with the Dnmt3 family of de novo DNA methyltransferases to establish maternal imprints in mice. Development *129*, 1983-1993.

Hauer, M.H., and Gasser, S.M. (2017). Chromatin and nucleosome dynamics in DNA damage and repair. Genes & development *31*, 2204-2221.

Hayashi, K., Ohta, H., Kurimoto, K., Aramaki, S., and Saitou, M. (2011). Reconstitution of the mouse germ cell specification pathway in culture by pluripotent stem cells. Cell *146*, 519-532.

He, Y.F., Li, B.Z., Li, Z., Liu, P., Wang, Y., Tang, Q., Ding, J., Jia, Y., Chen, Z., Li, L.*, et al.* (2011). Tet-mediated formation of 5-carboxylcytosine and its excision by TDG in mammalian DNA. Science *333*, 1303-1307.

Henckel, A. (2009). Histone methylation is mechanistically linked to DNA methylation at imprinting control regions in mammals. Hum Mol Genet *18*, 3375-3383.

Heras, S., Smits, K., De Schauwer, C., and Van Soom, A. (2017). Dynamics of 5-methylcytosine and 5-hydroxymethylcytosine during pronuclear development in equine zygotes produced by ICSI. Epigenetics & chromatin *10*, 13.

Hill, P.W.S., Leitch, H.G., Requena, C.E., Sun, Z., Amouroux, R., Roman-Trufero, M., Borkowska, M., Terragni, J., Vaisvila, R., Linnett, S.*, et al.* (2018). Epigenetic reprogramming enables the transition from primordial germ cell to gonocyte. Nature *555*, 392-396.

Hirasawa, R. (2008). Maternal and zygotic DNMT1 are necessary and sufficient for the maintenance of DNA methylation imprints during preimplantation development. Genes Dev *22*, 1607-1616.

Hochegger, H., Dejsuphong, D., Fukushima, T., Morrison, C., Sonoda, E., Schreiber, V., Zhao, G.Y., Saberi, A., Masutani, M., Adachi, N.*, et al.* (2006). Parp-1 protects homologous recombination from interference by Ku and Ligase IV in vertebrate cells. Embo J *25*, 1305-1314.

Hoeijmakers, J.H. (2001). Genome maintenance mechanisms for preventing cancer. Nature *411*, 366-374.

Hon, G.C., Song, C.X., Du, T., Jin, F., Selvaraj, S., Lee, A.Y., Yen, C.A., Ye, Z., Mao, S.Q., Wang, B.A.*, et al.* (2014). 5mC oxidation by Tet2 modulates enhancer activity and timing of transcriptome reprogramming during differentiation. Molecular cell *56*, 286-297.

Hou, J., Lei, T.H., Liu, L., Cui, X.H., An, X.R., and Chen, Y.F. (2005). DNA methylation patterns in in vitro-fertilised goat zygotes. Reproduction, fertility, and development *17*, 809-813.

Howe, J.A., Howell, M., Hunt, T., and Newport, J.W. (1995). Identification of a developmental timer regulating the stability of embryonic cyclin A and a new somatic A-type cyclin at gastrulation. Genes & development *9*, 1164-1176.

Howlett, S.K., and Reik, W. (1991). Methylation levels of maternal and paternal genomes during preimplantation development. Development *113*, 119-127.

Hsia, K.T., Millar, M.R., King, S., Selfridge, J., Redhead, N.J., Melton, D.W., and Saunders, P.T. (2003). DNA repair gene Ercc1 is essential for normal spermatogenesis and oogenesis and for functional integrity of germ cell DNA in the mouse. Development *130*, 369-378.

Hsieh, P., and Zhang, Y. (2017). The Devil is in the details for DNA mismatch repair. Proceedings of the National Academy of Sciences of the United States of America *114*, 3552-3554.

Hu, L., Lu, J., Cheng, J., Rao, Q., Li, Z., Hou, H., Lou, Z., Zhang, L., Li, W., Gong, W.*, et al.* (2015). Structural insight into substrate preference for TET-mediated oxidation. Nature *527*, 118-122.

Hübscher, U., Spadari, S., Villani, G., Maga, G. (2010). DNA polymerases: Discovery, Characterization and Functions in Cellular DNA Transactions, Vol 1 (World Scientific).

Hunt, P.A., and Hassold, T.J. (2008). Human female meiosis: what makes a good egg go bad? Trends in genetics : TIG *24*, 86-93.

Hurst, L.D., and Ellegren, H. (1998). Sex biases in the mutation rate. Trends in genetics : TIG *14*, 446-452.

Hwang, K., and Lamb, D.J. (2012). Molecular mechanisms of male infertility. In Male Infertil- ity (Springer).

Ichijima, Y., Ichijima, M., Lou, Z., Nussenzweig, A., Camerini-Otero, R.D., Chen, J., Andreassen, P.R., and Namekawa, S.H. (2011). MDC1 directs chromosome-wide silencing of the sex chromosomes in male germ cells. Genes Dev *25*, 959-971.

Inoue, A., Shen, L., Dai, Q., He, C., and Zhang, Y. (2011). Generation and replication-dependent dilution of 5fC and 5caC during mouse preimplantation development. Cell Res *21*, 1670-1676.

Inoue, A., and Zhang, Y. (2011). Replication-dependent loss of 5-hydroxymethylcytosine in mouse preimplantation embryos. Science *334*, 194.

Iqbal, K., Jin, S.G., Pfeifer, G.P., and Szabo, P.E. (2011). Reprogramming of the paternal genome upon fertilization involves genome-wide oxidation of 5-methylcytosine. Proc Natl Acad Sci U S A *108*, 3642-3647.

Ishikawa, M. (1993). [Oxygen radicals-superoxide dismutase system and reproduction medicine]. Nihon Sanka Fujinka Gakkai zasshi *45*, 842-848.

Ito, S. (2010). Role of TET proteins in 5mC to 5hmC conversion, ES-cell self-renewal and inner cell mass specification. Nature *466*, 1129-1133.

Ito, S., D'Alessio, A.C., Taranova, O.V., Hong, K., Sowers, L.C., and Zhang, Y. (2010). Role of Tet proteins in 5mC to 5hmC conversion, ES-cell self-renewal and inner cell mass specification. Nature *466*, 1129-1133.

Ito, S., Shen, L., Dai, Q., Wu, S.C., Collins, L.B., Swenberg, J.A., He, C., and Zhang, Y. (2011). Tet proteins can convert 5-methylcytosine to 5-formylcytosine and 5-carboxylcytosine. Science *333*, 1300-1303.

Iwasaki, Y.W., Siomi, M.C., and Siomi, H. (2015). PIWI-Interacting RNA: Its Biogenesis and Functions. Annu Rev Biochem *84*, 405-433.

Iyama, T., and Wilson, D.M., 3rd (2013). DNA repair mechanisms in dividing and non-dividing cells. DNA repair *12*, 620-636.

Jachowicz, J.W., Santenard, A., Bender, A., Muller, J., and Torres-Padilla, M.-E. (2013). Heterochromatin establishment at pericentromeres depends on nuclear position. Genes & development *27*, 2427-2432.

Jackson, S.P., and Bartek, J. (2009). The DNA-damage response in human biology and disease. Nature *461*, 1071-1078.

Jafarpour, F., Hosseini, S.M., Ostadhosseini, S., Abbasi, H., Dalman, A., and Nasr-Esfahani, M.H. (2017). Comparative dynamics of 5-methylcytosine reprogramming and TET family expression during preimplantation mammalian development in mouse and sheep. Theriogenology *89*, 86-96.

Jaroudi, S., Kakourou, G., Cawood, S., Doshi, A., Ranieri, D.M., Serhal, P., Harper, J.C., and SenGupta, S.B. (2009). Expression profiling of DNA repair genes in human oocytes and blastocysts using microarrays. Human reproduction *24*, 2649-2655.

Jaroudi, S., and SenGupta, S. (2007). DNA repair in mammalian embryos. Mutation research *635*, 53-77.

Jazayeri, A., Balestrini, A., Garner, E., Haber, J.E., and Costanzo, V. (2008). Mre11–Rad50–Nbs1-dependent processing of DNA breaks generates oligonucleotides that stimulate ATM activity. Embo J *27*, 1953-1962.

Jenuwein, T., and Allis, C.D. (2001). Translating the histone code. Science *293*, 1074-1080.

Jeong, S., Liang, G., Sharma, S., Lin, J.C., Choi, S.H., Han, H., Yoo, C.B., Egger, G., Yang, A.S., and Jones, P.A. (2009). Selective anchoring of DNA methyltransferases 3A and 3B to nucleosomes containing methylated DNA. Mol Cell Biol *29*, 5366-5376.

Jesaitis, M.A. (1957). THE NUCLEIC ACIDS OF T(2), T(4), AND T6 BACTERIOPHAGES. The Journal of Experimental Medicine *106*, 233-246.

Ji, B.T., Shu, X.O., Linet, M.S., Zheng, W., Wacholder, S., Gao, Y.T., Ying, D.M., and Jin, F. (1997). Paternal cigarette smoking and the risk of childhood cancer among offspring of nonsmoking mothers. Journal of the National Cancer Institute *89*, 238-244.

Jozwik, M., Wolczynski, S., Jozwik, M., and Szamatowicz, M. (1999). Oxidative stress markers in preovulatory follicular fluid in humans. Molecular human reproduction *5*, 409-413.

Jurkowska, R.Z., Jurkowski, T.P., and Jeltsch, A. (2011). Structure and function of mammalian DNA methyltransferases. Chembiochem *12*, 206-222.

Kagiwada, S., Kurimoto, K., Hirota, T., Yamaji, M., and Saitou, M. (2013). Replication-coupled passive DNA demethylation for the erasure of genome imprints in mice. Embo J *32*, 340-353.

Kanaar, R., and Wyman, C. (2008). DNA repair by the MRN complex: break it to make it. Cell *135*, 14-16.

Kaneda, M. (2004). Essential role for de novo DNA methyltransferase DNMT3A in paternal and maternal imprinting. Nature *429*, 900-903.

Kaneda, M., Hirasawa, R., Chiba, H., Okano, M., Li, E., and Sasaki, H. (2010). Genetic evidence for Dnmt3a-dependent imprinting during oocyte growth obtained by conditional knockout with Zp3-Cre and complete exclusion of Dnmt3b by chimera formation. Genes Cells *15*, 169-179.

Kaneda, M., Sado, T., Hata, K., Okano, M., Tsujimoto, N., Li, E., and Sasaki, H. (2004). Role of de novo DNA methyltransferases in initiation of genomic imprinting and X-chromosome inactivation. Cold Spring Harb Symp Quant Biol *69*, 125-129.

Kato, Y. (2007). Role of the DNMT3 family in de novo methylation of imprinted and repetitive sequences during male germ cell development in the mouse. Hum Mol Genet *16*, 2272-2280.

Kato, Y., Kaneda, M., Hata, K., Kumaki, K., Hisano, M., Kohara, Y., Okano, M., Li, E., Nozaki, M., and Sasaki, H. (2007). Role of the Dnmt3 family in de novo methylation of imprinted and repetitive sequences during male germ cell development in the mouse. Hum Mol Genet *16*, 2272-2280.

Kawamoto, T., Araki, K., Sonoda, E., Yamashita, Y.M., Harada, K., Kikuchi, K., Masutani, C., Hanaoka, F., Nozaki, K., Hashimoto, N.*, et al.* (2005). Dual roles for DNA polymerase eta in homologous DNA recombination and translesion DNA synthesis. Molecular cell *20*, 793-799.

Keeney, S., Baudat, F., Angeles, M., Zhou, Z.H., Copeland, N.G., Jenkins, N.A., Manova, K., and Jasin, M. (1999). A mouse homolog of the Saccharomyces cerevisiae meiotic recombination DNA transesterase Spo11p. Genomics *61*, 170-182.

Keeney, S., Giroux, C.N., and Kleckner, N. (1997). Meiosis-specific DNA double-strand breaks are catalyzed by Spo11, a member of a widely conserved protein family. Cell *88*, 375-384.

Khalil, A.M., Boyar, F.Z., and Driscoll, D.J. (2004). Dynamic histone modifications mark sex chromosome inactivation and reactivation during mammalian spermatogenesis. Proc Natl Acad Sci U S A *101*, 16583-16587.

Khil, P.P., Smirnova, N.A., Romanienko, P.J., and Camerini-Otero, R.D. (2004). The mouse X chromosome is enriched for sex-biased genes not subject to selection by meiotic sex chromosome inactivation. Nat Genet *36*, 642-646.

Kikyo, N., and Wolffe, A.P. (2000). Reprogramming nuclei: insights from cloning, nuclear transfer and heterokaryons. Journal of cell science *113 (Pt 1)*, 11-20.

Kim, Y.J., and Wilson, D.M., 3rd (2012). Overview of base excision repair biochemistry. Curr Mol Pharmacol *5*, 3-13.

Kimura, Y., and Yanagimachi, R. (1995). Mouse oocytes injected with testicular spermatozoa or round spermatids can develop into normal offspring. Development *121*, 2397-2405.

Kishikawa, S., Murata, T., Ugai, H., Yamazaki, T., and Yokoyama, K.K. (2003). Control elements of Dnmt1 gene are regulated in cell-cycle dependent manner. Nucleic Acids Res, 307-308.

Klaunig, J.E., and Kamendulis, L.M. (2004). The role of oxidative stress in carcinogenesis. Annual review of pharmacology and toxicology *44*, 239-267.

Ko, M., An, J., Bandukwala, H.S., Chavez, L., Aijo, T., Pastor, W.A., Segal, M.F., Li, H., Koh, K.P., Lahdesmaki, H.*, et al.* (2013). Modulation of TET2 expression and 5-methylcytosine oxidation by the CXXC domain protein IDAX. Nature *497*, 122-126.

Kobayashi, H., Sakurai, T., Imai, M., Takahashi, N., Fukuda, A., Yayoi, O., Sato, S., Nakabayashi, K., Hata, K., Sotomaru, Y.*, et al.* (2012). Contribution of intragenic DNA methylation in mouse gametic DNA methylomes to establish oocyte-specific heritable marks. PLoS genetics *8*, e1002440.

Kobayashi, H., Sakurai, T., Miura, F., Imai, M., Mochiduki, K., Yanagisawa, E., Sakashita, A., Wakai, T., Suzuki, Y., Ito, T.*, et al.* (2013). High-resolution DNA methylome analysis of primordial germ cells identifies gender-specific reprogramming in mice. Genome research *23*, 616-627.

Kohli, R.M., and Zhang, Y. (2013). TET enzymes, TDG and the dynamics of DNA demethylation. Nature *502*, 472-479.

Kojima, Y., Tam, O.H., and Tam, P.P. (2014). Timing of developmental events in the early mouse embryo. Seminars in cell & developmental biology *34*, 65-75.

Kolas, N.K., and Cohen, P.E. (2004). Novel and diverse functions of the DNA mismatch repair family in mammalian meiosis and recombination. Cytogenetic and genome research *107*, 216-231.

Korkmaz, F., Malama, E., Siuda, M., Leiding, C., and Bollwein, H. (2017). Effects of sodium pyruvate on viability, synthesis of reactive oxygen species, lipid peroxidation and DNA integrity of cryopreserved bovine sperm. Anim Reprod Sci *185*, 18-27.

Kota, S.K., and Feil, R. (2010). Epigenetic transitions in germ cell development and meiosis. Dev Cell *19*, 675-686.

Kourmouli, N., Jeppesen, P., Mahadevhaiah, S., Burgoyne, P., Wu, R., Gilbert, D.M., Bongiorni, S., Prantera, G., Fanti, L., Pimpinelli, S.*, et al.* (2004). Heterochromatin and tri-methylated lysine 20 of histone H4 in animals. Journal of cell science *117*, 2491.

Kriaucionis, S., and Heintz, N. (2009). The nuclear DNA base 5-hydroxymethylcytosine is present in Purkinje neurons and the brain. Science *324*, 929-930.

Krishnan, N., Jeong, D.G., Jung, S.K., Ryu, S.E., Xiao, A., Allis, C.D., Kim, S.J., and Tonks, N.K. (2009). Dephosphorylation of the C-terminal tyrosyl residue of the DNA damage-related histone H2A.X is mediated by the protein phosphatase eyes absent. The Journal of biological chemistry *284*, 16066-16070.

Krokan, H.E., and Bjoras, M. (2013). Base excision repair. Cold Spring Harb Perspect Biol *5*, a012583.

Krokan, H.E., Drablos, F., and Slupphaug, G. (2002). Uracil in DNA--occurrence, consequences and repair. Oncogene *21*, 8935-8948.

Kubo, N., Toh, H., Shirane, K., Shirakawa, T., Kobayashi, H., Sato, T., Sone, H., Sato, Y., Tomizawa, S., Tsurusaki, Y.*, et al.* (2015). DNA methylation and gene expression dynamics during spermatogonial stem cell differentiation in the early postnatal mouse testis. BMC genomics *16*, 624.

Kuo, L.J., and Yang, L.X. (2008). Gamma-H2AX - a novel biomarker for DNA double-strand breaks. In vivo *22*, 305-309.

Kuramochi-Miyagawa, S., Watanabe, T., Gotoh, K., Totoki, Y., Toyoda, A., Ikawa, M., Asada, N., Kojima, K., Yamaguchi, Y., Ijiri, T.W.*, et al.* (2008). DNA methylation of retrotransposon genes is regulated by Piwi family members MILI and MIWI2 in murine fetal testes. Genes Dev *22*, 908-917.

Kurimoto, K. (2008). Complex genome-wide transcription dynamics orchestrated by BLIMP1 for the specification of the germ cell lineage in mice. Genes Dev *22*, 1617-1635.

Kurimoto, K., and Saitou, M. (2015). Mechanism and Reconstitution In Vitro of Germ Cell Development in Mammals. Cold Spring Harbor symposia on quantitative biology *80*, 147-154.

Ladstatter, S., and Tachibana-Konwalski, K. (2016). A Surveillance Mechanism Ensures Repair of DNA Lesions during Zygotic Reprogramming. Cell *167*, 1774-1787 e1713.

Lahn, B.T., Tang, Z.L., Zhou, J., Barndt, R.J., Parvinen, M., Allis, C.D., and Page, D.C. (2002). Previously uncharacterized histone acetyltransferases implicated in mammalian spermatogenesis. Proceedings of the National Academy of Sciences of the United States of America *99*, 8707-8712.

Lan, J., Lepikhov, K., Giehr, P., and Walter, J. (2017). Histone and DNA methylation control by H3 serine 10/threonine 11 phosphorylation in the mouse zygote. Epigenetics Chromatin *10*, 5.

Lane, M., McPherson, N.O., Fullston, T., Spillane, M., Sandeman, L., Kang, W.X., and Zander-Fox, D.L. (2014). Oxidative stress in mouse sperm impairs embryo development, fetal growth and alters adiposity and glucose regulation in female offspring. PloS one *9*, e100832.

Lane, N., Dean, W., Erhardt, S., Hajkova, P., Surani, A., Walter, J., and Reik, W. (2003). Resistance of IAPs to methylation reprogramming may provide a mechanism for epigenetic inheritance in the mouse. Genesis *35*, 88-93.

Law, J.A., and Jacobsen, S.E. (2010). Establishing, maintaining and modifying DNA methylation patterns in plants and animals. Nature reviews Genetics *11*, 204-220.

Lee, J., Inoue, K., Ono, R., Ogonuki, N., Kohda, T., Kaneko-Ishino, T., Ogura, A., and Ishino, F. (2002). Erasing genomic imprinting memory in mouse clone embryos produced from day 11.5 primordial germ cells. Development *129*, 1807-1817.

Lee, J.H., and Paull, T.T. (2005). ATM activation by DNA double-strand breaks through the Mre11-Rad50-Nbs1 complex. Science *308*, 551-554.

Lee, J.H., Voo, K.S., and Skalnik, D.G. (2001). Identification and characterization of the DNA binding domain of CpG-binding protein. The Journal of biological chemistry *276*, 44669-44676.

Lee, M.T., Bonneau, A.R., and Giraldez, A.J. (2014). Zygotic genome activation during the maternal-to-zygotic transition. Annual review of cell and developmental biology *30*, 581-613.

Leemans, B., Gadella, B.M., Stout, T.A., De Schauwer, C., Nelis, H., Hoogewijs, M., and Van Soom, A. (2016). Why doesn't conventional IVF work in the horse? The equine oviduct as a microenvironment for capacitation/fertilization. Reproduction *152*, R233-R245.

Lei, H., Oh, S.P., Okano, M., Juttermann, R., Goss, K.A., Jaenisch, R., and Li, E. (1996). De novo DNA cytosine methyltransferase activities in mouse embryonic stem cells. Development *122*, 3195-3205.

Leonhardt, H., Page, A.W., Weier, H.U., and Bestor, T.H. (1992). A targeting sequence directs DNA methyltransferase to sites of DNA replication in mammalian nuclei. Cell *71*, 865-873.

Lepikhov, K., and Walter, J. (2004). Differential dynamics of histone H3 methylation at positions K4 and K9 in the mouse zygote. BMC developmental biology *4*, 12.

Lepikhov, K., Zakhartchenko, V., Hao, R., Yang, F., Wrenzycki, C., Niemann, H., Wolf, E., and Walter, J. (2008). Evidence for conserved DNA and histone H3 methylation reprogramming in mouse, bovine and rabbit zygotes. Epigenetics & chromatin *1*, 8.

Lewis, S.E., and Aitken, R.J. (2005). DNA damage to spermatozoa has impacts on fertilization and pregnancy. Cell and tissue research *322*, 33-41.

Li, E., Beard, C., and Jaenisch, R. (1993). Role for DNA methylation in genomic imprinting. Nature *366*, 362-365.

Li, E., Bestor, T.H., and Jaenisch, R. (1992a). Targeted mutation of the DNA methyltransferase gene results in embryonic lethality. Cell *69*, 915-926.

Li, E., Bestor, T.H., and Jaenisch, R. (1992b). Targeted mutation of the DNA methyltransferase gene results in embryonic lethality. Cell *69*, 915-926.

Li, G.-M. (2007). Mechanisms and functions of DNA mismatch repair. Cell Research *18*, 85.

Li, J.Y., Lees-Murdock, D.J., Xu, G.L., and Walsh, C.P. (2004). Timing of establishment of paternal methylation imprints in the mouse. Genomics *84*, 952-960.

Li, X. (2008). A maternal-zygotic effect gene, ZFP57, maintains both maternal and paternal imprints. Dev Cell *15*, 547-557.

Liang, G. (2002). Cooperativity between DNA methyltransferases in the maintenance methylation of repetitive elements. Mol Cell Biol *22*, 480-491.

Lin, C.J., Conti, M., and Ramalho-Santos, M. (2013). Histone variant H3.3 maintains a decondensed chromatin state essential for mouse preimplantation development. Development *140*, 3624-3634.

Lindahl, T. (1993). Instability and decay of the primary structure of DNA. Nature *362*, 709.

Liu, C.Y., Lee, C.F., Hong, C.H., and Wei, Y.H. (2004a). Mitochondrial DNA mutation and depletion increase the susceptibility of human cells to apoptosis. Annals of the New York Academy of Sciences *1011*, 133-145.

Liu, H., Kim, J.M., and Aoki, F. (2004b). Regulation of histone H3 lysine 9 methylation in oocytes and early pre-implantation embryos. Development *131*, 2269-2280.

Liu, K., Rajareddy, S., Liu, L., Jagarlamudi, K., Boman, K., Selstam, G., and Reddy, P. (2006). Control of mammalian oocyte growth and early follicular development by the oocyte PI3 kinase pathway: new roles for an old timer. Developmental biology *299*, 1-11.

Liu, X., Wang, C., Liu, W., Li, J., Li, C., Kou, X., Chen, J., Zhao, Y., Gao, H., Wang, H.*, et al.* (2016). Distinct features of H3K4me3 and H3K27me3 chromatin domains in pre-implantation embryos. Nature *537*, 558-562.

Lord, T., and Aitken, R.J. (2015). Fertilization stimulates 8-hydroxy-2'-deoxyguanosine repair and antioxidant activity to prevent mutagenesis in the embryo. Developmental biology *406*, 1-13.

Lou, H., Le, F., Zheng, Y., Li, L., Wang, L., Wang, N., Zhu, Y., Huang, H., and Jin, F. (2014). Assisted reproductive technologies impair the expression and methylation of insulin-induced gene 1 and sterol regulatory element-binding factor 1 in the fetus and placenta. Fertility and sterility *101*, 974-980 e972.

Lu, F., Liu, Y., Jiang, L., Yamaguchi, S., and Zhang, Y. (2014). Role of Tet proteins in enhancer activity and telomere elongation. Genes & development *28*, 2103-2119.

Lucifero, D., La Salle, S., Bourc'his, D., Martel, J., Bestor, T.H., and Trasler, J.M. (2007). Coordinate regulation of DNA methyltransferase expression during oogenesis. BMC Dev Biol *7*, 36.

Lucifero, D., Mann, M.R., Bartolomei, M.S., and Trasler, J.M. (2004). Gene-specific timing and epigenetic memory in oocyte imprinting. Hum Mol Genet *13*, 839-849.

Mackay, D.J., Callaway, J.L., Marks, S.M., White, H.E., Acerini, C.L., Boonen, S.E., Dayanikli, P., Firth, H.V., Goodship, J.A., Haemers, A.P.*, et al.* (2008). Hypomethylation of multiple imprinted loci in individuals with transient neonatal diabetes is associated with mutations in ZFP57. Nature genetics *40*, 949-951.

Mahaney, B.L., Meek, K., and Lees-Miller, S.P. (2009). Repair of ionizing radiation-induced DNA double-strand breaks by non-homologous end-joining. The Biochemical journal *417*, 639-650.

Maiti, A., and Drohat, A.C. (2011). Thymine DNA glycosylase can rapidly excise 5-formylcytosine and 5-carboxylcytosine: potential implications for active demethylation of CpG sites. The Journal of biological chemistry *286*, 35334-35338.

Maloisel, L., Fabre, F., and Gangloff, S. (2008). DNA polymerase delta is preferentially recruited during homologous recombination to promote heteroduplex DNA extension. Molecular and cellular biology *28*, 1373-1382.

Manipalviratn, S., DeCherney, A., and Segars, J. (2009). Imprinting disorders and assisted reproductive technology. Fertility and sterility *91*, 305-315.

Manzo, M., Wirz, J., Ambrosi, C., Villasenor, R., Roschitzki, B., and Baubec, T. (2017). Isoform-specific localization of DNMT3A regulates DNA methylation fidelity at bivalent CpG islands. EMBO J *36*, 3421-3434.

Marchetti, F., Essers, J., Kanaar, R., and Wyrobek, A.J. (2007). Disruption of maternal DNA repair increases sperm-derived chromosomal aberrations. Proceedings of the National Academy of Sciences of the United States of America *104*, 17725-17729.

Marchetti, F., and Wyrobek, A.J. (2008). DNA repair decline during mouse spermiogenesis results in the accumulation of heritable DNA damage. DNA repair *7*, 572-581.

Marsin, S., Vidal, A.E., Sossou, M., Menissier-de Murcia, J., Le Page, F., Boiteux, S., de Murcia, G., and Radicella, J.P. (2003). Role of XRCC1 in the coordination and stimulation of oxidative DNA damage repair initiated by the DNA glycosylase hOGG1. The Journal of biological chemistry *278*, 44068-44074.

Martianov, I., Brancorsini, S., Catena, R., Gansmuller, A., Kotaja, N., Parvinen, M., Sassone-Corsi, P., and Davidson, I. (2005). Polar nuclear localization of H1T2, a histone H1 variant, required for spermatid elongation

and DNA condensation during spermiogenesis. Proceedings of the National Academy of Sciences of the United States of America *102*, 2808-2813.

Masala, L., Burrai, G.P., Bellu, E., Ariu, F., Bogliolo, L., Ledda, S., and Bebbere, D. (2017). Methylation dynamics during folliculogenesis and early embryo development in sheep. Reproduction *153*, 605-619.

Matsuda, Y., Seki, N., Utsugi-Takeuchi, T., and Tobari, I. (1989). Changes in X-ray Sensitivity of Mouse Eggs from Fertilization to the Early Pronuclear Stage, and Their Repair Capacity. International Journal of Radiation Biology *55*, 233-256.

Matzuk, M.M., McKeown, M.R., Filippakopoulos, P., Li, Q., Ma, L., Agno, J.E., Lemieux, M.E., Picaud, S., Yu, R.N., Qi, J.*, et al.* (2012). Small-molecule inhibition of BRDT for male contraception. Cell *150*, 673-684.

Mayer, W., Niveleau, A., Walter, J., Fundele, R., and Haaf, T. (2000). Demethylation of the zygotic paternal genome. Nature *403*, 501-502.

Mazzilli, F., Rossi, T., Marchesini, M., Ronconi, C., and Dondero, F. (1994). Superoxide anion in human semen related to seminal parameters and clinical aspects. Fertility and sterility *62*, 862-868.

McCarrey, J.R., Geyer, C.B., and Yoshioka, H. (2005). Epigenetic regulation of testis-specific gene expression. Annals of the New York Academy of Sciences *1061*, 226-242.

McKAY, D.J., RENAUX, B.S., and DIXON, G.H. (1986). Human sperm protamines. European Journal of Biochemistry *156*, 5-8.

McPherson, S., and Longo, F.J. (1993). Chromatin structure-function alterations during mammalian spermatogenesis: DNA nicking and repair in elongating spermatids. European journal of histochemistry : EJH *37*, 109-128.

Meek, K., Dang, V., and Lees-Miller, S.P. (2008). DNA-PK: the means to justify the ends? Advances in immunology *99*, 33-58.

Meistrich, M.L., Mohapatra, B., Shirley, C.R., and Zhao, M. (2003). Roles of transition nuclear proteins in spermiogenesis. Chromosoma *111*, 483-488.

Meistrich, M.L., Trostle-Weige, P.K., Lin, R., Bhatnagar, Y.M., and Allis, C.D. (1992). Highly acetylated H4 is associated with histone displacement in rat spermatids. Molecular reproduction and development *31*, 170-181.

Melamed, N., Choufani, S., Wilkins-Haug, L.E., Koren, G., and Weksberg, R. (2015). Comparison of genome-wide and gene-specific DNA methylation between ART and naturally conceived pregnancies. Epigenetics *10*, 474-483.

Menezo, Y., Dale, B., and Cohen, M. (2010). DNA damage and repair in human oocytes and embryos: a review. Zygote *18*, 357-365.

Menezo, Y., Jr., Russo, G., Tosti, E., El Mouatassim, S., and Benkhalifa, M. (2007). Expression profile of genes coding for DNA repair in human oocytes using pangenomic microarrays, with a special focus on ROS linked decays. Journal of assisted reproduction and genetics *24*, 513-520.

Mertineit, C., Yoder, J.A., Taketo, T., Laird, D.W., Trasler, J.M., and Bestor, T.H. (1998). Sex-specific exons control DNA methyltransferase in mammalian germ cells. Development *125*, 889-897.

Messerschmidt, D.M., Knowles, B.B., and Solter, D. (2014). DNA methylation dynamics during epigenetic reprogramming in the germline and preimplantation embryos. Genes Dev *28*, 812-828.

Meyer-Ficca, M.L., Lonchar, J.D., Ihara, M., Meistrich, M.L., Austin, C.A., and Meyer, R.G. (2011). Poly(ADP-ribose) polymerases PARP1 and PARP2 modulate topoisomerase II beta (TOP2B) function during chromatin condensation in mouse spermiogenesis. Biol Reprod *84*, 900-909.

Modrich, P., and Lahue, R. (1996). Mismatch repair in replication fidelity, genetic recombination, and cancer biology. Annual review of biochemistry *65*, 101-133.

Montellier, E., Boussouar, F., Rousseaux, S., Zhang, K., Buchou, T., Fenaille, F., Shiota, H., Debernardi, A., Hery, P., Curtet, S.*, et al.* (2013). Chromatin-to-nucleoprotamine transition is controlled by the histone H2B variant TH2B. Genes & development *27*, 1680-1692.

Moran-Crusio, K., Reavie, L., Shih, A., Abdel-Wahab, O., Ndiaye-Lobry, D., Lobry, C., Figueroa, M.E., Vasanthakumar, A., Patel, J., Zhao, X.*, et al.* (2011). Tet2 loss leads to increased hematopoietic stem cell self-renewal and myeloid transformation. Cancer Cell *20*, 11-24.

Moretti, C., Vaiman, D., Tores, F., and Cocquet, J. (2016). Expression and epigenomic landscape of the sex chromosomes in mouse post-meiotic male germ cells. Epigenetics Chromatin *9*, 47.

Morris, S.A., Teo, R.T., Li, H., Robson, P., Glover, D.M., and Zernicka-Goetz, M. (2010). Origin and formation of the first two distinct cell types of the inner cell mass in the mouse embryo. Proceedings of the National Academy of Sciences of the United States of America *107*, 6364-6369.

Mostafa, T., Tawadrous, G., Roaia, M.M., Amer, M.K., Kader, R.A., and Aziz, A. (2006). Effect of smoking on seminal plasma ascorbic acid in infertile and fertile males. Andrologia *38*, 221-224.

Motosugi, N., Bauer, T., Polanski, Z., Solter, D., and Hiiragi, T. (2005). Polarity of the mouse embryo is established at blastocyst and is not prepatterned. Genes & development *19*, 1081-1092.

Mueller, J.L., Mahadevaiah, S.K., Park, P.J., Warburton, P.E., Page, D.C., and Turner, J.M. (2008). The mouse X chromosome is enriched for multicopy testis genes showing postmeiotic expression. Nat Genet *40*, 794-799.

Nabel, C.S., Jia, H., Ye, Y., Shen, L., Goldschmidt, H.L., Stivers, J.T., Zhang, Y., and Kohli, R.M. (2012). AID/APOBEC deaminases disfavor modified cytosines implicated in DNA demethylation. Nat Chem Biol *8*, 751-758.

Nakamura, J., Walker, V.E., Upton, P.B., Chiang, S.Y., Kow, Y.W., and Swenberg, J.A. (1998). Highly sensitive apurinic/apyrimidinic site assay can detect spontaneous and chemically induced depurination under physiological conditions. Cancer research *58*, 222-225.

Nakamura, T. (2012). PGC7 binds histone H3K9me2 to protect against conversion of 5mC to 5hmC in early embryos. Nature *486*, 415-419.

Nakane, H., Hirota, S., Brooks, P.J., Nakabeppu, Y., Nakatsu, Y., Nishimune, Y., Iino, A., and Tanaka, K. (2008). Impaired spermatogenesis and elevated spontaneous tumorigenesis in xeroderma pigmentosum group A gene (Xpa)-deficient mice. DNA repair *7*, 1938-1950.

Namekawa, S.H., Park, P.J., Zhang, L.F., Shima, J.E., McCarrey, J.R., Griswold, M.D., and Lee, J.T. (2006). Postmeiotic sex chromatin in the male germline of mice. Curr Biol *16*, 660-667.

Nashun, B., Yukawa, M., Liu, H., Akiyama, T., and Aoki, F. (2010). Changes in the nuclear deposition of histone H2A variants during pre-implantation development in mice. Development *137*, 3785.

Navarro-Costa, P., Nogueira, P., Carvalho, M., Leal, F., Cordeiro, I., Calhaz-Jorge, C., Goncalves, J., and Plancha, C.E. (2010). Incorrect DNA methylation of the DAZL promoter CpG island associates with defective human sperm. Human reproduction *25*, 2647-2654.

Neale, M.J., and Keeney, S. (2006). Clarifying the mechanics of DNA strand exchange in meiotic recombination. Nature *442*, 153-158.

Neeley, W.L., and Essigmann, J.M. (2006). Mechanisms of formation, genotoxicity, and mutation of guanine oxidation products. Chemical research in toxicology *19*, 491-505.

Newport, J., and Kirschner, M. (1982a). A major developmental transition in early Xenopus embryos: I. characterization and timing of cellular changes at the midblastula stage. Cell *30*, 675-686.

Newport, J., and Kirschner, M. (1982b). A major developmental transition in early Xenopus embryos: II. Control of the onset of transcription. Cell *30*, 687-696.

O'Flaherty, C., de Lamirande, E., and Gagnon, C. (2006). Positive role of reactive oxygen species in mammalian sperm capacitation: triggering and modulation of phosphorylation events. Free radical biology & medicine *41*, 528-540.

Obata, Y., and Kono, T. (2002). Maternal primary imprinting is established at a specific time for each gene throughout oocyte growth. J Biol Chem *277*, 5285-5289.

Oestrup, O., Hall, V., Petkov, S.G., Wolf, X.A., Hyldig, S., and Hyttel, P. (2009). From zygote to implantation: morphological and molecular dynamics during embryo development in the pig. Reproduction in domestic animals = Zuchthygiene *44 Suppl 3*, 39-49.

Ogura, A., Matsuda, J., and Yanagimachi, R. (1994). Birth of normal young after electrofusion of mouse oocytes with round spermatids. Proc Natl Acad Sci U S A *91*, 7460-7462.

Okano, M., Bell, D.W., Haber, D.A., and Li, E. (1999a). DNA methyltransferases Dnmt3a and Dnmt3b are essential for de novo methylation and mammalian development. Cell *99*, 247-257.

Okano, M., Bell, D.W., Haber, D.A., and Li, E. (1999b). DNA methyltransferases DNMT3A and DNMT3B are essential for de novo methylation and mammalian development. Cell *99*, 247-257.

Olsen, A.K., Lindeman, B., Wiger, R., Duale, N., and Brunborg, G. (2005). How do male germ cells handle DNA damage? Toxicology and applied pharmacology *207*, 521-531.

Ooi, S.K., Qiu, C., Bernstein, E., Li, K., Jia, D., Yang, Z., Erdjument-Bromage, H., Tempst, P., Lin, S.P., Allis, C.D.*, et al.* (2007). DNMT3L connects unmethylated lysine 4 of histone H3 to de novo methylation of DNA. Nature *448*, 714-717.

Orsi, G.A., Couble, P., and Loppin, B. (2009). Epigenetic and replacement roles of histone variant H3.3 in reproduction and development. Int J Dev Biol *53*, 231-243.

Oswald, J. (2000). Active demethylation of the paternal genome in the mouse zygote. Curr Biol *10*, 475-478.

Oswald, J., Engemann, S., Lane, N., Mayer, W., Olek, A., Fundele, R., Dean, W., Reik, W., and Walter, J. (2000). Active demethylation of the paternal genome in the mouse zygote. Curr Biol *10*, 475-478.

Otani, J., Nankumo, T., Arita, K., Inamoto, S., Ariyoshi, M., and Shirakawa, M. (2009). Structural basis for recognition of H3K4 methylation status by the DNA methyltransferase 3A ATRX-DNMT3-DNMT3L domain. EMBO reports *10*, 1235-1241.

Pacheco, S.E., Houseman, E.A., Christensen, B.C., Marsit, C.J., Kelsey, K.T., Sigman, M., and Boekelheide, K. (2011). Integrative DNA methylation and gene expression analyses identify DNA packaging and epigenetic regulatory genes associated with low motility sperm. PLoS One *6*, e20280.

Papadopoulos, S., Rizos, D., Duffy, P., Wade, M., Quinn, K., Boland, M.P., and Lonergan, P. (2002). Embryo survival and recipient pregnancy rates after transfer of fresh or vitrified, in vivo or in vitro produced ovine blastocysts. Animal reproduction science *74*, 35-44.

Park, J.S., Jeong, Y.S., Shin, S.T., Lee, K.K., and Kang, Y.K. (2007). Dynamic DNA methylation reprogramming: active demethylation and immediate remethylation in the male pronucleus of bovine zygotes. Developmental dynamics : an official publication of the American Association of Anatomists *236*, 2523-2533.

Park, J.S., Lee, D., Cho, S., Shin, S.T., and Kang, Y.K. (2010). Active loss of DNA methylation in two-cell stage goat embryos. Int J Dev Biol *54*, 1323-1328.

Park, K.E., Magnani, L., and Cabot, R.A. (2009). Differential remodeling of mono- and trimethylated H3K27 during porcine embryo development. Mol Reprod Dev *76*, 1033-1042.

Payer, B., Saitou, M., Barton, S.C., Thresher, R., Dixon, J.P., Zahn, D., Colledge, W.H., Carlton, M.B., Nakano, T., and Surani, M.A. (2003). Stella is a maternal effect gene required for normal early development in mice. Current biology : CB *13*, 2110-2117.

Pepling, M.E. (2006). From primordial germ cell to primordial follicle: mammalian female germ cell development. Genesis *44*, 622-632.

Pepling, M.E., and Spradling, A.C. (2001). Mouse ovarian germ cell cysts undergo programmed breakdown to form primordial follicles. Developmental biology *234*, 339-351.

Perry, G. (2016). Statistics of embryo collection and transfer in domestic farm animals. Embryo Technology Newsletter, 10-25.

Pfaffeneder, T., Hackner, B., Truss, M., Munzel, M., Muller, M., Deiml, C.A., Hagemeier, C., and Carell, T. (2011). The discovery of 5-formylcytosine in embryonic stem cell DNA. Angewandte Chemie *50*, 7008-7012.

Plastira, K., Msaouel, P., Angelopoulou, R., Zanioti, K., Plastiras, A., Pothos, A., Bolaris, S., Paparisteidis, N., and Mantas, D. (2007). The effects of age on DNA fragmentation, chromatin packaging and conventional semen parameters in spermatozoa of oligoasthenoteratozoospermic patients. Journal of assisted reproduction and genetics *24*, 437-443.

Polanski, Z., Motosugi, N., Tsurumi, C., Hiiragi, T., and Hoffmann, S. (2008). Hypomethylation of paternal DNA in the late mouse zygote is not essential for development. Int J Dev Biol *52*, 295-298.

Popp, C., Dean, W., Feng, S., Cokus, S.J., Andrews, S., Pellegrini, M., Jacobsen, S.E., and Reik, W. (2010). Genome-wide erasure of DNA methylation in mouse primordial germ cells is affected by AID deficiency. Nature *463*, 1101-1105.

Prasad, R., Dianov, G.L., Bohr, V.A., and Wilson, S.H. (2000). FEN1 stimulation of DNA polymerase beta mediates an excision step in mammalian long patch base excision repair. The Journal of biological chemistry *275*, 4460-4466.

Prasad, R., Lavrik, O.I., Kim, S.J., Kedar, P., Yang, X.P., Vande Berg, B.J., and Wilson, S.H. (2001). DNA polymerase beta -mediated long patch base excision repair. Poly(ADP-ribose)polymerase-1 stimulates strand displacement DNA synthesis. The Journal of biological chemistry *276*, 32411-32414.

Probst, A.V., Santos, F., Reik, W., Almouzni, G., and Dean, W. (2007). Structural differences in centromeric heterochromatin are spatially reconciled on fertilisation in the mouse zygote. Chromosoma *116*.

Ptak, G.E., D'Agostino, A., Toschi, P., Fidanza, A., Zacchini, F., Czernik, M., Monaco, F., and Loi, P. (2013). Post-implantation mortality of in vitro produced embryos is associated with DNA methyltransferase 1 dysfunction in sheep placenta. Human reproduction *28*, 298-305.

Puschendorf, M., Terranova, R., Boutsma, E., Mao, X., Isono, K., Brykczynska, U., Kolb, C., Otte, A.P., Koseki, H., Orkin, S.H.*, et al.* (2008). PRC1 and Suv39h specify parental asymmetry at constitutive heterochromatin in early mouse embryos. Nature genetics *40*, 411-420.

Quenneville, S. (2011). In embryonic stem cells, ZFP57/KAP1 recognize a methylated hexanucleotide to affect chromatin and DNA methylation of imprinting control regions. Mol Cell *44*, 361-372.

Quenneville, S., Verde, G., Corsinotti, A., Kapopoulou, A., Jakobsson, J., Offner, S., Baglivo, I., Pedone, P.V., Grimaldi, G., Riccio, A.*, et al.* (2011). In embryonic stem cells, ZFP57/KAP1 recognize a methylated hexanucleotide to affect chromatin and DNA methylation of imprinting control regions. Molecular cell *44*, 361-372.

Rangasamy, D., Berven, L., Ridgway, P., and Tremethick, D.J. (2003). Pericentric heterochromatin becomes enriched with H2A.Z during early mammalian development. Embo J *22*, 1599-1607.

Rasmussen, K.D., and Helin, K. (2016). Role of TET enzymes in DNA methylation, development, and cancer. Genes Dev *30*, 733-750.

Rathke, C., Baarends, W.M., Awe, S., and Renkawitz-Pohl, R. (2014). Chromatin dynamics during spermiogenesis. Biochimica et biophysica acta *1839*, 155-168.

Rathke, C., Baarends, W.M., Jayaramaiah-Raja, S., Bartkuhn, M., Renkawitz, R., and Renkawitz-Pohl, R. (2007). Transition from a nucleosome-based to a protamine-based chromatin configuration during spermiogenesis in <em>Drosophila</em&gt. Journal of cell science *120*, 1689.

Ray, S.D., Lam, T.S., Rotollo, J.A., Phadke, S., Patel, C., Dontabhaktuni, A., Mohammad, S., Lee, H., Strika, S., Dobrogowska, A.*, et al.* (2004). Oxidative stress is the master operator of drug and chemically-induced programmed and unprogrammed cell death: Implications of natural antioxidants in vivo. BioFactors (Oxford, England) *21*, 223-232.

Reik, W., Dean, W., and Walter, J. (2001). Epigenetic reprogramming in mammalian development. Science *293*, 1089-1093.

Reis e Silva, A.R., Bruno, C., Fleurot, R., Daniel, N., Archilla, C., Peynot, N., Lucci, C.M., Beaujean, N., and Duranthon, V. (2012). Alteration of DNA demethylation dynamics by in vitro culture conditions in rabbit pre-implantation embryos. Epigenetics *7*, 440-446.

Reis Silva, A.R., Adenot, P., Daniel, N., Archilla, C., Peynot, N., Lucci, C.M., Beaujean, N., and Duranthon, V. (2011). Dynamics of DNA methylation levels in maternal and paternal rabbit genomes after fertilization. Epigenetics *6*, 987-993.

Rinaudo, P.F., Giritharan, G., Talbi, S., Dobson, A.T., and Schultz, R.M. (2006). Effects of oxygen tension on gene expression in preimplantation mouse embryos. Fertility and sterility *86*, 1252-1265, 1265.e1251-1236.

Romanienko, P.J., and Camerini-Otero, R.D. (1999). Cloning, characterization, and localization of mouse and human SPO11. Genomics *61*, 156-169.

Ronen, A., and Glickman, B.W. (2001). Human DNA repair genes. Environmental and molecular mutagenesis *37*, 241-283.

Rooney, A.P., and Zhang, J. (1999). Rapid evolution of a primate sperm protein: relaxation of functional constraint or positive Darwinian selection? Molecular biology and evolution *16*, 706-710.

Rougier, N., Bourc'his, D., Gomes, D.M., Niveleau, A., Plachot, M., Paldi, A., and Viegas-Pequignot, E. (1998). Chromosome methylation patterns during mammalian preimplantation development. Genes & development *12*, 2108-2113.

Royo, H., Prosser, H., Ruzankina, Y., Mahadevaiah, S.K., Cloutier, J.M., Baumann, M., Fukuda, T., Hoog, C., Toth, A., de Rooij, D.G.*, et al.* (2013). ATR acts stage specifically to regulate multiple aspects of mammalian meiotic silencing. Genes Dev *27*, 1484-1494.

Sabeti, P., Pourmasumi, S., Rahiminia, T., Akyash, F., and Talebi, A.R. (2016). Etiologies of sperm oxidative stress. Int J Reprod Biomed (Yazd) *14*, 231-240.

Saitou, M., Barton, S.C., and Surani, M.A. (2002). A molecular programme for the specification of germ cell fate in mice. Nature *418*, 293-300.

Saitou, M., Kagiwada, S., and Kurimoto, K. (2012). Epigenetic reprogramming in mouse pre-implantation development and primordial germ cells. Development *139*, 15-31.

Saitou, M., and Miyauchi, H. (2016). Gametogenesis from Pluripotent Stem Cells. Cell stem cell *18*, 721-735.

Saitou, M., Payer, B., Lange, U.C., Erhardt, S., Barton, S.C., and Surani, M.A. (2003). Specification of germ cell fate in mice. Philos Trans R Soc Lond B Biol Sci *358*, 1363-1370.

Salamone, D.F., Canel, N.G., and Rodriguez, M.B. (2017). Intracytoplasmic sperm injection in domestic and wild mammals. Reproduction *154*, F111-F124.

Saleh, R.A., and Agarwal, A. (2002). Oxidative stress and male infertility: from research bench to clinical practice. Journal of andrology *23*, 737-752.

Salilew-Wondim, D., Fournier, E., Hoelker, M., Saeed-Zidane, M., Tholen, E., Looft, C., Neuhoff, C., Besenfelder, U., Havlicek, V., Rings, F.*, et al.* (2015). Genome-Wide DNA Methylation Patterns of Bovine Blastocysts Developed In Vivo from Embryos Completed Different Stages of Development In Vitro. PloS one *10*, e0140467.

Salvaing, J., Peynot, N., Bedhane, M.N., Veniel, S., Pellier, E., Boulesteix, C., Beaujean, N., Daniel, N., and Duranthon, V. (2016). Assessment of 'one-step' versus 'sequential' embryo culture conditions through embryonic genome methylation and hydroxymethylation changes. Human reproduction *31*, 2471-2483.

Sánchez, F., and Smitz, J. (2012). Molecular control of oogenesis. Biochimica et Biophysica Acta (BBA) - Molecular Basis of Disease *1822*, 1896-1912.

Sanocka, D., and Kurpisz, M. (2004). Reactive oxygen species and sperm cells. Reproductive biology and endocrinology : RB&E *2*, 12.

Santenard, A., Ziegler-Birling, C., Koch, M., Tora, L., Bannister, A.J., and Torres-Padilla, M.E. (2010). Heterochromatin formation in the mouse embryo requires critical residues of the histone variant H3.3. Nature cell biology *12*, 853-862.

Santos, F., Peters, A.H., Otte, A.P., Reik, W., and Dean, W. (2005). Dynamic chromatin modifications characterise the first cell cycle in mouse embryos. Dev Biol *280*, 225-236.

Santos, R.R., Schoevers, E.J., and Roelen, B.A. (2014). Usefulness of bovine and porcine IVM/IVF models for reproductive toxicology. Reprod Biol Endocrinol *12*, 117.

Sasaki, H., and Matsui, Y. (2008). Epigenetic events in mammalian germ-cell development: reprogramming and beyond. Nat Rev Genet *9*, 129-140.

Schärer, O.D. (2013). Nucleotide Excision Repair in Eukaryotes. Cold Spring Harbor Perspectives in Biology *5*, a012609.

Schiesser, S., Hackner, B., Pfaffeneder, T., Muller, M., Hagemeier, C., Truss, M., and Carell, T. (2012). Mechanism and stem-cell activity of 5-carboxycytosine decarboxylation determined by isotope tracing. Angewandte Chemie *51*, 6516-6520.

Schreiber, V., Dantzer, F., Ame, J.C., and de Murcia, G. (2006). Poly(ADP-ribose): novel functions for an old molecule. Nat Rev Mol Cell Biol *7*, 517-528.

Schulte, R.T., Ohl, D.A., Sigman, M., and Smith, G.D. (2010). Sperm DNA damage in male infertility: etiologies, assays, and outcomes. Journal of assisted reproduction and genetics *27*, 3-12.

Sebesta, M., Burkovics, P., Haracska, L., and Krejci, L. (2011). Reconstitution of DNA repair synthesis in vitro and the role of polymerase and helicase activities. DNA repair *10*, 567-576.

Seisenberger, S. (2012). The dynamics of genome-wide DNA methylation reprogramming in mouse primordial germ cells. Mol Cell *48*, 849-862.

Seisenberger, S., Andrews, S., Krueger, F., Arand, J., Walter, J., Santos, F., Popp, C., Thienpont, B., Dean, W., and Reik, W. (2012). The dynamics of genome-wide DNA methylation reprogramming in mouse primordial germ cells. Mol Cell *48*, 849-862.

Seki, Y. (2005). Extensive and orderly reprogramming of genome-wide chromatin modifications associated with specification and early development of germ cells in mice. Dev Biol *278*, 440-458.

Sepaniak, S., Forges, T., Fontaine, B., Gerard, H., Foliguet, B., Guillet-May, F., Zaccabri, A., and Monnier-Barbarino, P. (2004). [Negative impact of cigarette smoking on male fertility: from spermatozoa to the offspring]. Journal de gynecologie, obstetrique et biologie de la reproduction *33*, 384-390.

Shang, E., Nickerson, H.D., Wen, D., Wang, X., and Wolgemuth, D.J. (2007). The first bromodomain of Brdt, a testis-specific member of the BET sub-family of double-bromodomain-containing proteins, is essential for male germ cell differentiation. Development *134*, 3507-3515.

Shang, E., Salazar, G., Crowley, T.E., Wang, X., Lopez, R.A., Wang, X., and Wolgemuth, D.J. (2004). Identification of unique, differentiation stage-specific patterns of expression of the bromodomain-containing genes Brd2, Brd3, Brd4, and Brdt in the mouse testis. Gene expression patterns : GEP *4*, 513-519.

Shannon, M., Lamerdin, J.E., Richardson, L., McCutchen-Maloney, S.L., Hwang, M.H., Handel, M.A., Stubbs, L., and Thelen, M.P. (1999). Characterization of the mouse Xpf DNA repair gene and differential expression during spermatogenesis. Genomics *62*, 427-435.

Sharif, J., Muto, M., Takebayashi, S., Suetake, I., Iwamatsu, A., Endo, T.A., Shinga, J., Mizutani-Koseki, Y., Toyoda, T., Okamura, K.*, et al.* (2007). The SRA protein Np95 mediates epigenetic inheritance by recruiting Dnmt1 to methylated DNA. Nature *450*, 908-912.

Sharma, S., Hicks, J.K., Chute, C.L., Brennan, J.R., Ahn, J.Y., Glover, T.W., and Canman, C.E. (2012). REV1 and polymerase zeta facilitate homologous recombination repair. Nucleic acids research *40*, 682-691.

Shen, L., Inoue, A., He, J., Liu, Y., Lu, F., and Zhang, Y. (2014). Tet3 and DNA replication mediate demethylation of both the maternal and paternal genomes in mouse zygotes. Cell Stem Cell *15*, 459-471.

Shimura, T., Inoue, M., Taga, M., Shiraishi, K., Uematsu, N., Takei, N., Yuan, Z.M., Shinohara, T., and Niwa, O. (2002). p53-dependent S-phase damage checkpoint and pronuclear cross talk in mouse zygotes with X-irradiated sperm. Molecular and cellular biology *22*, 2220-2228.

Shinagawa, T., Huynh, L.M., Takagi, T., Tsukamoto, D., Tomaru, C., Kwak, H.G., Dohmae, N., Noguchi, J., and Ishii, S. (2015). Disruption of Th2a and Th2b genes causes defects in spermatogenesis. Development *142*, 1287-1292.

Shirane, K., Toh, H., Kobayashi, H., Miura, F., Chiba, H., Ito, T., Kono, T., and Sasaki, H. (2013). Mouse oocyte methylomes at base resolution reveal genome-wide accumulation of non-CpG methylation and role of DNA methyltransferases. PLoS genetics *9*, e1003439.

Shirazi, A., Derakhshan-Horeh, M., Pilvarian, A.A., Ahmadi, E., Nazari, H., and Heidari, B. (2011). Effect of pre-treatment of ovine sperm on male pronuclear formation and subsequent embryo development following intracytoplasmic sperm injection. Reproduction in domestic animals = Zuchthygiene *46*, 87-94.

Sikka, S.C., Rajasekaran, M., and Hellstrom, W.J. (1995). Role of oxidative stress and antioxidants in male infertility. Journal of andrology *16*, 464-468.

Simmet, K., Zakhartchenko, V., Philippou-Massier, J., Blum, H., Klymiuk, N., and Wolf, E. (2018). OCT4/POU5F1 is required for NANOG expression in bovine blastocysts. Proc Natl Acad Sci U S A *115*, 2770-2775.

Smallwood, S.A., Tomizawa, S., Krueger, F., Ruf, N., Carli, N., Segonds-Pichon, A., Sato, S., Hata, K., Andrews, S.R., and Kelsey, G. (2011). Dynamic CpG island methylation landscape in oocytes and preimplantation embryos. Nature genetics *43*, 811-814.

Smith, T.B., Dun, M.D., Smith, N.D., Curry, B.J., Connaughton, H.S., and Aitken, R.J. (2013). The presence of a truncated base excision repair pathway in human spermatozoa that is mediated by OGG1. J Cell Sci *126*, 1488-1497.

Smith, Z.D., Chan, M.M., Mikkelsen, T.S., Gu, H., Gnirke, A., Regev, A., and Meissner, A. (2012). A unique regulatory phase of DNA methylation in the early mammalian embryo. Nature *484*, 339-344.

Song, J., Rechkoblit, O., Bestor, T.H., and Patel, D.J. (2011a). Structure of DNMT1-DNA complex reveals a role for autoinhibition in maintenance DNA methylation. Science *331*, 1036-1040.

Song, N., Liu, J., An, S., Nishino, T., Hishikawa, Y., and Koji, T. (2011b). Immunohistochemical Analysis of Histone H3 Modifications in Germ Cells during Mouse Spermatogenesis. Acta Histochemica et Cytochemica *44*, 183-190.

Spada, F., Haemmer, A., Kuch, D., Rothbauer, U., Schermelleh, L., Kremmer, E., Carell, T., Langst, G., and Leonhardt, H. (2007). DNMT1 but not its interaction with the replication machinery is required for maintenance of DNA methylation in human cells. J Cell Biol *176*, 565-571.

Spermon, J.R., Ramos, L., Wetzels, A.M., Sweep, C.G., Braat, D.D., Kiemeney, L.A., and Witjes, J.A. (2006). Sperm integrity pre- and post-chemotherapy in men with testicular germ cell cancer. Human reproduction *21*, 1781-1786.

Stadler, J., and Richly, H. (2017). Regulation of DNA Repair Mechanisms: How the Chromatin Environment Regulates the DNA Damage Response. International journal of molecular sciences *18*.

Steger, K., Failing, K., Klonisch, T., Behre, H.M., Manning, M., Weidner, W., Hertle, L., Bergmann, M., and Kliesch, S. (2001). Round spermatids from infertile men exhibit decreased protamine-1 and -2 mRNA. Human reproduction *16*, 709-716.

Stewart, K.R., Veselovska, L., and Kelsey, G. (2016). Establishment and functions of DNA methylation in the germline. Epigenomics *8*, 1399-1413.

Stucki, M., Pascucci, B., Parlanti, E., Fortini, P., Wilson, S.H., Hubscher, U., and Dogliotti, E. (1998). Mammalian base excision repair by DNA polymerases delta and epsilon. Oncogene *17*, 835-843.

Suetake, I., Hayata, D., and Tajima, S. (2006). The amino-terminus of mouse DNA methyltransferase 1 forms an independent domain and binds to DNA with the sequence involving PCNA binding motif. J Biochem *140*, 763-776.

Sugino, N., Takiguchi, S., Kashida, S., Karube, A., Nakamura, Y., and Kato, H. (2000). Superoxide dismutase expression in the human corpus luteum during the menstrual cycle and in early pregnancy. Molecular human reproduction *6*, 19-25.

Sugitani, N., Sivley, R.M., Perry, K.E., Capra, J.A., and Chazin, W.J. (2016). XPA: A key scaffold for human nucleotide excision repair. DNA repair *44*, 123-135.

Suzuki, M.M., and Bird, A. (2008). DNA methylation landscapes: provocative insights from epigenomics. Nat Rev Genet *9*, 465-476.

Suzuki, T., Sugino, N., Fukaya, T., Sugiyama, S., Uda, T., Takaya, R., Yajima, A., and Sasano, H. (1999). Superoxide dismutase in normal cycling human ovaries: immunohistochemical localization and characterization. Fertility and sterility *72*, 720-726.

Svilar, D., Goellner, E.M., Almeida, K.H., and Sobol, R.W. (2011). Base excision repair and lesion-dependent subpathways for repair of oxidative DNA damage. Antioxidants & redox signaling *14*, 2491-2507.

Tachiwana, H., Kagawa, W., Osakabe, A., Kawaguchi, K., Shiga, T., Hayashi-Takanaka, Y., Kimura, H., and Kurumizaka, H. (2010). Structural basis of instability of the nucleosome containing a testis-specific histone variant, human H3T. Proceedings of the National Academy of Sciences *107*, 10454-10459.

Tachiwana, H., Osakabe, A., Kimura, H., and Kurumizaka, H. (2008). Nucleosome formation with the testis-specific histone H3 variant, H3t, by human nucleosome assembly proteins in vitro. Nucleic acids research *36*, 2208-2218.

Tahiliani, M. (2009). Conversion of 5-methylcytosine to 5-hydroxymethylcytosine in mammalian DNA by MLL partner TET1. Science *324*, 930-935.

Tahiliani, M., Koh, K.P., Shen, Y., Pastor, W.A., Bandukwala, H., Brudno, Y., Agarwal, S., Iyer, L.M., Liu, D.R., Aravind, L.*, et al.* (2009). Conversion of 5-methylcytosine to 5-hydroxymethylcytosine in mammalian DNA by MLL partner TET1. Science *324*, 930-935.

Takahashi, M. (2012). Oxidative stress and redox regulation on in vitro development of mammalian embryos. The Journal of reproduction and development *58*, 1-9.

Tam, P.P., and Loebel, D.A. (2007). Gene function in mouse embryogenesis: get set for gastrulation. Nature reviews Genetics *8*, 368-381.

Tam, P.P.L., and Behringer, R.R. (1997). Mouse gastrulation: the formation of a mammalian body plan. Mechanisms of development *68*, 3-25.

Tanaka, H., Iguchi, N., Isotani, A., Kitamura, K., Toyama, Y., Matsuoka, Y., Onishi, M., Masai, K., Maekawa, M., Toshimori, K.*, et al.* (2005). HANP1/H1T2, a novel histone H1-like protein involved in nuclear formation and sperm fertility. Molecular and cellular biology *25*, 7107-7119.

Taylor, R.W., and Turnbull, D.M. (2005). Mitochondrial DNA mutations in human disease. Nature reviews Genetics *6*, 389-402.

Taylor, W.R., and Stark, G.R. (2001). Regulation of the G2/M transition by p53. Oncogene *20*, 1803-1815.

Tegelenbosch, R.A., and de Rooij, D.G. (1993). A quantitative study of spermatogonial multiplication and stem cell renewal in the C3H/101 F1 hybrid mouse. Mutation research *290*, 193-200.

Tesarik, J., Greco, E., and Mendoza, C. (2004). Late, but not early, paternal effect on human embryo development is related to sperm DNA fragmentation. Human reproduction *19*, 611-615.

Thiriet, C., and Hayes, J.J. (2005). Chromatin in need of a fix: phosphorylation of H2AX connects chromatin to DNA repair. Mol Cell *18*, 617-622.

Tian, X.C., Kubota, C., Enright, B., and Yang, X. (2003). Cloning animals by somatic cell nuclear transfer--biological factors. Reprod Biol Endocrinol *1*, 98.

Torregrosa, N., Dominguez-Fandos, D., Camejo, M.I., Shirley, C.R., Meistrich, M.L., Ballesca, J.L., and Oliva, R. (2006). Protamine 2 precursors, protamine 1/protamine 2 ratio, DNA integrity and other sperm parameters in infertile patients. Human reproduction *21*, 2084-2089.

Torres-Padilla, M.E., Bannister, A.J., Hurd, P.J., Kouzarides, T., and Zernicka-Goetz, M. (2006). Dynamic distribution of the replacement histone variant H3.3 in the mouse oocyte and preimplantation embryos. Int J Dev Biol *50*, 455-461.

Tremellen, K. (2008). Oxidative stress and male infertility--a clinical perspective. Human reproduction update *14*, 243-258.

Trounson, A., and Mohr, L. (1983). Human pregnancy following cryopreservation, thawing and transfer of an eight-cell embryo. Nature *305*, 707-709.

Trounson, A., Wood, C., and Kausche, A. (1994). In vitro maturation and the fertilization and developmental competence of oocytes recovered from untreated polycystic ovarian patients. Fertility and sterility *62*, 353-362.

Trummer, H., Habermann, H., Haas, J., and Pummer, K. (2002). The impact of cigarette smoking on human semen parameters and hormones. Human reproduction *17*, 1554-1559.

Tubbs, A., and Nussenzweig, A. (2017). Endogenous DNA Damage as a Source of Genomic Instability in Cancer. Cell *168*, 644-656.

Turner, J.M. (2015). Meiotic Silencing in Mammals. Annu Rev Genet *49*, 395-412.

Urieli-Shoval, S., Gruenbaum, Y., and Razin, A. (1983). Sequence and substrate specificity of isolated DNA methylases from Escherichia coli C. Journal of Bacteriology *153*, 274-280.

Valinluck, V., and Sowers, L.C. (2007). Endogenous cytosine damage products alter the site selectivity of human DNA maintenance methyltransferase DNMT1. Cancer Res *67*, 946-950.

Valko, M., Leibfritz, D., Moncol, J., Cronin, M.T., Mazur, M., and Telser, J. (2007). Free radicals and antioxidants in normal physiological functions and human disease. The international journal of biochemistry & cell biology *39*, 44-84.

van der Heijden, G.W., Derijck, A.A., Posfai, E., Giele, M., Pelczar, P., Ramos, L., Wansink, D.G., van der Vlag, J., Peters, A.H., and de Boer, P. (2007). Chromosome-wide nucleosome replacement and H3.3 incorporation during mammalian meiotic sex chromosome inactivation. Nat Genet *39*, 251-258.

van der Heijden, G.W., Dieker, J.W., Derijck, A.A., Muller, S., Berden, J.H., Braat, D.D., van der Vlag, J., and de Boer, P. (2005). Asymmetry in histone H3 variants and lysine methylation between paternal and maternal chromatin of the early mouse zygote. Mechanisms of development *122*, 1008-1022.

van der Heijden, G.W., Ramos, L., Baart, E.B., van den Berg, I.M., Derijck, A.A., van der Vlag, J., Martini, E., and de Boer, P. (2008). Sperm-derived histones contribute to zygotic chromatin in humans. BMC Dev Biol *8*, 34.

Vega, M., Johnson, M.C., Diaz, H.A., Urrutia, L.R., Troncoso, J.L., and Devoto, L. (1998). Regulation of human luteal steroidogenesis in vitro by nitric oxide. Endocrine *8*, 185-191.

Vidal, A.E., Boiteux, S., Hickson, I.D., and Radicella, J.P. (2001). XRCC1 coordinates the initial and late stages of DNA abasic site repair through protein-protein interactions. Embo J *20*, 6530-6539.

Villalta, J., Ballesca, J.L., Nicolas, J.M., Martinez de Osaba, M.J., Antunez, E., and Pimentel, C. (1997). Testicular function in asymptomatic chronic alcoholics: relation to ethanol intake. Alcoholism, clinical and experimental research *21*, 128-133.

Vincent, J.J., Huang, Y., Chen, P.Y., Feng, S., Calvopina, J.H., Nee, K., Lee, S.A., Le, T., Yoon, A.J., Faull, K.*, et al.* (2013). Stage-specific roles for tet1 and tet2 in DNA demethylation in primordial germ cells. Cell stem cell *12*, 470-478.

Vinson, R.K., and Hales, B.F. (2002). DNA repair during organogenesis. Mutation research *509*, 79-91.

von Meyenn, F., Berrens, R.V., Andrews, S., Santos, F., Collier, A.J., Krueger, F., Osorno, R., Dean, W., Rugg-Gunn, P.J., and Reik, W. (2016). Comparative Principles of DNA Methylation Reprogramming during Human and Mouse In Vitro Primordial Germ Cell Specification. Dev Cell *39*, 104-115.

Walczak-Jedrzejowska, R., Wolski, J.K., and Slowikowska-Hilczer, J. (2013). The role of oxidative stress and antioxidants in male fertility. Cent European J Urol *66*, 60-67.

Wallace, S.S. (2014). Base excision repair: A critical player in many games. DNA repair *19*, 14-26.

Walsh, C.P., and Bestor, T.H. (1999). Cytosine methylation and mammalian development. Genes & development *13*, 26-34.

Wang, L., Zhang, J., Duan, J., Gao, X., Zhu, W., Lu, X., Yang, L., Zhang, J., Li, G., Ci, W*., et al.* (2014). Programming and inheritance of parental DNA methylomes in mammals. Cell *157*, 979-991.

Weber, A.R., Krawczyk, C., Robertson, A.B., Kusnierczyk, A., Vagbo, C.B., Schuermann, D., Klungland, A., and Schar, P. (2016). Biochemical reconstitution of TET1-TDG-BER-dependent active DNA demethylation reveals a highly coordinated mechanism. Nature communications *7*, 10806.

Wells, P.G., McCallum, G.P., Chen, C.S., Henderson, J.T., Lee, C.J.J., Perstin, J., Preston, T.J., Wiley, M.J., and Wong, A.W. (2009). Oxidative Stress in Developmental Origins of Disease: Teratogenesis, Neurodevelopmental Deficits, and Cancer. Toxicological Sciences *108*, 4-18.

West, S.C. (2003). Molecular views of recombination proteins and their control. Nat Rev Mol Cell Biol *4*, 435-445.

White, C.R., Denomme, M.M., Tekpetey, F.R., Feyles, V., Power, S.G., and Mann, M.R. (2015). High Frequency of Imprinted Methylation Errors in Human Preimplantation Embryos. Scientific reports *5*, 17311.

Williams, R.S., Williams, J.S., and Tainer, J.A. (2007). Mre11-Rad50-Nbs1 is a keystone complex connecting DNA repair machinery, double-strand break signaling, and the chromatin template. Biochemistry and cell biology = Biochimie et biologie cellulaire *85*, 509-520.

Wilmut, I., Schnieke, A.E., McWhir, J., Kind, A.J., and Campbell, K.H. (1997). Viable offspring derived from fetal and adult mammalian cells. Nature *385*, 810-813.

Wossidlo, M. (2010). Dynamic link of DNA demethylation, DNA strand breaks and repair in mouse zygotes. EMBO J *29*, 1877-1888.

Wossidlo, M. (2011). 5-hydroxymethylcytosine in the mammalian zygote is linked with epigenetic reprogramming. Nature Commun *2*, 241.

Wossidlo, M., Arand, J., Sebastiano, V., Lepikhov, K., Boiani, M., Reinhardt, R., Scholer, H., and Walter, J. (2010). Dynamic link of DNA demethylation, DNA strand breaks and repair in mouse zygotes. Embo J *29*, 1877-1888.

Wu, H., Coskun, V., Tao, J., Xie, W., Ge, W., Yoshikawa, K., Li, E., Zhang, Y., and Sun, Y.E. (2010). Dnmt3a-dependent nonpromoter DNA methylation facilitates transcription of neurogenic genes. Science *329*, 444-448.

Wu, H., and Zhang, Y. (2014). Reversing DNA methylation: mechanisms, genomics, and biological functions. Cell *156*, 45-68.

Wu, J., Huang, B., Chen, H., Yin, Q., Liu, Y., Xiang, Y., Zhang, B., Liu, B., Wang, Q., Xia, W*., et al.* (2016). The landscape of accessible chromatin in mammalian preimplantation embryos. Nature *534*, 652-657.

Wu, S.C., and Zhang, Y. (2010). Active DNA demethylation: many roads lead to Rome. Nat Rev Mol Cell Biol *11*, 607-620.

Xu, Y., Ashley, T., Brainerd, E.E., Bronson, R.T., Meyn, M.S., and Baltimore, D. (1996). Targeted disruption of ATM leads to growth retardation, chromosomal fragmentation during meiosis, immune defects, and thymic lymphoma. Genes & development *10*, 2411-2422.

Xu, Y., Xu, C., Kato, A., Tempel, W., Abreu, J.G., Bian, C., Hu, Y., Hu, D., Zhao, B., Cerovina, T.*, et al.* (2012). Tet3 CXXC domain and dioxygenase activity cooperatively regulate key genes for Xenopus eye and neural development. Cell *151*, 1200-1213.

Yabuta, Y., Kurimoto, K., Ohinata, Y., Seki, Y., and Saitou, M. (2006). Gene expression dynamics during germline specification in mice identified by quantitative single-cell gene expression profiling. Biol Reprod *75*, 705-716.

Yamaguchi, S., Hong, K., Liu, R., Shen, L., Inoue, A., Diep, D., Zhang, K., and Zhang, Y. (2012). Tet1 controls meiosis by regulating meiotic gene expression. Nature *492*, 443-447.

Yan, W., Ma, L., Burns, K.H., and Matzuk, M.M. (2003). HILS1 is a spermatid-specific linker histone H1-like protein implicated in chromatin remodeling during mammalian spermiogenesis. Proceedings of the National Academy of Sciences *100*, 10546-10551.

Zhang, B., Zheng, H., Huang, B., Li, W., Xiang, Y., Peng, X., Ming, J., Wu, X., Zhang, Y., Xu, Q.*, et al.* (2016). Allelic reprogramming of the histone modification H3K4me3 in early mammalian development. Nature *537*, 553-557.

Zhang, H., Zhang, X., Clark, E., Mulcahey, M., Huang, S., and Shi, Y.G. (2010). TET1 is a DNA-binding protein that modulates DNA methylation and gene transcription via hydroxylation of 5-methylcytosine. Cell Res *20*, 1390-1393.

Zhao, M., Shirley, C.R., Hayashi, S., Marcon, L., Mohapatra, B., Suganuma, R., Behringer, R.R., Boissonneault, G., Yanagimachi, R., and Meistrich, M.L. (2004). Transition nuclear proteins are required for normal chromatin condensation and functional sperm development. Genesis (New York, NY : 2000) *38*, 200-213.

Zheng, P., Schramm, R.D., and Latham, K.E. (2005). Developmental regulation and in vitro culture effects on expression of DNA repair and cell cycle checkpoint control genes in rhesus monkey oocytes and embryos. Biol Reprod *72*, 1359-1369.

Zhou, B.B., and Elledge, S.J. (2000). The DNA damage response: putting checkpoints in perspective. Nature *408*, 433-439.

Zhou, L.-q., and Dean, J. (2015). Reprogramming the genome to totipotency in mouse embryos. Trends in cell biology *25*, 82-91.

Zhou, Y., Connor, E.E., Bickhart, D.M., Li, C., Baldwin, R.L., Schroeder, S.G., Rosen, B.D., Yang, L., Van Tassell, C.P., and Liu, G.E. (2018). Comparative whole genome DNA methylation profiling of cattle sperm and somatic tissues reveals striking hypomethylated patterns in sperm. GigaScience *7*.

Zhu, J.K. (2009). Active DNA demethylation mediated by DNA glycosylases. Annual review of genetics *43*, 143-166.

Zhu, P., Guo, H., Ren, Y., Hou, Y., Dong, J., Li, R., Lian, Y., Fan, X., Hu, B., Gao, Y.*, et al.* (2018). Single-cell DNA methylome sequencing of human preimplantation embryos. Nature genetics *50*, 12-19.

Ziegler-Birling, C., Helmrich, A., Tora, L., and Torres-Padilla, M.E. (2009a). Distribution of p53 binding protein 1 (53BP1) and phosphorylated H2A.X during mouse preimplantation development in the absence of DNA damage. Int J Dev Biol *53*, 1003-1011.

Ziegler-Birling, C., Helmrich, A., Tora, L., and Torres-Padilla, M.E. (2009b). Distribution of p53 binding protein 1 (53BP1) and phosphorylated H2A.X during mouse preimplantation development in the absence of DNA damage. Int J Dev Biol *53*, 1003-1011.

Zini, A., and Agarwal, A. (2012). Spermatogenesis. In Sperm Chromatin (Springer).

Zitzmann, M., Rolf, C., Nordhoff, V., Schrader, G., Rickert-Fohring, M., Gassner, P., Behre, H.M., Greb, R.R., Kiesel, L., and Nieschlag, E. (2003). Male smokers have a decreased success rate for in vitro fertilization and intracytoplasmic sperm injection. Fertility and sterility *79 Suppl 3*, 1550-1554.

Zuo, X., Sheng, J., Lau, H.T., McDonald, C.M., Andrade, M., Cullen, D.E., Bell, F.T., Iacovino, M., Kyba, M., Xu, G.*, et al.* (2012). Zinc finger protein ZFP57 requires its co-factor to recruit DNA methyltransferases and

maintains DNA methylation imprint in embryonic stem cells via its transcriptional repression domain. The Journal of biological chemistry *287*, 2107-2118.